THÈSE

Pour obtenir le grade de

DOCTEUR DE L'UNIVERSITÉ GRENOBLE ALPES

École doctorale : CSV- Chimie et Sciences du Vivant
Spécialité : Physiologie-Physiopathogies-Pharmacologie
Unité de recherche : LPCV - Laboratoire de Physiologie Cellulaire Végétale

Rôle du peroxysome et de la β-oxydation dans le remodelage des lipides membranaires en réponse à la carence en phosphate chez *Arabidopsis thaliana*

Role of peroxisome and β-oxidation in membrane lipid remodeling in response to phosphate starvation in *Arabidopsis thaliana*

Présentée par :

Siqi YAN

Direction de thèse :

Juliette JOUHET CNRS Alpes	Directrice de thèse
Morgane MICHAUD CNRS Alpes	Co-encadrante de thèse

Rapporteurs :

Sébastien MONGRAND
DIRECTEUR DE RECHERCHE, CNRS délégation Aquitaine
Hubert SCHALLER
DIRECTEUR DE RECHERCHE, CNRS délégation Alsace

Thèse soutenue publiquement le **28 octobre 2024**, devant le jury composé de :

Christelle BRETON, PROFESSEURE DES UNIVERSITES, Université Grenoble Alpes	Présidente
Juliette JOUHET, DIRECTRICE DE RECHERCHE, CNRS délégation Alpes	Directrice de thèse
Morgane MICHAUD, CHARGEE DE RECHERCHE HDR, CNRS délégation Alpes	Co-directrice de thèse
Sébastien MONGRAND, DIRECTEUR DE RECHERCHE, CNRS délégation Aquitaine	Rapporteur
Hubert SCHALLER, DIRECTEUR DE RECHERCHE, CNRS délégation Alsace	Rapporteur
Sabine D'ANDREA, PROFESSEURE, INRAE Ile-de-France - Versailles Saclay	Examinatrice

Acknowledgements

I would like to first thank Eric Maréchal, as director, for welcoming me to the Laboratoire de Physiologie Cellulaire et Végétale (LPCV).

I would also like to thank the members of my thesis jury, Sébastien Mongrand, Hubert Schaller, Sabine d'Andréa, and Christelle Breton, for agreeing and taking the time to evaluate my work. I would like to extend my thanks to the members of my CSI committee, Emmanuelle Bayer, Stefanie Müller-Schüssele, and Robert Blanvillain, for their valuable and insightful advice they provided throughout my thesis journey.

My sincere appreciation then goes to Morgane Michaud, my co-supervisor, who effectively co-directed this thesis. Morgane, I greatly appreciated your guidance, patience and kindness. You are always available to answer my questions and assist me at the lab bench for experiments. We spent three and a half years together from my Master 2 internship to the end of my PhD. We faced many challenges, both scientific and personal, I deeply thank you for always supporting and encouraging me. Congratulations again to you Morgane on receiving your HDR this year. I would also like to thank Juliette Jouhet, my thesis director, for always being there to answer my questions, to discuss science, and to wisely advise me. Morgane and Juliette are both amazing supervisors, and I am sure that your future PhD students will have an enrich experience as I have had.

This thesis project was a team effort, with many people contributing in various ways. Therefore, I would like to express my gratitude first to everyone in the Lipid team, especially people in the team who contributed to my thesis project: Catherine Albrieux and Marion Schilling. I also want to thank those who gave me fruitful suggestions during meetings, Juliette Salvaing, Florence Corellou, and Sylvaine Roy. I would also like to thank Gaëlle Villain, Séverine Beille, Mathilde Cussac, Mathilde Louwagie, Yacine Diagne, Sassia Hadjadji, Jade Ezzedine, and many others with whom we shared great moments in the lab.

The happiness I experienced during my thesis would not have been possible without all the wonderful friends I met here, so a huge thank you to Sarah Salomon, Marta Carletti, Siraba Gueye, Ana-Belèn Benitez Tellez, Aline Janeau, Rachel Bonnarde, Aleksandra Mironova, Soumiya Muthukumar, Sara Pullara, Eva Cavallari, Camille Varrel, Batoul Moubarak, Laura Turchi, Aourégane Toussaint, Moïra Arnoux-Courseaux, Lorraine Pennera, Pierre Guenzi-Tiberi, Damien Le Moigne, Yannick Sérès, Paul Montmayeul, Benjamin Fel, Chems Amari, Armando Ávila Cárdenas, and Vangeli Geshkovski. A special thanks to Sarah, whose kindness and supports keep my spirits up and reinforce my trust to this world, and I enjoyed every moment with you for hikings, drinks, and trips. Thanks also to Marta for always bringing us energy, spreading the happiness and standing by me during my tough time. Thanks to Rachel and Pierre, the best

bakers in the world, who generously shared their delicious cakes and were always ready to stand up for others. I was so glad to meet you all and have such wonderful companions over these three years. Finally, I would like to extend my thanks to everyone else in the team, even if I cannot list you all here, but without you, the great atmosphere would not have been the same.

Teamwork does not end within our lab. A big thank you to our collaborators, Julia Novion Ducassou and Yohann Couté from EDyP Lab in Grenoble, who helped me for proteomic analysis in this project. I particularly want to thank Yohann for all your valuable advice.

During these past three years, my journey would not have been as enjoyable without the support of my parents and all my friends. A big thank you to my dear parents for their unconditional supports. Thanks to my dear cousin for her emotional supports. Thanks to my besties, 紫菜, 金鱼, and 大虾 from China, for always being there even from afar. I missed a lot spending time and traveling with you all. Special thanks to 紫菜 for letting me annoy you at any time even with the time difference. I am also grateful to my alcohol friends, including Bingyu in Denmark right now, Wang and many others in France and China, who released me from stressful moments.

Lastly, I would like to thank myself as well for being brave and strong enough to complete this great journey. Five years ago, I stood before the world, met friends like stars tracing the night sky. I thought I saw the world, but in truth, I saw myself. These years spent in France, I harvested seeds of thought. Yet, I knew well, this was not my final stop. Nowadays, the world lies before me, pointing to everywhere; I master myself, completely, absolutely.

Finally, to those reading this thesis, especially if you have made it to the end here, it would have been much more challenging without you. I wish you all happiness and fulfillment in your own journeys ahead.

“路漫漫其修远兮，吾将上下而求索。- 〈〈离骚〉〉

On and on stretched my road, long it was and far; I would go high and go low to seek my heart’s desire.”

Abbreviations

AAEs	acyl-activating enzymes
AAPT	aminoalcohol aminophosphotransferase
AAs	amino acids
ABC	ATP-binding cassette
ABCD	ABC transporters of subfamily D
ABI1	hormone-related abscisic acid insensitive 1
ACBD2/ECI2	enoyl-CoA δ isomerase 2
ACCase	acetyl-CoA carboxylase
ACO	aconitase
ACP	acyl carrier protein
ACX	acyl-CoA oxidase
ADP	adenosine diphosphate
AGT1	alanine:glyoxylate aminotransferase 1
AH	amphipathic helix
AIM1	Abnormal inflorescence meristem 1
ALDP	adrenoleukodystrophy protein
APX	ascorbate peroxidase
ARF1	ADP-ribosylation factor 1
At	*Arabidopsis thaliana*
ATGLL	Adipose triglyceride lipase-LIKE
ATP	adenosine triphosphate
B14.7	mitochondrial preprotein and amino acid transporter
BA	benzoic acid
BCase	biotin carboxylase
BCC	biotin carboxy-carrier
BiFC	bimolecular fluorescence complementation
BioID	proximity biotin labeling
BIP2	Luminal binding protein
BPPs	β-propeller phytases
C	carbon
CA	cinnamic acid
CAT	catalase
CDC48A	cell division cycle 48A
CDS	CDP-DAG synthase
CGI-58	comparative gene identifier 58
Chloro IE	chloroplast inner envelope
Chloro OE	Chloroplast outer envelope
CK	Cho kinase
CL	cardiolipin
CoA	coenzyme A
co-IP	co-immunoprecipitation
Col0	Columbia 0

COX2	Cytochrome c oxidase subunit 2
CSD	copper/zinc superoxide dismutases
CSY	citrate synthase
CTP	cytidine triphosphate
CTS	COMATOSE
DAG	diacylglycerol
DAGLs	DAG lipases
2D IEF/SDS-PAGE	two-dimensional iso-electric focusing/sodium dodecyl sulfate polyacrylamide gel electrophoresis
2,4-DB	2,4-dichlorophenoxybutyric acid
DCl	4-dienoyl-CoA isomerase
DGAT	diacylglycerol acyltransferase
DGD	DGDG synthase
DGDG	digalactosyldiacylglycerol
DPG	diphosphatidylglycerol
ECH	2-trans enoyl-CoA hydratase
ECH2	enoyl-CoA hydratase 2
EK	Etn kinase
EM	electron microscopy
EPR	electron paramagnetic resonance
ER	endoplasmic reticulum
ESCRT	endosomal sorting complex required for transport
Etn	ethanolamine
FAD	fatty acid desaturase
FAMEs	fatty acid methyl esters
FAs	fatty acids
FAS	fatty-acid synthase
FATA	FatA acyl-ACP thioesterase
FAX1	fatty acid export 1
FFAs	free FAs
FFE	free-flow electrophoresis
FM	fluorescence microscopy
FRET	fluorescence resonance energy transfer
G3P	glycerol-3-phosphate
GGGT	galactolipid galactosyltransferase
GlcADG	glucuronosyldiacylglycerol
GO	glycolate oxidase
GPAT	acyl-CoA:*sn*-glycerol-3-phosphate acyltransferase
GPD	glycerophosphodiester
GPDEs	glycerophosphodiesterases
H_2O_2	hydrogen peroxide
$H_2PO_4^-$	dihydrogen phosphate ion
HACD	l-3-hydroxyacyl-CoA dehydrogenase
HAPs	histidine acid phosphatases

HII	hexagonal II
HM	homozygous
13-HOD	(9Z,11E,13S)-13-hydroxy octadeca-9,11-dienoic acid
HPO_4^{2-}	hydrogen phosphate
13-HPOD	(9Z,11E,13S)-13-hydroperoxy octadeca-9,11-dienoic acid
HPR	hydroxypyruvate reductase
HZ	heterozygous
IAA	indole-3-acetic acid
IBA	indole-3-butyric acid
ICL	isocitrate lyase
IM	inner membrane
IMS	intermembrane space
JA	jasmonate
KAS	3-ketoacyl-ACP synthase
KAT	3-ketoacyl-CoA thiolase
KO	knockout
LACS	long-chain acyl-CoA synthetase
LAH	lipid acyl hydrolase
LB	left T-DNA border primer
LD	lipid droplets
Ler	Landsberg erecta
LIDL	LD-associated lipase
LOX	lipoxygenase
LP	left genomic primer
LPA	lyso-phosphatidic acid
LPAAT	acyl-CoA lysophosphatidic acid acyltransferase
LPC	lyso-phosphatidylcholine
LPE	lyso-phosphatidylethanolamine
LRs	lipid rafts
LTPs	lipid transfer proteins
MAG	monoacylglycerol
MAGLs	MAG lipases
MCMT	malonyl-CoA:ACP malonyltransferase
MCSs	membrane contact sites
MDAR	monodehydroascorbate reductase
MDH	malate dehydrogenase
MFP	multifunctional protein
MGD	MGDG synthase
MGDG	monogalactosyldiacylglycerol
MICOS complex	mitochondrial contact site cristae organizing system complex
MIEL1	MYB30-interacting E3 ligase 1
MLS	malate synthase
MOPs	mitochondrial outer membrane protrusions
MS	mass spectrometry
MTL complex	mitochondrial transmembrane lipoprotein complex

MUFA	monounsaturated fatty acid
MYA2	myosin XI
N	nitrogen
NBDs	nucleotide binding domains
NDPK3	nucleoside diphosphate kinase 3
NO	nitrite oxide
NPC	non-specific PLC
OB	oil body
OBL1	oil body lipase 1
OEP21	outer envelope protein 21
OLE	oleosin
OM	outer membrane
OPC:8	3-oxo-2-(2'-pentenyl)-cyclopentane-1-octanoic acid
OPDA	(9S,13S)-12-oxo-phytodienoic acid
OPR	12-oxo-phytodienoate reductase
P	phosphorus
PA	phosphatidic acid
PAH	phosphatidate phosphohydrolase
PAP	PA-phosphatase
PAPs	purple acid phosphatases
PC	phosphatidylcholine
P-Cho	phospho-choline
PDAT	phospholipid:diacylglycerol acyltransferase
PDHC	pyruvate dehydrogenase complex
PE	phosphatidylethanolamine
PED3	Peroxisome deficient 3
pER	pre-peroxisomal ER
P-Etn	phospho-ethanolamine
PEX11e	Peroxin 11e
PEX14	Peroxin 14
PG	phosphatidylglycerol
6PGL	6-phosphogluconolactonase
PGP	phosphatidylglycerolphosphate
PGPP	PGP phosphatase
PGPS	PGP synthase
PHTs	phosphate transporters
PI	phosphatidylinositol
Pi	phosphate
PIPs	protein-protein interactions
PIS	PI synthase
PL	phospholipid
PLA	phospholipase A
PLC	phospholipase C
PLD	phospholipase D
PLMT	phospholipid *N*-methyltransferase

PM	plasma membrane
PMD2	peroxisomal and mitochondrial division factor 2
PMF	peptide mass fingerprinting
PMP70	70-kDa peroxisomal membrane protein
PMP70R/PMP69	PMP70-related protein
PMPs	peroxisomal membrane proteins
POPC	1-palmitoyl-2-oleoyl-sn-glycerol-3-phosphocholine
PPARs	peroxisome proliferator-activated receptors
ppVs	pre-peroxisomes vesicles
PS	phosphatidylserine
PTMs	post-translational modifications
PTSs	peroxisome targeting signals
PUE	phosphorus use efficiency
PUFA	polyunsaturated fatty acid
PUX10	plant ubiquitin regulatory X (UBX) domain-containing protein 10
PXA1	Peroxisomal ABC transporter 1
RDO2	embryo reduced dormancy 2
RISP	reinitiation supporting protein
RNS	reactive nitrogen species
ROS	reactive oxygen species
RP	right genomic primer
SA	salicylic acid
SAD	Δ^9 stearoyl-ACP desaturase
SAR1	Secretion-associated RAS 1
SDC	serine decarboxylase
SDP1	Sucrose dependent 1
SDP1L	SDP1-LIKE
SDR	short-chain dehydrogenase/reductase superfamily
SEs	sterol esters
SFA	saturated fatty acid
SIT	sitosterol
SLS	sulfolipid synthase
SQDG	sulfoquinovosediacylglycerol
SQS	UDP-sulfoquinovose synthase
STI	stigmasterol
TAG	triacylglycerol
TCA cycle	tricarboxylic cycle
TGD	trigalactosyldiacylglycerol
Tgl4	triacylglycerol lipase 4
TGLs	TAG lipases
TIC40	Translocon at the inner envelope membrane of chloroplasts 40
TMDs	transmembrane domains
TOM complex	translocase of the outer membrane complex
UBX	ubiquitin regulatory X

UDP	uridine diphosphate
UDP-Gal	UDP-galactose
UDP-GlcA	UDP-glucuronic acid
UFA	unsaturated fatty acid
UGP3	UDP-Glc pyrophosphorylase
UGPase	UDP-glucose pyrophosphorylase
UTP	uridine triphosphate
VDAC	voltage-dependent anion channels
VPS29	vacuolar protein sorting 29
WT	wild type
Y2H	yeast two-hybrid
YFP	yellow fluorescent protein
α-CTase	α-carboxyltransferase
β-CTase	β-carboxyltransferase

Table of contents

General introduction

1 Overview of plant lipids 3

1.1 Fatty acids (FAs) in plants 3

1.2 Lipid composition in plants 4

2 Glycerolipid metabolism in plants 8

2.1 Fatty acid synthesis 8

2.2 Glycerolipids synthesis 10

2.2.1 Membrane lipid synthesis 10

2.2.2 TAG synthesis 14

2.3 Degradation of glycerolipids 16

2.3.1 Phospholipase-mediated hydrolysis 16

2.3.2 Glycolipase/sulfolipase-mediated hydrolysis 17

2.3.3 Stored TAG breakdown 17

3 Roles of lipids in response to phosphate starvation in plants 29

3.1 Phosphate starvation 29

3.2 Adaptations in phosphate-starved plants 30

3.2.1 PL-to-DGDG exchange 31

3.2.2 LDs accumulation during stress 39

3.3 Phosphate starvation-induced mitochondrial membrane lipid remodeling through MTL complex in *Arabidopsis thaliana* 39

Materials and Methods

1 Plant material and growth conditions 47

1.1 *Arabidopsis thaliana* 47

1.2 *Nicotiana benthamiana* plants 47

1.3 Culture conditions 47

1.3.1 Seed sterilization and stratification 47

1.3.2 Plants grown on soil 47

1.3.3 β-oxidation mutants seeds germination on solid media 47

1.3.4 Calli generation from *Arabidopsis thaliana* seedlings 48

1.3.5 *Arabidopsis thaliana* calli growth in liquid Murashige & Skoog media 48

1.3.6 *Arabidopsis thaliana* seedlings growth in Murashige & Skoog liquid or solid media 49
2 Molecular biology 49
2.1 Molecular cloning 49
2.1.1 Plasmids 49
2.1.2 Polymerase chain reaction (PCR) 52
2.1.3 DNA fragment purification on agarose gel 53
2.1.4 Restriction Enzyme Digestion of plasmid vectors 53
2.1.5 DNA fragment assembly by the Gibson method 54
2.1.6 *Escherichia coli* transformation and selection of transformants 54
2.1.7 PCR screening and Sanger sequencing 54
2.1.8 *Agrobacterium tumefaciens* transformation 55
2.1.9 Cryopreservation of *Escherichia coli* and *Agrobacterium tumefaciens* strains 55
2.2 Transient transgene expression in *Nicotiana benthamiana* by agroinfiltration 55
2.3 *Agrobacterium*-mediated transformation of *Arabidopsis thaliana* by floral dip 56
2.4 β-oxidation mutants genotyping 56
2.4.1 Genotyping of Arabidopsis plant leaves without prior DNA purification 56
2.4.2 Genotyping of Arabidopsis calli 57
3 Protein analysis 57
3.1 Total protein extraction from *Arabidopsis thaliana* leaves or calli 57
3.2 Protein concentration determination 58
3.2.1 Bradford assay 58
3.2.2 Coomassie blue staining 58
3.3 Polyacrylamide gel electrophoresis in denaturing conditions (SDS-PAGE) 58
3.4 Protein immunoblotting (Western Blot) 58
4 Plant phenotype analysis 61
4.1 *Arabidopsis thaliana* calli growth assay 61
4.2 *Arabidopsis thaliana* root growth assay 61
5 Subcellular organelle fractionation 61
5.1 Peroxisome purification by Percoll gradients centrifugation from *Arabidopsis thaliana* calli in the presence or absence of Pi 61
5.2 Proteomic analysis of isolated peroxisomal proteins from *Arabidopsis thaliana* calli in the presence or absence of Pi 63
6 Lipid analysis 63
6.1 Glycerolipid extraction by the Folch method 63
6.2 Methanolysis of total lipid extracts 64

6.3 Fatty acid and lipid quantification 64
6.3.1 Quantification of fatty acid methyl esters (FAMEs) by gas chromatography coupled to ion flame detection 32 (GC-FID) 64
6.3.2 Quantification of glycerolipids by high performance liquid chromatography coupled to triple quadrupole mass spectrometry (HPLC-MS/MS) 65
7 Imaging techniques 65
7.1 Laser scanning confocal microscopy 65

Chapter 1: Optimization of a peroxisome isolation protocol from *Arabidopsis thaliana* calli to study peroxisomal lipidome and proteome in response to Pi starvation

1 Overview of plant peroxisomes 69
2 Studies for the purification of Arabidopsis peroxisomes and proteomic analysis 71
3 Results 75
3.1 Western blot analysis of isolated peroxisome fractions by Percoll gradients centrifugation from *A. thaliana* calli under both +/-Pi conditions 76
3.2 Lipid analysis of isolated peroxisome fractions from *A. thaliana* calli under +/-Pi conditions .. 78
3.3 Proteomic analysis of isolated peroxisome fractions from *A. thaliana* calli under +/-Pi conditions 79
3.2.1 Comparative analysis of Western blot results and proteomic data 81
3.2.2 Proteomic analysis of identified peroxisomal proteins 82
4 Discussion and perspectives 91
4.1 We successfully enriched peroxisomes in the harvested peroxisomal fractions, although the purity was not sufficient to assess the lipidomic and proteomic differences in response to Pi deficiency 92
4.2 Distinguishing differences in lipidome of isolated peroxisome fraction between Pi-enriched and Pi-stressed conditions is challenging 93
4.3 Proteins related to oxidative stress response and nitrogen metabolism exhibited significant differences between normal growth conditions and Pi deficiency 96
4.4 The complexity to define the complete peroxisome proteome 98

Chapter 2: Role of PXA1 and peroxisomal β-oxidation in membrane lipid remodeling in response to Pi starvation

1 Pi-stress response of the core β-oxidation enzymes 101
2 Peroxisomal ABC transporter - PXA1 102

3 Peroxisomal multifunctional protein - MFP2 105
4 Results 107
4.1 Isolation of the homozygous *pxa1* (CS3950) and *mfp2* (SALK_098016) mutants 107
4.2 Phenotypic observations of *pxa1* and *mfp2* mutants under standard and Pi-starved conditions 109
4.2.1 Growth examination of Arabidopsis *pxa1* and *mfp2* calli 109
4.2.2 Seedling establishment examination of *mfp2* mutant 111
4.3 Lipid analysis of the *pxa1* and *mfp2* mutants under standard and Pi-starved conditions 112
4.3.1 Preliminary data of lipid analysis of Col0 and *mfp2* seedling grown under standard and Pi-starved conditions 112
4.3.2 Lipid analysis of Col0, *mfp2* and *pxa1* cell suspension cultures under standard and Pi-starved conditions 113
4.4 Preliminary data of electron microscopy observation of mitochondrial morphology in *mfp2* and *pxa1* mutant grown in cell suspension cultures under standard and Pi-starved condition 117
4.5 Preliminary measurements of β-oxidation activity in *A. thaliana* cell cultures under standard and Pi-starved conditions 120
5 Discussion and perspectives 121
5.1 The unexpected germination defect was found in M_2 *pxa1-1* mutants 121
5.2 Lack of Pi inhibits the growth of Col0 and *mfp2* calli, but likely not affects growth of *pxa1* calli 121
5.3 β-oxidation pathway is not involved in the metabolic processes of lipid remodeling in response to Pi starvation in *A. thaliana* cell cultures 123
5.4 Other aspects of lipid metabolism may play metabolic roles in membrane lipid remodeling in response to Pi deficiency 125
5.5 The abnormal mitochondrial morphology observed in β-oxidation mutants under standard conditions suggests a potential association with ROS accumulation 126

Chapter 3: Identification of interactions between peroxisomal PXA1 protein and mitochondrial TOM complex at peroxisome-mitochondria membrane contact sites

1 Peroxisome-mitochondria membrane contact sites (MCSs) 131
2 Methods for protein-protein interactions at MCSs 132
3 Preliminary BiFC results to confirm PXA1-TOM complex interaction 134
4 Conclusions and perspectives 139
4.1 There exists some methodological issues associated with split fluorescent protein and overexpression systems to confirm specific protein-protein interactions between organelles 139

4.2 BioID strategy is suitable to confirm PXA1-TOM complex interactions and to further identify potential partners in plant cells 139

General conclusion and perspectives 141

Publications 147

References 181

General introduction

1 Overview of plant lipids

First of all, to define lipid, lipids are fatty, waxy, or oily compounds that are soluble in organic solvents and insoluble in polar solvents such as water (Ahmed et al., 2024); chemically lipids are mainly composed of carbon and hydrogen, but also oxygen, nitrogen, phosphorous, and sulfur; biologically lipids consist of repeating units combining saturated and unsaturated fatty acids and perform widespread biological roles in terms of energy storage, cell membranes formation, intracellular signaling or local hormonal regulation etc. (Beenakkers et al., 1981; Dall'Armi et al., 2013; Dowhan & Bogdanov, 2002).

Lipids are fundamental building blocks in all living organisms. Despite their biological and economic importance, we still have a much poor understanding of lipids due to their complexity and diversity. Mammalian cells synthesize thousands of different lipid species through actions of hundreds of proteins that metabolize and transport them (for a review, Muro et al., 2014). The lipid profile of the yeast *Saccharomyces cerevisiae* has been also thoroughly investigated, and the effects of lipids on *S. cerevisiae* cellular functions, especially during wine alcoholic fermentation, has been well documented (Mbuyane et al., 2021). Although other yeast species currently used in various industries are gaining attention in winemaking, however, their lipid metabolism remains less explored (Mbuyane et al., 2021). Plant lipids has been studied for centuries due to their important roles in plant physiology and development, but also their diverse applications in the industries, such as food and biofuel (Li-Beisson & Wada, 2019). In the 1980s, the team of Professor Chris Somerville at Michigan State University pioneered the utilization of *Arabidopsis thaliana* in lipid research (Li-Beisson & Wada, 2019; Singh et al., 2016). Since then, novel discoveries in the area of plant lipids are getting overwhelming and subsequently expanded to multiple crop species, which have indispensable societal and economic values (Li-Beisson & Wada, 2019). Additionally, microalgae began to attract significant attention in lipid research due to their superior ability of substantial lipid productivity, rapid growth rate and environmental benefits, and therefore a great promise as sustainable feedstock for biofuel and bio-products (Li-Beisson & Wada, 2019; Singh et al., 2016).

1.1 Fatty acids (FAs) in plants

Fatty acids (FAs) are building-blocks for the majority of cellular lipids. The categorization of FAs can be determined by the length of their aliphatic chain, including short-chain fatty acids (with aliphatic tails containing up to 5 or 7 carbons), medium-chain fatty acids (ranging from 6–8 up to 12–14 carbons), long-chain fatty acids (spanning 13–18 up to 22 carbons), and very long-chain fatty acids (with aliphatic tails longer than 22 carbons; >C22; Kamp & Hamilton, 2006). Typically, the number of carbon atoms in plant tissues falls within the range of 14 to 24. Furthermore, aliphatic chains can be either saturated (resulting in saturated fatty acids, SFA) or unsaturated (resulting in unsaturated fatty acids, UFA). Unsaturated fatty acids can be further classified into monounsaturated fatty acids (MUFA) and polyunsaturated fatty acids

(PUFA), based on the presence of exactly one or at least two double bonds, respectively (Castro et al., 2016).

Nowadays, a comprehensive understanding of about 400 distinct fatty acids in plant kingdom has been documented (C. Li et al., 2017). Plant FAs not only play diverse roles in plant cells, but also exhibit positive effects on human diet and human health. In plant seeds, FAs can serve as a reservoir for the energy storage, function as lipid-derived signaling molecules and hormones, and constitute vital components of plant structures, such as glycerolipids found in plant membranes. Moreover, plant can synthesize several unique fatty acids, coupled with genetic engineering, holding promising applications in 'green chemistry' (Burgal et al., 2008). Additionally, concerning the benefits of FAs on human health, noteworthy examples included their antibacterial (Cateni et al., 2008) and antiparasitic activities (Mishra et al., 2005), as well as their anti-inflammatory (Cateni et al., 2004) and anticancer potentials (Maeda et al., 2008).

1.2 Lipid composition in plants

The model plant *Arabidopsis thaliana* is more often implemented into the research on lipids (Reszczyńska & Hanaka, 2020). Lipids can establish a hydrophobic barrier, separating cells and organelles from the surrounding environment (Ohlrogge & Browse, 1995). Elucidating the function of lipids, and the mechanisms for the unique lipid composition of each membrane in terms of different head group and acyl composition, is a paramount challenge in life science. To date, many studies on membrane lipid composition of Arabidopsis have been conducted (W. Li et al., 2004; Szymanski et al., 2014; Wolter et al., 1992).

In plant membranes, three main lipid classes were evident: glycerolipids, sphingolipids, and sterols. Glycerolipids, the most abundant lipid class, are further categorized into three groups: phospholipids (PL), glycolipids (including galactolipids, sulpholipids, glucolipids), and neutral lipids (triacylglycerols and diacylglycerol; Reszczyńska & Hanaka, 2020). The quantity of sphingolipids differs significantly across the plant species, tissues, and organelles within cells, but generally constituting up to 10% of total plant lipids (D. V. Lynch & Dunn, 2004). Sterols, the third lipid class, are commonly considered as reinforcers of cell membranes. Two 24-ethyl sterols, stigmasterol (STI) and sitosterol (SIT), are the major constituents of the sterol profiles of plant species and play essential roles in the embryonic plant growth (Dufourc, 2008). In addition, increasing evidences specialize a plant plasma membrane microdomain, known as lipid rafts (LRs; Borner et al., 2005; Mongrand et al., 2010; Simon-Plas et al., 2011; Simons & Ikonen, 1997), which are enriched in sphingolipids and sterols, whereas largely excluding phospholipids (Mongrand et al., 2004; Pike, 2003).

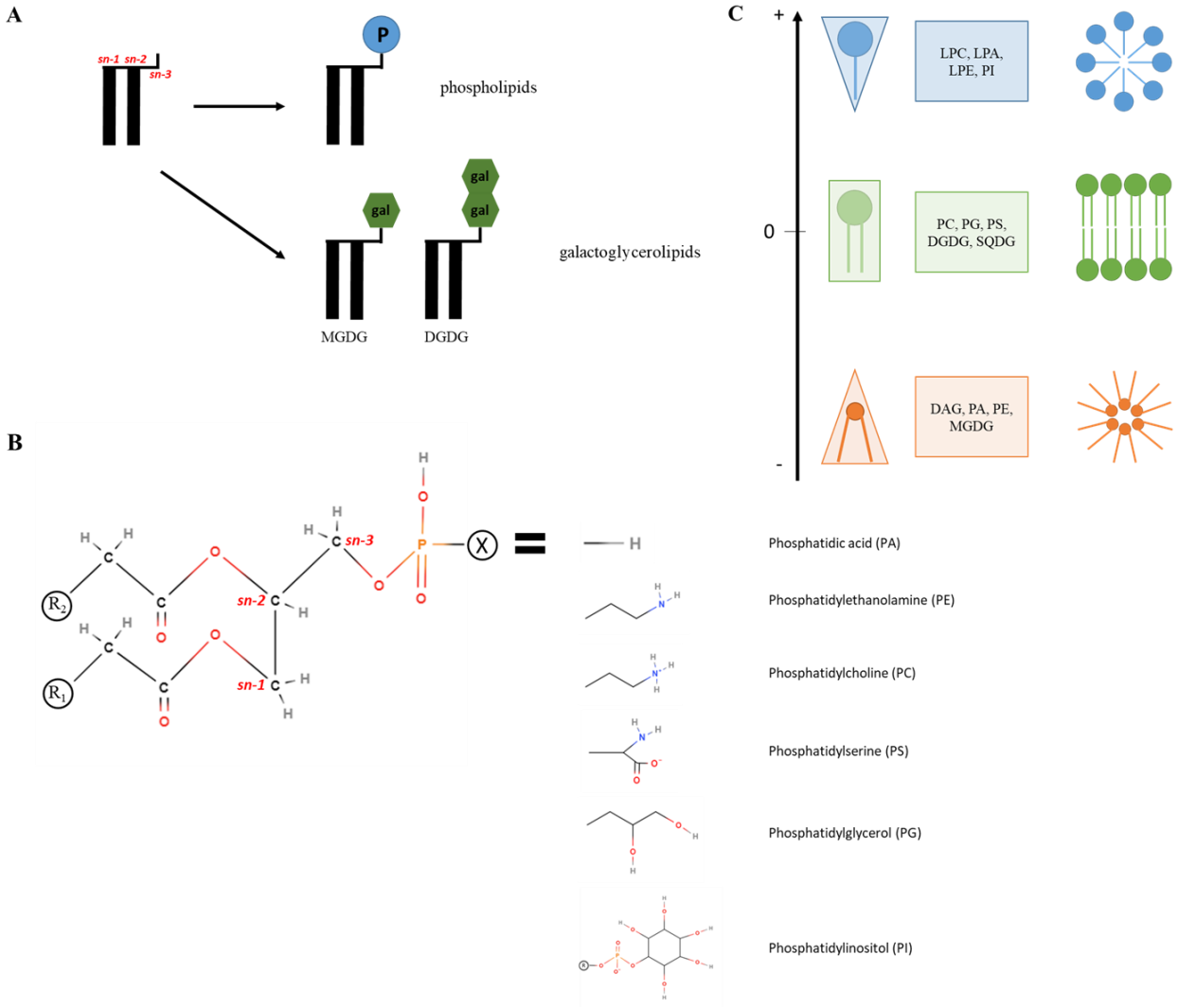


Figure 1. General structure and the physical properties of phospholipids (PLs) and galactoglycerolipids. A. Glycerolipids are composed of a glycerol backbone esterified with two fatty acids (FAs) at the *sn*-1 and *sn*-2 positions. Phospholipids and galactoglycerolipids contain a Pi moiety or galactose residues in their polar head at the *sn*-3 position, respectively. B. The different head groups attached to the Pi moiety at the *sn*-3 position of PLs are indicated here. C. Phase behavior of typical glycerolipids, adapted from *Thiam et al., 2013*. The phase behavior of typical surfactants is determined by the difference between the areas occupied by their hydrophilic head and their lipophilic tail respectively. Positive curvatures indicate the predominant hydrophilic part, such as lyso-phospholipids and PI. Conversely, monolayers, mainly constituted by DAG, PA, PE and MGDG exhibit negative curvature. Lipids, such as PC, PG, PS, DGDG and SQDG, which have similar cross-sectional areas for the polar head and hydrophobic region, look like cylinders. Therefore, they generally assemble into lamellar phases and serve as the primary component of bilayer membranes, with minimal curvature. MGDG, monogalactosyldiacylglycerol; DGDG, digalactosyldiacylglycerol; PA, phosphatidic acid; PE, phosphatidylethanolamine; PC, phosphatidylcholine; PS, phosphatidylserine; PG, phosphatidylglycerol; PI, phosphatidylinositol; LPC, lyso-phosphatidylcholine; LPA, lyso-phosphatidic acid; LPE, lyso-phosphatidylethanolamine; DAG, diacylglycerol; SQDG, sulfoquinovosediacylglycerol.

Glycerolipids are a class of lipids containing a glycerol backbone esterified with two fatty acids at the *sn*-1 and *sn*-2 positions. The different families of glycerolipids are distinguished by the different polar head group attached to the *sn*-3 position (Reszczyńska & Hanaka, 2020). Hereby, we primarily lay emphasis on the phospholipid and galactoglycerolipid families, containing a phosphate (Pi) moiety or galactose residues in their polar head, respectively (**Figure 1A**).

Phospholipids (PLs) are glycerolipids containing a polar head group attached with the phosphate (Pi) group at the *sn*-3 position, and are the major glycerolipid constituents of the cellular membranes, with the exception of chloroplast membranes. Phosphatidic acid (PA), phosphatidylethanolamine (PE), phosphatidylcholine (PC), phosphatidylserine (PS), phosphatidylglycerol (PG) and phosphatidylinositol (PI) represent different lipid classes in which a hydrogen, ethanolamine, choline, serine, glycerol or inositol group have been added on the phosphate group, respectively (**Figure 1B**; Aktas et al., 2014; Korn, 1966; Simon, 1974; van Meer et al., 2008). Additionally, cardiolipin (CL), also known as diphosphatidylglycerol (DPG), is a unique mitochondrial phospholipid, with a dimeric structure containing four acyl groups bound to two glycerol moieties, which are linked via two phosphate groups to a third glycerol (Y. Zhou et al., 2016).

Galactoglycerolipids, the non-phosphorous glycerolipids with galactose residues in their polar heads, are the major components of plastid membranes, and are categorized mainly into two classes, monogalactosyldiacylglycerol (MGDG) and digalactosyldiacylglycerol (DGDG; **Figure 1A**; Ben Hamed et al., 2005). In addition, sulfur-containing sulfolipids, such as sulfoquinovosyldiacylglycerol (SQDG), are also plastidial non-phosphorous lipids with an anionic polar head. Synthesis of these three lipids occurs exclusively in chloroplasts (Awai et al., 2001; Härtel et al., 2000; Kobayashi et al., 2007; Pugh et al., 1995). The high content of MGDG in chloroplasts is responsible for the membrane permeability and thermal stability (Dlouhý et al., 2020), as well as promoting membrane stacking and stabilizing the inner membrane leaflet in grana discs (Seiwert et al., 2018) and aiding in the conservation of photosynthetic energy (Kirchhoff, 2018).

The significant roles of glycerolipids in membrane architecture lie not only in their complex chemical structures, but also in their overall shape and bi-functional properties. These molecules are featuring one or two elongated hydrophobic acyl chain chains at positions *sn*-1 and *sn*-2, and a hydrophilic polar head at position *sn*-3 (Simon, 1974). The difference between the volume/size of hydrophilic polar head and the lipophilic tail results in different phase behavior of membrane lipids (**Figure 1C**; Jouhet, 2013; Thiam et al., 2013). Lipids with positive curvatures indicate the predominant hydrophilic part, forming tubular (hexagonal I phase) structures, such as lyso-phospholipids (LPC, LPA and LPE) and PI (**Figure 1C**). Conversely, monolayers are mainly constituted by diacylglycerol (DAG), PA, PE and MGDG exhibiting

negative curvature (**Figure 1C**), and tending to form hexagonal II (HII) phase or cubic (bicontinuous) phase. Lipids with minimal curvature, such as PC, PG, PS, DGDG and SQDG, have similar cross-sectional areas for the polar head and hydrophobic region, and look like cylinders (**Figure 1C**). Therefore, they generally assemble into lamellar phases and serve as the primary component of bilayer membranes (Jouhet, 2013; Thiam et al., 2013). This partially interprets why most natural bilayer membranes are primarily composed of the couple PC/PE, with lesser amount of lyso-phospholipids (Tauchi-Sato et al., 2002; Thiam et al., 2013). Those highly curved membranes, for instance, tubules of the ER network, the mitochondrial inner membrane, and thylakoid grana margins, are thus believed to be enriched in HII-phase forming lipid (Jouhet, 2013).

The plant lipidome is highly complex, which is evident by the significant variations in FAs composition across different tissues within a single Arabidopsis plant (**Table 1**, adapted from Li-Beisson et al., 2013). Likewise, diverse membrane lipid compositions are observed among different tissue types (**Table 2**, adapted from Li-Beisson et al., 2013).

Tissue type	Predominant Fatty Acids	Proportion (mol%)
Seed	18:2	15.0
	18:3	19.2
	20:1	20.2
Root	16:0	20.7
	18:2	36.5
	18:3	24.6
Leaf	16:0	15.0
	16:3	13.8
	18:2	15.7
	18:3	46.0

Table 1. The predominant fatty acids compositions of different Arabidopsis tissues. Data are presented in mol%.

Tissue type	Major Membrane Lipids	Proportion (mol%)
Seed	PC	48.1
	PE	22.1
	PI + PS	18.9
Root	MGDG	43.2
	DGDG	18.6
	PC	13.8
	PG	13.5
Leaf	PC	45.4
	PE	27.5
	PI + PS	12.9

Table 2. The major membrane lipid compositions of different Arabidopsis tissues. Data are presented in mol%.

In Arabidopsis seeds, the most abundant FAs are 18:2 (~15%), 18:3 (~19%) and 20:1 (~20%), and the major lipids are phospholipids PC (~48%), PE (~22%), PI and PS (~19%; Li-Beisson et al., 2013; Peng et al., 2020). In Arabidopsis roots, the proportion of the main FAs, 16:0, 18:2 and 18:3, is approximately 20%, 36% and 24%, respectively, along with a distinctive lipid composition featuring a high proportion of

galactoglycerolipids (~19% DGDG and ~43% MGDG) and reduced level of PLs (~14% PC, ~7% PE and ~13% PG; Li-Beisson et al., 2013; Shah et al., 1997). Arabidopsis leaves contain around 15% of 16:0, 14% of 16:3, 15% of 18:2 and 46% of 18:3, as the major fatty acids, alongside the similar major lipid compositions as Arabidopsis seeds (~45% PE, ~27% PC, ~13% PI and PS; Li-Beisson et al., 2013; Z. Yang & Ohlrogge, 2009).

In addition, lipid classes are unevenly distributed between different organelle membranes in different cells (Mackender & Leech, 1974; Nakamura, 2017). Moreover, the fatty acid composition of each lipid class, including the length of FAs chains and the ratio of saturated to unsaturated FAs, also significantly varies among different organelle membranes (Reszczyńska & Hanaka, 2020). The most exemplary glycerolipid composition and fatty acid composition of individual glycerolipids from Arabidopsis chloroplasts and mitochondria were well summarized in the review by Li-Beisson et al., 2013 and will be discussed in the first chapter of "Results" in this study (**Table 13**, please refer to **Chapter 1**, section 4.2).

Subsequently, in lipid researches, there exists a general question about how various lipid species are synthesized in cells, encompassing the inquiries into the locations and mechanisms, the regulatory factors, and the processes of lipid trafficking.

2 Glycerolipid metabolism in plants

2.1 Fatty acid synthesis

Plastidial acetyl-CoA, a two-carbon molecule, likely serves as the exclusive precursor for *de novo* fatty acid production (**Figure 2**). In Arabidopsis, the most straightforward pathway to rapidly generate acetyl-CoA and maintain the pool is the oxidative decarboxylation of pyruvate catalyzed by the plastidial pyruvate dehydrogenase complex (PDHC; **Figure 2**; Johnston et al., 1997). In prokaryotes, PDHC is localized in the cytoplasm, whereas in eukaryotes, it resides within the mitochondrial matrix. Plants, however, are unique, in which two distinct complexes exist: one in the plastids, functioning in *de novo* FAs synthesis, and one in the mitochondria, producing acetyl-CoA for carbon entry into the TCA cycle (Johnston et al., 1997; Tovar-Méndez et al., 2003).

Initially, acetyl-CoA is converted to malonyl-CoA by acetyl-CoA carboxylase (ACCase) dependent on light (**Figure 2**; Ohlrogge & Browse, 1995). Two physically distinct ACCases have been identified: the heteromeric and homomeric forms. In contrast to fungi and animals, in most plants (excluding Graminae), the heteromeric ACCase is plastidic, whereas the homomeric ACCase is cytosolic (Choi et al., 1995; Hasslacher et al., 1993; Ke et al., 2000; S. J. Li & Cronan, 1992; López-Casillas et al., 1988). The plastidic heteromeric ACCase is formed by the assembly of three nuclear-coded subunits (biotin carboxy-carrier, BCC; biotin carboxylase, BCase; and α-carboxyltransferase, α-CTase) and one plastid-coded subunit (β-

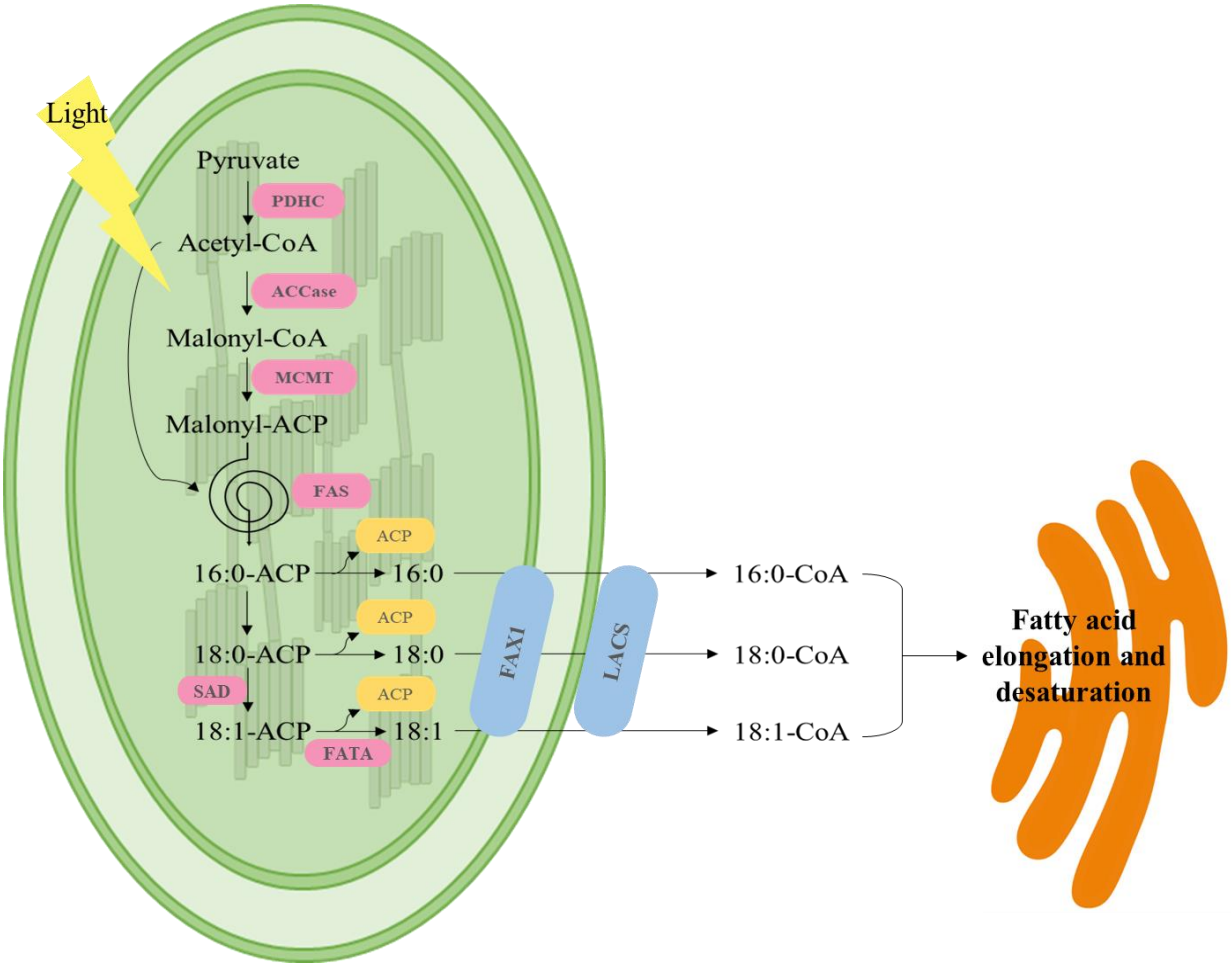


Figure 2. Fatty acids synthesis and export from plastid. The acetyl-coenzyme A generated by plastidial pyruvate dehydrogenase complex was used as a building block for *de novo* fatty acid production, followed by the sequential condensation of two-carbon units by enzymes of the fatty acid synthase complex, ultimately leading to the predominant production of C16 and C18 fatty acids. These resulting fatty acids are then exported to ER for further elongation or/and desaturation. PDHC, pyruvate dehydrogenase complex; ACCase, acetyl-CoA carboxylase; CoA, coenzyme A; ACP, acyl carrier protein; MCMT, malonyl-CoA:acyl carrier protein malonyltransferase; FAS, fatty acid synthase; SAD, Δ^9 stearoyl-ACP desaturase; FATA, FatA acyl-ACP thioesterase; FAX1, fatty acid export 1; LACS, long-chain acyl-CoA synthetase.

carboxyltransferase, β-CTase); therefore, a fully functional ACCase requires the coordination of the expression of both the nuclear and plastidic genes (Ke et al., 2000). In Arabidopsis, four genes for these subunits have been characterized, the *CAC1* gene encodes BCC (Choi et al., 1995), the *CAC2* gene encodes BCase (Bao et al., 1997), the *CAC3* gene encodes for α-CT, and the plastidic *accD* gene encodes for β-CT (Ke et al., 2000). The loss of any of these genes is lethal in Arabidopsis (Baud et al., 2003).

Subsequently, before entering the fatty acid synthesis pathway, the plastidic malonyl-CoA has to be transferred from coenzyme A (CoA) to acyl carrier protein (ACP) through the catalysis of malonyl-CoA:ACP malonyltransferase (MCMT; **Figure 2**). An Arabidopsis At2g30200 gene has been shown to

have sequence similarity to human (*Homo sapiens*) MCAMT, and mutations in the At2g30200 gene results in embryo lethality (Bryant et al., 2011; Jung et al., 2019; L. Zhang et al., 2003).

In the plant cell, 95% of fatty acids are *de novo* produced by the plastidial fatty-acid synthase (FAS) during FA elongation cycle, resulting in the formation of C16 or C18 acyl-ACP (**Figure 2**; Hölzl & Dörmann, 2019). This biosynthetic pathway is not restricted to specific tissues or organs but is present in every cell of the plant (Li-Beisson et al., 2013). FAS is a dissociable multi-subunit homodimer, consisting of monofunctional enzymes, including acyl carrier, acyl transferase, 3-ketoacyl-ACP synthase 1, 2, and 3 (KAS I, II, and III, respectively), β-ketoacyl reductase, β-hydroxylacyl dehydratase, enoyl-ACP reductase, and thioesterase (Brown et al., 2006; Pidkowich et al., 2007). Most of 18:0-ACP are then efficiently desaturated to 18:1-ACP by Δ^9 stearoyl-ACP desaturase (SAD) in the plastid stroma (**Figure 2**; Li-Beisson et al., 2013). These resulting fatty acids are subsequently hydrolyzed by FatA acyl-ACP thioesterase (FATA), exported into the cytosol by fatty acid export 1 (FAX1) and activated by long-chain acyl-CoA synthetase (LACS) to be used in the endoplasmic reticulum (ER) for further elongation or/and desaturation and glycerolipid synthesis (**Figure 2**; Jessen et al., 2015; LaBrant et al., 2018; Mou et al., 2000).

2.2 Glycerolipids synthesis

2.2.1 Membrane lipid synthesis

In Arabidopsis, fatty acids are used for the synthesis of glycerolipids by two different pathways, called the prokaryotic and the eukaryotic pathways, located in the chloroplast and ER, respectively (**Figure 3**; (Buchanan-Wollaston et al., 2005; Li-Beisson et al., 2013; Negi et al., 2018; Ohlrogge & Browse, 1995; Somerville & Browse, 1996).

These two pathways can be easily distinguished by the fatty acid specificity of the *sn*-2 acyltransferases. The ER-localized enzymes exhibit a pronounced specificity for C18 fatty acids, whereas the plastid-localized enzyme prefers C16 fatty acids (Li-Beisson et al., 2013). Thus, PA lipids containing a C16 fatty acid at the *sn*-2 position of glycerol is a distinctive marker for their plastidial origin, which can be either used for the synthesis of PG, or hydrolyzed to form DAG backbones as the precursors for the synthesis of prokaryotic galactolipids and sulfolipids (**Figure 3**; Mongrand et al., 1998). Lipids that contain C18 fatty acids exclusively at the *sn*-2 position and either C18 or C16:0 fatty acids at the *sn*-1 position are originated from the eukaryotic pathway in the ER (Mongrand et al., 1998).

In Arabidopsis, both eukaryotic and prokaryotic pathways contribute equally to the synthesis of chloroplastic galactolipids and sulfolipids (MGDG, DGDG, and SQDG; Fan et al., 2015; Li-Beisson et al., 2013; Nakamura et al., 2009), derived from the conversion of PC backbones synthesized in the ER , or plastidic DAG backbones, respectively. However, along with the evolutionary processes, the prokaryotic

pathway exclusively produce only one lipid, PG, and prokaryotic-synthesized chloroplast lipids were even diminished in many species of higher plants, such as pea (Goss et al., 2000; Negi et al., 2018; Ohlrogge & Browse, 1995). In addition, Negi et al., 2018 illustrated a distinctive contribution of these two pathways in lipid metabolism between Arabidopsis guard cells and mesophyll cells, in which the prokaryotic pathway of guard cells was significantly suppressed. Taken all together, these findings suggest that different plant species or even different tissues from the same plant can exhibit different proportions between prokaryotic and eukaryotic pathways in lipid biosynthesis (Ohlrogge & Browse, 1995).

Membrane lipid biosynthesis generally starts with the formation of phosphatidic acid (**Figure 3**), coming from the acylation of glycerol-3-phosphate (G3P) in positions *sn*-1 and *sn*-2 in plastids or in the ER, and serving as the precursors for the glycerolipids synthesis. Diacylglycerol (DAG), also as the main precursors, can be produced from the dephosphorylated PA (**Figure 3**) by a PA-phosphatase (PAP) in the plastids or *de novo* synthesized in ER (Karki et al., 2019; Ohlrogge & Browse, 1995). Subsequently, PA or/and DAG enter into the biosynthesis of galactolipids, sulfolipids or phospholipids at plastids or/and the ER in plant cells (**Figure 3**).

The galactolipids synthesis from DAG backbones contains two steps catalyzed by two different galactosyltransferases, transferring a galactose moiety from uridine diphosphate (UDP)-galactose (UDP-

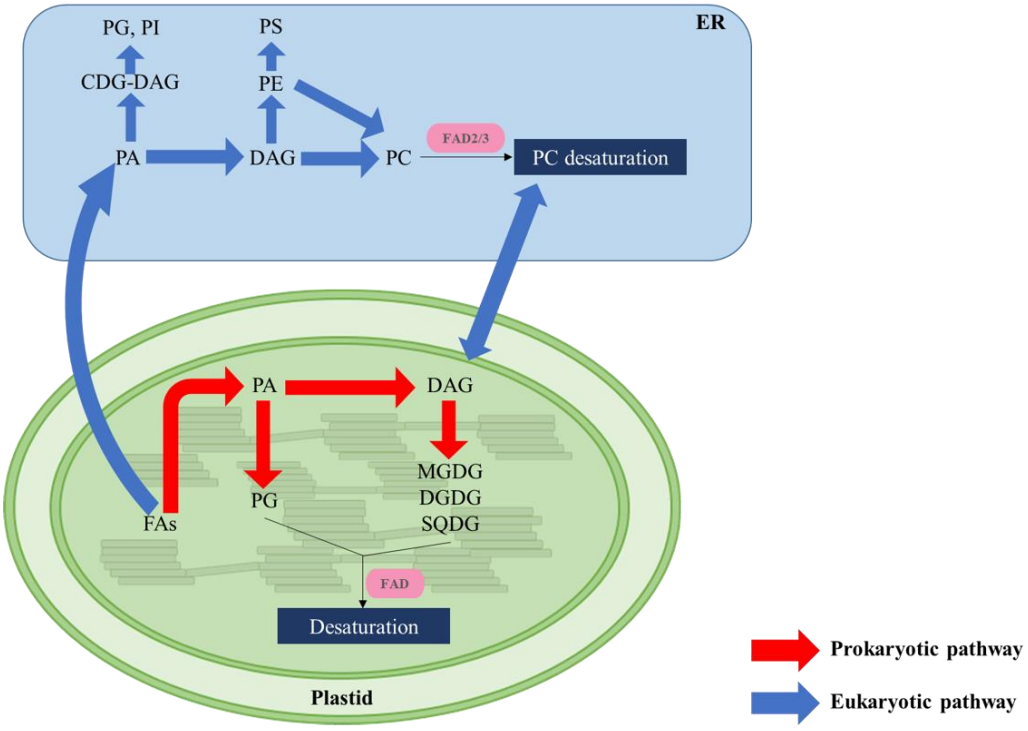


Figure 3. Schematic diagram of membrane lipid synthesis in plants, inspired by *Negi et al., 2018*. Fatty acids (FAs) were employed in membrane lipids synthesis through two distinct pathways, namely the prokaryotic (in red) and eukaryotic (in blue) routes in the plastids and endoplasmic reticulum (ER), respectively.

Gal). The MGDG synthase (MGD) transfers one galactose moiety to DAG to synthesize MGDG, which can be further galactosylated by the DGDG synthase (DGD) to form DGDG. In *A. thaliana*, the main enzymes responsible for MGDG and DGDG synthesis in green tissues are the IE-localized MGD1 and OE-localized DGD1, respectively (Andersson & Dörmann, 2008; Kelly & Dörmann, 2004). In addition, two others MGD synthases, MDG2 and 3, and another DGD synthase, DGD2, exist in *A. thaliana* and are thought to be mainly responsible for galactolipid synthesis in non-photosynthetic tissues or in response to stress, such as phosphate starvation (Awai et al., 2001; Kelly & Dörmann, 2002; Klaus et al., 2002; Kobayashi et al., 2004, 2009).

Biosynthesis of SQDG in the chloroplast envelope comprises three enzymatic steps (Benning, 2008). UDP-glucose is generated from the action of stroma-localized UDP-Glc pyrophosphorylase (UGP3), which utilizes uridine triphosphate (UTP) and glucose-1-phosphate as substrates (Okazaki et al., 2009). UDP 6-sulfoquinovosyl is assembled in the plastid stroma from sulfite and UDP-glucose, facilitated by stroma-localized UDP-sulfoquinovose synthase (SQS; Essigmann et al., 1998). Subsequently, sulfoquinovosyl, serving as the head group of SQDG, is transferred onto DAG, mediated by sulfolipid synthase (SLS) located in the chloroplast membranes (Yu et al., 2002). In Arabidopsis, genes encode the proteins SQD1, and SQD2, have been isolated, which are involved in the biosynthesis of UDP-sulfoquinovose from UDP-glucose, and in the transfer of the sulfoquinovose moiety to DAG, respectively (Essigmann et al., 1998; Yu et al., 2002).

Subsequently, to introduce double bonds in the acyl chains of glycerolipids synthesized in the plastids, various plastidial desaturases are present, identified as fatty acid desaturases (FAD; **Figure 3**; Benning et al., 2006; Hölzl & Dörmann, 2019; Jarvis et al., 2000; Kobayashi et al., 2007). Several *A. thaliana* chloroplast-localized lipid desaturases, FAD5, 6, 7 and 8, and a PG-specific FAD4, have been characterized (Gao et al., 2009).

ER and ER-localized eukaryotic pathway are the major site and process for phospholipid biosynthesis. The eukaryotic pathway contributes to the synthesis of the six phospholipid classes, PA, PC, PE, PG, PI, and PS, as well as synthesis of MGDG, DGDG and SQDG (**Figure 3**; Li-Beisson et al., 2013; Negi et al., 2018).

Cytidine diphosphate diacylglycerol (CDP-DAG), synthesized from PA and cytidine triphosphate (CTP) by CDP-DAG synthase (CDS) at the ER, is a critical intermediate in the metabolism of two phospholipids, PG and PI (**Figure 3**; Jennings & Epand, 2020; Michaud et al., 2017)**.** PG undergoes a two-step synthesis from CDP-DAG, firstly being catalyzed into phosphatidylglycerolphosphate (PGP) by PGP synthase (PGPS), and then dephosphorylated by PGP phosphatase (PGPP). In Arabidopsis, two PGPS enzymes, PGPS1 dual-targeted to mitochondria and chloroplasts and PGPS2 localized only in the ER, and one PGPP enzyme, PGPP1 located at chloroplasts, have been characterized (Lin et al., 2016; Y. Zhou et al., 2017). PI

is synthesized from CDP-DAG by PI synthase (PIS). Two genes encoding PIS enzymes, *AtPIS1* and *AtPIS2*, have been previously reported to be localized in the ER and possibly the Golgi apparatus (Löfke et al., 2008).

Ethanolamine (Etn) is a crucial metabolite for PE and PC synthesis in plants, which can be converted directly or indirectly from serine by serine decarboxylase (SDC). Etn can be also methylated to choline, a precursor for PC synthesis (Kwon et al., 2012). The PE or PC biosynthesis begins with the phosphorylation of Etn or choline by Etn kinase (EK) or Cho kinase (CK) to form phospho-ethanolamine (P-Etn) or phospho-choline (P-Cho), respectively (Michaud et al., 2017). P-Etn or P-Cho is subsequently attached to the DAG backbone (**Figure 3**), catalyzed by aminoalcohol aminophosphotransferase (AAPT) to form PE or PC, respectively (Michaud et al., 2017; Nakamura, 2017; Reszczyńska & Hanaka, 2020). Two AAPT genes, *AtAAPT1* and *AtAAPT2*, isolated from an *Arabidopsis thaliana* cDNA library, have been characterized (Goode & Dewey, 1999). The double knockout (KO) mutant *aapt1aapt2* is embryo-lethal, whereas single KO plants *aapt1* or *aapt2* exhibits no significant phenotypic changes, suggesting that AAPTs are essential for plant growth and reproduction, and that AAPT1 and AAPT2 have overlapping functions (Liu et al., 2015). Additionally, phospholipid *N*-methyltransferase (PLMT) may play a bypass role in the PE methylation to PC biosynthesis (**Figure 3**; Michaud et al., 2017). An *AtPLMT* gene has been identified and functionally studied; however, defects in *AtPLMT* does not appear to cause any significant perturbations in PC synthesis, or affect the plant growth and development (Keogh et al., 2009). Moreover, PE may also serve as a substrate for PS biosynthesis in Arabidopsis (**Figure 3**; Yamaoka et al., 2011).

Subsequently, extraplastidic fatty acids on phospholipid molecules, principally PC, can be desaturated directly by desaturases located in the ER (**Figure 3**; Speerling & Heinz, 1993). Two enzymes, FAD2 (Okuley et al., 1994) and FAD3 (Browse et al., 1993), are shown to be responsible for the conversion of PC-bound oleate to linoleate and then to linolenate, respectively (**Figure 3**).

In addition, as mentioned before, PC could be a substrate for MGDG and DGDG synthesis through the eukaryotic pathway (**Figure 3**). Throughout the plant life cycle, there is a dynamic transport of PC backbones between the chloroplast and ER. The exact nature of the transported molecule is still a matter of debate. This exchange may involve the transport of PC, or the DAG moiety of PC, or lyso-PC, or PA, or a combination of all these molecules, from ER to the chloroplast envelope, which eventually enriches the chloroplast DAG reservoir utilized in plastidic glycolipid synthesis (Kunst et al., 1989; Miquel & Browse, 1992; Mongrand et al., 2000; Mueller-Schuessele et al., 2024; Negi et al., 2018; L. Wang et al., 2014). A trigalactosyldiacylglycerol (TGD) protein complex, consisting of TGD1, 2, 3, 4 and 5 subunits, has been suggested to play a role in the lipid transfer of PA from the ER to chloroplasts (Fan et al., 2015; Roston et al., 2012; Z. Wang et al., 2012). TDG1, 2, and 3 form an ABC transport in the IE of chloroplasts, TGD4 is

in outer envelope membrane and could play a tethering role between the ER and chloroplast, while TGD5, physically interacts with all of the other four TGD proteins and is hypothesized to serve as a bridge between the OE and the IE and to play a regulatory role in the lipid transfer from ER to the chloroplast envelopes by a still unknown mechanism (Andersson & Dörmann, n.d.; LaBrant et al., 2018; Moreau et al., 1998; Mueller-Schuessele et al., 2024).

2.2.2 TAG synthesis

In Arabidopsis, triacylglycerols (TAG), serving as the primary storage form for energy and carbon, accumulate in various tissues such as senescing leaves, floret tapetosomes, pollen grains and seeds (Kaup et al., 2002, p. 2002; Kim et al., 2002). Synthesis of TAG mainly occurs at the ER and subsequently forms lipid droplets (LDs) in the cytosol (**Figure 4**; Chapman & Ohlrogge, 2012; Troncoso-Ponce et al., 2013). TAG biosynthesis can be driven by different pathways. The most straightforward process seems to be the pathway involving the sequential acylation followed by the subsequent dephosphorylation of glycerol-3-phosphate (**Figure 4**), which is originated from the reduction of dihydroxyacetonephosphate.

Utilizing acyl-CoA pool from plastids and G3P as primary substrates, the stepwise acylation is facilitated by two fatty acyltransferases, namely acyl-CoA:*sn*-glycerol-3-phosphate acyltransferase (GPAT) and acyl-CoA lysophosphatidic acid acyltransferase (LPAAT), leading to the formation of PA (**Figure 4**; Chapman & Ohlrogge, 2012).

Gidda et al., 2009, Kang et al., 2020, and Zheng et al., 2003 have reported an Arabidopsis GPAT gene family, consisting of ten members (*GPAT1–9*, and one soluble *ATS1*). AtGPAT1/2/3 are found in the mitochondria, AtGPAT4-9 are ER membrane-bound and ATS1 is specifically located in the plastid (Y. Cheng et al., 2011; Gidda et al., 2009; Jayawardhane et al., 2018; Liu et al., 2023). Among all, AtGPAT9 is suggested to be the ER-localized GPAT enzyme responsible for TAG biosynthesis in plant, and is found to interact with other enzymes involved in TAG synthesis, such as AtLPAAT2 (J. Shockey et al., 2016; S. U. Yang et al., 2019). GPAT9 is highly conserved throughout evolution, due to its indispensable roles in the synthesis of storage and membrane lipids required for life (J. Shockey et al., 2016). Furthermore, a loss-of-function mutant of mitochondrial *GPAT1* leads to a significant reduction of TAG content in flower buds and seeds, suggesting that GPAT1 may also participate in TAG biosynthesis in different plant tissues (Bai et al., 2021; Zheng et al., 2003).

Five Arabidopsis genes, encoding one plastidic and four cytoplasmic LPAAT proteins (LPAAT1-5), have been characterized based on sequence similarity to those of other species (Kim & Huang, 2004). LPAAT1 and LPAAT2 have been shown to play essential roles in plastid- and ER-localized *de novo* glycerolipid biosynthesis pathways, respectively, while LPAAT4 and LPAAT5 are N-starvation-inducible in the ER-

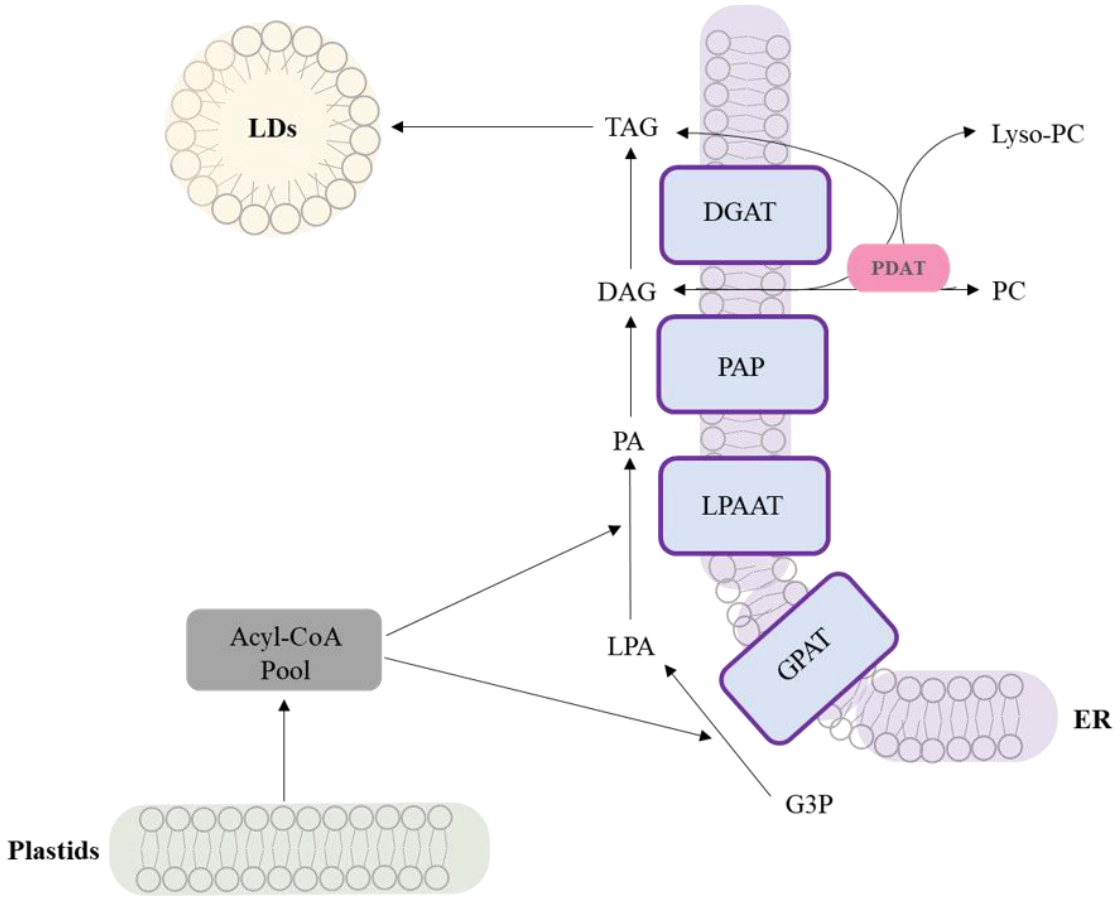


Figure 4. Simplified model of TAG synthesis in plants. TAG synthesis is mediated by GPAT, LPAAT, PAP, and DGAT, as well as the reaction steps of PC-derived DAGs via PDAT in the ER network. G3P, (*sn*)-glycerol-3-phosphate; GPAT, acyl-CoA:*sn*-glycerol-3-phosphate acyltransferase; LPAAT, acyl-CoA lysophosphatidic acid acyltransferase; PAP, phosphatidic acid phosphatase; DGAT, diacylglycerol acyltransferase; PDAT, phospholipid:diacylglycerol acyltransferase.

localized *de novo* phospholipids and TAG biosynthesis in seedling growth, however, the role of LPAAT3 remains unclear (Angkawijaya et al., 2019; Kim et al., 2005).

Subsequently, PAP performs the dephosphorylation of PA, resulting in the production of DAG, which can be then acylated at the *sn*-3 position using a fatty acyl-CoA molecule by diacylglycerol acyltransferase (DGAT) to generate TAG (**Figure 4**). This PA dephosphorylation appears to be the major source of DAG, as the immediate precursor for TAG synthesis in plant leaves (Li-Beisson et al., 2013). A yeast *PAH1* knockout mutant shows an accumulation of PA and decreased levels of DAG and TAG (Han et al., 2006). Eastmond et al., 2010 demonstrated that the Arabidopsis homologs of yeast PAH1 (AtPAH1 and AtPAH2) play regulatory roles in phospholipid synthesis in the ER.

Three Arabidopsis DGAT proteins, DGAT1 and 2 at the ER membrane, and the soluble DGAT3, have been identified (Aymé et al., 2018; Zhou et al., 2013). These proteins lack sequence homology, probably due to the convergent evolution. To date, AtDGAT1 has been shown to play the major role in seed TAG synthesis

(Li-Beisson et al., 2013), while transient expressions of AtDGAT2 and AtDGAT3, respectively, in the *Nicotiana benthamiana* leaves also lead to increased TAG levels, as observed in the parallel expression of AtDGAT1 (Aymé et al., 2018; Zhou et al., 2013), suggesting their potential involvements in TAG biosynthesis. Moreover, Zhou et al., 2013 revealed that AtDGAT2 displayed different acyl-CoA substrate preferences compared to AtDGAT1.

Overall, this entire process is known as the *Kennedy pathway* or the *glycerol phosphate pathway* (**Figure 4**; Kennedy, 1961), and it shares most of the initial steps with the membrane lipids synthesis.

Additionally, in most seeds, TAG can be generated independently of acyl-CoA donors by phospholipid:diacylglycerol acyltransferase (PDAT; **Figure 4**), which transfers an acyl group from the *sn*-2 position of PC to the *sn*-3 position of DAG as the major donor to form TAG and yields lyso-PC that can be then reacylated to form PC (Banaś et al., 2000; Chapman & Ohlrogge, 2012, p. 2012; Dahlqvist et al., 2000; C. Xu & Shanklin, 2016; M. Zhang et al., 2009). PDAT1 and PDAT2, two closest homologs to the yeast *LRO1* gene that encodes the PDAT, have been identified in Arabidopsis (Mhaske et al., 2005; Ståhl et al., 2004; J. Xu et al., 2012). Xu et al., 2012 suggested that PDAT1, rather than PDAT2, played the dominant role in TAG biosynthesis in the developing seeds and pollen. Notably, the interaction and physical association between DGAT1 and PDAT1 have been found in Arabidopsis seeds to enhance the efficiency of TAG production (Lee et al., 2018; Lee & Seo, 2018). The double mutants of *PDAT1* and *DGAT1* are lethal to pollen, and may affect embryo development (M. Zhang et al., 2009).

Furthermore, upon the conditions of lipid overload, excess FAs released from membrane lipids can be biologically converted into inactive neutral lipids in the form of TAG packaged in LDs, thereby effectively sequestering them away from cellular membranes.

2.3 Degradation of glycerolipids

Understanding of lipids metabolism (synthesis and degradation) is essential to study their regulatory role in the growth and development of plants. Glycerolipid degradation in plants involves multiple enzymatic pathways that break down phospholipids, galactolipids, sulfolipids, TAG, and eventually FAs.

2.3.1 Phospholipase-mediated hydrolysis

In Arabidopsis, PLs can be hydrolyzed by phospholipases to generate PA, DAG, bioactive lyso-PLs, free FAs (FFAs) and soluble head groups. The enzymes responsible for the hydrolysis of membrane phospholipids can be categorized into three groups: acyl-hydrolyzing phospholipase A (PLA), head group-hydrolyzing phospholipase C (PLC) and phospholipase D (PLD; Ali et al., 2022; M. Li, Qin, et al., 2006). According to the DNA/protein sequences and conserved domains, these phospholipases can be further divided into different families and subfamilies (Scherer et al., 2010). PLAs can cleave the *sn*-1 and/or *sn*-2

position of PLs to release FFAs and lysolipids. PLCs hydrolyze the phosphodiester bond on the glycerol side, resulting in the formation of DAG and phosphorylated head groups. PLDs hydrolyze the phosphodiester bond at the head group to produce PA and free head groups (Ali et al., 2022). All these phospholipases play crucial roles in signaling pathways during plant growth, development, and responses to stress, particularly during Pi starvation (Ali et al., 2022).

2.3.2 Glycolipase/sulfolipase-mediated hydrolysis

A number of lipase involved in galactolipid and sulfolipid turnover have also been identified in plants (Harwood & Okanenko, 2003; Moellering et al., 2010; Seo et al., 2009). For instance, an Arabidopsis galactolipid galactosyltransferase (GGGT) at the chloroplast outer envelope, encoded by the *SENSITIVE TO FREEZING 2* (*AtSFR2*) gene and highly induced during cold stress, can transfer the galactosyl residues from MGDG to a variety of galactolipid receptors to form oligogalactolipids and DAG (Moellering et al., 2010). Arabidopsis PLA1 was shown to have moderate hydrolase activity towards DGDG (Seo et al., 2009). It is generally believed that SQDG is only initially hydrolyzed by specific acyl hydrolases and glycosidases or glycosyltranferases to produce DAG, but is hardly metabolized by higher plants to release sulfate (Harwood & Okanenko, 2003).

2.3.3 Stored TAG breakdown

In general, a lipid droplet (LD), also known as oil or oil body (OB), is composed of 94-98% (w/w) stored neutral lipids (TAG; and sterol esters, SEs), 0.6-2.0% (w/w) phospholipids (PLs), and 0.6-3.0% (w/w) protein (Tzen et al., 1993). The size of seed LDs typically varies from 0.5 to 2 μm in diameter and can constitute approximately 60% of the volume of a mature embryonic cell (Tzen et al., 1993). Lipid in the chemical form of TAG is a high-energy storage compound present in the seeds of a variety of "oilseed" species, such as sunflower, cucumber or Arabidopsis. The transition from seed to seedling is a crucial stage in the plant life cycle, primarily fueled by the TAG breakdown from the seed LDs (Chapman & Trelease, 1991; Graham, 2008; Y. Hayashi et al., 2001; Kao et al., 2018).

LDs mobilization is progressive, it is required to degrade the surface proteins and phospholipid monolayer of LDs to promote certain lipid-mobilizing enzymes access into the stored TAG (**Figure 5**). Although the rapid disappearance of LD surface proteins (Hsiao & Tzen, 2011; Radetzky & Langheinrich, 1994; Sadeghipour & Bhatla, 2002), and the presence of phospholipase activities (Gupta & Bhatla, 2007), have been noted in the LD fraction of some plant species, such as sunflower, anise and Arabidopsis (Deruyffelaere et al., 2015; Jia & Li, 2018); the mechanisms underlying the breakdown of the phospholipid monolayer and the subsequent metabolic fate of the degradation products remain to be further elucidated.

2.3.3.1 The removal of LD surface proteins

In Arabidopsis seeds, there are at least three classes of functionally characterized surface proteins of LDs: oleosins (OLE), caleosins, and steroleosins (C. Xu & Shanklin, 2016). Oleosins are seed-specific LD proteins that are absent in vegetative tissues, and are the major LD structural proteins served to protect stored TAG from lipolytic enzymes (Beisson et al., 2001; Jacquier et al., 2013; Winichayakul et al., 2013). Caleosins and steroleosins are minor proteins found in seed LDs, and the genes encoding these proteins are primarily expressed in the vegetative tissues, especially in response to stresses (C. Xu & Shanklin, 2016).

It has been revealed by studies in Arabidopsis seeds that oleosins are ubiquitinated at the onset of lipid degradation (Deruyffelaere et al., 2015) and removed from the LD membrane to reach the cytosolic

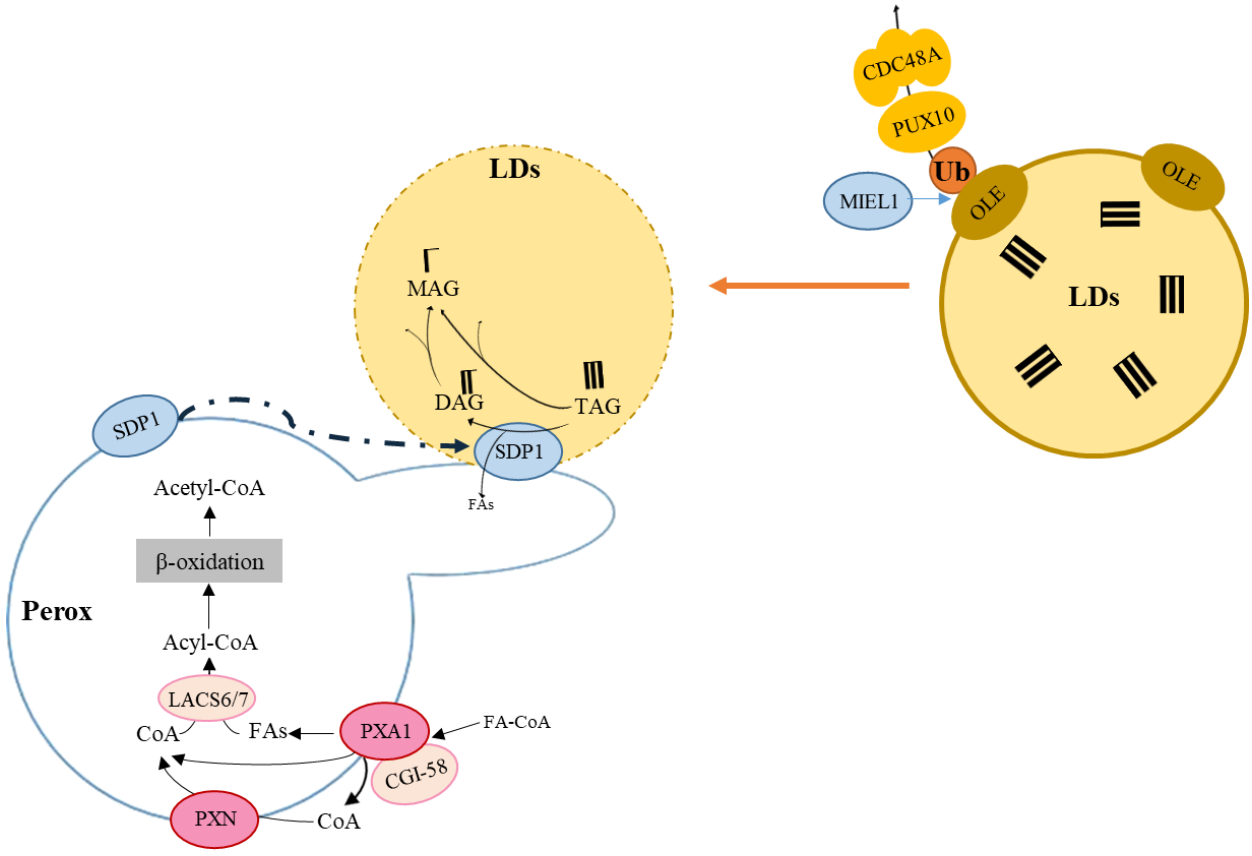


Figure 5. Stored TAGs breakdown in *Arabidopsis thaliana*. LDs mobilization begins with the degradation of the surface proteins and phospholipid monolayer to promote lipid-hydrolyzing enzymes access into the stored TAGs. The TAG lipase, SDP1, is recruited from peroxisomes to the surface of LDs with the assistance of multiple proteins through the peroxisomal tabulation. TAGs are preferentially hydrolyzed into DAG or MAG to release FAs via SDP1/SDP1L. FAs released from TAG hydrolysis are transported into peroxisomes by PXA1. CoA moieties, released by the acyl-CoA thioesterase activity of PXA1, on the cytosolic side are imported via PXN proteins. The imported FAs, along with CoA inside peroxisomes, are then activated by LACS6/7 into acyl-CoA for further β-oxidation to generate C-2 units, acetyl-CoA. CGI-58 interacts with PXA1 and promotes the functions of PXA1, specifically in Arabidopsis leaves. OLE, oleosin; Ub, ubiquitinated surface proteins; PUX10, plant ubiquitin regulatory X (UBX) domain-containing protein10; CDC48A, cell division cycle 48A ATPase; MIEL1, MYB30-interacting E3 ligase 1; LDs, lipid droplets; SDP1, sucrose-dependent lipase 1; SDP1L, SDP1-LIKE; DAG, diacylglycerol; MAG, monoacylglycerol; FAs, fatty acids; LACS6/7, long-chain acyl-CoA synthetases; PXA1, peroxisomal ABC transporter 1; CGI-58, comparative gene identifier 58; perox, peroxisomes.

proteasome, where they are sequentially degraded by proteases (**Figure 5**; Sharma et al., 2016). Five *A. thaliana* oleosin isoforms, OLE1-OLE5, have been reported (Jolivet et al., 2004). The degradation sequence of oleosins begins with the minor OLE5, followed by OLE2 and OLE4; whereas OLE1 and OLE3 are degraded slightly later, occurring concomitantly with the breakdown of stored TAG, indicating that they may have distinct and specific degradation pathways (Deruyffelaere et al., 2015).

For the regulation of the oleosin extraction from the LDs monolayer, three Arabidopsis ubiquitin-mediated enzymes have been characterized: plant ubiquitin regulatory X (UBX) domain-containing protein 10 (PUX10), cell division cycle 48A (CDC48A) ATPase, and MYB30-interacting E3 ligase 1 (MIEL1; **Figure 5**; Deruyffelaere et al., 2018; Kretzschmar et al., 2018; Traver & Bartel, 2023). The recent study of Traver & Bartel, 2023 demonstrated that the peroxisome-localized MIEL1 firstly ubiquitinates OLE1, the main LD surface protein, and then other seed oleosins during germination (**Figure 5**). This oleosin ubiquitination by MIEL1 occurs prior to the actions of LD-associated PUX10 and CDC48A (Traver & Bartel, 2023). Subsequently, PUX10 localizes LDs through its hydrophobic domain, binds to the ubiquitinated oleosins, and recruits CDC48A and interacts with ubiquitin and CDC48A via its UBA and UBX domains, respectively (**Figure 5**; Kretzschmar et al., 2018). Oleosins are then removed from LDs by the segregase activity of CDC48A (Deruyffelaere et al., 2018; Kretzschmar et al., 2018) and proteolytically digested (Deruyffelaere et al., 2018; Vandana & Bhatla, 2006).

2.3.3.2 The degradation of LD phospholipid monolayer

Besides the LDs surface proteins, the degradation of PLs at phospholipid monolayer are necessary to be investigated. PC is the major lipid class constituting the phospholipid monolayer of LDs, with a small amount of PE, PI and PS (Payne et al., 2014). Evidences of LDs phospholipid monolayer degradation by the recruited phospholipases have been revealed in Arabidopsis, cucumber and sunflower (Jia & Li, 2018; Qin et al., 2023). However, the mechanisms of the recruitment, migration and regulation of the specific phospholipase involved in degrading the LDs surface in Arabidopsis remain less known.

In Arabidopsis, 1-butanol, the inhibitor of PLD activity, have been found to exhibit a delayed TAG mobilization and inhibited Arabidopsis seed germination, and it potentially disrupts the expression of genes necessary for LD mobilization, suggesting a possible involvement of PLD in LDs membrane degradation (Jia & Li, 2018).

During seed germination of cucumber, PLA2 was accumulated and localized to LDs, and a simultaneous enhancement of *in vivo* PLA2 activity was observed, proposing an involvement of this enzyme in the partial degradation of the LDs membrane (C. May et al., 1998; Rudolph et al., 2011). Moreover, at the stage of maximal PLA2 expression during germination, holes of approximately 80 nm in width and 2.45 +/- 0.46

nm in depth were found, which are sufficiently large to provide access for 100 kDa enzymes, such as lipoxygenase (LOX) and lipases, to reach the TAG (Noll et al., 2000). The preferential PLA2 activity on LDs membrane in sunflower cotyledons during seed germination has also been reported (Mansfeld et al., 2014). Furthermore, the degradation of PC, concomitant with the accumulation of lyso-PC, was observed during the germination of dark-grown sunflower seedlings (Gupta & Bhatla, 2007). Although four secretory low-molecular-weight PLA2s (sPLA2) (AtPLA2α-δ) have been identified in Arabidopsis, their impacts on LDs membrane phospholipid hydrolysis are currently unclear (Mansfeld et al., 2014).

2.3.3.3 The classical pathway of storage TAG hydrolysis by lipases

The classical pathway to mobilize stored TAG of LDs, known as lipolysis, is induced by endogenous, seedling-specific TAG lipases (TGLs), such as the patatin-like lipase SUCROSE DEPENDENT1 (SDP1) in Arabidopsis, which can hydrolyze TAG into energy-rich FFAs and glycerol. SDP1 is the first identified and the major lipase involved in TAG mobilization during seedling germination in Arabidopsis (Eastmond, 2006). The *sdp1* mutant exhibited a dramatic TAG accumulation (Kelly et al., 2013) and a growth arrest phenotype after germination, which can be rescued by external sugar supply (Eastmond, 2006).

SDP1 is initially localized on peroxisomes and then delivered to lipid droplets with the assistance of the Golgi retromer complex through the peroxisomal tubulation (**Figure 5**; Eastmond, 2006; Thazar-Poulot et al., 2015; Cui et al., 2016). The core retromer vacuolar protein sorting 29 (VPS29) complex interacts with SDP1 at the peroxisomal membrane surface and regulates the translocation of SDP1 from peroxisomes to LDs through the peroxisomal tubular extensions (Kelly et al., 2013; Thazar-Poulot et al., 2015), although the precise mechanistic details are elusive. This migration process of SDP1 also involves the participation of the endosomal sorting complex required for transport (ESCRT) machinery and PEROXIN 11e (PEX11e) (Huang et al., 2022). FYVE DOMAIN PROTEIN REQUIRED FOR ENDOSOMAL SORTING 1 (FREE1/FYVE1), a plant-unique ESCRT component identified in Arabidopsis, was shown to interact with the amphipathic helix (AH) motif of PEX11e that has membrane remodeling capacity, resulting in the peroxisomal tubulation and the trafficking of SDP1 to the LD surface for TAG mobilization (Gao et al., 2014; Yoshida et al., 2015; Huang et al., 2022). Arabidopsis PEX11 proteins were demonstrated to be essential for stimulating peroxisomal proliferation and tubule formation (Orth et al., 2007). The interaction between PEX11e and SDP1 relies on the presence of FREE1, suggesting that FREE1 might act as a scaffold to link PEX11e and SDP1 (Huang et al., 2022).

In Arabidopsis, the small GTPase RABC2a localized on the surface of LDs and RABE1d localized to the Golgi complex and cytosol are also associated with peroxisomes (Hashimoto et al., 2008; Cui et al., 2013). RabC2a can interact with myosin XI (MYA2) to rapidly migrate peroxisomes to LDs (Hashimoto et al., 2008). AtRABC2a and AtRABE1d were hypothesized to collaborate to promote the contact between LDs

and peroxisomes and the delivery of lipases from peroxisomal extensions to LDs in Arabidopsis (Huang et al., 2019).

SDP1-LIKE (SDP1L), an Arabidopsis homolog of SDP1, sharing 74% similarity of the predicted patatin-like domain as SDP1, was also shown to be responsible for TAG hydrolysis in LDs (Scherer et al., 2010). The two Arabidopsis lipases SDP1 and SDP1L, homologous to triacylglycerol lipase 4 (Tgl4) in *Saccharomyces cerevisiae*, are mainly expressed in seeds and can contribute to over 95% of TAG hydrolysis during seed germination (Eastmond, 2006; Kelly et al., 2011; Kelly et al., 2013). It has been demonstrated that SDP1L exhibits an overlapping function with SDP1 in TAG breakdown during seed germination (Kelly et al., 2011), but not plays a substantial role in TAG hydrolysis within the roots and leaves of mature plants (Fan et al., 2014; Kelly et al., 2013). The Arabidopsis double knockout mutant of *sdp1sdp1L* displayed phenotypes of delayed germination and significantly reduced post-germinative seedling growth (Kelly et al., 2011), as well as TAG accumulation in oilseeds (Kelly et al., 2013). In addition, *in vitro* assays suggested that both SDP1 and SDP1L hydrolyze TAG in preference to diacylglycerol (DAG) or monoacylglycerol (MAG) (Eastmond, 2006; Kelly et al., 2011), suggesting that patatin domain TAG lipases need to collaborate with other lipases to effectively hydrolyze TAG into FFAs and glycerol.

Diacylglycerol lipases (DAGLs) are widely present in bacteria, fungi, plants, and animals, with different substrate preferences. Microbial DAGLs can catalyze DAG and MAG into FFAs, MAG, or glycerol. Animal DAGLs mainly hydrolyze DAG and exhibit minimal activity of monoacylglycerol lipase (MAGL) (reviewed in Qin et al., 2023). In plants, only several putative DAGLs and MAGLs have been characterized, but their exact roles in DAG and MAG mobilization are less known (Yuan et al., 2016). A chloroplast non-regioselective lipase, ADIPOSE TRIGLYCERIDE LIPASE-LIKE (ATGLL), has been identified in *Arabidopsis thaliana* (Yu et al., 2023). ATGLL displays a preference to remove 16:0 from unsaturated DAGs. However, analysis of *atgll* mutant indicated that ATGLLs might not contribute significantly to TAG hydrolysis in Arabidopsis seeds (James et al., 2010). Moreover, Kim et al., 2016 has revealed that AtMAGL8 exhibits a notable substrate preference for MAG containing C20:1 fatty acids and is associated with the surface of LDs in germinating seeds and leaves, suggesting its potential involvement in LDs lipolysis. In addition, a cytosolic member of the DAD1-like acyl-hydrolase family encoded by At4g18550 demonstrates a specific ability to hydrolyze DAG and MAG at the *sn*-1 position, and this protein is involved in the regulation of storage oil mobilization and the establishment of early seedlings in Arabidopsis (Kim et al., 2011). Nevertheless, none of them has been proved to coordinate with SDP1 or SDP1L in LDs degradation.

In mammals, the TAG lipase candidate, ATGLL, is regulated by a coactivator protein named comparative gene identifier 58 (CGI-58) localized on LDs (Eastmond, 2006; Lass et al., 2006). CGI-58 may help ATGLL to access its substrate for TAG hydrolysis (Lass et al., 2006). ADP-RIBOSYLATION FACTOR1 (ARF1) and SECRETION-ASSOCIATED RAS1 (SAR1) were reported to mediate the delivery of ATGLL to LD surfaces in mammal cells, suggesting their potential roles in LDs degradation (Soni et al., 2009). However, these possible impacts on LDs degradation in plants require further investigations.

In humans, mutation in *CGI-58* leads to Chanarin-Dorfman syndrome, an uncommon disorder of abnormal neutral lipids storage, which can be characterized by an increase of LDs in cell types that typically do not store lipids, including skin, skeletal muscle, liver and blood cells (Lefèvre et al., 2001). Loss of CGI-58 activity not only results in an accumulation in TAG, but also in diacylglycerol, ceramides and PG, as well as changes in the composition of the phospholipid pool (Igal & Coleman, 1996; James et al., 2010; Brown et al., 2010; Park et al., 2013). Additionally, mammalian CGI-58 also has been demonstrated to have LPAAT activity for the production of PA (**Figure 4)** *in vitro* (Ghosh et al., 2008; Montero-Moran et al., 2010; Park et al., 2013). In mice, disruption of CGI-58 appeared to have reduced PA level during tumor necrosis factor signaling (Lord et al., 2012). However, conflicts existed, as *Radner et al., 2010* indicated that total LPAAT activity remained unaffected in the skin tissues of CGI-58 disrupted mice. Furthermore, since TAG are increased rather than decreased in *CGI-58* disrupted plants or animals, CGI-58 is more likely to contribute to TAG breakdown, rather than to the LPAAT activity in TAG synthesis.

The homologous protein of CGI-58 in Arabidopsis has been shown to be present at peroxisomes (**Figure 5**) and exhibits TAG lipase and phospholipase activity, as well as influences TAG content in vegetative tissues (Ghosh et al., 2009; James et al., 2010; Radner et al., 2011). However, lipid levels in the seeds of loss-of-function *CGI-58* plants appeared not to affect significantly, neither the rate of TAG mobilization nor the total lipid amount (James et al., 2010; Kelly, et al., 2011; Fan et al., 2014), and the *cgi-58* mutant seeds germinated well and grew normally; whereas disruption of *CGI-58* in Arabidopsis mature leaves led to the TAG accumulation and a Chanarin–Dorfman syndrome-like phenotype (James et al., 2010; Yamaguchi and Osumi, 2009), indicating that the impacts of CGI-58 may vary between different plant cell types. Additionally, all these observations in both plant and mammals implied that certain aspects of CGI-58 function are evolutionarily conserved (Chapman et al., 2012).

Furthermore, the oil body lipase 1 (AtOBL1), a homolog of *Ricinus communis* acid lipase RcOBL1, was found to localize to LDs and be able to hydrolyze TAG in Arabidopsis (Eastmond, 2004; Müller and Ischebeck, 2018). The *Atobl1* mutant shows similar germination rate and TAG breakdown as the wild-type plants, but impaired pollen tube growth (Müller and Ischebeck, 2018). Additionally, a LD-ASSOCIATED LIPASE (LIDL) was identified by quantitative proteomic analysis of LD-enriched fractions derived from

Arabidopsis seedlings (Kretzschmar et al., 2020). The *Saccharomyces cerevisiae* homolog of Arabidopsis LIDL1 and LIDL2, Tgl1p, is a putative lipase with sterol esterase activity, and the *tgl1p* mutant exhibits the accumulation of sterol esters (Jandrositz et al., 2005). This suggested that LIDL1 and LIDL2 might function as sterol esterases specific to LDs. However, the question of whether LIDL1 and LIDL2 are involved in the LDs mobilization in Arabidopsis remained to be further elucidated (Kretzschmar et al., 2020). In addition, three other enzymes derived from Arabidopsis, a leaf senescence-associated protein SAG101 (At5g14930; He & Gan, 2002), a TAG hydrolase homologous to mammalian lysosomal acid lipase (At2g15230; El-Kouhen et al., 2005), and a plastid TAG lipase (At2g31690; Padham et al., 2007), also exhibit TAG hydrolytic activities in *in vitro* assays using recombinant proteins. However, further investigations into their involvements in *in vivo* TAG hydrolysis are pending.

2.3.3.4 LOX-dependent pathway

In addition to the classical storage TAG degradation pathway via SDP1/SDP1L, a novel LD-specific lipoxygenase (LOX)-dependent pathway for lipid mobilization during seed germination has been proposed in various plant species, such as Arabidopsis, cucumber, barley, potato, tomato, sunflower and tobacco (Feussner et al., 2001; Viswanath et al., 2020; Singh et al., 2022). Both pathways may occur in parallel in 'oilseeds' species, as reported in cucumber, sunflower, and linseed (Liavonchanka and Feussner, 2006).

LOX is an oxidoreductase enzyme widely distributed in both plants and animals, and contribute to degrading the stored LDs in plant seeds. It was reported that the expression of 13-LOX was muted in dormant seeds but strongly induced at the early stage of germination (Höhne et al., 1996). In addition, the LOX-dependent fatty acid peroxide pathway is also the first step in the biosynthesis of biologically active fatty acid metabolites, collectively referred as oxylipins, which are known to function as signaling molecules or phytoalexins (Singh et al., 2022).

Based on their specific positions in linoleic acid oxygenation, plant LOXs can be categorized into two groups: 9-LOXs and 13-LOXs (Brash, 1999; Viswanath et al., 2020). In the LOX-mediated pathway, after the rupture of the LDs membrane, stored TAG are accessible to the LOX enzymes and the breakdown commences with the hydroperoxidation of polyunsaturated fatty acids (PUFAs), such as linoleic or linolenic acid residues within TAG, by LOX enzymes, to produce the corresponding hydroperoxyl derivatives (Feussner et al., 2001). The generated hydroperoxy fatty acids can be preferentially liberated by a LD lipase activity and subsequently metabolized via several secondary pathways to produce bioactive compounds, such as jasmonate (JA) or lipid mediators (Mashima & Okuyama, 2015). The free hydroperoxy fatty acids can be reduced into hydroxy derivatives, which might in turn undergo β-oxidation (Feussner et al., 2001).

For instance, 13-LOX, synthesized at free ribosomes and originally appeared in the cytosol but then mainly localized at LDs membranes (Hause, et al. 2000), can access to the released TAG after the degradation of the surface proteins and phospholipids monolayer of LDs. 13-LOX can catalyze the hydroperoxidation of linoleic or linolenic acid residues to generate (9Z,11E,13S)-13-hydroperoxy octadeca-9,11-dienoic acid (13-HPOD). Subsequently, 13-HPOD is released from LDs lipase and converted to (9Z,11E,13S)-13-hydroxy octadeca-9,11-dienoic acid (13-HOD), likely through the peroxygenase activity of caleosin. The hydroperoxyl fatty acids, 13-HOD, are then preferentially cleaved by a TGL and metabolized via peroxisomal β-oxidation to provide reducing equivalents and acetyl-CoA for synthetic processes in seedling growth (Feussner et al., 1995; Feussner et al., 2001; Gerhardt et al., 2005). However, the reducing enzymes responsible for the reduction from free hydroperoxy polyenoic fatty acids to the hydroxy compounds have not yet been elucidated.

For the mobilization of storage lipids, the classical peroxisomal-associated lipase degradation or the LOX-dependent pathway, or a hypothetical fatty acid CoA-synthetase-independent pathway (Zou et al., 1999) may exist in parallel in plants (Feussner et al., 2001). Moreover, this also questioned interestingly whether either of these metabolic pathways is selectively used across different plant tissue types. So far, there is no accurate answer; but evidences suggested that various plant species exhibit preferences for different pathways during seed germination (Feussner et al., 2001).

2.3.3.5 The import of FAs into peroxisomes

The free fatty acids released by membrane lipids degradation or TAG lipolysis are subsequently transported into peroxisome for the FAs breakdown. Inside peroxisomes, the imported fatty acids are β-oxidized to C-2 units, acetyl-CoA (**Figure 5 & 6**), which can be subsequently converted into succinate through the glyoxylate cycle and transported to mitochondria, where they are converted into malate. The malate is then exported to the cytosol, entering the gluconeogenesis process to produce sucrose (**Figure 6**; Graham, 2008).

An ABC transporter protein, independently named as PEROXISOMAL ABC TRANSPORTER 1 (PXA1; **Figure 5 & 6**; Zolman et al., 2001), PEROXISOME DEFICIENT 3 (PED3; Hayashi et al., 2002), and COMATOSE (CTS; Footitt, 2002) in three different genetic screens, has been identified to mediate the uptake of substrates for β-oxidation into the peroxisome in Arabidopsis. CGI-58 interacts with the C-terminal Walker B Motif of Peroxisomal PXA1 (**Figure 5**; Yun et al., 2022). This interaction can enhance PXA1 function specifically in leaves, but is not observed in germinating seeds (Park et al., 2013).

There exists arguments in favor of either/both free fatty acids or/and CoA esters as the transport substrates of plant PXA1. In yeast (*Saccharomyces cerevisiae*), homologs of plant PXA1, Pxa1p (peroxisomal ABC-transporter 1) and Pxa2p, operate as a heterodimer to form a fully functional transporter. The Pxa1p/Pxa2p

transporter imports long-chain acyl-CoA ester (Verleur et al., 1997), whereas the medium-chain FAs enter yeast peroxisomes as free FAs independently of Pxa1p/Pxa2p (Hettema et al., 1996). The human ATP-binding cassette (ABC) transporters of subfamily D (ABCD) transporter subfamily includes four members: adrenoleukodystrophy protein (ALDP), ALD-related protein, the 70-kDa peroxisomal membrane protein (PMP70), and PMP70-related protein (PMP70R/PMP69), although their precise biochemical functions in lipid transport across the peroxisomal membrane are not fully understood (Nyathi et al., 2010). Of all, it has been hypothesized that human ALDP plays a role in the transport of long- and very-long-chain FA-CoAs, rather than unesterified FAs, across the peroxisome membrane (Guimarães et al., 2005).

In plants, several studies have suggested that the plant PXA1 protein transports acyl-CoAs across the peroxisomal membrane, the same as its *S. cerevisiae* homologs and as proposed for mammalian ABCD proteins (Footitt, 2002; Fulda et al., 2004; Guimarães et al., 2005; Roermund et al., 2012; Zolman et al., 2001). The current model in plant posits that PXA1 cleaves CoA through its thioesterase activity and imports the FA, which is then acylated by long-chain acyl-CoA synthetases (LACSs) within peroxisomes (**Figure 5**). The evidence in favor of this model includes: 1) The analysis of acyl-CoA levels in germinating *pxa1* seedlings uncovered a significant accumulation, compared to that in the wild-type controls (Footitt et al., 2002). 2) Acyl-CoA can induce the basal ATPase activity of PXA1 (De Marcos Lousa et al., 2013). 3) The fatty acyl-CoA thioesterase activity of plant PXA1 stimulated by ATP, which cleaves the CoA moiety upon transport, was reported to support β-oxidation (Carrier et al., 2019; De Marcos Lousa et al., 2013; Nyathi et al., 2010). This cleavage of CoA has also been revealed for yeast Pxa1p/2p prior to acyl-CoA import and for the human ALDP protein (Roermund et al., 2012). 4) LACSs are essential to sustain germination and seedling establishment in the absence of sugar (Fulda et al., 2004). Therefore, taken all together, these findings support the specificity of acyl-CoA as a substrate for plant PXA1 transporter.

The release of CoA moieties by PXA1 on the cytosolic side was proposed to have an independent uptake route. The Arabidopsis peroxisome membrane protein PXN, originally identified as an NAD+ transporter, has been found to import CoA into peroxisome (**Figure 5**; Agrimi et al., 2012). However, the *pxn* knockout mutants are still able to degrade fatty acids at a relatively reduced rate, indicating the potential existence of other alternative route for CoA import, or the possibility of CoA moiety releases on the luminal side of the peroxisome membrane (**Figure 5**; Agrimi et al., 2012). It was proposed from the yeast model that free CoA is released in the peroxisomal lumen, and PXA1 could also import free CoA (van Roermund et al., 2021).

Subsequently, along with the CoA moieties within the peroxisomes, FAs are activated to acyl-CoAs by long-chain acyl-CoA synthetases (LACSs) before entering the peroxisome β-oxidation pathway (**Figure 5**; (Fulda et al., 2002; Rinaldi et al., 2016). Arabidopsis LACSs are encoded by a family of nine genes, and most, with the exception of LACS5, are expressed in various tissues including leaves and roots (J. M.

Shockey et al., 2002). Numerous investigations have been performed to functionally characterize Arabidopsis LACSs (Fulda et al., 2002; Lü et al., 2009; Schnurr et al., 2004; Zhao et al., 2010). Fulda et al., 2002 showed that LACS6 and LACS7 are responsible for activating FAs targeted for peroxisomal β-oxidation. In addition, a functional and physical interaction between PXA1 and LACS6/7 has been demonstrated in plants and yeast (De Marcos Lousa et al., 2013).

2.3.3.6 The FAs β-oxidation pathway

The β-oxidation pathway is responsible for breaking down FAs from the mobilization of storage TAG or the membrane lipid turnover. In higher plants and most fungi, the catabolism of straight-chain fatty acids

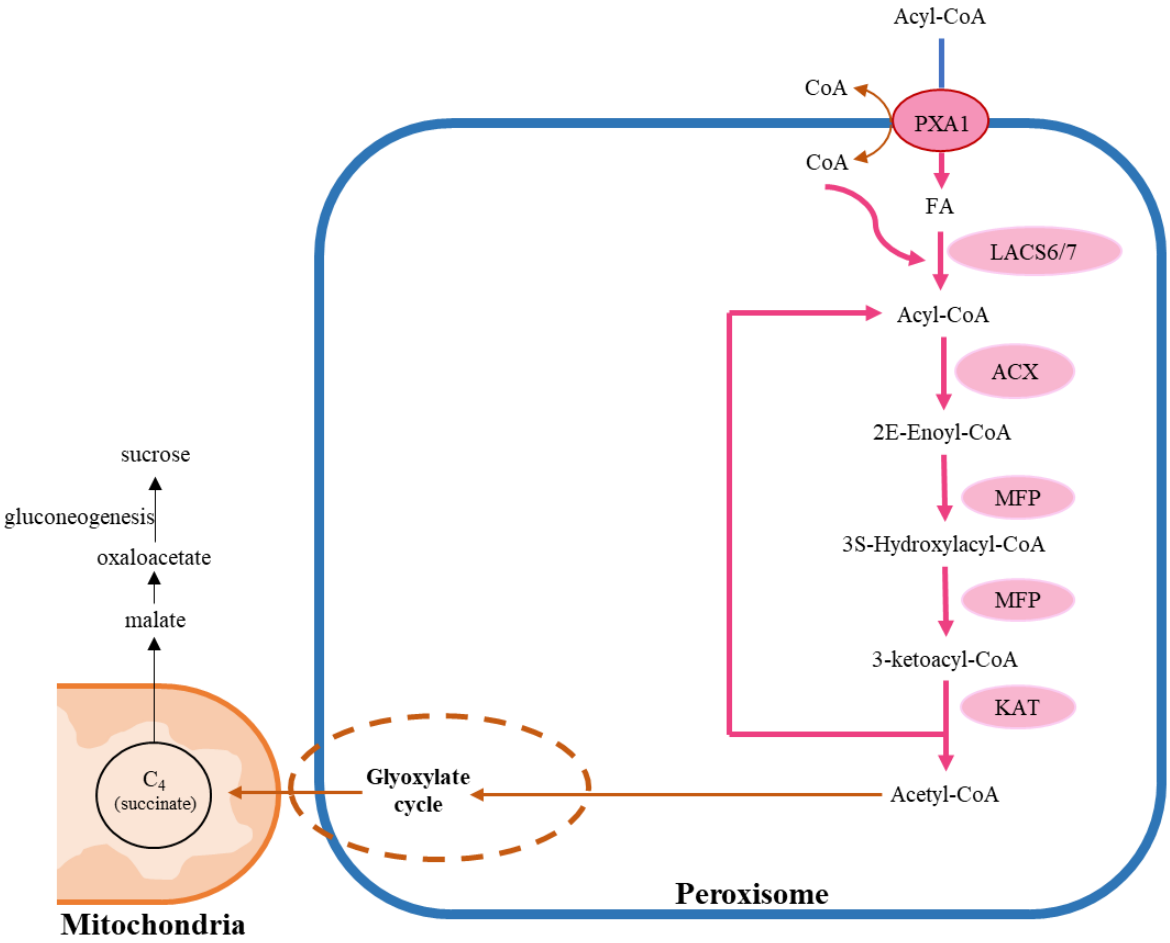


Figure 6. Peroxisomal key metabolic pathways in plants. Activated fatty acids esterified with CoA are imported into peroxisomes by PXA1, which hydrolyzes CoA upon transport. Inside peroxisomes, fatty acids are re-activated by LACS6/7 and catabolized to acetyl-CoA through β-oxidation process (in pink), which requires ACX, MFP and KAT enzymes. The 2-carbon acetyl-CoA is subsequently converted to 4-carbon compound (succinate) via glyoxylate cycle (in orange), which involves enzymes localized inside or outside the peroxisome. The generated succinate is then transferred from peroxisome to mitochondria, where it can undergo the conversion to malate within the Krebs cycle. Synthesized malate is transported to the cytoplasm and converted into oxaloacetate, which is further metabolized through gluconeogenesis to yield sucrose. PXA1, peroxisomal ABC transporter 1; LACS6/7, long-chain acyl-CoA synthetases; ACX, acyl-CoA oxidase; MFP, multifunctional protein 2; KAT, 3-ketoacyl-CoA thiolase; C_4, 4-carbon compound.

through the β-oxidation exclusively occurs only in peroxisomes, whereas within the human body it occurs in both mitochondria and peroxisome (Talley & Mohiuddin, 2024). Genes responsible for the core and auxiliary activities of β-oxidation in Arabidopsis have been well identified (**Figure 6**; Graham, 2008; Li-Beisson et al., 2013). However, there still requires ongoing efforts to address gaps in our understanding, particularly regarding the substrate specificity of certain enzymes and their interactions (Arent et al., 2010; Pye et al., 2010).

The β-oxidation pathway involves the core sequential actions of acyl-CoA oxidase (ACX), multifunctional protein (MFP), and 3-ketoacyl-CoA thiolase (KAT) for oxidation, hydration/dehydrogenation, and thiolytic cleavage, respectively (**Figure 6**).

The β-oxidation cycle initiates with the oxidation process of acyl-CoA carried out by one of the six ACX isozymes with overlapping but distinct specificities identified in Arabidopsis (Adham et al., 2005; Eastmond, Hooks, et al., 2000) to produce 2-trans-enoyl-CoA (**Figure 6**). The ACX1 (C12:0 to C16:0), ACX2 (C14:0 to C20:0), ACX3 (C8:0 to C14:0), and ACX4 (C4:0 to C8:0) have been well characterized in Arabidopsis (Adham et al., 2005; Eastmond, Hooks, et al., 2000; Froman et al., 2000). During Arabidopsis seed germination and early post-germinative growth, ACX1, ACX2, ACX3, and ACX4 genes exhibit coordinated upregulation, correlating with the rapid storage TAG breakdown (Rylott et al., 2001). The Arabidopsis double mutants disrupted in both *ACX1* and *ACX2* display impaired seed germination and seedling establishment (Pinfield-Wells et al., 2005). However, ACX6 unlikely significantly affect β-oxidation in seedlings, while ACX5 may make contributions that are masked by redundancy (Adham et al., 2005).

The subsequent two steps are performed by the partially redundant MFP proteins (**Figure 6**), including a MFP2 protein and an ABNORMAL INFLORESCENCE MERISTEM1 (AIM1) protein, both possessing 2-trans-enoyl-CoA hydratase and l-3-hydroxyacyl-CoA dehydrogenase activities (Richmond & Bleecker, 1999; Rylott et al., 2006b). In addition, MFP can contribute to some auxiliary activities necessary for the β-oxidation of certain unsaturated FAs (Graham, 2008; Poirier et al., 2006). The isoform MFP2 is highly expressed during post-germinative seedling growth (Eastmond & Graham, 2000) and its 2-trans-enoyl-CoA hydratase is exclusively active towards long-chain (C18:0) substrates, whereas the L3-hydroxyacyl-CoA dehydrogenase activity of MFP2 acts on C6:0, C12:0, and C18:0 substrates (Rylott et al., 2006b). The *mfp2* mutant exhibits a sucrose dependence for seedling establishment and a compromised capacity for storage oil breakdown, but not as severe as observed in the *acx1 acx2* double mutant, or in the *pxa1* mutant and *kat2* mutant (Rylott et al., 2006a; Zolman et al., 2001).

Finally, KAT enzymes release acetyl-CoA, and a truncated fatty acyl-CoA that can participate in further rounds of β-oxidation (**Figure 6**; Germain et al., 2001; M. Hayashi et al., 1998). Three loci encoding KAT enzymes have been demonstrated in the Arabidopsis genome, including KAT1, KAT2, and KAT5 (corresponding to At1g04710, At2g33150, and At5g48880, respectively; reviewed in Li-Beisson et al., 2013). KAT5 generates two polypeptides, KAT5.1 and KAT5.2, likely due to alternative RNA splicing Carrie et al., 2007; Germain et al., 2001). KAT2 stands out as the only KAT2 gene significantly expressed during Arabidopsis seed germination, suggesting an essential role of KAT2 for the efficient TAG mobilization (Footitt et al., 2007; Germain et al., 2001). Germain et al., 2001 showed that KAT1, KAT5 or other thiolases cannot substitute KAT2 activity in the *kat2* mutant seddlings.

In addition, concerning the unsaturated FAs with a *cis* double bond at even-numbered carbon or odd-numbered carbon positions, utilizing only the core set of enzymes of β-oxidation will result in metabolic blocks for the β-oxidation pathway. Two alternative pathways have been proposed for the continued β-oxidation of the intermediate derived from those unsaturated fatty acids (Goepfert et al., 2006)(Schulz and Kunau, 1987). In the hydratase/epimerase pathway, the intermediates eventually produced from unsaturated FAs with a *cis* double bond on an even-numbered carbon are converted to 2-trans-enoyl-CoA by an epimerase activity or an auxiliary enzyme, enoyl-CoA hydratase2 (ECH2/Hydratase; Goepfert et al., 2006), which allows the intermediate to re-enter the normal set of core reactions of β-oxidation. For the complete breakdown of unsaturated fatty acids with *cis* double bonds at odd-numbered carbons, it is reported that the functional D3, 5, D2, 4-dienoyl-CoA isomerase (DCl/lsomerase) and the D3, D2,-enoyl-CoA isomerases from Arabidopsis are also involved (reviewed in Li-Beisson et al., 2013).

2.3.3.7 From lipids to sugar

Subsequently, the acetyl-CoA derived from β-oxidation undergoes metabolism through the glyoxylate cycle to produce four-carbon organic acids (C_4, succinate), which can be transported into mitochondria for energy production via mitochondrial respiration or converted to malate to produce sucrose through gluconeogenesis process in the cytosol used for growth (**Figure 6**; Graham, 2008). It is generally suggested that in plants the glyoxylate cycle occurs in the specialized peroxisomes, termed glyoxysomes, and cytoplasm. The glyoxysomal steps of the glyoxylate cycle are catalyzed by malate synthase (MLS), isocitrate lyase (ICL), and citrate synthase (CSY), while the reactions catalyzed by aconitase (ACO) and malate dehydrogenase (MDH) occur outside the peroxisome (Cornah et al., 2004; De Bellis et al., 2020; Eastmond, Germain, et al., 2000; Lazarow, 2022; Pracharoenwattana et al., 2007).

During the germination phase of oilseeds, when the plant is not yet able to perform the photosynthesis, the glyoxylate cycle enables to efficiently synthesize sugars from stored TAG, without any carbon lost as CO_2. After the seed germination, this rapid conversion also supports the growth during early seedling

development (Eastmond & Graham, 2001). Subsequently, as Arabidopsis seedlings develop, glyoxylate cycle genes, such as ICL and MLS, do not continue to be expressed in the mature Arabidopsis plants (Buchanan-Wollaston et al., 2005; Rylott et al., 2001; van der Graaff et al., 2006).

The generated succinate from glyoxylate cycle is then transferred from the peroxisome to the mitochondria (**Figure 6**), where it can undergo the conversion to malate within the Krebs cycle. Synthesized malate is subsequently transported to the cytoplasm (**Figure 6**), where it is converted into oxaloacetate. These four-carbon molecules are further metabolized through gluconeogenesis to yield soluble sugar (**Figure 6**), which served as energy sources for seedling development. Furthermore, glycerol originating from TAG, can be channeled into both glycolysis and gluconeogenesis pathways (for reviews, Li-Beisson et al., 2013; Qin et al., 2023).

3 Roles of lipids in response to phosphate starvation in plants

3.1 Phosphate starvation

Plants take up P from the exogenous inorganic phosphate (Pi), such as hydrogen phosphate (HPO_4^{2-}) and dihydrogen phosphate ion ($H_2PO_4^-$), only when the soil pH is less than 7.0 (López-Arredondo et al., 2013; Preuss et al., 2011; Sentenac & Grignon, 1985). The assimilation of the orthophosphates depends on root phosphate transporters (PHTs), which can transport Pi between organs and cells within the plant, (reviewed in Dissanayaka et al., 2021; López-Arredondo et al., 2014; Nussaume et al., 2011). However, because of low levels of Pi in the soils and mostly forming in the covalently or non-covalently bound complexes under acid conditions, like acid-weathered soils of the tropics and subtropics (Marschner 1995; Vance et al., 2003), the availability of Pi is very low in the nature and the agricultural ecosystems. Claims that these complexed insoluble forms cannot be assimilated by the root system have been substantiated in tons of studies (Paungfoo-Lonhienne et al., 2010; Plaxton & Tran, 2011; Lambers, 2022). Thus, Pi limitation affects a lot the plant growth, development and productivity. Crop yields on 30-40% of the global arable land are constrained by Pi availability (Ros et al., 2020). Consequently, Pi starvation is a frequent nutrient stress that significantly affects plant growth and crop yield.

To enhance soil Pi availability, Pi-enriched fertilizers are commonly applied. However, the efficiency of Pi fertilizers is notably low with less than 20% of applied Pi being absorbed by plants, while the remaining Pi becomes immobile in the soil or leaches into and pollutes nearby water sources (Plaxton & Tran, 2011). Therefore, a more comprehensive understanding of how plant itself can adapt to Pi starvation biochemically and physiologically could benefit invaluably in optimizing agricultural productions with less reliance on unsustainable Pi fertilizers.

3.2 Adaptations in phosphate-starved plants

During land plant evolutionary transition, the ancestral aquatic species originating from mineral-rich aquatic environments had to cope with the challenge of limited Pi in the newly colonized terrestrial habitats (López-Arredondo et al., 2013). Thus, plants have developed various strategies to obtain phosphate during Pi-limited condition, for instance, to increase Pi uptake. At the overall root level, Pi deficiency can increase the root/shoot ratio (J. Lynch, 1995) and alter the root architecture (Williamson et al., 2001; López-Bucio et al., 2002), including root skewing (Matthus et al., 2020), the production of lateral roots (Robinson, 1994) and the proliferation of long root hairs (T. R. Bates & Lynch, 2001) to promote Pi uptake. Moreover, Pi starvation can affect the plant root to stimulate the exudation of compounds, which increases the availability of phosphate in the soil (Vance et al., 2003).

Additionally, Pi limitation can lead to the activation or suppression of over 1000 genes associated with various biological processes, including genes involved in Pi uptake, signaling, and translocation (Bergkemper et al., 2016; López-Arredondo et al., 2013; Morcuende et al., 2007; Mudge et al., 2002; Smith et al., 2003), and in the synthesis of Pi-solubilizing organic acids in soil and apoplast (Raghothama, 1999), as documented by numerous expression profiling studies (Hammond et al., 2003; Misson et al., 2005; Wu et al., 2003).

Furthermore, plant also develop another strategy to remobilize the phosphorus (P) reserves within the cells. P plays a vital role as a fundamental component of intermediates involved in central and energy metabolism in cells, as adenosine triphosphate (ATP), signaling molecules and genetic backbones as nucleic acids (DNA and RNA), and structural macromolecules as phospholipids (for a review, Jiménez et al., 2016). P enters metabolism via non-dedicated pathways, involving the synthesis of ATP from adenosine diphosphate (ADP) and Pi, followed by the subsequent transfer to other nucleotides and phosphorylated intermediates. Most of Pi can be rapidly recycled; some are directed towards the formation of P-containing end products (Abel et al., 2002; Lenburg & O'Shea, 1996; O'Neill et al., 1996; Wanner, 1993).

When Pi is limited, increased gene expression of phosphatases (del Pozo et al., 1999; D. Li et al., 2002) and RNAases (Bariola et al., 1994) are observed, in order to promote the mobilization of organically bound P within the plant cells. These changes lead to a general reduction in P-containing intermediates and cofactors such as ADP, ATP, uridine diphosphate-glucose (UDP-Glc) (Dancer et al., 1990), nucleotides (Zrenner et al., 2006) and RNA levels (Hewitt et al., 2005), as well as phospholipids (Dörmann & Benning, 2002; Kelly et al., 2003), although certain specific mechanisms remain to be further elucidated. However, these metabolic adjustments could be reversed within 3 h after Pi re-supply (Morcuende et al., 2007).

Pi-deprived plants also exhibited significant alterations in the expression of genes related to secondary metabolism and photosynthesis, however, these changes did not reverse rapidly upon Pi re-supply and were likely secondary in origin (Morcuende et al., 2007). For instance, Pi-deficient seedlings displayed a notable accumulation of starch and sucrose, along with relatively stable or slightly increased levels of most major amino acids, particularly glycine. After Pi re-addition, there was no significant decrease in carbohydrates, and certain amino acids (e.g., Gly, Ser, His, Phe, Tyr) remained unaltered for the initial 3 h, following with a decline in other amino acids (Gln, Glu, Asp, Ala, Asn, Ile, Leu, Val, Lys, Met) from the 8-hour mark onward (Morcuende et al., 2007).

Therefore, to artificially improve the phosphorus use efficiency (PUE) and thus Pi acquisition capacity in plants, especially during Pi starvation, the applied attempts to induce genes, which encode enzymes capable of promoting P uptake or mobilizing intracellular P sources, are potentially promising and have been validated successfully in crop fields (reviewed in López-Arredondo et al., 2013). For instance, phytate are the primary organic form of P accumulated by animals and plants. The phytate hydrolytic enzymes, collectively termed phytases, are categorized into four groups based on their catalytic properties: histidine acid phosphatases (HAPs), purple acid phosphatases (PAPs), Cys phosphatases, and β-propeller phytases (BPPs; Brinch-Pedersen et al., 2002; Ma et al., 2009). A transgenic expression or an introduction of a subset of PAPs enzymes, exhibiting phytase activity, from *M. truncatula* in Arabidopsis or soybean were shown to have the enhancements in dry weight and total P content, when phytate was provided as the sole P source (X. Wang et al., 2009; Xiao et al., 2006).

3.2.1 PL-to-DGDG exchange

Regarding strategies for the remobilization of intracellular P, in the past decades, the replacement of phospholipids with non-phosphate containing membrane lipids, such as galactolipids (DGDG) and/or sulfolipids (SQDG), has come to light. The replacement of phospholipids (PL) to phosphate-free lipids was initially reported in prokaryotes and photosynthetic bacteria, leading to the substitution of PG with SQDG, under Pi-starved conditions (Benning, 1998; Minnikin et al., 1974). Subsequently, a similar replacement of PG with SQDG due to phosphate deficiency was documented in the leaves and roots of *Arabidopsis thaliana* (Essigmann et al., 1998; Härtel et al., 2000; Jouhet et al., 2004; M. Li, Qin, et al., 2006; M. Li, Welti, et al., 2006). Nowadays this phenomenon of substituting phospholipids with non-phosphate lipids during phosphate limitation is widespread across various plant species, including shoots and roots of oat (Andersson et al., 2003), sycamore maple cell cultures (Jouhet et al., 2003) and soybean (Gaude et al., 2004), etc..

Apart from SQDG, various species have been reported to replace a significant portion of PLs with DGDG in response to phosphate limitation, including three monocot species (oat, rice, maize) with the exception

of timothy grass, and six dicot species (Arabidopsis, bean, garden nasturtium, radish, sunflower, sycamore maple; Tjellström et al., 2008). Although there are restricted range of plant species being studied, neither the phylogenetic relationships, nor the degree of domestication, influences the phenomenon of PL-to-DGDG replacement, indicating that it is a general mechanism for Pi-limited response in most of plants (Tjellström et al., 2008). However, there is a minimum threshold for the definition of Pi-starved conditions, Härtel et al., 2000 revealed that when the exogenous phosphate level is below than 1 mM, DGDG started to accumulate in Arabidopsis roots.

In addition, it is now well investigated that this non-P lipid replacement induced by phosphate deficiency occurs not only in plastids but also in extra-plastidic membranes. This extraplastidic PL-to-DGDG replacement (or DGDG accumulation) has been demonstrated to occur in plasma membrane (Andersson et al., 2003, 2005; Nakamura et al., 2005), mitochondria (Jouhet et al., 2004), and tonoplast (Andersson et al., 2005). Several studies have evidenced that when the replacement occurs outside plastids, DGDG serves as the main lipid undergoing replacement (Andersson et al., 2003, 2005; Jouhet et al., 2004; Nakamura et al., 2005). The uncharged DGDG replaces phospholipids in membranes, thus the overall charge of the membrane can be largely maintained. Moreover, the shape of the replacing lipid is also a critical factor to maintain membrane integrity (**Figure 1C**, see section 1.2), even more than its charge (Morcuende et al., 2007). DGDG, along with the majority of the PL it substituted (such as PC, PG, and PI), can readily form bilayers independently (Burger, 2000). However, the exact mechanisms of DGDG transport from plastid envelopes to other organelle membranes still requires further investigations.

This phospholipid-to-galactolipid membrane lipid remodeling in response to Pi limitation is an integral system, which consists the induction of two steps: 1) the phospholipid hydrolysis pathway to yield DAGs and 2) the galactolipid biosynthetic pathway using DAGs as the substrates (for a review, Nakamura, 2013). Hereby, I will provide an overview for proposed metabolic pathways governing membrane lipid remodeling in Pi-starved plants (**Figure 7A**), while the key enzymes involved in these metabolic pathways are listed in **Table 3**.

3.2.1.1 Phospholipids conversions

Considering that Pi starvation generally decreases the total phospholipid content and extraplastidic phospholipids (thus except for PG), and that the acylation patterns of DGDG formation are similar to those of degraded PC under phosphate-free condition in Arabidopsis, it suggests that a part of the degraded PC backbone is channeled to plastids to feed the synthesis of galactolipids (Heinz, 1977; Jouhet et al., 2003; Nakamura, 2013; Roughan, 1970).

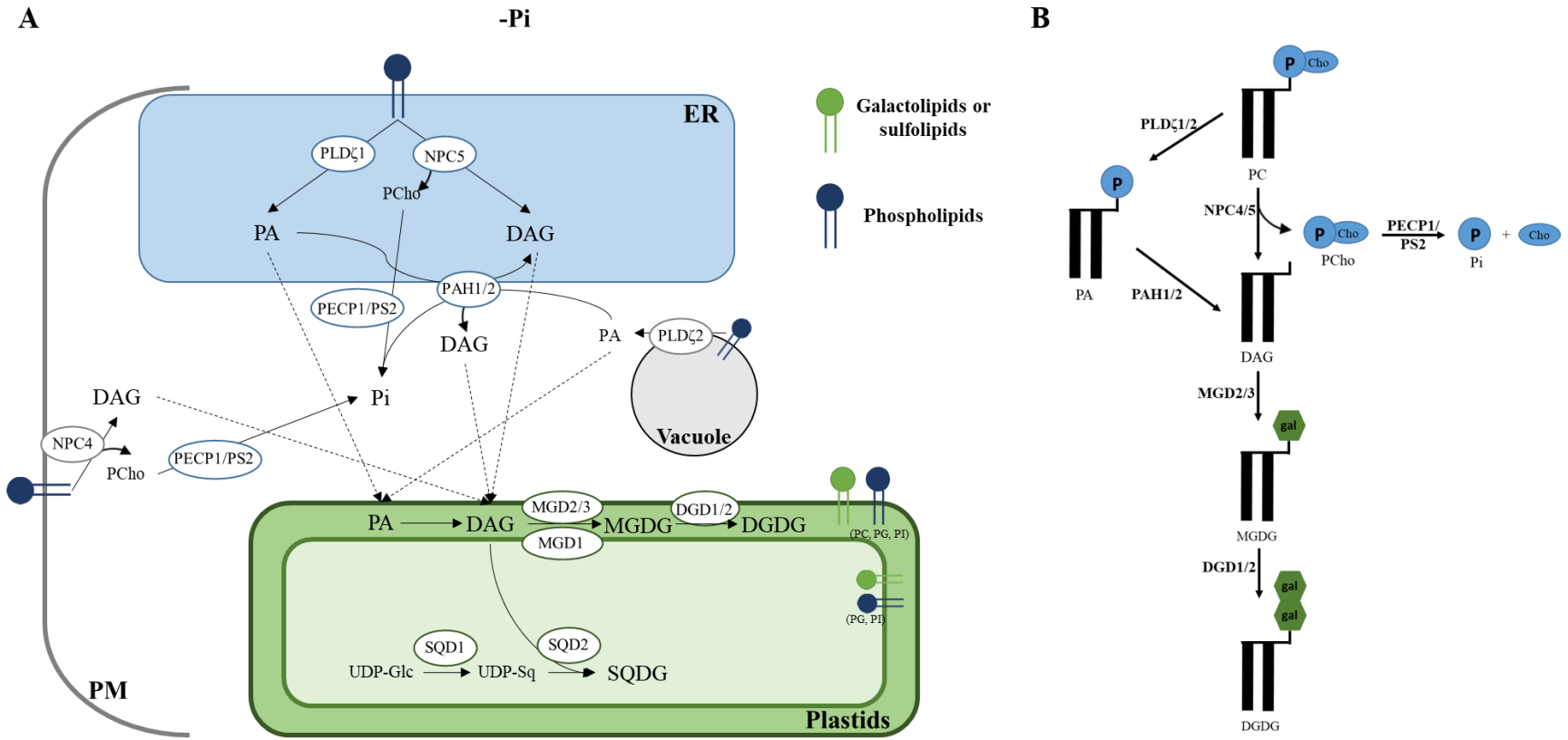


Figure 7. A model for proposed metabolic pathways governing membrane lipid remodeling in Pi-starved plant. A. Solid black arrows represented the metabolic pathways among different lipid molecules, while dashed black arrows suggested possible transport of lipid molecules between organelles. **Table 3** summarizes the characteristics of the involved enzymes. The subcellular localization of the metabolic pathways is based on the characterized subcellular localizations of the involved enzymes. Pcho, phosphocholine; UDP-Glc, uridine diphosphate glucose; UDP-Sq, uridine diphosphate sulfoquinovose. B. An example of the conversion of PC-to-DGDG presented in their chemical forms in Pi-starved plants.

Protein name	Accession	Pi starvation-induced	Substrates	Subcellular localization
Phospholipids hydrolysis				
NPC4	At3g03530	yes	PC > PE	PM
NPC5	At3g03540	yes	PE > PC	soluble fraction
PECP1	At1g17710	yes	PCho, PEth	unknown
PS2	At1g73010	yes	PCho, PEth	unknown
PLDζ1	At3g16790	yes	PC >> PE > PS	cytoplasmic space
PLDζ2	At3g05630	yes	n.d.	tonoplast
PAH1	At3g09560	hypothetically yes	PA	cytosol
PAH2	At5g42870	hypothetically yes	PA	cytosol
Galactolipid/sulfolipid accumulation				
SQD1	At4g33030	yes	UDP-Glc	Chloroplast
SQD2	At5g01220	yes	DAG and UDP-Sq	Chloroplast
MGD1	At4g31780	no	DAG and UDP-Gal	Plastid inner envelope
MGD2	At5g20410	yes		Plastid outer envelope
MGD3	At2g11810	yes		Plastid outer envelope
DGD1	At3g11670	yes	MGDG and UDP-Gal	Plastid outer envelope
DGD2	At4g00550	yes		Plastid outer envelope

Table 3. List of the key enzymes involved in metabolic pathways governing membrane lipid remodeling in Pi-starved plants, adapted from Nakamura, 2013. n.d., not determined.

Two pathways are extensively studied to hydrolyze extraplastidic phospholipids: 1) a one-step reaction by PLC to produce DAG and soluble polar heads of PLs, such as phosphocholine (PCho) and phosphoethanolamine (PEth) from PC and PE, respectively; and 2) a two-step reaction firstly by PLD to generate PA and then by phosphatidic acid phosphatase (PAP) to release Pi and DAG (Angkawijaya & Nakamura, 2017; Nakamura, 2013).

3.2.1.1.1 Pi starvation-induced PLC hydrolysis

The significant transcriptional activation of two Arabidopsis PC-hydrolyzing PLC (also called non-specific PLC, NPC), NPC4 and NPC5, upon phosphate limitation has been reported by Nakamura et al., 2005 and Gaude et al., 2008 (**Figure 7**). Thus, taking the PC-to-DGDG conversion as an example, PC is firstly hydrolyzed by NPC4/5 to produce DAG and PCho (**Figure 7B**).

NPC was initially identified in bacteria as a toxin that aids in host cell invasion by digesting the surrounding membrane (Titball, 1993). Homologs of bacterial NPC are exclusively found in Arabidopsis and other seed plants, suggesting that NPCs have evolved a specific role in plants for a conditional degradation of phospholipids at the cost of potential toxicity (Nakamura, 2013). Arabidopsis NPC4 and NPC5 share high similarity across their entire amino acid sequence, but exhibit distinct characteristics. Notably, NPC4 and NPC5 have substantially different subcellular localizations; NPC4 localizes primarily at the plasma membrane, while NPC5 is mainly found in the soluble fraction (**Figure 7A**). The recombinant NPC5, when expressed and purified in *Escherichia coli*, demonstrates 40-fold lower PC-PLC activity compared to NPC4 (Gaude et al., 2008). Moreover, the T-DNA knockout *npc5* mutants do not exhibit a reduction in total PC-

PLC activity in leaves under Pi starvation (Gaude et al., 2008), whereas the Pi-replete *npc4* mutants show PC-PLC activity almost as low as the Pi-limited wild-type plants (Nakamura et al., 2005). These findings suggested that NPC4 is shown to play the major role of PC-PLC activity during Pi deprivation. However, the Pi-starved *npc5* mutants display significantly reduced DGDG levels compared to the wild-type, whereas in *npc4* mutants DGDG accumulation is unaffected, indicating that NPC5 contributes more to DGDG accumulation under Pi starvation (**Figure 7A**; Gaude et al., 2008; Nakamura et al., 2005). This may be explained by the localization of NPC5, since the soluble NPC5 can access to the intracellular leaflet of organellar membranes, including the ER for phospholipid biosynthesis, and the outer envelope membrane of plastids for galactolipid biosynthesis (Nakamura, 2013).

Subsequently, in the PC-to-DGDG conversion, the generated PCho can be further dephosphorylated to release Pi (**Figure 7B**). The strong induction of a PEth/PCho phosphatase PECP1, and a HAD-type phosphatases PS2 (also called as PPsPase1) has been observed under Pi-deprived conditions (**Figure 7**; Angkawijaya & Nakamura, 2017; Chandrika et al., 2013; Hanchi et al., 2018; May et al., 2012). Angkawijaya & Nakamura, 2017 demonstrated that PECP1 and PS2 function redundantly as the PCho phosphatases to release Pi and produce choline under phosphate starvation (**Figure 7B**). Analysis of KO mutants and overexpressing lines of *PECP1* and *PS2* revealed significant effects on both PEth and PCho content in plants, indicating that both PEth and PCho serve as substrates by these two enzymes (Hanchi et al., 2018). Therefore, along with NPC4/5, they form a putative pathway for hydrolyzing PLs and further dephosphorylating polar heads of PLs to supply free Pi and DAGs. However, the subcellular localizations of PECP1 and PS2 enzymes remain unclear. Additionally, although *pecp1* and *ps2* mutants display almost complete loss of PCho phosphatase activity under phosphate starvation, no severe phenotypes were observed (Angkawijaya & Nakamura, 2017), suggesting that the dephosphorylation of PCho is not likely the major source to produce Pi in response to phosphate limitation.

3.2.1.1.2 Pi starvation-induced PLD hydrolysis

In addition, for the PC-to-DGDG conversion, PC can be initially hydrolyzed by PLD activity to generate PA (**Figure 7B**). However, studies in root tissues revealed that the up-regulation of PLD activity in response to Pi starvation is relatively minor compared to NPC activity (Nakamura et al., 2005). The Arabidopsis PLDζ1 localized to cytoplasmic space, and PLDζ2 localized to the tonoplasts, are found to be highly expressed under Pi-limited conditions in Arabidopsis (**Figure 7A**; M. Li, Welti, et al., 2006; Misson et al., 2005; Shimamura et al., 2022; X. Wang, 2001). Under Pi deprivation, the total root PC levels of *pldζ1pldζ2* double knockout mutants were significantly increased and the root DGDG levels were notably decreased compared to the wild type (M. Li, Qin, et al., 2006), suggesting a role for PLDζs in PC hydrolysis and DGDG accumulation during Pi starvation in roots (**Figure 7**). However, the single *pldζ1* and *pldζ2* mutants

did not show significant differences in PC and DGDG levels in Pi-starved roots, indicating that PLDζ1 and PLDζ2 have overlapping functions on PC hydrolysis and DGDG accumulation in Arabidopsis roots (M. Li, Qin, et al., 2006). In contrast, in Arabidopsis leaves, the contribution of PLDζ1/2 to DGDG production in membrane lipid remodeling induced by Pi deficiency is negligible, suggesting that the major pathways for phospholipid hydrolysis and DAG supply exhibit tissue specificity (Gaude et al., 2008).

Subsequently, the dephosphorylation of PA, produced either from the PLD-mediated phospholipid hydrolysis or *de novo* glycerolipid metabolism, can be catalyzed by PAPs to release Pi and produce DAG backbones (**Figure 7**). Nakamura et al., 2009 proposed that two Arabidopsis homologs of the human protein lipin, phosphatidate phosphohydrolase 1 and 2 (AtPAH1 and AtPAH2), function in membrane lipid remodeling during Pi starvation (**Figure 7**). It has been revealed that AtPAH1 and AtPAH2 regulate phospholipid synthesis at the ER in Arabidopsis (**Figure 7A**; Eastmond et al., 2010). In mammals and yeast, defect in lipin leads to abnormal lipid metabolism (Adeyo et al., 2011; Péterfy et al., 2001). Arabidopsis double mutant of *PAH1* and *PAH2* has a severe growth defect under Pi starvation and exhibits a 60% reduction in total soluble PAP activity, a significantly increased PA levels and an impaired DGDG accumulation, although the single mutants of *PAH1* or *PAH2* show no visible phenotype (Nakamura et al., 2009). These marked phenotypes in response to Pi deprivation are observed even under normal conditions in the double mutant *pah1pah2*, suggesting that both PAH1 and PAH2 are not conditional PAPs in response to Pi starvation, but are the general PAPs that regulate overall glycerolipid metabolism under standard growth conditions (Nakamura et al., 2009).

3.2.1.1.3 A potential pathway for phospholipid hydrolysis under Pi starvation

Additionally, phospholipids may be degraded through a third pathway mediated by lipid acyl hydrolase (LAH) and glycerophosphodiesterases (GPDEs) in Arabidopsis. In this pathway, phospholipids are initially hydrolyzed via LAH into free FAs and glycerophosphodiester (GPD) that can be further hydrolyzed to yield G3P, as the initial substrate to be converted into DAG for DGDG accumulation. Notably, this metabolic pathway does not release free Pi (Nakamura, 2013). In Arabidopsis, several LAH genes were characterized to be up-regulated by Pi deficiency (Morcuende et al., 2007); however, their roles in the phospholipid metabolism in response to Pi starvation remain largely unexplored (Zhu et al., 2022). Morcuende et al., 2007 also uncovered that four GPDE genes (At3g02040, At5g08030, At1g74210, and At5g41080) were reversibly induced by 3- to 30-fold in P-deprived seedlings. The T-DNA knockout mutant of one *GPDE* gene (At5g08030) leads to a significant reduction in GDPD activity, G3P content, Pi content, and seedling growth rate under Pi starvation; however, it exhibits no difference in lipid classes comparing with the wild type under both Pi-deprived and Pi-enriched conditions (Y. Cheng et al., 2011; Gaude et al., 2004; Nakamura et al., 2005), which may suggest significant redundancy in other phospholipid turnover pathways,

or their alternative functions beyond membrane lipid reconstruction during Pi starvation (L. Cheng et al., 2011).

3.2.1.2 Galactolipid/sulfolipid accumulation

Härtel et al., 2000 and Kelly et al., 2003 noticed that Pi deprivation triggered the activation of genes essential for galactolipid synthesis, and proposed that phospholipids were replaced by galactolipids during Pi starvation to recycle phosphate and to conserve membrane integrity. Thereafter, Misson et al., 2005 showed the strong induction of a cluster of genes associated with galacto- and sulpholipid synthesis, including several MGDs (MGD2/3) and DGDs (DGD1/2), as well as SQD1 and SQD2 synthases (**Figure 7**). However, no induction of MGD1, the major enzyme involved in galactolipid biosynthesis under standard conditions, is observed in response to Pi starvation (Awai et al., 2001). Moreover, three genes encoding UDP-Glc 4-epimerase (At4g23920) and UDP-galactose 4-epimerase (At1g10960 and At2g34850), which are potentially required to provide UDP-galactose for galactolipid synthesis, are also weakly induced (two-to-four fold) during midterm and long-term of Pi-starved seedlings (Misson et al., 2005; Morcuende et al., 2007).

3.2.1.2.1 Pi starvation-induced SQDG biosynthesis

As described before, SQDG was found to be increased upon Pi starvation. SQD1 and SQD2 are proteins involved in the synthesis of SQDG, regulating the conversion from UDP-glucose (UDP-Glc) to UDP-sulfoquinovose (UDP-Sq), and the transfer of the sulfoquinovose moiety to DAG, respectively (**Figure 7A**; Essigmann et al., 1998; Yu et al., 2002). The up-regulation of *SQD* levels are observed in Arabidopsis leaves during Pi deficiency (Sanda et al., 2001; Yu et al., 2002). In the Arabidopsis mutants of *SQD1* and *SQD2*, SQDG is completely absent, but these mutants show normal growth under Pi-enriched conditions (Essigmann et al., 1998; Yu et al., 2002). Under Pi-limited conditions, the *sqd2* mutant exhibits more severe growth defects than the *sqd1* mutant (Okazaki et al., 2013). Detailed analysis of Pi-starved *sqd1* and *sqd2* mutants revealed an accumulation of PG and PI compared to the wild-type, whereas other lipid classes were unaffected (Okazaki et al., 2013). PE levels were also slightly elevated in *sqd1* mutants compared to the wild-type even under P sufficiency, suggesting that these phospholipids (PG, PI and PE) may compensate the loss of negatively charged lipids in the thylakoid membranes of the *sqd* mutants, as they have similar biophysical properties (**Figure 1C**; Bolik et al., 2022; Okazaki et al., 2013). The contributions of these PLs in this compensatory mechanism are likely following the order of PG>PI>PE (Okazaki et al., 2013). Moreover, the absence of trans-16:1, a signature acyl species in PG, in the Pi starvation-induced SQDG indicates that PG is not the precursor of Pi-starved SQDG (Okazaki et al., 2013).

3.2.1.2.2 Pi starvation-induced MGDG/DGDG biosynthesis

Under standard growth conditions, MGD2 and MGD3, localized in the outer envelope membrane of chloroplast (**Figure 7A**), are mainly expressed in flowers and roots, respectively. MGD2 and MGD3 cannot compensate for the loss of IE-localized MGD1 function, as the *mgd2 mgd3* double mutant displays a similar MGDG level compared with wild type (**Figure 7A**; Kobayashi et al., 2009). Although Pi starvation strongly activates the gene expression of MGD2 and MGD3 in the shoot and root, the overall MGDG level does not increase, suggesting that MGD2 and MGD3 may produce MGDG primarily as the substrate for the DGDG synthesis to replace phospholipids (**Figure 7**; Awai et al., 2001; Kobayashi et al., 2004). Indeed, the DGDG accumulation under Pi starvation is almost completely abolished in the roots of the *mgd2mgd3* double mutant (Kobayashi et al., 2009), indicating that these two MGDG synthases are crucial for the DGDG accumulation during Pi starvation in Arabidopsis roots (**Figure 7**). However, the leaf DGDG level still increases in the Pi-free *mgd2 mgd3* mutant, suggesting that MGD1 also plays a role in the membrane lipid remodeling under Pi deprivation, particularly in leaves (**Figure 7A**; Kobayashi et al., 2009).

The two Arabidopsis DGDG synthases DGD1 and DGD2 localized in the outer envelope of chloroplasts, are also induced by Pi starvation, DGD2 being the most induced (**Figure 7**; Awai et al., 2001). The *dgd1* and *dgd2* single knockout mutants exhibit an decreased level of DGDG accumulation under Pi-limited conditions compared to wild-type (Kelly et al., 2003; Kelly & Dörmann, 2002), whereas no increase in DGDG was detected in the double mutant line *dgd1 dgd2*, indicating that single mutants *dgd1* and *dgd2* carry null mutations, and that the Pi-starvation induced DGDG synthesis was mediated only by DGD1 and DGD2.

Furthermore, the PL-to-DGDG replacement is reversible, not only at the gene expression level (Morcuende et al., 2007), but also in lipid composition of the overall tissues (Tjellström et al., 2008). Morcuende et al., 2007 revealed that phosphate starvation-induced transcriptional changes of the genes involved in PL-to-DGDG replacement in Arabidopsis were reversed within 3 hours of Pi re-supplementation. When re-supplying the radiolabeled Pi to oat seedlings, a significant allocation occurred into shoot phospholipids, primarily in PC (Tjellström et al., 2008). The preferential allocation of phosphate to shoot PC rather than root PC in Pi-enriched plants may reflect a transient role of PC as a DAG backbone carrier in chloroplast lipid synthesis (P. D. Bates et al., 2007; Slack et al., 1977). Over the time, allocation to PE and PG became more pronounced, consistent with findings in pea leaf aging studies showing that PC synthesis decreased and turnover of PG and PE increased (Hellgren & Sandelius, 2001). However, the plasma membrane lipid composition cannot completely be restored after 1 week of fully nutrient supply, as experimented in oat, suggesting that the adjustment in lipid metabolism at the subcellular level lags behind (Tjellström et al., 2008).

3.2.2 LDs accumulation during stress

LDs are known to serve as energy storage, yet various studies have explored their alternative functions in transiently sequestering free FAs that can be harmful to the cell, particularly numerously generated in response to stress (for a review, Yang & Benning, 2018). TAG accumulation has been commonly observed in response to Pi deprivation in higher plants (Pant et al., 2015; Shimojima et al., 2015). However, limited information is available regarding the regulators involved in TAG accumulation and LDs formation during stress. Therefore, further investigations are required to demonstrate if specific stress-responsive proteins exist, for instance, whether proteins associated with LD biogenesis, like SEIPINS in the incorporation of additional proteins and lipids into the growing LD, are upregulated, or enzymes involved in TAG breakdown are down-regulated.

TAG accumulation under senescence and nitrogen starvation conditions has shown to be related to the transcriptional activation of the key steps in TAG biosynthesis, including DGAT1 and OLEOSIN1 (Kaup et al., 2002; Y. Yang et al., 2011). However, Shimojima et al., 2015 and Pant et al., 2015 found that the expression levels of these genes in wild-type shoots and roots were clearly shown to be unchanged during Pi starvation, suggesting that the enhanced TAG accumulation under Pi-depleted conditions was not associated with the transcriptional up-regulation of TAG synthesis genes. However, it may be attributed to the down-regulation of genes involved in TAG breakdown during Pi depletion (James et al., 2010; Kelly et al., 2013).

3.3 Phosphate starvation-induced mitochondrial membrane lipid remodeling through MTL complex in *Arabidopsis thaliana*

It had been described in section 1.2 that plant organelles membranes have different lipid composition and the lipid composition in each organelle is usually stable, whereas glycerolipid synthesis happens mainly in plastids and ER compartments (section 2.2.1), thus indicating the existence of glycerolipid trafficking systems in plant cells for lipid distribution and homeostasis under standard culture conditions.

Lipid transfer between organelles can be mediated through both the secretory vesicular pathway and non-vesicular pathways occurring at membrane contact sites (MCSs), which are specialized cellular structures formed between two membranes in close proximity, typically within a distance ≤ 30 nm (detailed overview of MCSs please refer to **Chapter 3**; Block et al., 2007; Holthuis & Levine, 2005; Jouhet et al., 2007; Leterme & Michaud, 2022; Moreau et al., 1991, 1998). The vesicle pathway is involved in the transport of all phospholipids between organelles connected to the endomembrane system, such as the ER, the vacuole, the Golgi or the plasma membrane (PM; Cevher-Keskin, 2020). Furthermore, there are some indications supporting that vesicular trafficking may occur in plastids for the transportation of MGDG, DGDG, PG and

SQDG, synthesized in the plastid envelopes, selectively from the inner envelope to the thylakoids (Joyard et al., 1980; Lindquist & Aronsson, 2018; Rawyler et al., 1995; Q. Wang et al., 2004).

Although the vesicular pathways are involved in the lipid distribution, they do not fully mediate the entire required lipids for organelles. Another lipid transfer mechanism, independent of the vesicular pathway, has been proposed between organelles MCSs: the non-vesicular pathway (for a review, Leterme & Michaud, 2022). In contrast to vesicular trafficking, non-vesicular transfer does not entail the transfer of a portion of a bilayer but rather a direct transfer of lipid molecules from one membrane to another (Jouhet et al., 2007; Leterme & Michaud, 2022). Four types of proteins for non-vesicular lipid transfer can be found at organelle MCSs: 1) lipid transfer proteins (LTPs) that contain a soluble domain with a hydrophobic cavity for accommodating lipid molecules; 2) flippases/scramblases that transfer lipids from one leaflet of a membrane to another; 3) proteins that can promote non-vesicular lipid transport by favoring lipid extrusion or insertion from the donor or acceptor membranes respectively, and 4) multi-subunits complexes that can mediate lipid transport crossing two or several membranes (for a review, Leterme & Michaud, 2022).

As our lab is primarily focused on the study of lipid transport to mitochondria, I will provide a detailed overview of the phosphate starvation-induced lipid remodeling through a mitochondria-localized complex in plants (**Figure 8A**).

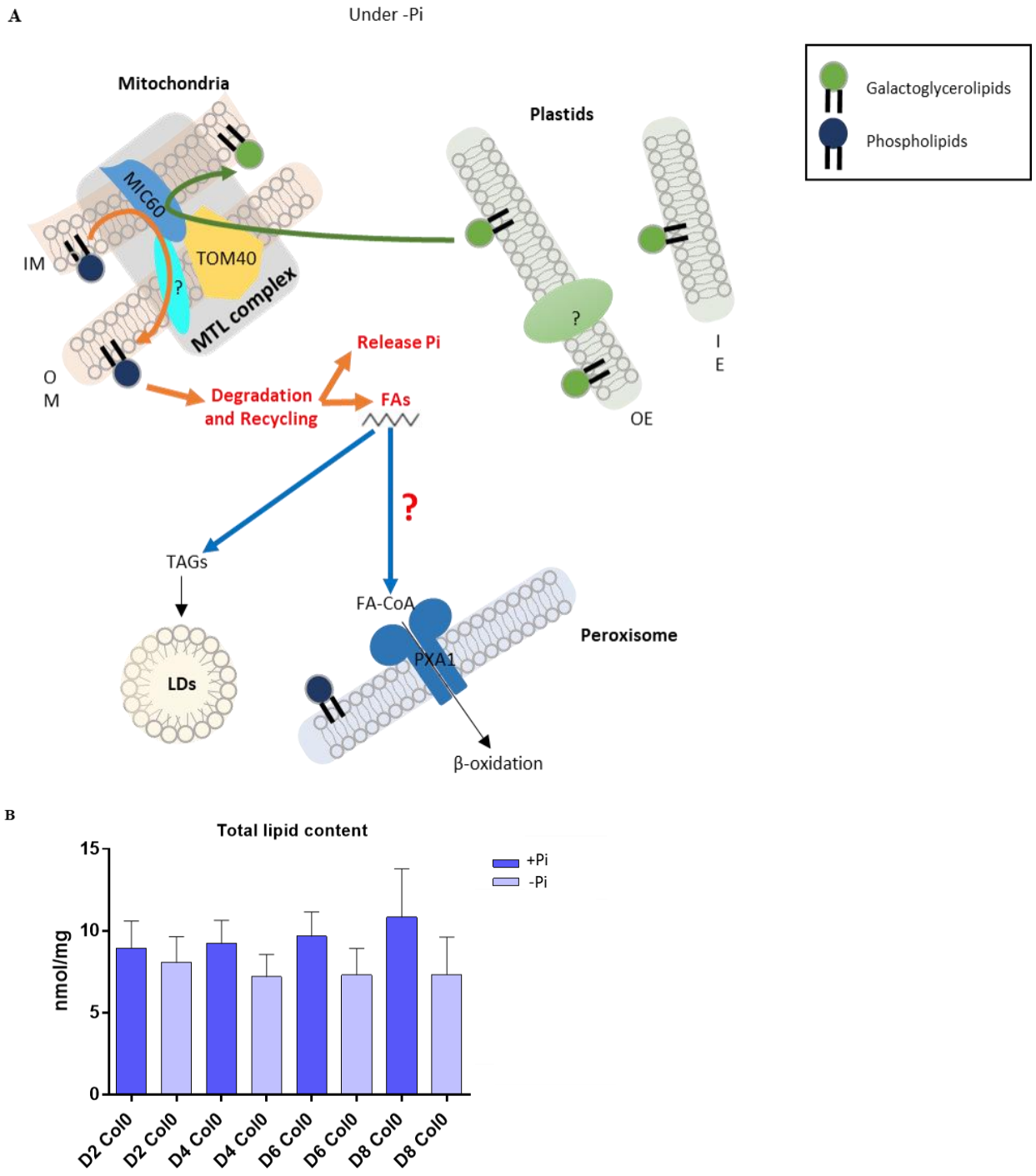


Figure 8. Phosphate starvation-induced mitochondrial membrane lipid remodeling in *Arabidopsis thaliana*. A. During Pi starvation, mitochondrial phospholipids (in dark blue) are partially degraded to release Pi and recycle, and replaced by the galactoglycerolipids DGDG (in green) transported from plastids to maintain the integrity of mitochondrial membranes. In the MTL complex, Tom40 interacts with Mic60, are involved in DGDG import and PE export from mitochondria. Some peroxisomal proteins involved in β-oxidation, such as PXA1, were found in the co-IPs results with Tom40 protein, suggesting that peroxisomes and β-oxidation pathway might play a role in lipid remodeling during Pi starvation. In addition, the released free FAs could also participate in TAG synthesis resulting in an enhanced TAG and lipid droplets (LDs) accumulation under stress conditions. B. Total amount of lipids per mg of fresh weight from Col0 (wild type) calli grown in phosphate replete (+Pi) and deplete (-Pi) conditions within 8 days. Five biological triplicates were performed.

Previous studies in our lab have identified a mitochondrial lipoprotein complex called MTL (mitochondrial transmembrane lipoprotein) complex involved in mitochondrial lipid transport in response to Pi starvation (Michaud, 2018; Michaud et al., 2016, 2017). The MTL complex is a huge lipid-rich structure comprising approximately 200 proteins located across the dual mitochondrial membranes and migrated at about 800 kDa on native gel (Michaud, 2018; Michaud et al., 2016). The protein and lipid composition of the MTL complex is dynamic and varies during Pi starvation. Proteomic analysis of the MTL complex revealed that it contained mainly mitochondrial proteins and several proteins located in other organelles, including plastids and peroxisomes, possibly suggesting a role in mediating lipid transfer between mitochondria and other organelles.

Interestingly, all the components of the translocase of the outer membrane (TOM) complex and AtMic60, a protein located in the inner membrane (IM), were found in the MTL complex (**Figure 8A;** Michaud et al., 2016). AtMic60 has been identified as a functional homolog of yeast Mic60, a key constituent of the mitochondrial contact site cristae organizing system (MICOS) complex (Pfanner et al., 2014). MICOS complex plays a central role in mitochondrial membrane architecture, protein import dynamics and lipid homeostasis (Michaud et al., 2017; Mukherjee et al., 2021; Pfanner et al., 2014). In yeast and mammals, Mic60 interacts with multiple partners located in the OM, including Tom40, SAM50, VDAC and DNAJC11 (Mukherjee et al., 2021). Michaud et al., 2016 revealed that the Arabidopsis homolog AtMic60 also interacts with AtTom40 (**Figure 8A**). The *atmic60* mutants display a decreased level in AtTom40 content in MTL complex fractions (Michaud et al., 2016), likely indicating a role of AtMic60 in regulating the OM-IM tethering. Moreover, under Pi-starved conditions, there were observed elevations in the abundance of AtMic60-AtTom40 within the MTL, implying their potential involvements in adaptation to the Pi-deprived effects (Michaud et al., 2016). Thus, lipid analysis of the MTL complex was performed in *atmic60* knockout mutants. The results showed a diminished DGDG accumulation and an unusual PE accumulation in the MTL complex under Pi limitation, suggesting an impairment in mitochondrial PE export and DGDG import resulting from the deletion of AtMic60. Thereafter, this observation was further supported by the analysis of isolated mitochondrial lipids from the same *atmic60* knockout mutants, revealing a reduction in DGDG levels and an elevation in PE levels under Pi starvation, in contrast to the wild type (Michaud et al., 2016). These findings collectively suggest a role for AtMic60 in the PE export and DGDG import of intra-mitochondrial lipid trafficking (**Figure 8A**). In addition, AtMic60 could induce the destabilization of liposomes *in vitro*, potentially indicating that it favors lipid desorption from membranes prior to transport (Michaud et al., 2016). Further investigations are necessary to explore the effects of AtMic60 deficiency at the subcellular level (Michaud et al., 2016, 2017). The other putative candidates identified in the MTL complex, Tom40, are multifunctional proteins, and the *tom40* KO plants are embryolethal (Murcha et al., 2014), thus its involvement cannot be confirmed by conventional genetic approaches. Therefore, it would

be a challenge to characterize novel mutant plants that are strongly affecting the plant mitochondria lipid trafficking without inducing lethality. Even though AtMic60 and AtTom40 have been recognized as key components for mitochondrial lipid transport, the precise lipid transport mechanisms via MTL complex and its partners remain to be unraveled.

Recently, in the framework of Sébastien Leterme's thesis, our team identified and characterized an Arabidopsis vacuolar protein sorting 13 protein located at the surface of mitochondria in leaves, AtVPS13M1 as a lipid transfer protein involved in phospholipid degradation in response to Pi starvation (Leterme et al., 2024). To date, apart from these, no other protein involved in mitochondrial lipid transport has been characterized in plants.

Since the MTL complex also encompassed several extra-mitochondrial proteins, it prompts the speculations regarding its potential interplays with other organelles in lipid exchange in response to stress. For instance, if, as in yeast, the plant TOM complex is able to interact with ER proteins, such as an ER complex (EMC; Lahiri et al., 2014), the plant MTL complex via TOM40 and/or other partners might also be involved in the tethering and/or lipid transfer between these two organelles. This would provide additional insights for understanding the roles of the MTL complex in lipid trafficking.

Consequently, to identify potential candidates outside mitochondria, based on Tom40 protein at the outer membrane of mitochondria, we performed co-immunoprecipitation (co-IP) with Tom40-HA tagged protein (Michaud and Albrieux, unpublished data). Unexpectedly we found peroxisomal proteins involved in β-oxidation as putative partners of AtTom40, such as PXA1, opening a new perspective into the role of peroxisome, β-oxidation and mitochondria-peroxisome MCSs in phosphate starvation-induced membrane lipid remodeling (**Figure 8A**).

Furthermore, as shown in **Fig 8B**, the total lipid contents in plant cells gradually decreased with the increasing duration of Pi deprivation. Given that, we hypothesized a potential association between the MTL complex and peroxisomal β-oxidation, a lipid degradation pathway (see section 2.3), it prompts us to further investigate if the β-oxidation pathway would be highly induced for the recycling of free FAs derived from the remodeled phospholipids under Pi deprivation.

Overall, this study will focus on the metabolic involvements of peroxisome and peroxisomal β-oxidation in membrane lipid remodeling in response to Pi starvation. Particularly, it is unknown whether peroxisomal membrane lipid composition is modified in response to Pi starvation. Therefore, this work is divided into three main parts: 1) the characterization of peroxisome lipid composition under both Pi-enriched and Pi-limited conditions from *A. thaliana* cell suspension cultures, 2) the metabolic determination of β-oxidation pathway using the key enzymes KO mutants in the context of Pi starvation in plants, and 3) preliminary

work that has been performed to investigated putative mitochondria-peroxisomes contact sites mediated by PXA1.

Materials and Methods

1 Plant material and growth conditions

1.1 *Arabidopsis thaliana*

Experiments were performed using *Arabidopsis thaliana* plant lines including wild-type Columbia-0 (Col0), and two β-oxidation mutants obtained from the Arabidopsis Stock Center: *pxa1-1* (CS3950; an ethyl methanesulfonate-generated, a splice-site mutant of Col0; homozygous; Zolman et al., 2001b) and *mfp2-2* (SALK_098016; Col0 background; homozygous T-DNA insertion line; Alonso et al., 2003) that are in a Col0 background.

1.2 *Nicotiana benthamiana* plants

Nicotiana benthamiana is an angiosperm from the *Solanaceae* family. All the plants used in this study are wild type *Nicotiana benthamiana*.

1.3 Culture conditions

1.3.1 Seed sterilization and stratification

To avoid unwanted pests from spreading in the phytotrons, the seeds were subjected to a treatment at -80°C for 3h and then surface sterilized under a sterile laminar flow hood with 70% (v/v) ethanol and spinning for 2 min on a rotative wheel, followed by a treatment with 0.4% (v/v) bleach solution for 12 min. After sedimentation, the seeds were washed five times in 1 mL of sterile water and put at 4°C in dark for a minimum of 48 h to allow seed vernalization. After 48 h, the seeds were sown on a soil mix containing 35 L of soil, 7 L vermiculite and 10 g of biological fungicide (Prestop, Lallemand), or on *in vitro* agar plates.

1.3.2 Plants grown on soil

Plants were grown in long day (16-h light and 8-h dark photoperiod) or short day (8-h light and 16-h dark photoperiod) conditions in phytotrons maintaining a temperature at 22°C/20°C light/dark, an hygrometry at 60-70% and a photon flux density of 100 µmol/m^2/s. Plants were watered 3 times a week.

1.3.3 β-oxidation mutants seeds germination on solid media

β-oxidation mutants seeds were sterilized and sown on sterile Murashige & Skoog (MS)-agar plates (**Table 4**; José A. *et al.*, 2019) and grown in phytotrons in long day condition (16h-8h light-dark photoperiod). The

Component	
MS with vitamins	4.41 g/L
Sucrose	5 g/L
MES	0.5 g/L
Agar	7 g/L

Table 4. Murashige & Skoog solid media for β-oxidation mutants seeds germination. PH was adjusted to 5.7 with KOH.

temperature maintained at 22°C during the day, 20°C during the night. The photon flux density was at 30-60 µmol/m^2/s. After 2 weeks of growth, the seedlings of mutants were planted on soil as described above.

1.3.4 Calli generation from *Arabidopsis thaliana* seedlings

Arabidopsis seeds were sterilized and grown on sterile Murashige & Skoog (MS)-agar plates (**Table 4**) at long day conditions. After two weeks of growth, the cotyledons of the seedlings were cut in four pieces using a sterile scalpel and placed on new solid MS medium (**Table 5**). After approximately 3 weeks of growth in continuous light at 22°C, the dedifferentiated cells form the genotyped calli were transferred on new solid MS medium (**Table 5**). Calli were then passed to new plates once per month.

Component	
MS with vitamins	4.41 g/L
Sucrose	30 g/L
2,4-D (2,4-dichlorophenoxyacetic acid)	1.2 g/L
Agar	0.8% (w/v)

Table 5. Murashige & Skoog solid media for A. thaliana calli growth. PH was adjusted to 5.7 with KOH.

1.3.5 *Arabidopsis thaliana* calli growth in liquid Murashige & Skoog media

Murashige & Skoog liquid calli growth medium was prepared with (+Pi) or without phosphate (-Pi) as described in **Table 6**. This medium contained 2,4-dichlorophenoxyacetic acid (2,4-D) to maintain the cells undifferentiated.

Component	Concentration in +Pi medium	Concentration in -Pi medium
MS including vitamins W/O KH_2PO_4 (DU1072, Duchefa)	4.235 g/L	4.235 g/L
Sucrose	15 g/L	15 g/L
2,4-D	1.2 mg/L	1.2 mg/L
Phosphate	0.5 mM	0 mM

Table 6. Murashige & Skoog liquid medium composition for calli growth. PH was adjusted to 5.7 using NaOH.

After a month of cultivation on plates, calli were subsequently transferred to liquid culture in round flasks containing 200 mL of MS +Pi medium (**Table 6**). These cultures were maintained under 125 rpm agitation and constant illumination, and were passed into new liquid medium once a week.

For the experimental treatments under both Pi-enriched (+Pi) and Pi-limited (-Pi) conditions, approximately 5 mL of calli grown in liquid cultures were initially collected. These calli were then thoroughly washed five times with the respective +Pi or -Pi media (**Table 6**) to ensure a consistent nutrient environment. Following the washing process, the calli were transferred into new flasks containing 200 mL of the corresponding +Pi or -Pi media. Calli samples for the subsequent analysis were collected after 4, 6, or 8 days, depending on the specific experimental setup.

1.3.6 *Arabidopsis thaliana* seedlings growth in Murashige & Skoog liquid or solid media

Arabidopsis seeds were sterilized and incubated for 4 days on Murashige & Skoog (MS) solid media with 1 mM phosphate (Pi) shown in **Table 7**. Seedlings of comparable sizes were selected and subsequently transferred into liquid or onto solid MS media, depending on the experimental conditions. For those seedlings grown in liquid MS medium, a thorough washing step using the corresponding +Pi or -Pi media (**Table 7**) was performed to ensure a consistent nutrient environment. Seedlings grown in liquid MS medium were cultured in the 6-well plates containing 5 mL of the respective MS medium (**Table 7**) per well under 100 rpm agitation and constant illumination. Seedlings grown on solid MS medium (**Table 7**) were placed vertically in phytotrons under long day conditions to observe the root growth.

Component	Liquid medium		Solid medium	
	1 mM Pi	0 mM Pi	1 mM Pi	0.005 mM Pi
MS including vitamins W/O KH_2PO_4 (DU1072, Duchefa)	4.235 g/L	4.235 g/L	1.0575 g/L	1.0575 g/L
Sucrose	10 g/L	10 g/L	10 g/L	10 g/L
KH_2PO_4	1 mM	0 mM	1 mM	0.005 mM
Agar (A7921, Sigma)	-	-	12g/L	12g/L

Table 7. Murashige & Skoog liquid or solid medium composition for seedlings growth. PH was adjusted to 5.8

2 Molecular biology

2.1 Molecular cloning

2.1.1 Plasmids

2.1.1.1 Plant expression vectors pFP108, pMM100, and pMM125

The plant vector pFP108 (From F. PARCY; To et al., 2006), pMM100 and pMM125 created by Morgane Michaud were used as basis to construct the plasmids for protein-protein interactions (PPIs) identifications *in vitro* or *in vivo*.

pFP108 is a plant vector for protein expression under the control of a Cauliflower Mosaic Virus 35S promoter (CaMV 35S) repeated in tandem to constitutively drive strong protein expression (Error! Reference source not found.). Transcription is terminated by the nopaline synthase (NOS) terminator. A multiple cloning site allows efficient cloning between the CaMV 35S promoter and NOS terminator. The promoter, multiple cloning site and nos terminator are inserted between the T-DNA left and right borders.

The pMM100 corresponds to the pFP108 plasmid in which the EGFP gene were C-terminally fused in the multiple cloning site according to the Gibson cloning method downstream of the inducible CaMV 35S

promoter and using SpeI and BamHI restriction sites to linearize the plasmid backbone (Error! Reference source not found.).

pMM125 corresponds to the insertion of 3xHA-TurboID (amplified via PCR from Addgene constructs #107171) into pFP108 vector using BamHI restriction enzyme sites (**Figure 11**).

All the plasmids were selected with spectinomycin in bacteria and Basta in plants.

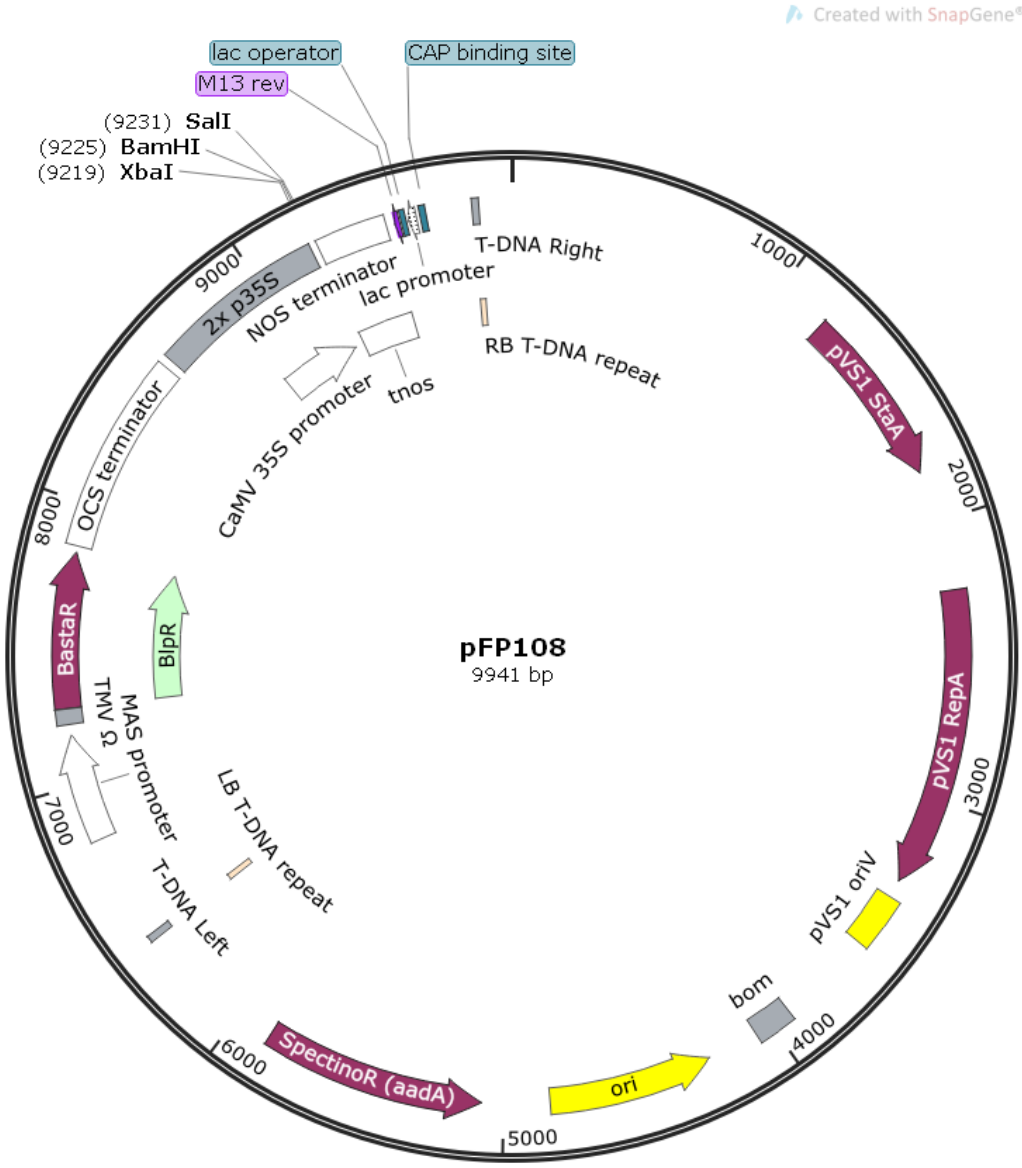


Figure 9. Map of the pFP108 plasmid created with SnapGene.

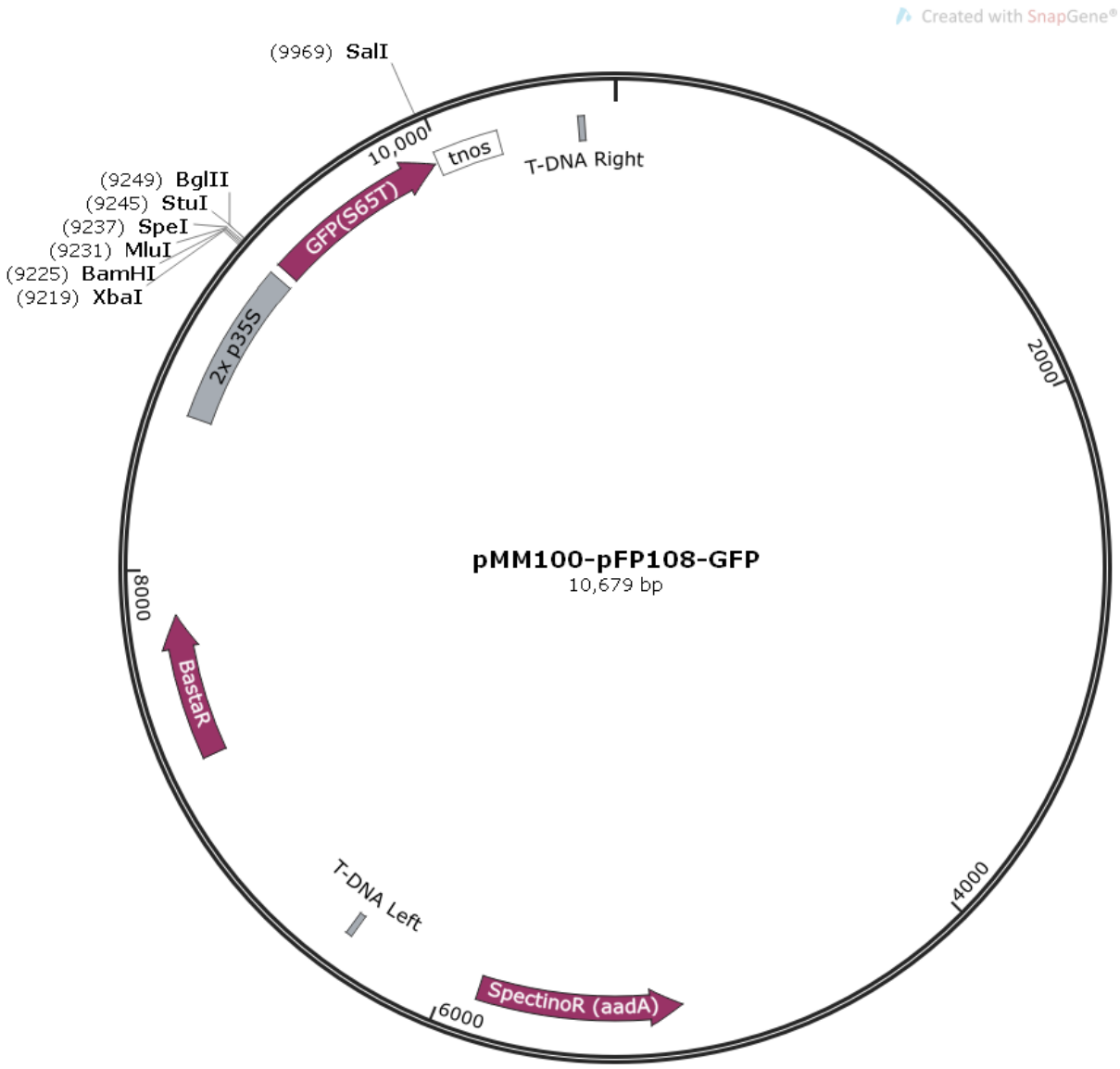


Figure 10. Map of the pMM100 (pFP108-GFP) plasmid used to constitutively overexpress GFP-fused proteins for localization studies.

2.1.1.2 Construction of plasmids for bimolecular fluorescence complementation (BiFC), *in vivo* expression of fluorescent proteins, and proximity-dependent biotin identification (BioID)

All the cell lines shown in the **Table 8** were sorted by *Agrobacterium tumefaciens* strain numbers. In this study, bimolecular fluorescence complementation (BiFC) was based on the split-YFP (yellow fluorescent protein). The *A. tumefaciens* strain bMM108 expresses P19 protein, a suppressor of post-transcriptional gene silencing, which can enhance transient transgene expression (Voinnet et al., 2003, retracted) in *Nicotiana benthamiana* after agroinfiltration. The *A. tumefaciens* strain bMM254 and bMM335 served as

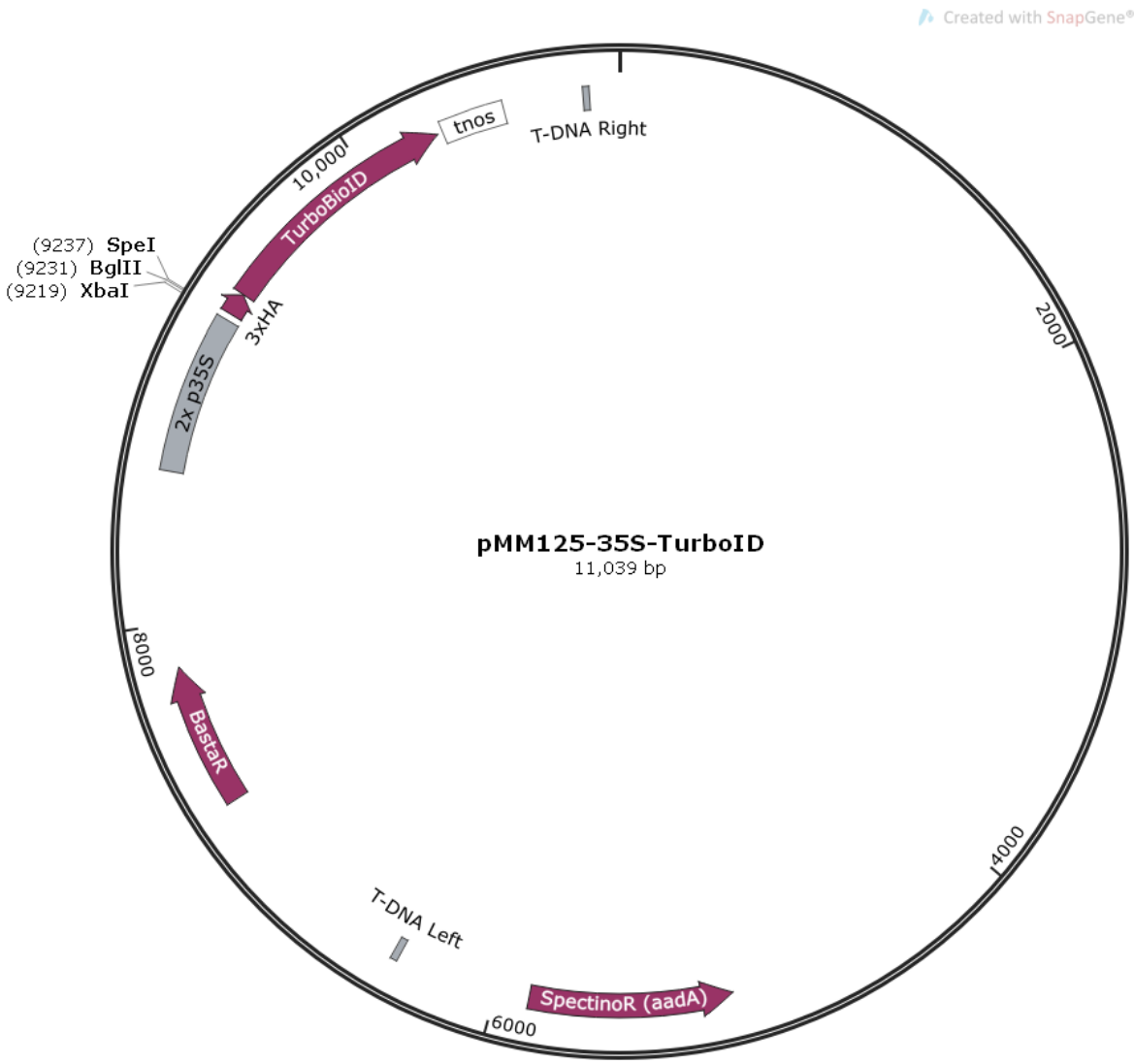


Figure 11. Map of the pMM125 (pFP108-3xHA-TurboID) used as the vector for the construction of BioID plasmids.

the peroxisomal and mitochondrial markers, respectively. The rest of the cell lines were generated to investigate the mitochondria-peroxisome interactions *in vitro* or *in vivo* by several protein-protein interactions (PPIs) methods, including bimolecular fluorescence complementation (BiFC), *in vivo* expression of fluorescent proteins and proximity-dependent biotin identification (BioID), which will be described detailedly in **Chapter 3**. All the constructions were cloned using Gibson assembly.

2.1.2 Polymerase chain reaction (PCR)

For molecular cloning purposes, the Phusion DNA Polymerase (New England Biolabs) was used for the accurate template amplification. The PCR reaction contained 1.5 mM $MgCl_2$, 0.2 mM of dNTPs (dTTP, dATP, dCTP, dGTP), 0.5 µM of forward and reverse primers, 0.02 U/µL of Phusion DNA polymerase and an adequate template DNA concentration for a final reaction volume of 25 µL. The samples were placed

Cell line	Description	Vector	Resistance	Application
bMM108*	P19	–	R, K	BiFC
bMM254*	**Perox-CFP**	**–**	**R, K**	**BiFC**
bMM335*	Mito-RFP	pFP108	R, G, S	BiFC
bMM381*	Tom20.2-CtYFP	pFP108	R, G, S	BiFC
bMM382*	Tom20.3-NtYFP	pFP108	R, G, S	BiFC
bMM409	Cbr1-TurboID	pFP108	R, G, S	BioID
bMM417	Pxa1-NtYFP	pFP108	R, G, S	BiFC
bMM418	At5g27520-NtYFP	pFP108	R, G, S	BiFC
bMM419	At5g27520-TurboID	pFP108	R, G, S	BioID
bMM421	TurboID-Tom20.2	pFP108	R, G, S	BioID
bMM422	Pxa1-TurboID	pMM125	R, G, S	BioID
bMM458	Pxa1-GFP	pMM100	R, G, S	*in vitro* expression

Table 8. All the cell lines used in this study. * represents the cell lines created previously in the laboratory. cDNA was generated from the extracted RNAs from Arabidopsis thaliana calli. Abbreviations: R = Rifampicin, K = Kanamycin, G = Gentamicin, S = Spectinomycin.

into a thermal cycler (T100™, BioRad). The PCR program started with a denaturation step for 5 minutes at 98°C. Then each amplification cycle initiated with a 10-second denaturation step at 98°C, followed by a 30-second primer annealing step at a temperature determined by the nature of the primer pair used (3°C below the calculated melting temperature) and concluded with an amplification step at 72°C, the duration of which was dependent on the template length (30 seconds per kilobase). The PCR cycle was repeated 35 times.

2.1.3 DNA fragment purification on agarose gel

The resulting PCR fragments were run on 1% agarose (w/v) gels by electrophoresis at 100V for 20 min. The fragments of interest were excised from the gel using a scalpel and subsequently purified with a Monarch DNA gel extraction kit (New England Biolabs N° T1020L) according to the manufacturer's protocol.

2.1.4 Restriction Enzyme Digestion of plasmid vectors

One or two selected restriction enzymes were used to digest the purified plasmid vectors, resulting in a directional insertion of PCR fragments of interest into the compatible plasmids. The restriction digestion reaction included ~500 ng of plasmid DNA, 0.5 U/µL of restriction enzyme, the recommended buffer for maximal enzyme activity in a final volume of 20 µL and was incubated at 37°C for 2 hours. The digested

plasmids were subjected to electrophoresis on 1% agarose (w/v) gels at 100V for 20 min, while ~100 ng non-digested vectors were loaded for comparative analysis.

2.1.5 DNA fragment assembly by the Gibson method

The Gibson assembly method enables the directional assembly of multiple DNA fragments with overlapping sequences (Gibson et al., 2009). The DNA fragments, generated by PCR and by backbone plasmid digestion, were assembled by combing about 15 fmol of each fragment in a Gibson reaction mix. The mix contained 100 mM Tris-HCl pH 7.5, 10 mM $MgCl_2$, 0.2 mM dATP, 0.2 mM dCTP, 0.2 mM dGTP, 0.2 mM dTTP, 10 mM dithiothreitol, 0.05 g/mL polyethylene glycol (PEG)-8000, 1 mM NAD, 2.5 mU/µL T5 exonuclease (New England Biolabs N°M0363S), 25 mU/µL Phusion High fidelity DNA polymerase (New England Biolabs N°M0530S) and 4 U/µL TAQ DNA ligase (New England Biolabs N°M0208S) in a final volume of 20 µL. Following incubation at 50°C for 1 hour, the reaction mix was ready for use in transformation experiments.

2.1.6 *Escherichia coli* transformation and selection of transformants

The commercially available NEB5-alpha competent *E. coli* cells (C2987H, New England Biolabs) were used for heat choc transformation according to the manufacturer's instructions. 5 µL of the Gibson reaction mix were incubated with 25 µL of competent cells, while the appropriate digested DNA backbone without any insertion was added as a negative control. Around 400 µL of the transformed bacteria were cultivated for a minimum of 12 h at 37°C. Colonies that appeared on the selection medium were screened by PCR to verify the presence of the desired construct, and thus the success of the transformation.

2.1.7 PCR screening and Sanger sequencing

To confirm the existence of a plasmid containing the construct of interest in an *Escherichia coli* colony cultivated on LB-agar, PCRs were conducted directly with the colonies using the Taq DNA polymerase (Euromedex). The PCR reaction contained 1.5 mM $MgCl_2$, 0.2 mM of dNTPs (dTTP, dATP, dCTP, dGTP), 0.5 µM of forward and reverse primers, 0.02 U/µL of Taq DNA polymerase for a final reaction volume of 15 µL. The bacterial colony was introduced using a pipette tip, while a blank template served as a negative control in an individual PCR reaction. The samples were put in a thermal cycler (T100™, BioRad) and subjected to denaturation for 5 min at 94°C. Each cycle commenced with a denaturing step at 94°C for 10 seconds, followed by a 30-second primer annealing step at a temperature specific to the primer pair's nature (3°C below the calculated melting temperature) and ended with an amplification step at 72°C. The length of the template determined the duration of the PCR amplification cycle, with a rate of 1 minute per kilobase. The PCR cycle was iterated 40 times. PCR products were analyzed on 1% agarose gel (w/v). Colonies with the proper insert size were selected to extract plasmid DNA using commercial Miniprep kits (Macherey-

Nagel NucleoSpin) according to the manufacturer's protocol. The quantity of extracted plasmid was assessed by spectrophotometry (NanoDrop 2000, Thermo).

Sanger sequencing was performed by the Macrogen sequencing service according to the Sanger sequencing technique (Sanger et al., 1977).

2.1.8 *Agrobacterium tumefaciens* transformation

The competent *A. tumefaciens* C58C1 cells were previously generated by the laboratory and dispensed into 100 µL aliquots per tube. 600 ng of plasmid DNA were introduced to 100 µL of competent cells, subjected to a 30-second incubation for cell thawing, followed by gentle mixing and a 5-minute incubation at 37°C in a water bath. 900 µL of LB were added, and the cells were incubated for 2 h at 28°C for recovery. Subsequently, the cells were spread on LB-agar containing the appropriate antibiotics for plasmid selection. The bacteria plates were cultivated at 28°C for 2-3 days until visible colonies appeared.

2.1.9 Cryopreservation of *Escherichia coli* and *Agrobacterium tumefaciens* strains

A single colony of either *E. coli* or *A. tumefaciens* strains was scratched from a corresponding selection LB-agar plate, and then inoculated in 10 mL of liquid LB medium containing the same selection antibiotics. *E. coli* and *A. tumefaciens* strains were cultivated at 37°C and 28°C, respectively, with agitation at 180 rpm for 16 h or 24 h, respectively. The bacterial cultures were blended with sterile glycerol to a final concentration of 20% (v/v) glycerol and flash-frozen in liquid nitrogen prior to storage at -80°C.

2.2 Transient transgene expression in *Nicotiana benthamiana* by agroinfiltration

A. tumefaciens C58C1 transformed with the desired constructs and the *A. tumefaciens* strain expressing P19 protein were inoculated in 10 mL of LB medium containing the prescribed antibiotics and 20 µM acetosyringone for 24 hours at 28°C with continuous agitation at 180 rpm, respectively. All the cultures were then centrifuged for 10 min at 4 000 rpm. The pellets were resuspended in 5 mL of agro-infiltration buffer ($MgCl_2$ 1 mM, acetosyringone 200 mM) and further diluted to achieve bacterial suspensions of 5 mL to 10 mL with an optical density measured at 600 nm set to one. Subsequently, different *A. tumefaciens* strains designated for agroinfiltration were combined in a 1:1 ratio.

A minor superficial laceration was created with a needle on the upper surface of young leaves from 4-week-old *Nicotiana benthamiana* grown under controlled conditions (see **section 1.3.2**). An appropriate volume of the mixed bacterial suspension was gently injected into the leaf laceration using a 1 mL syringe until the entire leaf surface was saturated. The agroinfiltrated plants were then returned back to the controlled growth conditions and grown for a minimum of 2 days before the observations by confocal microscopy.

2.3 *Agrobacterium*-mediated transformation of *Arabidopsis thaliana* by floral dip

Arabidopsis thaliana wild type plants were grown to the flowering stage (around 7 weeks) in a 16h-8h light-dark photoperiod until the inflorescences exhibited a substantial number of floral buds. To obtain more floral buds per plant, the initial inflorescence was clipped to relieve apical dominance and to promote simultaneous emergence of multiple secondary bolts. Meanwhile, pre-cultures of *Agrobacterium tumefaciens* strains were inoculated in 2 mL of liquid LB medium with the appropriate antibiotics from a single colony on the plate. Subsequently, the pre-cultures were transferred to 100 mL of liquid LB medium containing the same antibiotics supplemented with 50 µM acetosyringone and grown for an additional 16 hours at 28°C under 180 rpm agitation. After 16 h of growth, the OD600 values of the cultures were measured, and 140 OD equivalents were harvested following a centrifugation at 5 000 x g for 20 min. The bacterial pellets were collected and resuspended in 200 mL of floral dip buffer (2.1 g/L Murashige & Skoog with vitamins (MSP09, Caisson Labs), 5% (w/v) sucrose, 0.05% (v/v) Silwet L-77 adjuvant, 200 µM acetosyringone).

All the inflorescences of the plants were submerged in the *Agrobacterium* solution for 30 seconds. The dipped plants were isolated in a plastic tray and covered with a tall clear-plastic dome to maintain humidity, and kept in the dark for the initial 48 h, then returned to the greenhouse grown under standard conditions. The domes were removed around 24 hours after the treatments. The plants were grown for additional one month and stored on a drying room (25°C, low humidity) until the siliques attained a brown and dry state. Seeds were harvested and stored in the Eppendorf tubes at room temperature.

To select the putative transformants, seeds were surface sterilized and sown on soil. Two to three weeks after the sowing, seedlings were sprayed with an aqueous solution containing 0.1% (v/v) of Basta herbicide containing glufosinate-ammonium (Basta®, Profert). Seedlings effectively transformed with the transgene carrying a gene resistant to the herbicide, enabled to continue growing. Resistant plants were passed on new soil pot and grown to harvest seeds as described above.

2.4 β-oxidation mutants genotyping

2.4.1 Genotyping of Arabidopsis plant leaves without prior DNA purification

To begin the genotyping assay directly on Arabidopsis plant leaves, Phire Plant Direct PCR Kit (F130WH, ThermoScientific) (Chum et al., 2012) were used to formulate a 20 µL PCR reaction. A 0.50 mm punch was cut from the Arabidopsis mutant or Col0 as a control leaves using a puncher. The excised samples were dropped into 1.5 mL Eppendorf tubes containing the Phire PCR dilution buffer and ground with a 200 µL pipette tip by briefly pressing the leaf samples against the tube walls, followed by a microcentrifugation until the plant tissues were settled at the bottom of tubes. 0.5 µL of the supernatant were taken for the PCR

as a template, while negative controls with only water or wild type sample were also included as templates in the PCRs for comparative analysis. The PCR program was adapted from **section 2.1.2** with a difference of 40 amplification cycles. After PCR, the resulting products were run on agarose gel electrophoresis as described in **section 2.1.3** and, for *pxa1* lines, were sent for Sanger sequencing as described in **section 2.1.7** to confirm the homozygous lines.

2.4.2 Genotyping of Arabidopsis calli

Extraction of genomic DNA from *Arabidopsis thaliana* calli was performed following a method adapted from Dellaporta et al., 1983.

A small piece of calli (around 100 mg) was collected and placed in a 1.5 mL Eppendorf tube. 200 µL of CTAB (cetyltrimethylammonium bromide) buffer (CTAB 2% (w/v) heated at 60°C, NaCl 1.4 M, Tris-HCl 100 mM pH 7.5, EDTA 20 mM, dithiothreitol (DTT) 10 mM) were added to the tube. Calli were grounded on ice with a sterile piston. Subsequently, 800 µL of CTAB buffer were added, and the mixture was incubated at 60°C for 30 min in a water bath, followed by centrifugation for 15 min at 16 000 x g at room temperature. 500 µL of the supernatant typically were collected and transferred to a new tube, thoroughly mixing with an equivalent volume of chloroform-isoamylalcohol (24:1) for 10 s. After centrifugation for 10 min at 16 000 x g, 400 µL of the upper phase were collected and mixed with an equal volume of cold isopropanol. The mixture was incubated at -20°C for 1 h and then centrifuged for 15 min at 16 000 x g at 4°C to pellet genomic DNA. The pellet was then washed with 1 mL of cold 70% ethanol, air-dried for 10 min at 37°C, resuspended in sterile water and stored at -20°C.

The subsequent genotyping steps conducted via PCR were identical to those outlined in **section 2.4.1**.

3 Protein analysis

3.1 Total protein extraction from *Arabidopsis thaliana* leaves or calli

A small quantity of calli or plant leaves was collected and transferred into a resistant 2 mL bead-beater tissue homogenizer tube (PreCellys® 2 mL Empty Reinforced Tubes). 200 µL of protein buffer (8 M urea, 50 mM Tris-HCl pH 6.8, 1 mM EGTA, and 10 mM DTT) were added, along with approximately one spatula of 425-600 µm acid-washed glass beads (Sigma-Aldrich). The mixture was heated at 70°C for 5 min, and then grounded in a bead-beater tissue homogenizer (PreCellys® Evolution, Ozyme) at 4°C with 3 rounds of 20 s agitation at 10 000 rpm, between each step followed by a 30-second pause. This heating and grinding cycle was repeated once. Subsequently, the cell homogenate was centrifuged at 5 000 x g at 4°C for 5 min. The resultant supernatant, constituting the total protein extract, was transferred into a new Eppendorf tube, which either can be stored at -20°C or maintained on ice for the subsequent manipulations.

3.2 Protein concentration determination

3.2.1 Bradford assay

The protein concentration was determined by a colorimetric protein assay with Coomassie blue protein-dye binding (Bradford, 1976). The dye reagent (Bio-Rad, Protein Assay Dye Reagent Concentrate, composition undisclosed) was diluted five-fold in water and dispensed into spectrophotometry cuvettes, with each cuvette containing 1 mL of the diluted reagent. An appropriate volume of the sample (ranging from 0.2 µL to 10 µL) was thoroughly mixed with the dye, and the absorbance values were read at 595 nm using a spectrophotometer (Eppendorf Biophotometer D30). Protein concentration was determined by a bovine serum albumin (BSA) standard curve as a reference according to Lambert-Beer's law.

3.2.2 Coomassie blue staining

If BSA was originally present in the protein extraction buffers, protein concentrations could be further verified by SDS-PAGE (see **section 3.3**) followed by Coomassie blue staining. Gel was covered with 20 mL of Instant blue staining solution (InstantBlue® Coomassie Protein Stain (ISB1L), ABCAM) for 15 min at room temperature, and then washed for 3 times with water prior to photography by a luminescence detection system (GelDoc, Coomassie blue staining, Bio-Rad).

3.3 Polyacrylamide gel electrophoresis in denaturing conditions (SDS-PAGE)

Polyacrylamide gel electrophoresis (PAGE) under denaturing conditions using sodium dodecyl sulfate (SDS) as denaturing agent allows to separate proteins based on their molecular mass, independent of their intrinsic electric charge. Proteins samples, typically for 20 µg, were mixed with a denaturing buffer (LDS (4X) NuPAGE™, Life technologies) and a reducing buffer (Sample reducing agent (10X) NuPAGE™, Life technologies) in a final volume of 40 µL to impart a negative charge to the proteins and to disrupt their structure and unfold them. Samples were heated at 95°C for 5 min to complete the denaturation, and then loaded on a pre-cast polyacrylamide gel (NuPAGE™ 4 to 12 % Bis-Tris minigel, Life Technologies). 3 µL of a molecular weight marker (Precision Plus Protein™ Dual Color Standards, BioRad) was co-migrated alongside the samples to assess the molecular masses of the proteins contained in the samples. The gel electrophoresis was conducted in a Mini Gel Tank (Life Technologies) at 100V for around 2 h.

3.4 Protein immunoblotting (Western Blot)

Immunoblotting enables the specific identification of the protein of interest in a complex protein sample previously separated by SDS-PAGE using a specific antibody. Pieces of nitrocellulose membrane (Amersham Protran 0.2 µm) and Whatman papers were cut to match the size of the polyacrylamide gel, and immersed in containing 20% ethanol. A standard Western blot sandwich was then assembled as positioning the polyacrylamide gel on the negatively charged pole and directly adjacent to the nitrocellulose

membrane, allowing the migration of negatively charged proteins from the gel to the membrane. Transfer was performed in 1X transfer buffer (ThermoFisher Scientific) at 25 V for 1h with agitation and cooling in a Mini Gel Tank (Life Technologies). After the transfer, the membrane was washed for three times in water and reversibly stained with Ponceau red (0.2% (w/v) Ponceau red, 3% (v/v) trichloroacetic acid) to confirm the presence of proteins on the membrane and to probe their integrity and charged amount. Subsequently, the membrane was destained by three washes in Tris-buffered saline (TBS: Tris-HCl 20 mM, NaCl 150 mM, pH 7.6) containing 0.1% (v/v) Tween® 20 (TBS-T) and incubated in TBS-T milk 5% (w/v) for a minimum of 1 h with agitation for aspecific sites blocking. Primary antibodies (**Table 9**), appropriately diluted in TBS-T milk 5% (w/v), were then applied to the membrane overnight at 4°C with mild agitation. If the primary antibodies are not horseradish peroxidase (HRP)-conjugated, secondary antibodies (**Table 9**) coupled to the aforementioned enzyme diluted in TBS-T milk 5% (w/v) were mandatory to be used after three washes in TBS-T, and then incubated for 5 h at 4°C under mild agitation. The membrane was then washed three times for 10 min with TBS-T to eliminate the unbound antibodies. The entire incubation program was achieved by Bandmate™ Automated Western Blot Processor (ThermoFisher Scientific). The detection of HRP-conjugated antibodies was accomplished by applying Clarity™ or Clarity Max Western ECL Substrate (Bio-Rad) containing luminol and H_2O_2. HRP can catalyze luminol oxidation, which generates light emission at 428 nm that can be detectable using a luminescence detection system (Amersham ImageQuant 800). Quantifications of the detected bands density were performed by ImageQuantTL software.

Antibody name	Type	Dilution	Host	Application	Reference
Anti-PEX14	Polyclonal	1/20000	Rabbit	Organelle marker, peroxisome	Agrisera Ref. AS08372
Anti-CAT	Polyclonal	1/1000	Rabbit	Organelle marker, peroxisome	Agrisera Ref. AS09501
Anti-GOX	Polyclonal	1/1000	Rabbit	Organelle marker, peroxisome	Agrisera Ref. AS142772
Anti-DEG15	Polyclonal	1/500	Rabbit	Organelle marker, peroxisome	Agrisera Ref. AS10177
Anti-HPR	Polyclonal	1/10000	Rabbit	Organelle marker, peroxisomal matrix	Agrisera Ref. AS111797
Anti-UGPase	Polyclonal	1/1000	Rabbit	Organelle marker, cytosolic proteins	Agrisera Ref. AS05086
Anti-BIP2	Polyclonal	1/10000	Rabbit	Organelle marker, ER	Agrisera Ref. AS09481
Anti-COXII	Polyclonal	1/1000	Rabbit	Organelle marker, mitochondria inner membrane	Agrisera Ref. AS04053A
Anti-B14.7	Polyclonal	1/5000	Rabbit	Organelle marker, mitochondrial inner membrane	Biotem
Anti-RISP	Polyclonal	1/10000	Rabbit	Organelle marker, mitochondrial inner membrane	provided by Dr. Monika Murcha, University of Western Australia
Anti-NDPK	Polyclonal	1/5000	Rabbit	Organelle marker, mitochondrial intermembrane space	Agrisera Ref. AS08302
Anti-VDAC	Polyclonal	1/1000	Rabbit	Organelle marker, mitochondrial outer membrane	Provided by André Dietrich (IBMP, Strasbourg)
Anti-PMD2	Polyclonal	1/2000	Rabbit	Organelle marker, mitochondrial outer membrane	(Michaud et al., 2016)
Anti-V-ATPase	Polyclonal	1/2000	Rabbit	Organelle marker, vacuole	Agrisera Ref. AS07213
Anti-H^+-ATPase	Polyclonal	1/3000	Rabbit	Organelle marker, plasma membrane	Agrisera Ref. AS07260
Anti-TIC40	Polyclonal	1/2500	Rabbit	Organelle marker, chloroplast inner envelope	Agrisera Ref. AS10709
Anti-HA	Monoclonal	1/5000	Mouse	Protein tag	Sigma Ref. H9658
Anti-HA-HRP	Monoclonal	1/1000	-	Protein tag	Miltenyi Biotec
Anti-Rabbit (2°)	Polyclonal	1/10000	Goat	Secondary antibody	Interchim Ref. 115-035-003
Anti-Mouse (2°)	Polyclonal	1/10000	Goat	Secondary antibody	Interchim Ref. 111-035-003

Table 9. List of primary and secondary (2°) antibodies used in this study.

4 Plant phenotype analysis

4.1 *Arabidopsis thaliana* calli growth assay

Five pieces of calli of comparable size from the wild-type Arabidopsis and mutants, respectively, were carefully excised using a scalpel, and then placed onto a square plate containing 1 mM or zero Pi (**Table 6**). The plates were grown in continuous light conditions at 22°C, and the growth was monitored every 7 days over the span of one month. The area of each calli was quantified by Image J software.

4.2 *Arabidopsis thaliana* root growth assay

Seeds from wild type and mutants were surface sterilized and vernalized as described in **section 1.3.1**, and then placed onto square plates containing full MS and enriched Pi (**Table 7**) grown under normal conditions outlined in **section 1.3.3**. After the germination for 4 days, seedlings of similar size were carefully transferred onto either agar-plate culture system or into liquid culture system in 6-well plates (CytoOne®) in the presence or absence of Pi, as described in **section 1.3.6**. After growth periods of 3 to 6 days in liquid culture, or 7 to 14 days on agar plates, seedlings were used for experimental analysis, respectively. Quantifications of the length of the primary roots, or lateral roots or root hairs were performed manually using Image J software.

5 Subcellular organelle fractionation

5.1 Peroxisome purification by Percoll gradients centrifugation from *Arabidopsis thaliana* calli in the presence or absence of Pi

Protocol for peroxisome purification from calli was adapted from Taylor et al., 2014. The purification process was illustrated in **Figure 12**.

Plant peroxisomes are highly fragile, thus necessitating meticulous handling procedures. To preserve their structural integrity and functionality, all the manipulations (including grinding, centrifugation, and fractionation) must be conducted at 4°C, and all the equipment and reagents (such as blender, tubes, rotors, and buffers) must be pre-chilled to 4°C prior to use. Approximately 100 g of 4-day-old Arabidopsis calli were required for one peroxisome isolation fraction.

Arabidopsis thaliana calli were cultured in liquid medium with or without Pi for 4 days, followed by a filtration through a glass fiber filter (Merck, AP1509000) using a vacuum filtration unit. The filtered cells were weighed and immediately transferred into a pre-chilled blender. Two volumes of the extraction buffer (0.45 M mannitol, 0.05 M $Na_4P_2O_7$, 0.5% (w/v) bovine serum albumin (BSA), 0.5% (w/v) PVP40, 2 mM

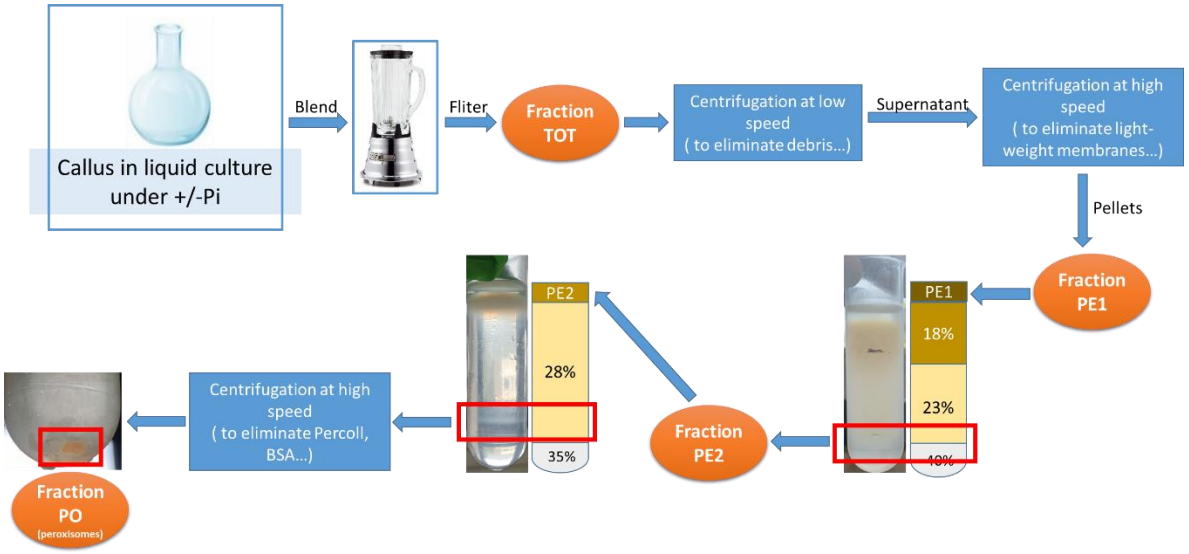


Figure 12. Protocol used to purify peroxisomes from *Arabidopsis thaliana* calli cultures, adapted from Taylor NL et al., 2014.

EGTA, 0.02 M cysteine, adjusted to pH 8.0 using phosphoric acid) per calli weight were added to the blender. The cells were blended at high speed for 15 s and at low speed for two-repeated 15 s, with 30-second intervals between each blending cycle. The resulting lysate was then filtered through one layer of Miracloth and two layers of muslin, applying consistent gentle pressure to eliminate starch, cell debris, and unbroken cells. 200 µL of the crude extract was taken for total proteins analyses as "TOT" fraction.

Subsequently, the crude extract was transferred into a 250 mL bucket that fitted in the JA10 (Beckman Coulter) rotor and centrifuged at 1 500 x g for 10 minutes at 4°C to pellet unbroken cells and heavy materials. The supernatant was collected with a pipette and distributed into 35 mL centrifuge tubes that fitted in a JA25.50 rotor (Beckman Coulter), followed by an ultracentrifugation at 18 000 x g for 15 minutes at 4°C. This step was repeated once. The pellets were then gently resuspended in cell peroxisome washing buffer I (0.3 M mannitol, 0.01 M TES-KOH pH 7.5) using a soft paintbrush and transferred to a Potter-Elvehjem tissue grinder. After homogenization, the crude peroxisome fraction was adjusted to a total volume of 16 mL with cell peroxisome washing buffer I. A 200 µL aliquot of the crude peroxisome fraction was reserved for proteins analyses as "PE1" fraction.

Eight discontinuous gradients were prepared by layering 40%, 23% and 18% Percoll solutions in 35 mL ultracentrifuge tubes. 2 mL of the "PE1" fraction was carefully added on top of each ultracentrifuge tube and centrifuged at 40 000 x g for 30 minutes at 4°C, with acceleration "Max" and deceleration "Slow". Peroxisomes were recovered at the 23%-40% Percoll interface. After the removal of the upper gradient portion, the peroxisome fraction was retrieved and washed by resuspending in cell peroxisome washing

buffer I and centrifuging for 30 min at 39 000 x g at 4°C. The pellets were then collected and homogenized. 200 µL of the crude peroxisome pellets was taken for proteins analyses as "PE2" fraction.

A second Percoll gradient was required to separate peroxisomes from mitochondria by layering 35% and 28% Percoll solutions in two 35 mL ultracentrifuge tubes. 2 mL of the "PE2" fraction were carefully added on top of each ultracentrifuge tube and centrifuged at 40 000 x g for 20 minutes at 4°C, with acceleration "Max" and deceleration "Slow". Peroxisomes should appear at the lower part of the 28% fraction as white bands. The peroxisome bands were then transferred into 38 mL SW 32 Ti ultracentrifuge tubes that fitted in SW 32 Ti Swinging-Bucket Rotor (Beckman Coulter) and resuspended with cell peroxisome wash buffer II (0.4 M sucrose, 0.01 M TES-KOH pH 7.5), followed by an ultracentrifugation at 39 000 x g for 30 min at 4°C, with acceleration "Max" and deceleration "Slow". The resultant pellets were collected for the subsequent ultracentrifugation at 100 000 x g for 30 min at 4°C. This ultracentrifugation step was repeated once to eliminate BSA. The final pellets were collected and immediately flash-frozen in liquid nitrogen, then stored at -80°C as the isolated "PO" sample.

5.2 Proteomic analysis of isolated peroxisomal proteins from *Arabidopsis thaliana* calli in the presence or absence of Pi

5 µg to 10 µg of isolated peroxisomal proteins from *Arabidopsis thaliana* calli in the presence or absence of Pi, mixing with a denaturing buffer (LDS (4X) NuPAGE™, Life technologies) and a reducing buffer (Sample reducing agent (10X) NuPAGE™, Life technologies) in a final volume of 30 µL to 80 µL, were loaded on a polyacrylamide gel (NuPAGE™ 4 to 12 % Bis-Tris minigel, Life Technologies) and blue-stained by Coomassie blue staining (InstantBlue® Coomassie Protein Stain (ISB1L), ABCAM).

Proteomic analysis were performed by Julia Novion Ducassou and Yohann Couté (EDyP-lab, Grenoble).

6 Lipid analysis

6.1 Glycerolipid extraction by the Folch method

The glycerolipids from solid biological samples were extracted using the Folch method (Folch et al., 1957).

Typically, approximately 0.3 g of calli or seedlings, or a quantity of isolated peroxisomes equivalent to approximately 100 µg of peroxisomal proteins were required for lipid extraction. Calli or seedlings were collected and immediately flash-frozen in liquid nitrogen and stored at -80°C to prevent lipase activity. Before extraction, the biological materials were lyophilized overnight using a lyophilizator (Christ Alpha 2-4 LDplus) to eliminate water from the samples and prevent lipase activity.

The lyophilized samples, which were constantly kept in liquid nitrogen to prevent lipase activity, were transferred to 35 mL Corex tubes pre-chilled in liquid nitrogen. Subsequently, the samples were ground using a Potter-Elvehjem pestle to ensure maximal surface contact with the solvents. 4 mL of boiling ethanol were added to the samples and then incubated for 5 min at 90°C to inhibit lipase activity. 2 mL of methanol and 8 mL of ethanol-stabilized chloroform were then added, and the samples were homogenized by bubbling argon through them to further safeguard the lipids from oxidation. Following this, samples were incubated for a minimum of 1 h at room temperature under an argon atmosphere before being filtrated through quartz wool into another Corex tube to eliminate cellular debris. The organic phase containing the lipids was separated from the hydrophilic phase by adding 3 mL of chloroform/methanol (2:1 v/v) and 5 mL of 1% (w/v) NaCl. After the homogenization by bubbling argon, the samples were centrifuged for 10 min at 2000 rpm at room temperature, and the inferior organic phase was collected. The lipid extracts were obtained by evaporating the organic phase under argon. Lipid films can be stored at -20°C for several months without degradation if maintained in an argon atmosphere.

6.2 Methanolysis of total lipid extracts

Methanolysis represents a nucleophilic transesterification process in which the acyl groups disengage from the glycerol skeleton and esterified to methanol, thereby generating fatty acid methyl esters (FAMEs). FAMEs can serve as indicators to determine the total lipid content of the lipid extracts.

The lipid extracts were resuspended in 1 mL of ethanol-stabilized chloroform, and 50 µL of lipid extracts, combining with 5 µg of internal standard (C15:0, a saturated odd chain fatty acid containing 15 carbons), were prepared for the methanolysis robot (LIPANG platform, LPCV). The hydrophobic FAMEs were automatically retrieved though the methanolysis program by the methanolysis robot and maintained in hexane phases. The collected hexane phases underwent evaporations under argon and the resultant FAMEs can be stored at -20°C.

6.3 Fatty acid and lipid quantification

6.3.1 Quantification of fatty acid methyl esters (FAMEs) by gas chromatography coupled to ion flame detection 32 (GC-FID)

The FAMEs were resuspended in 100 µL of hexane and analyzed by gas chromatography-flame ionization detector (GC-FID) (Perkin Elmer Clarus 580). The GC column was maintained at 180°C, and nitrogen served as the vector gas. FAMEs were identified by comparing their retention times to the standards (Sigma-Aldrich) and quantified by the surface peak method with the C15:0 fatty acid as the internal standard for calibration. The measured quantity of FAMEs allowed for the determination of the glycerolipid concentration in the original samples.

6.3.2 Quantification of glycerolipids by high performance liquid chromatography coupled to triple quadrupole mass spectrometry (HPLC-MS/MS)

The samples of lipid extracts, equivalent to 25 nmol of total fatty acids, were prepared in chloroform. Lipid analysis by high performance liquid chromatography (HPLC)-MS/MS was performed on the LIPANG (Lipid Analysis in Grenoble) platform directed by Juliette Jouhet. Quantification analyses by MS/MS were conducted by Juliette Jouhet, Morgane Michaud and Marion Schilling.

7 Imaging techniques

7.1 Laser scanning confocal microscopy

Laser scanning confocal microscopy was performed on a microscope Zeiss LSM880 equipped with a 40x and a 63x/1.4 oil-immersed Plan-Apochromat objective, running Zen 2.3 SP1 acquisition software (Platform μLife, IRIG, LPCV). The 63x objective was used for acquisitions.

The cell lines used for transient expression in *Nicotiana benthamiana* leaves for the confocal fluorescence microscopy were listed in **Table 8**. The employed mitochondrial organelle marker used in living cells was MitoTracker Orange CMTMRos (M7510, ThermoFisher).

YFP was excited at 513 nm at 2.8% laser capacity and its fluorescence was detected between 519 nm and 550 nm with a photomultiplier tube detector set to 800V. CFP was excited at 485 nm at 2.4%-8.0% laser capacity and its fluorescence was detected between 463 nm and 502 nm with a photomultiplier tube detector set to 800V. eGFP was excited at 488 nm at laser capacities between 2.6% and 2.8% and its fluorescence was detected between 507 nm and 556 nm with a photomultiplier tube detector set to 800V. Chlorophyll was excited at 633 nm at laser capacities between 2.8% and auto-fluorescence was detected between 642 nm and 698 nm with a photomultiplier tube detector set to 800V.

At least 10 images were taken randomly over the whole sample within two leaves. Images were visualized and quantified with the ImageJ software running the image processing package Fiji.

Chapter 1

Optimization of a peroxisome isolation protocol from *Arabidopsis thaliana* calli to study peroxisomal lipidome and proteome in response to Pi starvation

1 Overview of plant peroxisomes

Peroxisomes are small, ubiquitous organelles present in most eukaryotes, delineated by a single lipid bilayer membrane and lacking genetic material. Peroxisomal assembly and proliferation rely on peroxin (PEX) proteins (Jansen et al, 2021; Cross et al., 2016). Three models have co-existed regarding the biogenesis of peroxisomes and are likely to operate within the same cells in response to specific environmental cues. Initially, it was widely believed that peroxisomes originated from the growth and fission of pre-existing ones in a 3-step process, including the elongation of the peroxisomal membranes, the membrane constriction, and eventually the fission of peroxisomes (**Figure 13B**; Farré et al., 2019; Lazarow & Fujiki, 1985; Lodhi & Semenkovich, 2014). The second model invokes *de novo* peroxisome biogenesis, in which peroxisomes are integrated into the endomembrane system (**Figure 13A**). In this model, some peroxisomal membrane proteins (PMPs) are firstly inserted into the ER membrane and sorted to a region of the ER, called the pre-peroxisomal ER (pER), from where pre-peroxisomes vesicles (ppVs) budded off, carrying lipids and some membrane proteins. Subsequently, peroxisomes become mature followed by the fusion of distinct ppVs, either heterotypically or with a pre-existing peroxisome (**Figure 13A**; Farré et al., 2019; Hu et al., 2012; Tabak et al., 2013). The third model combines features of both the growth and division model and the *de novo* biogenesis model via the ER (Motley et al., 2015). Though most of the work were conducted in yeast, similarities have been found in plants (Farré et al., 2019; Hua et al., 2017; Mullen et al., 1999; Orth et al., 2007).

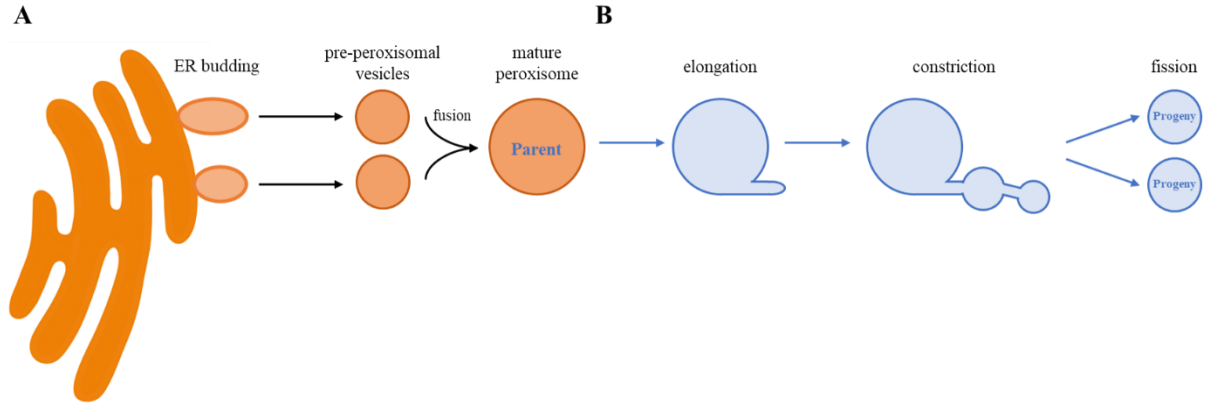


Figure 13. Peroxisome dynamics. A. *De novo* peroxisome formation (in orange). After pre-peroxisomal vesicles (ppVs) budded from the ER, peroxisomes become mature following the fusion of distinct ppVs. B. The growth and fission model. Peroxisomes can be generated autonomously through the division of the pre-existing organelles in a 3-step process, including the elongation of the peroxisomal membranes, the membrane constriction, and eventually the peroxisome fission (in blue).

Moreover, in plants, the extending tubules from peroxisomes, known as peroxules, were also observed to extend along ER tubules and mirror the dynamic behaviors of ER, particularly under oxidative stress conditions (Sinclair et al., 2009). However, despite the frequent close proximity and interaction between

peroxisomes and the ER, no evidence of a direct connection between their lumens was detected (Barton et al., 2013).

In plant cells, peroxisomes perform diverse functions, including reactive oxygen species (ROS) and reactive nitrogen species (RNS) metabolism, hormone catabolism and signaling, FAs metabolic pathways (β-oxidation, see "General Introduction", **section 2.3.1**; and glyoxylate cycle), and viral infection (**Figure 14**; Ferreira et al., 2022; Hu et al., 2012; Kao et al., 2018; Pan et al., 2020; Reumann & Bartel, 2016). ROS and RNS metabolism occurring within peroxisomes can generate hydrogen peroxide (H_2O_2) and nitrite oxide (NO), respectively, which can be detoxified by catalase (CAT) in the matrix, ascorbate peroxidase (APX) on the membrane, and other peroxisomal enzymes to exit the peroxisomes and function in stress signaling (**Figure 14**; Corpas et al., 2017; Kao et al., 2018). The produced hormones within plant peroxisomes, such as auxin, jasmonic acid (JA) and salicylic acid (SA), are essential for seedlings growth and root development (**Figure 14**; reviewed in Kao et al., 2018). Peroxisomal β-oxidation can be used to catabolize the imported fatty acids to generate acetyl-CoA, and the seedling acetyl-CoA can be further metabolized by peroxisomal glyoxylate cycle, resulting in the formation of four-carbon dicarboxylic acids as the precursors for the synthesis of sucrose used for seedling growth (**Figure 14**; reviewed in Kao et al., 2018). The impairment of peroxisomal β-oxidation activity has been linked to embryo lethality, suggesting a

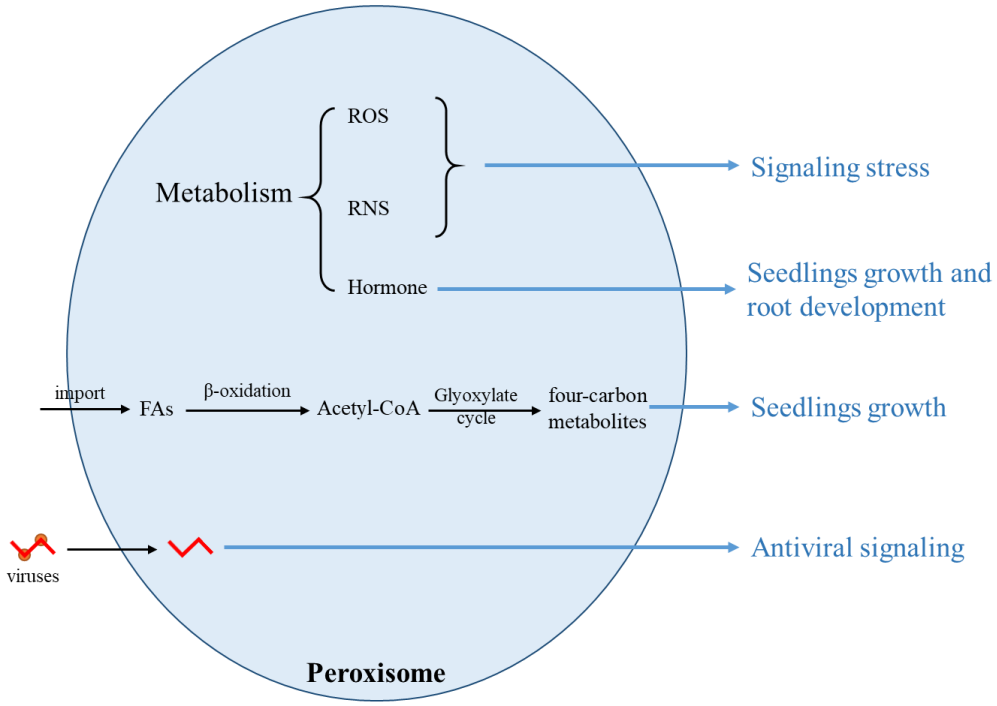


Figure 14. Plant peroxisome functions. Peroxisomes house a variety of biosynthetic and catabolic processes, including reactive oxygen species (ROS) and reactive nitrogen species (RNS) metabolism, hormone catabolism and signaling, FAs metabolic pathways (β-oxidation and glyoxylate cycle), and viral infection. ROS, reactive oxygen species; RNS, reactive nitrogen species; H_2O_2, hydrogen peroxide; FAs, fatty acids.

necessity for a role of β-oxidation process during embryogenesis (Footitt, 2002; Rylott et al., 2006). However, this observation seems to vary depending on the accession in Arabidopsis (Khan et al., 2012). Several plant viruses were reported to target peroxisomes to promote their propagation, suggesting that plant peroxisomes also play important roles in antiviral signaling (**Figure 14**; for a review, Ferreira et al., 2022).

2 Studies for the purification of Arabidopsis peroxisomes and proteomic analysis

Elucidating the protein and lipid composition of cellular compartment requires its isolation with certain experimental methods. However, the analytical depth concerning peroxisomes from the model plant *Arabidopsis thaliana* are lagging considerably behind other major cellular organelles, such as chloroplasts or mitochondria (Bussell et al., 2013). For instance, approximately 800 proteins have been identified through proteome studies in mitochondria (source: SUBA3; Tanz et al., 2013). Likewise, the number of reported plastidial proteins exceeds 2100 (source: SUBA3, http://suba.plantenergy.uwa.edu.au). Peroxisomes lack genetic components and proteins involved in genome replication, transcription or translation, therefore the predicted peroxisomal proteome of up to 670 proteins was clearly simpler compared to chloroplasts and mitochondria (Bussell et al., 2013).

The difficulties associated with plant peroxisomes purification is primarily because of 1) high peroxisome fragility *in vitro*, 2) much lower peroxisome abundance than, for example, mitochondria or chloroplasts, in most tissue types, 3) pronounced peroxisome adherence to plastids and mitochondria, particularly in photosynthetic tissue, 4) expected losses during the isolation procedure, and 5) high organ-specific and developmental plasticity in peroxisome functions (Bussell et al., 2013; Palma et al., 2009; Reumann, 2011; Reumann & Singhal, 2014). Therefore, the enriched peroxisome fractions often suffer from significant contaminations from other organelles. Low yields are also a common characteristic observed in peroxisome purification from Arabidopsis, consequently narrowing the error margins for the successful isolation and compromising the purity of peroxisome fractions.

Therefore, in terms of the challenges in isolating and purifying peroxisome, it is not surprising that the depth of investigation of the peroxisomal proteome has not yet reached that of other plant compartments fractions with good purity and detailed subcellular proteomes. So far, only a few research groups have achieved successfully to isolate peroxisome fractions from various tissue types and published their detailed isolation protocols (Eubel et al., 2008; Fukao et al., 2002, 2003; Reumann et al., 2007, 2009; Reumann & Singhal, 2014), with their experimental strategies summarized in **Table 10**.

	Fukao et al.	Reumann et al.	Eubel et al.	This study
Tissue type	greening or etiolated cotyledons	leaf	7-day-old cell suspension culture	4-day-old calli cell suspension cultures under +/-Pi
Minimum quantity of tissues	25 g	60-70 g	200 g	100 g
Grind methods	homogenizer (SMT COMPANY, Japan)	mortar and pestle	enzymatic digestion of the cell wall and then disruption by Potter-Elvehjem homogenizer	blender
A succession of differential centrifugation steps	to remove plastids and cell debris	to remove plastids and nuclei	to remove cell debris and concentrate the organelles	to remove cytosolic proteins, heavy organelles and cell debris
Density gradients	one discontinuous Percoll gradient	one discontinuous Percoll density gradient and one continuous sucrose density gradient	one discontinuous Percoll density gradient, followed by free-flow electrophoresis (FFE)	two discontinuous Percoll gradients
Analysis methods	measurements of enzymes activities, immunoblot analysis, proteomic analysis	enzymatic analyses, immunoblot analysis, proteomic analysis	enzymatic analyses, immunoblot analysis, proteomic analysis	immunoblot analysis, proteomic analysis
Relative evaluation of the strategy	high purity and high concentration	high purity at ~95%	high level of purity at 85% to 90%	low level of purity at ~10% (see **section 3.2**)

Table 10. Experimental strategies for the purification of Arabidopsis peroxisomes performed by Fukao et al., 2002, 2003; Reumann et al., 2007, 2009, 2014; Eubel et al., 2008; and in this study.

The proteomic analysis of mitochondria in *A. thaliana* have been documented for mitochondria from cell culture (Millar et al. 2001), from green tissue (leaves and stems; Kruft et al., 2001), etc. Likewise, proteomic analysis of peroxisomes in *A. thaliana* should be classified by different tissue origins and growth stages (**Table 10**), for example, glyoxysomes from cotyledons (Fukao et al., 2003), unspecialized peroxisomes from cotyledons, peroxisomes from cotyledons or mature plant leaves (Fukao et al., 2002; Reumann et al., 2007, 2009), and peroxisomes from cell cultures (Eubel et al., 2008).

Fukao et al., 2002, 2003 used peptide mass fingerprinting (PMF) to analyze proteins that were separated by two-dimensional iso-electric focusing/sodium dodecyl sulfate polyacrylamide gel electrophoresis (2D IEF/SDS-PAGE). 29 proteins were identified from greening Arabidopsis cotyledons (Fukao et al., 2002), whereas 19 proteins were detected in glyoxysomes of etiolated cotyledons (Fukao et al., 2003). The identified proteins included contaminants, which was assessed due to their reported presences in other organelles, the absence of peroxisome targeting signals (PTSs) that were used to confirm the peroxisomal matrix protein identity, and the lack of an apparent association with the expected metabolic functions in peroxisomes. In addition, only three proteins were notably found to overlap between these two studies from either greening or etiolated cotyledons (Fukao et al., 2002, 2003), indicating significant disparities in the protein composition of Arabidopsis leaf peroxisomes dependent on the cell's life cycle (Bussell et al., 2013; Michels et al., 2005).

Subsequently, because of the inherent technical limitations using 2D IEF/SDS-PAGE for protein separation, which biased against the identification of membrane proteins and abundant proteins, Reumann et al., 2007, 2009 employed alternative approaches complimented by shotgun MS to enhance analytical depth. They identified peroxisomal proteins by initially running the samples in a single lane of a SDS gel, followed by dividing the lane into 16 slices, each subjected to high-resolution tandem MS analysis. The subsequent validation of putative peroxisomal proteins was determined using *in vivo* subcellular localization of candidates fused to yellow fluorescent protein. In addition, a new purification method involving two density gradients was established. Throughout these studies, 43 novel peroxisomal proteins were identified, with approximately half of them (21; 49%) containing a previously defined PTS1 tripeptide (Reumann et al., 2007), contrasting with the peroxisomal proteome studies from greening and etiolated cotyledons (one protein with PTS signal out of 20; Fukao et al., 2002; three out of 13; Fukao et al., 2003). Additionally, Reumann et al., 2007 discovered three novel PTS1 tripeptides, expanding the putative PTS1 proteins encoded in the Arabidopsis genome by 40%, from 221 to 311. Therefore, the prediction of plant peroxisomal proteins significantly benefits from the proteomic data generated in these studies, in terms of increased sensitivity and specificity.

Unlike the earlier studies on Arabidopsis leaf peroxisomes, Eubel et al., 2008 chose non-green Arabidopsis cell suspension cultures grown in darkness for 7 days to elucidate the proteome of plant peroxisomes, thus reducing chloroplasts as a significant source of contamination in the peroxisomal fraction. Furthermore, to enhance the organelle purity, they utilized a free-flow electrophoresis (FFE) approach after the Percoll gradient, along with both gel-based (1D and 2D) and non-gel methodologies. This study identified 35 novel proteins via tandem MS, including hydrophobic ones that were not previously detected in leaf or cotyledon peroxisome studies (Fukao et al., 2002, 2003; Reumann et al., 2007, 2009; Reumann & Singhal, 2014). Of all, 21 proteins contained PTS1 or PTS2, and were predominantly involved in fatty acid oxidation (Eubel et al., 2008). However, the set of 29 proteins reported by Fukao et al., 2002, 2003 were missing in the study of Eubel et al., 2008, while none of the seven proteins associated with pathogen and herbivore defense in leaf peroxisomes documented by Reumann et al., 2007 were detected.

The differences between the sets from different tissues and developmental stages imply different requirements of peroxisomal functions. Glyoxysomes of cotyledons contain enzymes involved in fatty acid β-oxidation for the breakdown of fatty acids derived from storage TAGs during germination and the glyoxylate cycle to produce succinate, whereas leaf peroxisomes that are completely transformed from glyoxysomes in greening cotyledons additionally house enzymes for the photorespiration pathway prior to β-oxidation, such as glycolate oxidase (GO), hydroxypyruvate reductase (HPR) and alanine:glyoxylate aminotransferase 1 (AGT1; Fukao et al., 2002; Reumann et al., 2007). Moreover, leaf peroxisomes is also involved in signaling compounds and hormone production (Reumann et al., 2007, 2009). Peroxisome proteome of cell cultures included all of the classical peroxisomal pathways, such as fatty acid β-oxidation, ROS detoxification, hormone, carbon (C) and nitrogen (N) metabolism, organelle biogenesis, and surprisingly photorespiratory pathway even though they are not green and grown in the dark (Eubel et al., 2008). In addition, a notably absence of the glyoxylate cycle enzymes were observed in the study of Eubel et al., 2008, indicating that the cell culture organelles cannot be conclusively regarded to catalyze a glyoxylate cycle.

So far, there is an evident scarcity of studies examining the lipid composition of *A. thaliana* peroxisomes, regardless under stress conditions. Previous research has identified the phospholipid composition of peroxisomal membranes in various species, including rat liver, yeast, castor bean endosperm, and of glyoxysomal membranes from cotyledons of cotton seedlings (Chapman & Trelease, 1991; Donaldson & Beevers, 1977; Hardeman et al., 1990; Zinser et al., 1991). In this study, we attempted to determine the lipidome and proteome of Arabidopsis peroxisomes under standard conditions and during Pi starvation.

3 Results

In my PhD project, I chose to isolate peroxisomes from *A. thaliana* calli grown in liquid cultures, whose advantages are 1) the low abundance of plastid membranes and proteins that can be a source of contamination compared to green tissue, 2) that it is easier to control the media of cell cultures to study stress response and to obtain huge quantity of materials and 3) the possibility to obtain cell cultures from mutants of interest (Leterme et al., 2021). The purity of the isolated peroxisomes was assessed by Western blot using antibodies against proteins derived from different cell compartments and lipidomic analyses, as some lipids, such as the galactolipids and DPG, are specific plastidial and mitochondrial lipids, respectively.

I initially adapted a detailed protocol from Reumann & Singhal, 2014 for the isolation of leaf peroxisomes, as it has been successfully used to obtain peroxisomes of high purity for proteomic analyses. This protocol was based on a succession of Percoll/sucrose and sucrose gradients. However, our results were not satisfactory. Issues encountered with this protocol in our study included three aspects: low purity, low yield of the isolated peroxisomes, and non-reproducibility across separate experiments, as indicated by WB analyses from multiple attempts (data not shown). Several optimizations were conducted, such as modifying the grinding method for Arabidopsis calli to increase the yield, incorporating additional differential centrifugation steps to eliminate contaminations before loading onto the gradients, adding a continuous sucrose density gradients to enhance the purity, and culturing the Arabidopsis calli in the dark to reduce the physical organelle adherence between peroxisomes, chloroplasts, and mitochondria. However, the contaminations from mitochondria and chloroplast could still not be excluded, and none of these adjustments yielded satisfactory results (data not shown).

Subsequently, I employed another detailed protocol from Taylor et al., 2014 for the isolation of Arabidopsis green cell culture peroxisomes using two discontinuous Percoll gradient centrifugation. In our study, this protocol presented several challenges, including low yield, major contaminations from the cytosol and ER, minor contaminations from other organelles, and difficulties to pellet the eventual isolated peroxisomes fractions for lipid extraction (data not shown). To address these issues, multiple refinements were conducted, such as adding additional differential centrifugation steps to remove cell debris, heavy organelles and cytosolic proteins before loading onto the gradients, and increasing the final centrifugation speed to 100000 x g for 30 min to pellet isolated peroxisomes. The ultimately optimized protocol for peroxisome purification, which involved a succession of differential centrifugation steps and two-step purification by two Percoll density gradients (see “Materials and Methods”, **Figure 12**), proved to be highly successful and reproducible, as evidenced by WB results across replicates (data not shown). Western blot and lipidomic analyses were conducted to assess purity, and comparative lipidomic and proteomic analyses between Pi-

enriched (+Pi) and Pi-starved (-Pi) conditions were performed to characterize the lipidome and proteome of Arabidopsis peroxisomes under both standard and stress conditions.

3.1 Western blot analysis of isolated peroxisome fractions by Percoll gradients centrifugation from *A. thaliana* calli under both +/-Pi conditions

Peroxisomes were isolated from *A. thaliana* wild type (WT) calli in the presence and absence of Pi. The aliquots from different fractions were taken during peroxisome isolation ("TOT", "PE1", "PE2" and "PO", see "Materials and Methods", **Figure 12**) and were analyzed by Western Blot using antibodies against

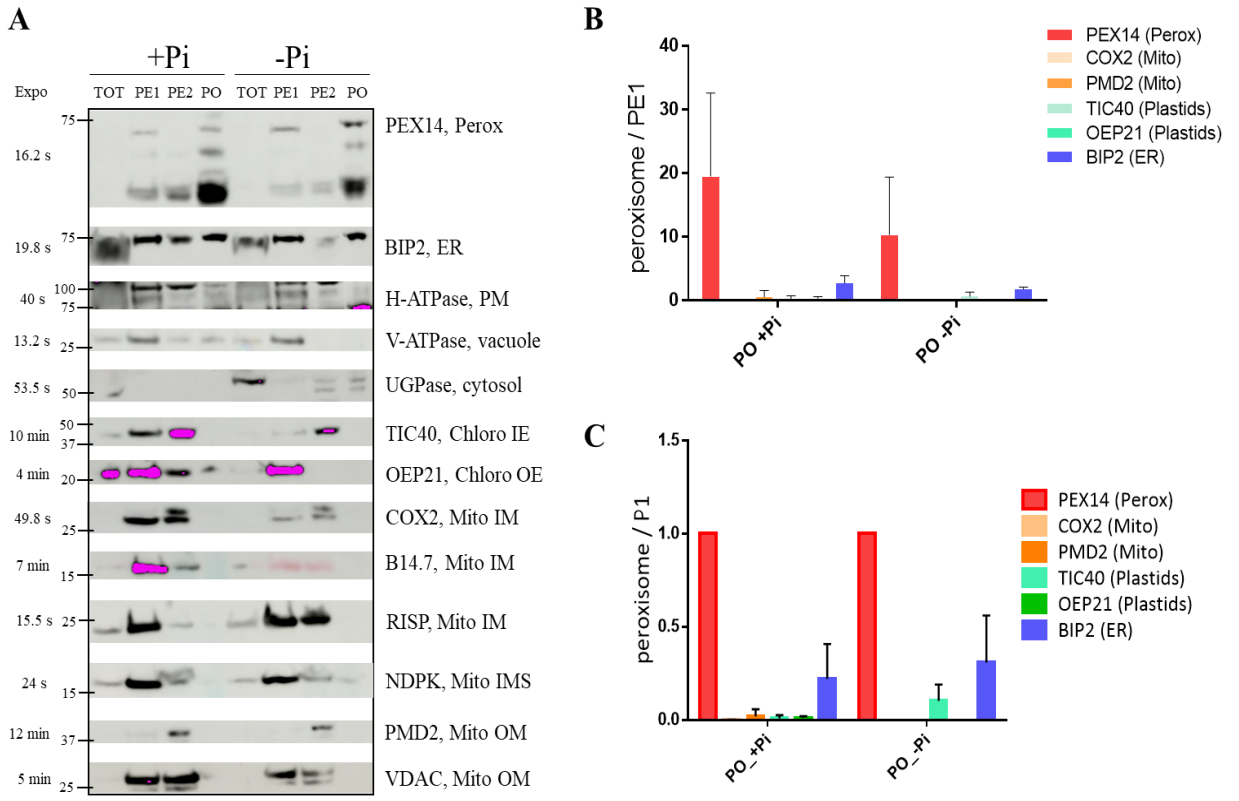


Figure 15. Analysis by Western Blots to assess the purity of the peroxisomal fractions isolated from *A. thaliana* calli cell cultures grown in presence or absence of phosphate. A. "TOT", "PE1", "PE2", "PO" fractions isolated from *A. thaliana* calli grown in +Pi or –Pi were collected to evaluate the enrichment of peroxisomes and the contaminations from other cell compartments at different purification steps by WB analysis. Aliquots of "TOT", "PE1", "PE2" containing 20µg of proteins, whereas fraction "PO" containing 10µg, verified by InstantBlue™ Coomassie Gel Staining, were loaded on each lane. Perox, peroxisome; ER, endoplasmic reticulum; PM, plasma membrane; IE, inner envelope; OE, outer envelope; IM, inner membrane; IMS, intermembrane space; OM: outer membrane. Observed molecular weights, in KDa, and the exposition times (Expo) on a chemiluminescence imager (Amersham ImageQuant 800), in second (s) or minute (min), were indicated on the left. B. Bar charts depicted the quantifications of the Western blot analyses in three separate experiments. Band intensities were quantified using the ImageQuant TL software. Values were firstly plotted taking the "PE1" fraction as a reference. Error bars represented the standard deviation (SD) from the average of three separate experiments. C. The PEX14 signals were then standardized to 1 in both + and –Pi conditions. The signals of other organelles were normalized relative to the PEX14 values, allowing for the comparison of contaminant levels between the two conditions.

proteins derived from different cell compartments (**Figure 15A**) to assess the purity of isolated peroxisomal fractions and the contamination levels from other cellular organelles.

Peroxin 14 (PEX14) is a peroxisomal membrane protein, hereby, served as the peroxisomal organelle marker. In addition, several peroxisomal markers were tested, including anti-catalase (Anti-CAT), anti-glycolate oxidase (Anti-GOX), anti-degradation of periplasmic proteins 15 (Anti-DEG15), and anti-hydroxypyruvate reductase (Anti-HPR). However, except Anti-PEX14, none of the rest peroxisomal markers were detected by Western blot and peroxisome enrichment was therefore probe only with Pex14. Luminal binding protein (BIP2) is a protein of endoplasmic reticulum (ER). H^+-ATPase is found in plasma membrane. Vacuolar-type H^+-ATPases (V-ATPase) is a protein of the vacuole membrane. UDP-glucose pyrophosphorylase (UGPase) is a cytoplasm marker in the cell. Translocon at the inner envelope membrane of chloroplasts 40 (TIC40) is a protein of the chloroplast inner envelope (Chloro IE), while outer envelope protein 21 (OEP21) is located at the chloroplast outer envelope (Chloro OE). Cytochrome c oxidase subunit 2 (COX2), mitochondrial preprotein and amino acid transporter (B14.7), reinitiation supporting protein (RISP), nucleoside diphosphate kinase 3 (NDPK3), peroxisomal and mitochondrial division factor 2 (PMD2) and voltage-dependent anion channels (VDAC) are mitochondrial proteins, dedicated to mitochondrial inner membrane (Mito IM), intermembrane space (IMS) and outer membrane (OM), as shown in **Fig. 15A**.

We can see that large amount of peroxisomal protein, PEX14, were enriched at the "PO" fractions in both +/-Pi conditions, while contaminations from other organelles, besides ER, were significantly reduced (**Figure 15A**). However, instead of the expected bands of PEX14 protein at 75 KDa, several degraded bands of its fragments were observed under both Pi-enriched and Pi-limited conditions (**Figure 15A**). According to the manufacturer, Pex14 is prone to degradation, which likely explained this result.

Subsequently, quantifications of the band intensities have been done by the ImageQuant TL software and the values of "PO" fractions were plotted taking the "PE1" fractions as a reference (**Figure 15B**), because peroxisomal protein, PEX14, as well as other protein markers, could not be successfully detected in "TOT" protein fractions (**Figure 15A**). Results showed that, at "PO" fractions in both +/-Pi conditions, peroxisomal proteins were concentrated 10-20 times more than the "PE1" fraction (**Figure 15B**). The PEX14 signals were then standardized to 1 under both + and -Pi conditions. The signals of other organelles were normalized relative to the PEX14 values, allowing for the comparison of contaminant levels under/between these two conditions (**Figure 15C**). The peroxisomal fractions exhibited negligible contamination by plastidial and mitochondrial proteins, while a major contamination from ER was observed under both normal growth and stress conditions (**Figure 15C**). Additionally, there was an increased level of

contamination by plastidial and ER proteins in the peroxisomal fractions under Pi-starved conditions, compared to the Pi-enriched conditions (**Figure 15C**).

3.2 Lipid analysis of isolated peroxisome fractions from *A. thaliana* calli under +/-Pi conditions

So far, no studies have information about the lipid composition of plant peroxisomes from *A. thaliana* calli, regardless under phosphate starvation condition. Thus, we analyzed the fatty acid and lipid composition of the peroxisome fractions isolated from *A. thaliana* calli grown under +/-Pi conditions, namely "PO +Pi" and "PO -Pi", in comparison with the collected calli samples served as controls, referred to "TOT +Pi" and "TOT -Pi" (**Figure 16**). Lipids were extracted by the standard Folch method and were subsequently analyzed via GC-FID and LC-MS/MS. The objective of this study was aimed not only to assess the contamination levels from plastidial or mitochondrial membranes, but also to have a better understanding of the lipid classes in plant peroxisomes under standard conditions, and to investigate the response of the lipid composition in our harvested peroxisome fractions to Pi starvation.

Upon the examination of FAs and lipid class composition in normal growth condition (**Figure 16A & 16B**; "TOT +Pi", in dark blue, and "PO +Pi", in dark green), the FA and lipid profile of the peroxisome fractions displayed significant differences from the "TOT" fraction. Peroxisome fractions exhibited elevated level

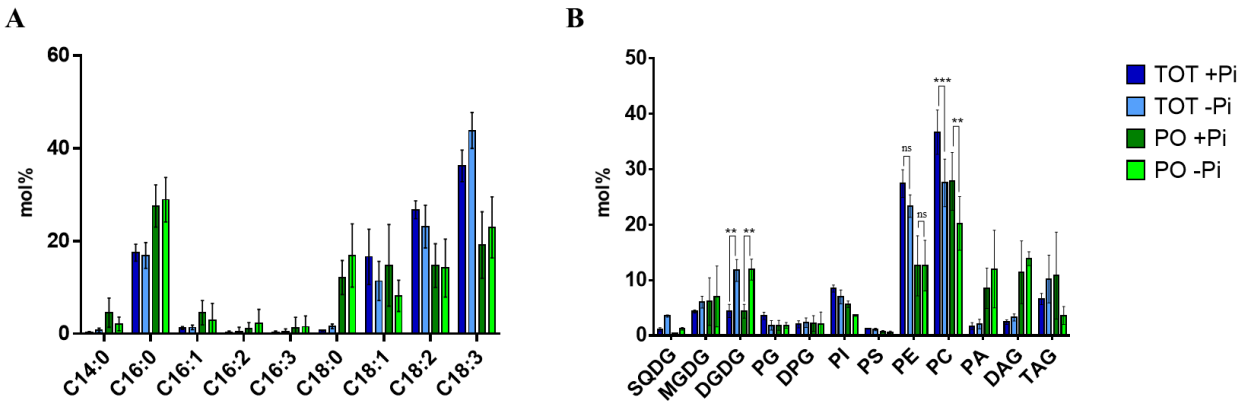


Figure 16. Fatty acid and lipid composition of total fraction and isolated peroxisome fractions from Arabidopsis calli in the presence or absence of Pi. Total lipids were extracted from lyophilized callus grown under +/-Pi conditions, taken as "TOT +Pi" and "TOT -Pi", respectively, while "PO +Pi" and "PO -Pi" samples were harvested after peroxisome purification as described in **Fig. 12**. A. GC-FID analysis of FA composition in the indicated samples in the presence or absence of Pi. B. LC-MS/MS analysis of lipid composition in the indicated samples in the presence or absence of Pi. Results were presented in mol%. Data represents Mean ± SD of 3 or 4 independent experiments. Statistical significant differences ($P < 0.01$) were shown by asterisks and were calculated by Two-way ANOVA using GraphPad Prism software: TOT +Pi vs TOT -Pi, or PO +Pi vs PO -Pi.

of 18:0 and reduced level of unsaturated 18:2 and 18:3 (**Figure 16A**), and were primarily comprised of phospholipids (over 60% of the total lipid content), including approximately 27.9% PC, 15.6% PE, 5.7% PI, 2.0% PG, 1.9% DPG, 0.7% PS, and 8.5% PA (**Figure 16B**). Additionally, the phospholipid composition in peroxisome fractions included lower levels of PE and PC, and higher levels of PA, and DAG, compared to the "TOT" fraction under standard conditions (**Figure 16B**). The level of SQDG, MGDG and DGDG, three lipids exclusively found in plastid membranes in normal growth condition, was low in peroxisome fractions (**Figure 16B**; "PO +Pi", in dark green), suggesting a minor contamination from plastid membranes, aligned with WB analysis (**Figure 15**). Similarly, the level of DPG, a mitochondria-specific lipid, was also low in peroxisome fractions (**Figure 16B**; "PO +Pi", in dark green), indicating a minimal contamination from mitochondrial membranes, consistent with WB analysis (**Figure 15**).

Furthermore, consistent with earlier findings (O'Quin et al., 2010), we observed the lipid remodeling adaptation to phosphate starvation in both "TOT" and "PO" fractions, evidenced by a significant increase of galactolipids DGDG (**Figure 16B**) and decrease of phospholipids, including PC, PE and PI (**Figure 16B**). SQDG levels also increased during Pi starvation, as observed in "TOT" fraction, but this lipid was not reported to be exported. Thus, the low level and slight increase of SQDG in peroxisome fraction under –Pi conditions might suggest a minimal contamination from plastids (**Figure 16B**). MGDG levels remained stable in both "TOT" and peroxisome fractions during Pi starvation, indicating that there was not a significant increase in contamination from plastids under –Pi conditions (**Figure 16B**). Furthermore, in comparison of "PO" fractions between +Pi (**Figure 16B**, in dark green) and –Pi conditions (**Figure 16B**, in light green), a decreased level in TAG was observed.

3.3 Proteomic analysis of isolated peroxisome fractions from *A. thaliana* calli under +/- Pi conditions

In order to elucidate the proteome of Arabidopsis peroxisomes under both standard and stress conditions, proteomic analyses on the isolated peroxisome fractions from *A. thaliana* calli grown in both conditions were performed.

In this study, in total we identified 2695 proteins under both +/-Pi conditions. Protein have been grouped with regarding to their subcellular locations based on the SUBA5 database. This identified proteome included mitochondrial, plastidial, nuclear, vacuolar, cytosolic and extracellular proteins, as well as categories dedicated to ER, Golgi and plasma membrane, and some unknown proteins (**Figure 17**).

Fig. 17A illustrated the relative distribution of proteins within these groups in +/-Pi conditions by plotting the summed abundances of each compartment against the total. The pie charts revealed the low abundance of peroxisomal proteins in our so-called isolated peroxisome fractions under both conditions (**Figure 17A**),

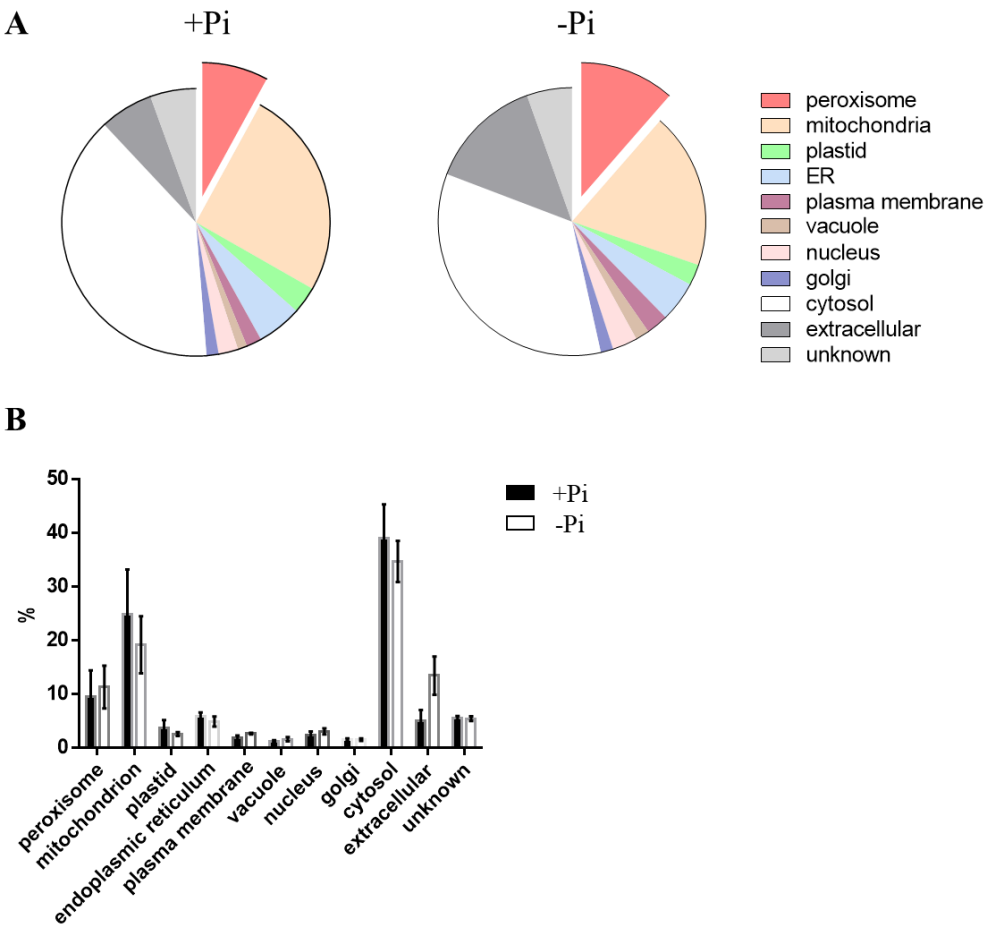


Figure 17. The relative distribution of proteins from each compartments in isolated "PO" fractions. A. The distributions of proteins were considered in percentage according to the summed abundances of each protein from the same compartment versus the summed abundances of all identified proteins. The protein abundances were taken as the arithmetic mean of four separate experiments. B. The histogram represented median with ranges of four independent experiments under +/-Pi conditions.

suggesting that the purity of our peroxisome isolation protocol was unexpectedly low (approximately 10%), which contrasted with our estimations based on WB and lipid results (**Figure 15 & 16**).

The largest classes of proteins were found to be cytosolic (30-40%) and mitochondrial (15-36%) proteins under +/-Pi conditions, following by a notable presence of peroxisomal proteins (~10% in both conditions; **Figure 17B**), contrasting with the findings we observed from WB and lipidomic analysis (**Figure 15 & 16**). The plastidial proteins accounted for a minor fraction (2-3%) as contaminants under both +/-Pi conditions (**Figure 17B**), aligning with the WB and lipidomic analysis (**Figure 15 & 16**). The other two main groups of proteins were those designated in ER (4-6%) and nucleus (2-3%; **Figure 17B**), consistent with WB analysis (**Figure 15**), as these two organelles are in close relation to the biogenesis of peroxisomes. The abundance of proteins with extracellular functions, primarily involved in stress-induced cell wall construction and modification, cell expansion and pathogen resistance, comprised 13.76% of the total

proteome identified in –Pi, which were higher than that detected in +Pi (6.45%; **Figure 17B**). Plasma membrane, vacuole and Golgi proteins represented a negligible proportion (1-2%) under both +/-Pi conditions, while proteins with unknown functions and locations represented approximately 5.5% (**Figure 17B**).

3.2.1 Comparative analysis of Western blot results and proteomic data

To better understand the discrepancies between the WB and proteomic results, we examined the proteomic data for the presence and abundance of various protein markers used in the WB (**Table 11)**. The rank of each protein presented in the table was determined based on the calculated values of protein abundances within the individual peroxisome fraction and referred as the arithmetic mean of four independent experiments.

In the WB experiments, the bands of the peroxisomal marker, PEX14, were clearly detected with some degradation observed (**Figure 15**); while in the proteomic results, it exhibited very low abundance (**Table 11**, ranking 1015 in +Pi), and there was no significant difference between standard and stress conditions. The ER marker BIP2 was consistently detected in all peroxisomal fractions under both conditions in WB (**Figure 15**), and was highly abundant in the proteome (**Table 11**, ranking 171 in +Pi). The plasma membrane and vacuole markers, H^+-ATPase and V-ATPase, were slightly detected in WB (**Figure 15A**) and was also low abundant in the proteome (**Table 11**, ranking 1487 in +Pi). Even though the cytoplasm

Rank (in +Pi)	Rank (in -Pi)	Accession	Protein name	Location	Differential (+Pi vs –Pi)	SDS-PAGE	
						+Pi	-Pi
1015	616	AT5G62810	PEX14	Perox	no	*	*
171	147	AT5G42020	BIP2	ER	no	*	*
1487	1364	AT4G30190	H^+-ATPase	PM	no	*	*
440	502	AT1G76030	V-ATPase	Vacuole	no	*	n.d.
1052	776	AT3G03250	UGPase	Cytosol	no	n.d.	*
n.d.	n.d.	AT5G16620	TIC40	Chloro IE	-	n.d.	n.d.
n.d.	n.d.	AT1G20816	OEP21	Chloro OE	-	*	n.d.
127	176	ATMG00160	COX2	Mito IM	no	n.d.	n.d.
258	316	AT2G42210	B14.7	Mito IM	no	n.d.	n.d.
115	156	AT5G13430	RISP	Mito IM	no	n.d.	n.d.
122	41	AT4G11010	NDPK	Mito IMS	no	n.d.	*
992	1166	AT1G06530	PMD2	Mito OM	no	*	n.d.
11	14	AT3G01280	VDAC	Mito OM	no	*	n.d.

Table 11. Analysis of the protein quantity determined by proteomic compared to Western blot analyses. The rank was determined based on the calculated values of protein abundances and referred as the arithmetic mean of four independent experiments. Whether the protein is identified as differentially abundant between +Pi and –Pi condition was indicated by the calculation of Log2 fold change of the protein enrichment. The proteins detected in Western blot in the peroxisomal fraction was as indicated with an asterisk. n.d.: not detected.

marker, UGPase, exhibited minimal detection in WB (**Figure 15A**) and low abundance in the proteome (**Table 11**, ranking 1052 in +Pi), the entire proteomic analysis revealed a large number of cytosolic contaminants (**Figure 17**), indicating that relying on a single organelle marker in the WB could not provide a comprehensive assessment. Two chloroplast markers, TIC40 and OEP21, were nearly detected in WB experiments (**Figure 15**) and were not identified in the proteome (**Table 11**), but few proteins involved in plastidial glycolytic pathway in non-green plastids and chloroplasts were found (**Figure 17**).

Due to the significant presence and high abundance of mitochondrial proteins as evidenced in the proteomic analysis (**Figure 17**), various mitochondrial markers located at different mitochondrial regions, including COX2, B14.7 and RISP at mitochondrial IM, NDPK at mitochondrial IMS, PMD2 and VDAC at mitochondrial OM, were utilized in WB experiments. All of them showed relatively high abundance in the proteome data, with the exception for PMD2, which was less abundant (**Table 11**); however, only NDPK, PMD2 and VDAC showed faint bands in WB experiments (**Figure 15A**).

3.2.2 Proteomic analysis of identified peroxisomal proteins

Of all the classified proteins, 133 have been previously identified as peroxisomal proteins based on fluorescent subcellular localization database, and compared with proteomic data from previous studies, as detailed in **Table 12**. Among the 133 peroxisomal proteins listed here, 78 have been previously reported in the peroxisomal proteome studies from various tissue types by Eubel et al., 2008; Fukao et al., 2002, 2003; Reumann et al., 2007, while 55 were newly detected in this study. However, due to the unsatisfactory purity of our peroxisome fractions, we cannot conclusively identify the newly detected proteins as novel components of the peroxisomal proteome from Arabidopsis calli and in vivo localization of protein fusion with fluorescent proteins should be done to confirm this result.

These detected peroxisomal proteins participate in all of the classical peroxisomal pathways, such as fatty acid β-oxidation, reactive oxygen species (ROS) detoxification, nitrogen and sulfur metabolism, hormone catabolism, and organelle biogenesis (**Table 12**). Moreover, some proteins involved in the peroxisomal steps of the photorespiratory pathway have been also identified in this study from Arabidopsis cell suspension cultures, even though they are not green tissues.

In the following paragraphs, we categorized different classes of these 133 proteins by their functions (**Table 12**). We primarily discussed newly detected peroxisomal proteins and previously reported peroxisomal proteins that were not detected in this study under normal growth condition, the differences of protein abundance in response to phosphate starvation in our proteome data, and the close association of peroxisomes with the ER.

Proteins involved in fatty acid β-oxidation and auxiliary enzymes

The core proteins involved in FAs β-oxidation pathway, At4g39850 (CTS/PXA1/PED3) as fatty acid transporters, two LACSs (AT3G05970 and AT5G27600) for re-activating FAs, five of the six known isoforms of acyl-CoA oxidases (ACXs) (At4g16760, ACX1; AT5G65110, ACX2; At1g06290, ACX3; At3g51840, ACX4; and At2g35690, ACX5), two isoforms of MFP (AT3G06860, MFP2; AT4G29010, AIM1), and two of three reported KAT enzymes (At1g04710, KAT1; At2g33150, KAT2) have been identified in this study, which encompassed a broader range of enzymes compared to the published reports from different plant tissues, although none of them showed significant differences between normal and stress conditions (**Table 12**; Eubel et al., 2008; Fukao et al., 2002, 2003; Reumann et al., 2007).

In this study, the isoforms, ACX6 (AT1G06310) and KAT5 (AT5G48880), were not detected. Even though ACXs enzymes partially overlap in substrate specificity, they seemed to prefer different types of substrates feeding into the β-oxidation process. ACX6 was reported to be implicated in the β-oxidation of IBA, expressed strongly in root tip and may be a pseudogene due to the lack of detected transcripts (Adham et al., 2005; Eubel et al., 2008). The absent KAT5 is highly expressed in flowers and siliques, indicating that thiolases may be functionally important in reproductive tissues (Wiszniewski et al., 2014). Although KAT5 does influence the composition of benzoylated metabolites in seeds (Bussell et al., 2014), little is known about the function of KAT5, particularly in its contributions to β-oxidation processes and to seed germination.

Our data also found two paralogous acetoacetyl CoA thiolase (At5g47720, AACT1; and At5g48230, AACT2) in these peroxisome fractions from Arabidopsis calli, which can catalyze the condensation of two acetyl CoA molecules to form acetoacetyl CoA (Jin et al., 2012). AACT2 was previously identified in Arabidopsis leaves by Reumann et al., 2007 but was not detected in cell culture peroxisomes by Eubel et al., 2008; while AACT1 was not reported in any earlier studies. Jin et al., 2012 demonstrated that AACT1 is primarily expressed in the vascular system, whereas AACT2 is highly expressed in root tips, young leaves, top stems and anthers. Moreover, plants lacking AACT1 function remained completely viable and exhibited no apparent growth phenotypes. In contrast, loss of AACT2 function resulted in a lethal phenotype, and AACT2 cannot be compensated only by AACT1 (Jin et al., 2012). These indicated that AACT1 is functionally redundant with respect to AACT2 function, which is consistent with the observation in our study that AACT1 was at lower abundance compared to AACT2.

A group of acyl-activating enzymes (AAEs) also has been revealed in our data, which provide the entry for various substrates with distinct specificities into the β-oxidation pathway. In addition to the four family proteins identified by Reumann et al., 2007 and Eubel et al., 2008 (AT1G20560, AAE1; AT5G16370, AAE5; AT3G16910, AAE7; AT5G23050, AAE17), two additional AAE proteins (AT3G48990, AAE3; AT1G55320, AAE18) were found at low abundance in this study. Arabidopsis AAE3 encodes an oxalyl-

CoA synthetase that is capable to specifically converting oxalate and CoA into oxalyl-CoA in the first step of oxalate catabolism (Lou et al., 2016). AAE18 has limited sequence similarity to acetyl-CoA synthetase, and is expressed in flowers and leaves, as well as at low levels in developing seeds (Shockey et al., 2003). Previous studies has demonstrated that Arabidopsis AAE18 is involved in activating auxin precursor 2,4-dichlorophenoxybutyric acid (2,4-DB) by peroxisomal β-oxidation to active auxins that inhibit root growth (Wiszniewski et al., 2009).

Moreover, two 4CL family proteins (At1g20510, 4CLL5; and At4g05160, 4CLL7) have been identified in our study, which were also reported by Reumann et al., 2007 and Eubel et al., 2008. They were reported to accept medium- to long-chain fatty acids as substrates, and play a role in jasmonic acid (JA) biosynthesis (Koo et al., 2006). An additional member of 4CL family detected in the study of Eubel et al., 2008, 4CLL2 (At1g20480), was absent in our study, which is predicted to localize in peroxisome but whose function in substrate activation for β-oxidation remains unclear.

At2g39970 (PXN), At5g27520 (PNC2) were found in our proteome data, consistent with finding by Eubel et al., 2008, but were not detected in plant leaves in the study of Reumann et al., 2007. These proteins are peroxisomal ADP/ATP transporters reported in yeast and closely related to mitochondrial carrier family (MCF; Eubel et al., 2008; McCammon et al., 1990; Millar & Heazlewood, 2003). In addition, an *Arabidopsis thaliana* gene that encodes peroxisomal adenine nucleotide carrier 1 (AT3G05290, PNC1) has been exceptionally detected in our study, which catalyzes the counter-exchange of ATP with AMP supplying ATP for FAs β-oxidation (Arai et al., 2008). Linka et al., 2008 has evidenced the peroxisomal protein identity of this protein, and demonstrated that, apart from the PNC proteins, no other ATP generating systems exists within plant peroxisomes.

Furthermore, three additional auxiliary oxidation-related enzymes have been identified in our study: AT5G17380 (HACL; absent in any previous studies), AT2G38180 (found in Eubel et al., 2008), and AT3G01980 (SDRc; found in Reumann et al., 2007). AtHACL, along with AtPAHX (At2g01490), are key enzymes of the α-oxidation pathway involved in phytol metabolism within Arabidopsis peroxisomes, which are sequence homologous to human 2-hydroxy-phytanoyl-CoA lyase (Yang et al., 2022). SDRc is a member of the short-chain dehydrogenase/reductase (SDR) superfamily, which are NAD(P)(H)-dependent oxidoreductases that participate in auxiliary FAs β-oxidation in plant peroxisomes. *In silico* expression profiling of Arabidopsis peroxisomal SDR genes indicated that SDRc has relatively high expression levels in floral organs, which is consistent with its roles in the biosynthesis of benzaldehyde, an important floral scent component, and in germinating seeds, which may suggest an involvement in fatty acid β-oxidation (Zhang et al., 2023). However, little is known about the biological function of AT2G38180, thus the reason why it appeared to be absent in leaves or in low abundance in cell culture is currently unclear.

ROS metabolism

Ten proteins have been identified that fit into the category of proteins involved in ROS metabolism: three isoforms of catalase (AT1G20630, CAT1; AT4G35090, CAT2; AT1G20620, CAT3), two isoforms of peroxisomal monodehydroascorbate reductase (AT3G52880, MDAR1; AT3G27820, MDAR4), L-ascorbate peroxidase 3 (AT4G35000, APX3), peroxisomal membrane protein (AT4G04470, PMP22), superoxide dismutase (AT5G18100, CSD3), and 6-phosphogluconolactonase (AT5G24400, PGL3).

In Arabidopsis, catalase (CAT) genes encode a small family of proteins, including CAT1, CAT2 and CAT3, which catalyze the decomposition of hydrogen peroxide (H_2O_2) and play a crucial role in maintaining ROS homeostasis (Du et al., 2008). These proteins were detectable either completely or partially in all the previous studies (Eubel et al., 2008; Fukao et al., 2002, 2003; Reumann et al., 2007). In our study, although CAT2 protein is relatively well abundant in the peroxisome fraction, in the WB analysis, it was not detected with the CAT2 antibody (AS09501, Agrisera), used as a peroxisomal marker, under both +/-Pi conditions (data not shown). This could be linked to the low efficiency of this antibody.

The H_2O_2 byproduct from FAs catabolism in plant peroxisomes can be also cleaved by ascorbate peroxidase (APX) and monodehydroascorbate reductase (MDAR), and might be more preferentially scavenged by the APX/MDAR system (Eastmond, 2007). Arabidopsis APX3, the primary APX isoform of the peroxisomal membranes, was identified in all earlier studies (Eubel et al., 2008; Fukao et al., 2002, 2003; Reumann et al., 2007). However, it was surprisingly found to be dispensable for Arabidopsis growth and development (Narendra et al., 2006). The two predominant MDAR isoforms in plant peroxisomes are AtMDAR1 and AtMDAR4, which reside in the matrix and membrane of Arabidopsis peroxisomes, respectively (Lisenbee et al., 2005). The physiological function of MDAR4 in maintaining redox balance in plant peroxisomes has been revealed in previous studies using mutants (Eastmond, 2007), but less attention has been paid to peroxisomal MDAR1. Unexpectedly, our study uncovered that MDAR1 was more abundant than MDAR4 in Arabidopsis cell cultures, and exhibited significant increase in abundance under Pi deprivation compared to normal growth conditions, which would open perspectives for investigating the role of MDAR1 in response to abiotic stress. In addition, it might suggest a link between the induction of oxidative-stressed proteins and phosphate deficiency in Arabidopsis calli.

At4g04470 (PMP22), also identified in cell culture peroxisomes by Eubel et al., 2008, is an integral membrane protein with similarities to known mammalian and yeast peroxisomal proteins, however its biological function in Arabidopsis remains largely unclear. It was hypothesized to function either as a nonselective membrane channel and/or as a reactive oxygen species forming protein in the peroxisome membrane (Eubel et al., 2008; Visser et al., 2007).

AT5G18100 (CSD3) and AT5G24400 (PGL3) were detected in our study and in leaf tissues by Reumann et al., 2007. *Arabidopsis thaliana* has three copper/zinc superoxide dismutases (CSD) isoforms: CSD1 in the cytoplasm, CSD2 in chloroplasts, and CSD3 in peroxisomes. CSD enzymes generally can catalyze the disproportionation of superoxide anion to oxygen and hydrogen peroxide. Among all, CSD3 has been reported to play an important role in the plant antioxidant defense system in Arabidopsis rosette leaves under stress conditions (Holzmeister et al., 2015; Huang et al., 2012; Kliebenstein et al., 1998). However, Arabidopsis CSD3 displayed no differences in response to Pi starvation in our studies. PGL3 was predicted to encode an isoform of 6-phosphogluconolactonase (6PGL) that localized to both plastids and peroxisomes, whereas PGL1, PGL2, PGL4 and PGL5 were predicted to encode cytosolic isoforms of 6PGL. Xiong et al., 2009 revealed that PGL3 contributed to maintaining cellular redox equilibrium in photosynthetic cells, and plays an essential role in plant growth and development.

Glyoxylate cycle

The glyoxylate cycle enzymes isocitrate lyase (AT3G21720, ICL) was found in our study, but was previously reported to be absent from plant leaf and the cell culture peroxisomes (Eubel et al., 2008; Reumann et al., 2007). Moreover, a notable absence of other glyoxylate cycle-related enzymes, such as malate synthase, citrate synthase, aconitase and malate dehydrogenase, was observed in our study and in Eubel et al., 2008, which might suggest that the isolated peroxisomes from Arabidopsis cell suspension cultures cannot be considered to be catalyzing a glyoxylate cycle.

Photorespiration and hormone biosynthesis

Even though the non-photosynthetic tissue, calli, was utilized in our study, multiple proteins associated with peroxisomal steps of photorespiration were identified. However, none of those proteins exhibited significant differences in response to stress. In addition, in tissues with low lipid consumption and requirement, peroxisomes perform reduced β-oxidation activity and are often involved in the production of signaling compounds and hormones, such as jasmonic acid (JA) biosynthesis and the conversion of indole-3-butyric acid (IBA) into indole-3-acetic acid. This explained the high abundance of the SDRA protein (AT4G05530), a peroxisomal member of SDR family, which is responsible for catalyzing a dehydrogenation step in the conversion of IBA to IAA (Wiszniewski et al., 2009).

Peroxisomal biogenesis factors

Genes regulating peroxisomal biogenesis in plants and their gene products have been designated with the acronym “PEX” (Nito et al., 2007). Our study identified several PEX proteins, with no significant differences observed under +Pi and -Pi conditions.

Alike Eubel et al., 2008, four of the five PEX11 family proteins, which were predicted to play roles in peroxisome proliferation in Arabidopsis, have been found in this study (PEX11a, -c, -d, and -e); whereas PEX11d was only detected in leaf peroxisomes by Reumann et al., 2007. PEX11b, undetected by any studies, was reported to be involved in peroxisome proliferation during seedling morphogenesis (Desai & Hu, 2008; Eubel et al., 2008).

Since calli grown in liquid culture performed a rapid cell division, peroxisomal biogenesis and proliferation may be enhanced, which might explain the relatively high abundance of PEX11 proteins, and the detection of the other PEX3-2, PEX5, PEX7, PEX10, PEX12, PEX14 and PEX16 proteins. Previous studies have demonstrated that PEX3, PEX11 and PEX16 contributed to morphology determination of peroxisomes; PEX5, PEX7 and PEX14 were involved in peroxisomal protein targeting; PEX10 and PEX12 are essential for embryogenesis (for a review, Kao et al., 2018).

N- and S- metabolism

Our study identified several peroxisome-localized proteins involved in nitrogen and sulfur metabolism, with notably one protein (AT4G36760, APP1) showing significantly higher abundance in Pi-stressed condition compared to normal growth condition. However, despite its activity on the auxin transport, little is known about this protein. Previous transcriptome data have revealed that phosphate starvation affects nitrogen metabolism, for instance, the upregulation of At1g08090 at cell membrane and the cytosolic At5g16570 under Pi-starved condition (Srivastava et al., 2023), whereas the connection between sulfur metabolism and phosphate starvation has been less studied.

Identification of ER Proteins

Within all our identified proteins, 161 appeared to be ER proteins (data not shown), which can be considered to be of particular interest as connections between the ER and peroxisomes due to the import of peroxisomal proteins from the ER. In the other hand, the case of these ER proteins considered as contamination, could be explained by the close interaction of these two organelles for peroxisomal biogenesis and the import of peroxisomal matrix proteins. While there is no doubt that these proteins are predominantly located in the ER, it is harder to tell whether they are also present in peroxisome, or if they are contaminants resulting from the co-purification of ER vesicles with the peroxisomes. Similar dilemmas have been discussed in other literatures (Eubel et al., 2008; Saleem et al., 2006).

Rank (in +Pi)	Rank (in -Pi)	Accession	Protein name	Differential (+Pi vs –Pi)	Presence (compare to +Pi)			
					Fukao et al.		Reumann et al., 2007	Eubel et al., 2008
					2002	2003		
Fatty acid β-oxidation								
10	5	AT2G33150	KAT2	no		yes	yes	yes
43	30	AT3G06860	MFP2	no			yes	yes
164	93	AT4G16760	ACX1	no				yes
177	109	AT4G29010	AIM1	no			yes	yes
182	133	AT3G05970	LACS6	no				yes
216	162	AT5G27600	LACS7	no			yes	yes
246	197	AT1G06290	ACX3	no				yes
301	263	AT3G51840	ACX4	no			yes	yes
444	325	AT5G65110	ACX2	no				
926	657	AT2G35690	ACX5	no				yes
1225	1237	AT1G04710	KAT1	no			yes	yes
Auxiliary β-oxidation enzymes								
86	75	AT3G12800	MBK21.18	no			yes	yes
159	121	AT4G16210	ECHIA	no			yes	yes
167	215	AT5G42890	SCP2	no			yes	yes
272	366	AT1G65520	ECI1	no			yes	yes
284	249	AT4G05160	4CLL7	no			yes	yes
296	240	AT3G16910	AAE7	no			yes	yes
299	296	AT1G49670	NQR	no			yes	yes
312	261	AT1G76150	ECH2	no			yes	yes
368	279	AT1G20510	4CLL5	no			yes	yes
382	272	AT5G16370	AAE5	no			yes	yes
393	408	AT3G02360	PGD2	no			yes	yes
401	338	AT2G39970	PXN	no				yes
444	348	AT4G14430	ECI2	no			yes	yes
511	456	AT3G05290	PNC1	no				
529	534	AT5G43280	DCI1	no			yes	yes
561	527	AT3G15290	At3g15290	no			yes	yes
669	723	AT5G48230	ACCT2	no			yes	
705	566	AT1G01710	ACH2	no			yes	yes
745	648	AT1G54340	ICDH	no		yes	yes	yes
812	712	AT5G27520	PNC2	no				yes
849	675	AT4G39850	PXA1	no				yes
967	802	AT1G20560	AAE1	no				yes
982	726	AT5G23050	AAE17	no				yes
1185	1070	AT4G02340	EH3	no			yes	yes
1444	1192	AT5G17380	HACL	no				
1587	2042	AT2G38180	At2g38180	no				yes
1752	1770	AT3G48990	AAE3	no				
1759	2031	AT3G01980	SDRc	no			yes	
2359	2066	AT5G47720	ACCT1	no				
2561	2466	AT1G55320	AAE18	no				

Rank (in +Pi)	Rank (in -Pi)	Accession	Protein name	Differential (+Pi vs –Pi)	Presence (compare to +Pi)			
					Fukao et al.		Reumann et al., 2007	Eubel et al., 2008
					2002	2003		
ROS metabolism								
13	8	AT1G20620	CAT3	no	yes	yes	yes	yes
60	52	AT4G35000	APX3	no	yes	yes	yes	yes
104	63	AT1G20630	CAT1	no			yes	yes
109	73	AT4G35090	CAT2	no	yes		yes	yes
534	308	AT3G52880	MDAR1	yes -1.268			yes	yes
630	893	AT4G04470	PMP22	no				yes
909	796	AT3G27820	MDAR4	no				
970	718	AT5G18100	CSD3	no			yes	
1721	1827	AT5G24400	PGL3	no			yes	
Glyoxylate cycle								
482	295	AT3G21720	ICL	no		yes		
Hormone biosynthesis								
95	68	AT4G05530	SDRA	no			yes	yes
199	118	AT3G06810	IBR3	no				yes
420	400	AT2G06050	OPR3	no			yes	yes
1226	988	AT5G63380	4CLL9	no				
1609	1491	AT1G24100	UGT74B1	no				
1966	2360	AT3G44320	NIT3	no				
Photorespiration								
127	94	AT2G22780	PMDH1	no	yes	yes	yes	yes
174	113	AT4G18360	GLO5	no			yes	yes
387	318	AT1G23310	GGAT1	no	yes		yes	yes
964	803	AT3G14150	GLO3	no				
1370	1759	AT3G14130	GLO4	no				
1394	814	AT1G70580	GGAT2	no	yes		yes	yes
1753	1516	AT1G79870	HPR2	no				
2335	2618	AT2G16640	TOC132	no				
Peroxisomal biogenesis factors								
131	56	AT3G61070	PEX11E	no				yes
220	192	AT1G01820	PEX11C	no				yes
742	627	AT1G47750	PEX11A	no				yes
764	741	AT2G45740	PEX11D	no			yes	yes
1015	616	AT5G62810	PEX14	no			yes	yes
1804	1669	AT1G29260	PEX7	no				yes
1935	2022	AT2G45690	PEX16	no				
2004	1774	AT1G48635	PEX3-2	no				
2425	2422	AT5G56290	PEX5	no				
2433	2398	AT2G26350	PEX10	no				
2450	2395	AT3G04460	PEX12	no				
N- and S- metabolism								
89	44	AT5G11520	ASP3	no	yes		yes	yes
324	254	AT3G01910	SOX	no			yes	yes

Rank (in +Pi)	Rank (in -Pi)	Accession	Protein name	Differential (+Pi vs –Pi)	Presence (compare to +Pi)			
					Fukao et al.		Reumann et al., 2007	Eubel et al., 2008
					2002	2003		
367	322	AT2G26230	Uricase	no			yes	yes
488	547	AT3G56490	HINT1	no				
618	596	AT5G65940	CHY1	no				yes
674	578	AT5G58220	TTL	no			yes	yes
726	674	AT2G17420	NTR2	no				yes
754	591	AT2G28760	UXS6	no				
859	654	AT4G16566	HINT4	no			yes	yes
1215	1639	AT1G78590	NADK3	no				
1289	1081	AT4G30530	GGP1	no				
1592	1852	AT5G66120	DHQS	no				
1677	1734	AT3G48690	CXE12	no				
1751	1255	AT2G43940	HOL3	no				
1976	1640	AT1G65840	PAO4	no				yes
2077	2229	AT3G59050	PAO3	no				
2145	2094	AT2G37040	PAL1	no				
2280	1650	AT4G36760	APP1	Yes -2.402				
2290	2199	AT5G19180	ECR1	no		yes		
2373	2236	AT3G06580	GAL1	no				
2426	2393	AT2G20610	SUR1	no				
Other functions								
123	75	AT3G58750	CSY2	no				yes
141	148	AT5G41210	GSTT1	no			yes	yes
183	131	AT2G42790	CSY3	no			yes	yes
260	236	AT3G48170	ALDH10A9	no			yes	yes
279	254	AT1G48320	DHNAT1	no				
314	298	AT1G72680	CAD1	no				
365	316	AT1G54100	ALDH7B4	no				
391	409	AT5G43940	ADH2	no			yes	
407	359	AT2G42490	CuAOzeta	no				yes
447	379	AT1G50510	PUMY	no				yes
763	629	AT1G17170	GSTU24	no				
767	809	AT1G06550	At1g06550	no				
787	958	AT5G04830	MUK11.15	no				
789	592	AT2G30140	UGT87A2	no				
864	872	AT1G52760	CSE	no				
928	849	AT2G37760	AKR4C8	no				
974	773	AT3G24170	GR1	no			yes	yes
1092	1009	AT5G47040	LON2	no				
1105	924	AT2G41790	PXM16	no				yes
1130	1012	AT2G30660	At2g30660	no				
1153	1508	AT1G64850	PXG4	no				
1257	969	AT2G29490	GSTU1	no				
1312	1102	AT1G04290	At1g04290	no			yes	yes
1420	1064	AT3G22850	At3g22850	no				

Rank (in +Pi)	Rank (in -Pi)	Accession	Protein name	Differential (+Pi vs –Pi)	Presence (compare to +Pi)			
					Fukao et al.		Reumann et al., 2007	Eubel et al., 2008
					2002	2003		
1513	1738	AT1G52400	BGLU18	no			yes	
1817	1717	AT5G11910	At5g11910	no				
1847	1405	AT2G29460	GSTU4	no				
1861	1895	AT1G28320	DEG15	no				yes
2150	1938	AT2G34690	ACD11	no				
2525	2591	AT5G20250	RFS6	no				
2619	2559	AT1G17580	XI-1	no				
Unknown								
727	507	AT5G64250	At5g64250	no				
1443	1224	AT4G21580	At4g21580	no				
2087	2177	AT3G51130	At3g51130	no				
2190	2005	AT4G13180	At4g13180	no				
2473	2360	AT3G19990	At3g19990	no				

Table 12. Results of the identified peroxisomal proteins performed on the peroxisomal "PO" fractions under both +/-Pi conditions in four separate experiments. The rank was determined based on the calculated values of protein abundances and referred as the arithmetic mean of four independent experiments. Whether the protein is identified as differentially abundant between +Pi and –Pi condition was indicated by the calculation of Log2 fold change of the protein enrichment. The negative Log2 fold change indicated an increased protein abundance in –Pi compared to +Pi conditions. Proteomic results of this study were compared with those of Fukao et al., 2002, 2003; Reumann et al., 2007; and Eubel et al., 2008.

4 Discussion and perspectives

The aim of this study was to elucidate the response of peroxisomes membrane lipidome and proteome during Pi starvation, which requires firstly obtaining the relatively pure peroxisomes from *A. thaliana* calli grown in presence or absence of Pi.

Here, we took advantage of a pre-existing peroxisome isolation protocol from plant leaves or cell suspension cultures, and attempted to optimize several steps with differential centrifugation and two-step purification by two Percoll density gradients to separate peroxisomes from the other cell compartments, especially plastids and mitochondria. Subsequently, we determined the proteome and lipidome of the isolated peroxisome fractions to see if there would be significant differences of protein abundances or lipid class distributions in response to Pi starvation. However, taking all our Western blot, lipidomic and proteomic data into consideration, we proposed that we successfully enriched peroxisomes and de-enriched plastids and mitochondria in the harvested peroxisomal fractions, however, the purity of peroxisomes was

not sufficient; thus, to distinguish differences in lipidome or proteome of isolated peroxisome fraction between Pi-stressed and Pi-enriched conditions is challenging.

4.1 We successfully enriched peroxisomes in the harvested peroxisomal fractions, although the purity was not sufficient to assess the lipidomic and proteomic differences in response to Pi deficiency

Western bolt results showed that in the isolated peroxisomal fractions ("PO"), peroxisomal protein PEX14 were concentrated 10-20-fold, with a minor contamination from ER and plastidial proteins (**Figure 15**). The other undetectable peroxisomal markers in WB experiments (data not shown), CAT2, DEG15 and HPR2 were less abundant according to the proteomic data, while GOX was completely absent (**Table 12**).

The low levels of galactoglycerolipids, typically found in plastid membranes under normal growth condition, observed in lipidomic analysis (**Figure 16**), along with the low abundance of plastidial proteins detected in proteomic analysis (**Figure 17**), suggested that our harvested peroxisomal fractions exhibited negligible contamination by plastids. Therefore, this low level of contamination from plastids in our peroxisomal fractions would be promising to elucidate the process of DGDG transfer in response to Pi starvation.

Based on the undetected results of multiple mitochondrial organelle markers in WB analysis (**Figure 15**) and the low proportion of the specific mitochondria lipid, DPG, in lipidomic analysis (**Figure 16**), it seemed that we also successfully reduced the mitochondrial contamination from the resultant peroxisomal fractions. However, proteomic results indicated that the mitochondrial and cytosolic proteins, rather than peroxisomal proteins, contributed the largest proportions among all the identified proteins (**Figure 17**). This contrasted to our observations in WB and lipidome data, and suggested that we still got a massive contamination from mitochondrial and cytosolic proteins. However, given that Arabidopsis calli is not a tissue abundant in peroxisomes, and that the total quantity of peroxisome in cells is originally much lower than mitochondria, we could infer that our fractions resulted in an enrichment of peroxisomes and a depletion of mitochondria, even though it was not sufficient.

Since mitochondria are probably the most abundant organelles in non-photosynthetic calli, and they are widely considered as the major contaminants in peroxisome proteome analyses (Eubel et al., 2008; Kikuchi et al., 2004; Saleem et al., 2006), this was not surprising. However, it was unexpected that the mitochondrial proteins, corresponding to the used mitochondrial markers used in WB experiments, were identified at relatively high abundance in proteome data, but were not detected in WB experiments (**Table 11**). The paradox between WB results and proteome data might be attributed to several reasons: 1) the different sensitivities of WB and proteomic analysis. Even though PEX14, the peroxisomal organelle marker, may

be present in fractions at relatively low abundance (ranking 1015 in +Pi, **Table 12**), it can be detected by proteomic technics that are now highly sensitives, and also by WB due to the high sensitivity of the PEX14 antibody; whereas it is opposite to the other undetectable mitochondrial markers by WB, which are likely less sensitive than the PEX14 one, but highly detectable by proteomic method. 2) Moreover, distinct immunoblot antibodies have different sensitivities, making it incomparable across those organelle markers in WB analysis, thus meaning that it cannot reveal the relative distribution of each compartment in samples. 3) Furthermore, post-translational modifications (PTMs) might affect the protein's abundance or make it less amenable to be detected by mass spectrometry techniques used in proteomic analysis.

In order to eliminate cytosolic proteins in cells, we adapted an ultracentrifugation step from a mitochondria isolation protocol from *Arabidopsis thaliana* cell cultures for lipidomic analysis (Leterme et al., 2021). However, there still existed a large amount of cytosolic proteins in our isolated peroxisome fractions according to proteomic data despite the use of two Percoll gradients (**Figure 17**), while WB results showed minimal detection of the cytoplasm marker, UGPase (**Figure 15**). Several factors could explain this discrepancy: 1) unfortunately, the purification protocol might be incomplete to separate peroxisomes from other cellular fractions, thus cytosolic proteins co-sedimented with peroxisomes or other organelles, leading to contamination; 2) though high-speed centrifugation were conducted to remove the cytosolic proteins, they may still adhere to the pelleted peroxisomes. Even though contamination by cytosolic proteins did not significantly influence our lipidomic analyses due to their non-membrane nature, interference from mitochondrial proteins was the major concern.

Additionally, the presence of multiple matrix peroxisomal proteins in our isolated fractions indicated that our peroxisome purification protocol from Arabidopsis calli was highly successful in maintaining intact peroxisome, which is typically challenging due to the inherent fragility of peroxisomes *in vitro*.

Taken all together, it suggested that this protocol allowed us to enrich peroxisomes with satisfactory yields for analysis under both normal and stress conditions, and de-enrich other organelles, however, the purity of peroxisomes was not sufficient to assess the lipidomic and proteomic differences in response to Pi deficiency.

4.2 Distinguishing differences in lipidome of isolated peroxisome fraction between Pi-enriched and Pi-stressed conditions is challenging

To the best of our knowledge, there is an evident scarcity of studies examining the lipid composition of *A. thaliana* peroxisomes, regardless under stress conditions. Previous research has determined the phospholipid composition of peroxisomal membranes in various species, such as rat liver, yeast, and castor bean endosperm. These studies have revealed that peroxisomal membranes are predominantly composed

of the phospholipids, including PC and PE as the major PLs, and distinct intermediate proportions of PI, PS, DPG, PG, and PA (**Table 13**; Reglinski et al., 2020; Rosenberger et al., 2009; Schneiter et al., 1999; Schrader et al., 2020; Tuller et al., 1999; Wriessnegger et al., 2007; Zinser et al., 1991).

In this study, although the purity of our peroxisome fraction was not sufficient to fully assess the Arabidopsis peroxisomal lipidome, we still observed a typical phospholipid-dominated composition, with highly abundant PC and PE, under both Pi-enriched and Pi-starved conditions (**Table 13**). The elevated levels of PA and DAG were also observed in our peroxisome fractions under both conditions (**Figure 16**), which was not mentioned in other studies. The PA high levels might be due to lipid degradation during the purification, while the presence of unusual high DAG content, the key intermediate in the biosynthesis of glycerolipids, may result from the degradation of phospholipids and require further investigation.

Subsequently, in comparison with the lipidome of isolated mitochondria from *A. thaliana* cell suspension cultures grown in standard conditions (Jouhet et al., 2004), the peroxisomal lipidome exhibited different phospholipid compositions. Mitochondria primarily contained PC and PE, each constituting equally for approximately 40% of the total, and were specifically rich in DPG (around 10%), whereas peroxisomes had a higher PC content, as reported in other species and observed in our study (**Table 13**). Moreover, as reported in earlier studies (Jouhet et al., 2004; Michaud & Jouhet, 2019), there appeared a significant replacement of phospholipids (PC decreasing from 39.4% to 32.6%, PE from 41.2% to 29%, PG from 3.0% to 0.3%) to galactoglycerolipids (increasing from 1.4% to 8.4%) in mitochondria lipidome during Pi starvation. During Pi deficiency, our so-called peroxisome fractions also exhibited an increase in galactoglycerolipids (from 11.3% to 20.3%), especially DGDG (**Figure 16**). This observation could be explained by that Pi starvation triggered the typical response of DGDG transfer from plastids to our harvested “peroxisome fractions” that included large proportion of mitochondrial proteins. Interestingly, PL degradation appeared to differ in our so-called “peroxisome fractions”, with a predominant degradation of PC, compared to the main degradation of PE in isolated mitochondria, which might propose an unique modification of Arabidopsis peroxisome lipidome in response to Pi starvation. Certainly, further investigations with highly purified peroxisomes are required to confirm these findings.

		Peroxisome					Mitochondria		Chloroplast
		Rat liver	Yeast	Germinating castor bean endosperm	This study		Arabidopsis cell culture[a]		Arabidopsis
		Hardeman et al., 1990	Zinser et al., 1991	Donaldson & Beevers, 1977	+Pi	-Pi	+Pi	-Pi	Browse & Somerville, 1994
PL	PC	56.4	48.2	51.4	27.9	22.6	39.4	32.6	12.0
	PE	27.5	22.9	27.2	15.6	15.8	41.2	29	-
	PI	4.7	15.8	9.0	5.7	3.6	3.3	2.3	-
	PS	3.0	4.5	1.5	0.7	0.5	0.7	0.6	-
	DPG (CL)	0	7.0	2.3	1.9	1.8	10.2	14.7	-
	PG & PA	-	1.6	2.7	9.7	17.2	3.0	0.3	9.5
DAG		-	-	-	13.0	14.5	2.5	5.0	-
TAG		-	-	-	10.7	3.5	0.5	1.3	-
Galactoglycerolipid		-	-	-	11.3	20.3	2.9	21.1	78.5
Others		6.3	-	-	-	-	-	-	-

Table 13. Glycerolipids composition of isolated peroxisomes from different species and this study, compared with isolated mitochondria and chloroplasts from *Arabidopsis thaliana*. Lipidomic results in this study were compared with peroxisomal lipidome of rat liver reported by Hardeman et al., 1990, of yeast by Zinser et al., 1991 and of germinating castor bean endosperm by Donaldson & Beevers, 1977, as well as with mitochondrial lipidome from Arabidopsis cell suspension culture by Jouhet et al., 2004 and Arabidopsis chloroplastdial lipidome by Browse & Somerville, 1994. -, not mentioned, or not detected. a, Jouhet et al., 2004.

In comparison with Arabidopsis chloroplast lipidome reported by an old study (Browse & Somerville, 1994), chloroplasts are highly enriched in galactoglycerolipids (78.5%), including 3.9% SQDG, 20.9% DGDG and 53.7% MGDG, and are less abundant in PC (12.0%) and PG (9.5%; **Table 13**). In our study, the isolated peroxisome fractions contained small amount of galactoglycerolipids under both conditions, indicating a low plastid contamination.

With regard to the differences in lipid membrane composition among organelles, it is tempting to speculate on the corresponding differences in membrane physiology (Schrader et al., 2020). PC has been traditionally regarded as a structural lipid since its discovery in the 19th century. However, this view began to evolve; for instance, Furse and Kroon (2015) suggested a functional role of PC interacting with peroxisome proliferator-activated receptors (PPARs) in muscle cells. PPARα is a transcription factor regulating the expression of several genes involved in fatty acid uptake and β-oxidation in lipid metabolism. Isoforms of PC, such as 1-palmitoyl-2-oleoyl-sn-glycerol-3-phosphocholine (16:0/18:1 PC, POPC), can serve as the endogenous ligand and a specific upstream effector of muscle PPARα to influence gene expression. Moreover, PC and PE are considered to be required for membrane bending and curvature (see "General Introduction", **Figure 1**). Thus, the relatively high concentrations of PC and PE in the peroxisomal membranes may mirror the highly dynamic nature of the membranes required for rapid fusion and fission (Schrader et al., 2020). Furthermore, the FAs compositions, including saturation grades and chain length, are also important determinants of biomembrane properties. However, the current lack of detailed information on the peroxisomal membrane composition from previous studies limited us to propose any reliable predictions on its architecture and function. Therefore, to address the challenge of revealing Arabidopsis peroxisomal lipid composition and its response to stress conditions will require cross-discipline approaches combining biochemical methods to separate intact peroxisomes with higher purity and to determine its lipidome and proteome.

4.3 Proteins related to oxidative stress response and nitrogen metabolism exhibited significant differences between normal growth conditions and Pi deficiency

Aside from enzymes related to ROS and nitrogen metabolism, none of these identified peroxisomal enzymes exhibited significant differences in response to Pi starvation.

Previous studies have uncovered the oxidative stress symptoms during Pi deficiency in bean plants (Hernández & Munné-Bosch, 2015; Juszczuk et al., 2001). In non-photosynthetic tissues, mitochondria were suggested to be the primary source of ROS. Under normal growth conditions, ROS were maintained at a non-damaging level by various antioxidant compounds and enzymes. However, environmental stress can overwhelm these mechanisms easily, resulting in an excessive production and accumulation of ROS,

leading to oxidative stress. Therefore, exhibiting oxidative stress symptoms was observed as a common feature of several abiotic stresses.

Juszczuk et al., 2001 observed that during phosphate starvation, the respiration rate of bean roots decreased, H_2O_2 concentration and the activities of catalase and total peroxidase increased, while in isolated mitochondria from Pi-deficient roots, the electron flow through the cytochrome pathway was restricted and the gene expression level of oxidase protein was enhanced. These observations indicated that phosphate starvation induced an oxidative stress, which may explain our findings of the significant differences in proteins related to ROS stress response under Pi-limited conditions. Moreover, the Pi-stressed conditions may induce alterations in mitochondrial membrane components via ROS reacting with membrane lipids, which leads to membrane damage and restrict electron transport through cytochrome respiratory chain, resulting in increasing the reduction level of ubiquinone and enhancing the ROS production (Kritsiligkou et al., 2017). Thus, proteins related to ROS stress response exhibited higher abundance under Pi-starved conditions. Based on the link between Pi-starved stress and oxidative stress, it suggested that the increased H_2O_2 level might serve as an important signal for evaluating stress levels. Moreover, the morphological changes resulting from oxidative stress induced by Pi deficiency would be of great interest to explore in plant cells. In our subsequent studies, abnormal mitochondrial morphology were observed in various peroxisomal β-oxidation mutants and will be discussed in Chapter 2 (**Figure 28**).

The impact of Pi-stressed condition on nitrogen metabolism has also been studied in legume, *Virgilia divaricata* (Valentine et al., 2017). Sustained N nutrition in legumes during Pi deficiency is crucial for the survival of both natural and agricultural systems. To maintain N metabolism, the legume nodules have developed several strategies to resist and to respond to the effects of Pi limitation, such as the mechanisms for the modification of N export products and the recycling of amino acids (AAs). Pi deficiency can induce alterations in organic acid synthesis, particularly malate and its subsequent metabolism involving peroxisomes, mitochondria, cytosol, etc. Perturbations in malate supply during Pi deficiency will subsequently reduce amino acid synthesis, limiting the recycling of organic N. Therefore, malate dehydrogenase (MDH), functioning in the reversible conversion of oxaloacetate to malate, also deserves further investigation for its potential to improve the AAs recycling during P deficiency. Additionally, in cotton, a mitochondrial MDH isoform (GhmMDH1) were greatly induced and has been associated with improved growth under Pi deficiency (Wang et al., 2015).

In this study, the APP1 gene related to N metabolism, which was found to be more abundant in Pi-free condition, may represent a novel potential target for the genetic improvement of legume crop. However, less is known about this protein, thus further identification and characterization of which would be required.

4.4 The complexity to define the complete peroxisome proteome

The detection of core and auxiliary enzymes involved in fatty acid β-oxidation in our study indicated that the dynamic range of protein identification was sufficient to cover enzymes primarily expressed in germinating seeds rather than Arabidopsis calli. Moreover, the relatively high abundances of β-oxidation–related enzymes may suggest their yet underestimated roles in calli peroxisomal metabolism. In addition, compared to earlier studies on peroxisomal proteomes from different plant tissues (Eubel et al., 2008; Fukao et al., 2002, 2003; Reumann et al., 2007), our study showed a broader range in the identification of all the core and auxiliary enzymes involved in β-oxidation. The comparison of the protein abundances of these enzymes across different plant organs or different developmental stages may be very promising to provide further insights into their different functions in priming substrates for the β-oxidation process.

However, let alone the unexpected low purity of peroxisomal proteins in this study and the substantial efforts of three other groups working on different Arabidopsis tissue types (Eubel et al., 2008; Fukao et al., 2002, 2003; Reumann et al., 2007), achieving a completely purified peroxisomal proteome in Arabidopsis remains challenging. Reumann et al., 2004 has screened the Arabidopsis genome to identify unknown proteins with putative major or minor peroxisome targeting signals type 1 or 2 (PTS1 or PTS2). However, less than 20% of the proteins with predicted PTS sequences were found in peroxisomal proteomic analyses (Eubel et al., 2008; Fukao et al., 2002, 2003; Reumann et al., 2007), which may be attributed to the lower sensitivity of bioinformatics prediction tools available between 2002 and 2008 compared to the more advanced methods we have nowadays. In addition, despite the few overlap between all these studies, significant discrepancies of peroxisomal proteins exist across different Arabidopsis tissue types, particularly for those newly identified peroxisomal proteins from each study, complicating the effort to define a comprehensive peroxisome proteome.

Therefore, in order to improve peroxisomal protein identification, to analyze peroxisomal functions in details, and to reconstruct the major metabolic pathways in plant cells, further advances in peroxisome purification techniques are required, such as integrating other protein characterization methods based on peptide fingerprinting, free-flow electrophoresis (FFE; Eubel et al., 2008), or immunopurification (Boussardon et al., 2020). Additionally, more quantitative data and thorough assessments of the protein targeting are necessary.

Chapter 2

Role of PXA1 and peroxisomal β-oxidation in membrane lipid remodeling in response to Pi starvation

1 Pi-stress response of the core β-oxidation enzymes

PXA1 and several peroxisomal proteins involved in β-oxidation pathway were found in our co-IP results with Tom40-HA (Michaud and Albrieux, unpublished data), suggesting a connection between mitochondria and peroxisomes, particularly regarding the β-oxidation pathway. As the total lipid content decreased in *A. thaliana* cell cultures in response to Pi starvation, this raised questions about the role of peroxisome and β-oxidation in membrane lipid remodeling in response to Pi starvation. Indeed, several studies have reported that FAs β-oxidation activity increased upon nutrient deprivation, for instance, carbon starvation (Contento & Bassham, 2010), cold stress (Dong et al., 2009) and extended darkness (Kunz et al., 2009). However, a clear role of FAs β-oxidation pathway in response to Pi starvation is not yet elucidated.

Multiple studies have documented the changes of genome-wide gene expression across different tissue types during Pi deprivation (J et al., 2012; Morcuende et al., 2007; Wu et al., 2003). **Table 14** summarized previous analyses of the expression levels of the core β-oxidation enzymes in response to Pi starvation across tissues.

Morcuende et al., 2007 presented the genome-wide data of the log2 transformation when comparing "full nutrient versus Pi-starved" and "Pi re-addition after 3 h versus Pi-starved" conditions. Log2 values ≥ 2-fold change (increase or decrease) in signal intensity between –Pi and +Pi conditions in replicates, along with an adjusted P-value < 0.05, were identified as Pi-starvation-induced genes from the 9-day-old seedling experiments, while log2 values > 5-fold indicated the strong Pi deprivation-induced genes. Of all the core

Gene name	Accession	Pi starvation-induced			Recovery after Pi re-addition	
		9-day-old seedlings (Morcuende et al., 2007)	Leaves (Wu et al., 2003)	Roots (Wu et al., 2003)	Seedlings (Morcuende et al., 2007)	Roots (J et al., 2012)
PXA1	At4g39850	nc	nc	nc	nc	nc
LACS6	At3g05970	nc	nc	nc	nc	nc
LACS7	At5g27600	+	nc	nc	nc	nc
ACX1	At4g16760	nc	+	nc	nc	nc
ACX1.2	At2g35690	nc	nc	nc	nc	nc
ACX2	At5g65110	nc	nc	nc	nc	nc
ACX3	At1g06290	nc	nc	nc	nc	nc
ACX3.2	At1g06310	nc	nc	nc	nc	nc
ACX4	At3g51840	nc	+	+	nc	nc
MFP2	At3g06860	nc	+	nc	nc	nc
AIM1	At4g29010	nc	nc	nc	nc	nc
KAT1	At5g46240	nc	nc	nc	nc	nc
KAT2	At4g18290	nc	nc	nc	nc	nc
KAT3	At4g32650	nc	nc	nc	nc	nc

Table 14. Pi-starved response and recovery of the core β-oxidation gene expression levels in various Arabidopsis tissues. +, induction; -, repression; nc, no change.

β-oxidation enzymes, only expression of *LACS7* showed a slight induction upon Pi limitation (**Table 14**). After 3 hours of Pi re-addition, none of these genes exhibited changes in expression levels (**Table 14**).

Wu et al., 2003 identified a set of genes that were induced or repressed over 2-fold in leaves and roots within a 72-hour course of Pi starvation. Notably, induction of *ACX1* and *MFP2* were observed in leaf tissues, while Pi deprivation altered the *ACX4* gene expression in both leaves and roots (**Table 14**). J et al., 2012 analyzed gene expression data in root materials after a 10-day treatment of Pi starvation and an additional 3-day period of Pi re-supply. None of the core β-oxidation genes showed changes in expression levels after Pi re-addition (**Table 14**).

However, minor changes observed in gene expression levels are insufficient to determine the contribution of β-oxidation pathway in response to Pi starvation. In this chapter, we attempted to analyze the response of two loss-of-function mutants in genes involved in β-oxidation: *PXA1*, encoding an upstream regulatory protein, which is completely impaired in β-oxidation pathway, and *MFP2* that may partially affect β-oxidation pathway, to Pi-limited conditions. By the comparison analysis between these two mutants with wild type, we aimed to investigate the roles of these two proteins and, consequently, the metabolic role of β-oxidation pathway in membrane lipid remodeling in response to Pi starvation.

2 Peroxisomal ABC transporter - PXA1

Substrates for β-oxidation enter peroxisomes via ATP-binding cassette (ABC) transporters of subfamily D (ABCD) for the subsequent metabolic processes. Arabidopsis AtABCD1, PXA1, is the most studied and comprehensively understood peroxisomal ABC transporter in plants (Baker et al., 2015). Plant *PXA1* gene is expressed throughout the plant life cycle and encodes a full-size ABC transporter with two duplicated

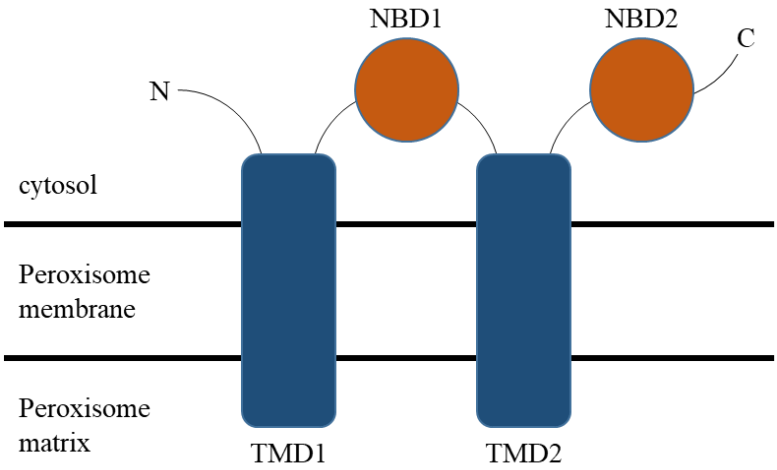


Figure 18. Diagram of a typical ABC transporter protein. The structure of a representative ABC protein is shown at the lipid bilayer of peroxisomal membrane. The transmembrane domains (TMD) are in blue, while the nucleotide binding domains (NBD) are fold in red. N, N terminal portion of PXA1; C, C terminus.

but distinct halves fused into a symmetrical heterodimer (Park et al., 2013). Hundreds homologs have been identified across bacteria, yeast and human (Dean et al., 2001; Nyathi et al., 2010, p. 1; Roermund et al., 2012; Shintre et al., 2013). However, these diverse proteins across different species share a common architecture, consisting of two transmembrane domains (TMDs) and two cytosol-exposed nucleotide binding domains (NBDs) in the arrangement of N-TMD1-NBD1-TMD2-NBD2-C (**Figure 18**; Dean et al., 2001; Shintre et al., 2013).

Each TMDs contains six putative long membrane-spanning domains that traverse the lipid bilayer, while the NBDs feature a signature or C motif, and the Walker A and B motifs (Dean et al., 2001; Park et al., 2013). During the transport cycle, the transporter transitions from open-inwards to an open-outwards state allow the substrates bind on one side of the membrane and release on the other side (Shintre et al., 2013). The Walker B motif of the second NBD (NBD2), oriented on the cytosolic side of peroxisomal membrane, is a region known to be important for the regulation of protein activity *in vivo* in planta (Dietrich et al., 2009; Park et al., 2013).

PXA1 mediates the transport of acyl-CoA for FAs β-oxidation (see "General Introduction", **section 2.3.3.5**), lipophilic hormone precursors for the jasmonate (JA) and auxin biosynthesis, precursors for ubiquinone (coenzyme Q) synthesis, and cinnamic acid (CA) required for the benzoic acid (BA) synthesis, into the peroxisome (Baker et al., 2015; Dave et al., 2011; Eastmond, 2006; Footitt, 2002; M. Hayashi et al., 2002; Theodoulou et al., 2005; Zolman et al., 2001).

JA synthesis is widely believed to begin with the release of the unsaturated fatty acid, linolenic acid (18:3), from galactolipids in plastids, followed by a series of metabolic transformations that eventually produce (9S,13S)-12-oxo-phytodienoic acid (OPDA), which is the precursor for JA synthesis and is transported into peroxisomes via PXA1 (Theodoulou et al., 2005). The synthesis of OPDA occurs in the chloroplast. Subsequently, OPDA is reduced by 12-oxo-phytodienoate reductase (OPR) into 3-oxo-2-(2'-pentenyl)-cyclopentane-1-octanoic acid (OPC:8) at peroxisome, where it is then shortened by three rounds of peroxisomal β-oxidation to yield JA (Theodoulou et al., 2005). Thus, JA biosynthesis initiates in the chloroplast and terminates in the peroxisome, implicating possible membrane-bound transporters between these two organelles. In Arabidopsis, a parallel hexadecanoid pathway based on the plastid 16:3 fatty acid to synthesize JA also exists (Weber et al., 1997).

PXA1 is also implicated in the peroxisomal import of indole 3-butyric acid (IBA), the precursor for auxin indole-3-acetic acid (IAA) synthesis (Damodaran & Strader, 2019). The conversion of IBA to IAA occurs in the peroxisome through the β-oxidation process with the actions of ACX3, AIM1, and PED1 enzymes (M. Hayashi et al., 2002; Zolman et al., 2001). IAA is a vital plant hormone that regulates numerous

developmental processes. However, the peroxisomal transporter responsible for the efflux of IBA-derived IAA from the peroxisome remains unclear (Damodaran & Strader, 2019).

Moreover, Block et al., 2014 demonstrated that PXA1 plays a critical role in the import of *p*-coumaric acid, a ubiquinone precursor. Additionally, Bussell et al., 2014 revealed that peroxisomal PXA1 is also required for the production of secondary metabolites derived from BA, thus pointing a potential role of PXA1 in the import of CA, the precursor for BA synthesis. The CA to BA conversions in Arabidopsis employ the same core set of β-oxidation enzymes involved in the synthesis of IAA from IBA (Bussell et al., 2014).

The loss-of-function alleles of *PXA1* have been independently studied in different laboratories (Footitt, 2002; Fulda et al., 2004; Hayashi et al., 2002; Russell et al., 2000; Zolman et al., 2001). Mutant genotypes and respective ecotypes are listed in **Table 15**. Different alleles exhibit distinct germination phenotypes, whereas all alleles show resistance to a toxic amount of 2,4-DB for seedling root growth (Footitt et al., 2006).

Protein	Accession	Mutant allele	Stock number	Nature of allele	Background	Ref
PXA1	At4g39850	*pxa1-1*	CS3950	Point mutation	Col0	(Zolman et al., 2001)
		pxa1-2	SALK_019334	Point mutation	Col0	(Kunz et al., 2009)
		pxa1-3	SALK_002100	Point mutation	Col0	(Kunz et al., 2009)
		cts-1	*cts-1*	Fast neutron translocation	Ler	(Footitt, 2002; Russell et al., 2000)
		cts-2	*cts-2*	T-DNA insertion	Ws2	(Footitt, 2002)
		ped3	*ped3*	-	Ler	(Hayashi et al., 1998, 2002)

Table 15. Description of *pxa1* mutant genes, alleles and ecotypes isolated in previous studies.

The *pxa1-1* mutant was shown to have normal germination potential; however, the mutant plants exhibit developmental defects, failing to develop beyond germination without exogenous sucrose (Zolman et al., 2001). The mutant plants display slower growth, slightly shorter roots, smaller rosettes, fewer leaves, and shorter inflorescence stems, compared to the wild type (Zolman et al., 2000, 2001). Moreover, it has defects in lateral root initiation, producing fewer lateral roots than the wild type. It is resistant to the inhibition of root elongation by IBA, but remains sensitive to the inhibition by IAA. The *pxa1-2* and *pxa1-3* alleles, also isolated from the collection of sequence-indexed T-DNA lines of the SALK Institute and named according to the nomenclature used by Zolman et al., 2001, were comparatively studied with *pxa1-1* mutant under

extended darkness conditions (Kunz et al., 2009). This study demonstrated that peroxisomal β-oxidation plays a major role in dark-treated plants (Kunz et al., 2009).

The *cts-1* and *cts-2* alleles, studied by Footitt, 2002 and Russell et al., 2000, are defective in lipid mobilization and accumulate acyl-CoAs. In contrast to *pxa1-1* mutant, the *cts-1* and *cts-2* mutant seeds do not completely germinate, and require sucrose for both germination and seedling establishment. The *cts-1* exhibits similar phenotypes in stunted root growth as *pxa1-1* mutant. There are no significant differences in peroxisomal size or morphology in the *cts-1* mutant cells, but it contains small vacuoles and distorted chloroplast morphology. It displays functional peroxisomal β-oxidation activity, thus addition of exogenous propionate or butyrate, short chain fatty acids that can potentially enter the peroxisome membrane, to the growth media can greatly enhance the germination potential of *cts-1* seeds. Moreover, it has been demonstrated that CTS interacts with genes promoting dormancy, such as embryo reduced dormancy 2 (RDO2), and hormone-related abscisic acid insensitive 1 (ABI1), meanwhile itself regulates in the embryo dormancy status, consequently leading to the defects in germination (Footitt, 2002; Russell et al., 2000). Thus, the *cts-1* allele was proposed to be in a "forever dormant" state.

The *ped3* mutant line has also been slightly previously described in some aspects (M. Hayashi et al., 2002). In the *ped3* mutants, peroxisomes are morphologically normal, and contain detectable amounts of enzymes for fatty acid β-oxidation and glyoxylate cycle (M. Hayashi et al., 2002).

Therefore, in order to avoid germination defects, we chose the *pxa1-1* mutant line (CS3950; Zolman et al., 2001) for the following analysis in this study.

3 Peroxisomal multifunctional protein - MFP2

The multifunctional proteins (MFP) involved in peroxisomal β-oxidation catalyzes four separate reactions, two of which (2-trans enoyl-CoA hydratase, ECH; and l-3-hydroxyacyl-CoA dehydrogenase, HACD) are the core actions essential for the FAs catabolism. In the Arabidopsis genome, *AIM1* and *MFP2* are the only MFP genes, which share 58% identity. Both AIM1 and MFP2 contain putative type 1 peroxisomal targeting signals (PTS-1), and MFP2 has been confirmed to localize to the peroxisome *in vivo* using a GFP fusion construct (Cutler et al., 2000). They both have ECH and HACD activity functioning in the β-oxidation pathway. The double mutant *mfp2aim1* is embryolethal, showing the importance of these proteins in plant development (Rylott 2006). However, *in vivo* and *in vitro* characterization indicated their different chain length specificities (Rylott et al., 2006). MFP2 functions as a long chain hydratase coupled with a short, medium, and long chain-specific dehydrogenase, whereas AIM1 appears to preferentially interact with short chain acyl-CoA, evidenced by the elevated levels of C18:1 and C18:2 unsaturated fatty acids in the *aim1* mutant plants (Rylott et al., 2006).

The *AIM1* gene is primarily expressed in silique, flower and older seedlings (> 8 days) at minimal expression levels during early post-germinative growth, while *MFP2* gene is significantly expressed in germinating seeds, suggesting a crucial role of MFP2 in lipid remobilization during seed germination (Eastmond & Graham, 2000). Moreover, MFP2 exhibits expression changes in leaves during Pi starvation (**Table 14**). Therefore, we chose to investigate the role of MFP2 in response to Pi starvation, and consider it as a partial regulator of the β-oxidation pathway, unlike PXA1, and as a control in this study.

Arent et al., 2010 has reported the structure of Arabidopsis MFP2, a 79-kDa protein comprising three domains arranged into two compact structural entities separately, and a linker helix in a stable monomer (**Figure 19**). Two regions corresponding to ECH and HACD activities, respectively, have been mapped, including one N-terminal ECH domain and a C-terminal HACD entity, which is further divided into two HACD domains ($HACD_N$ and $HACD_C$) with substantial interdomain interaction (**Figure 19**). MFP2 introduces H_2O to the double bond of enoyl-CoA through its ECH domain and oxidizes the hydroxyl-acyl group of the resultant hydroxylacyl-CoA to ketoacyl-CoA via its HACD domains (**Figure 19**).

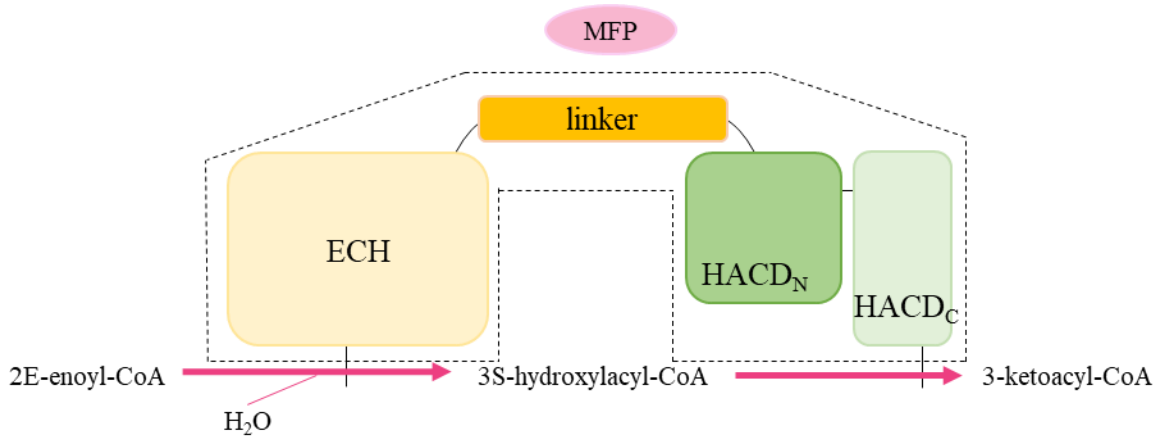


Figure 19. Diagram of the MFP2 protein. The Arabidopsis MFP2 protein consists of three domains and a linker helix. The ECH domain of MFP2 protein is shown in yellow, the linker to the HACD domains in orange, the N-terminal HACD domain in green, and the C-terminal HACD domain in light green. These domains form a stable MFP2 monomer. The ECH domain of MFP2 is responsible for introducing H_2O into the double bond of enoyl-CoA to produce hydroxylacyl-CoA, while the HACD domains oxidize the hydroxyl-acyl group of the produced hydroxylacyl-CoA into ketoacyl-CoA. 2-trans enoyl-CoA hydratase, ECH; l-3-hydroxyacyl-CoA dehydrogenase, HACD; N-terminal HACD domain, $HACD_N$; C-terminal HACD domain, $HACD_C$.

Five well-studied *mfp2* mutants, namely *mfp2-1*, *mfp2-2*, *mfp2-3*, *mfp2-4*, and *mfp2-5*, were identified (Rylott et al., 2006; Sussman et al., 2000). Mutant genotypes and their respective ecotypes are detailed in **Table 16**.

Mutations in the *MFP2* gene result in a general sucrose-dependent seedling phenotype (Rylott et al., 2006). Beyond seedling establishment, all the *mfp2* mutant plants exhibit an indistinguishable phenotype from wild-type plants throughout the rest of the life cycle, suggesting that, after seedling establishment, MFP2

activity is sufficiently compensated by AIM1 and/or additional hydratases. The *mfp2* mutants are sensitive to 2,4-DB, unlike *aim1* mutant exhibiting resistance. Moreover, all the *mfp2* mutants lack hydroxyacyl-CoA dehydrogenase activity, and showed reduced levels of long-chain enoyl-CoA hydratase activity. Additionally, the *mfp2* mutants display a reduction in storage TAG breakdown, an accumulation of long-chain acyl-CoAs during early post-germinative growth, and a reduced number of peroxisomes that are enlarged (Rylott et al., 2006). The increase in peroxisomal size may specifically result from the excess peroxisomal concentration of acyl-CoAs, similar as demonstrated in the *ped1* and *kat2* mutants (Graham et al., 2002; Rylott et al., 2006).

In order to ensure consistency with the backcrossed wild type Columbia 0 (Col0) used for *pxa1-1* mutant, we selected the *mfp2-2* mutant (SALK_098016; Rylott et al., 2006) for the subsequent analysis in this study.

Protein	Accession	Mutant allele	Stock number	Nature of allele	Background	Ref
MFP2	At3g06860	*mfp2-1*	*mfp2-1*	T-DNA insertion	WS	(Rylott et al., 2006; Sussman et al., 2000)
		mfp2-2	SALK_098016	T-DNA insertion	Col0	(Rylott et al., 2006)
		mfp2-3	*mfp2-3*	Point mutation	Col0	(Rylott et al., 2006)
		mfp2-4	*mfp2-4*	Point mutation	Col0	(Rylott et al., 2006)
		mfp2-5	*mfp2-5*	Point mutation	Col0	(Rylott et al., 2006)

Table 16. Description of *mfp2* mutant genes, alleles and ecotypes isolated in previous studies.

4 Results

4.1 Isolation of the homozygous *pxa1* (CS3950) and *mfp2* (SALK_098016) mutants

The *pxa1-1* mutant (CS3950) used in this study has a G-to-A mutation at position 5559, resulting in the absence of 5'-splice site of intron 24 and the generation of a truncated protein (**Figure 20A**; Zolman et al., 2001). To genotype *pxa1-1* mutants, two primers were designed at the both side of the point mutation to perform PCRs (**Figure 20A**), and subsequently the purified PCR products were sequenced to verify the point mutation. However, after genotyping, the harvested M_2 mutant population of homozygous *pxa1-1* mutant exhibited severe germination defects, even in the presence of sucrose, which contrasted with the observations reported by Zolman et al., 2001. Nevertheless, a germination defect in *pxa1-1* mutant was reported by another study (Footitt et al., 2006), suggesting that the germination ability of *pxa1-1* seeds might be influenced by the conditions of seed growth and storage.

Since germination inhibition was reported for others *pxa1* alleles (*cts-1* and *cts-2* mutant; Dietrich et al., 2009; Footitt, 2002; Russell et al., 2000), multiple strategies were employed to enhance the germination rate of the generated M_2 *pxa1-1* mutant seeds. Freshly harvested M_2 seeds were stored for over a year to increase germination potential. The imbibed seeds were pre-chilled in darkness for several weeks before being placed in the growth chamber, or an appropriate amount of exogenous gibberellin, propionate, or isobutyrate, respectively, were added to the growth media to promote germination of dormant seeds (Hooks et al., 2007; Russell et al., 2000). However, none of these methods significantly affected the eventual germination rate (data not shown).

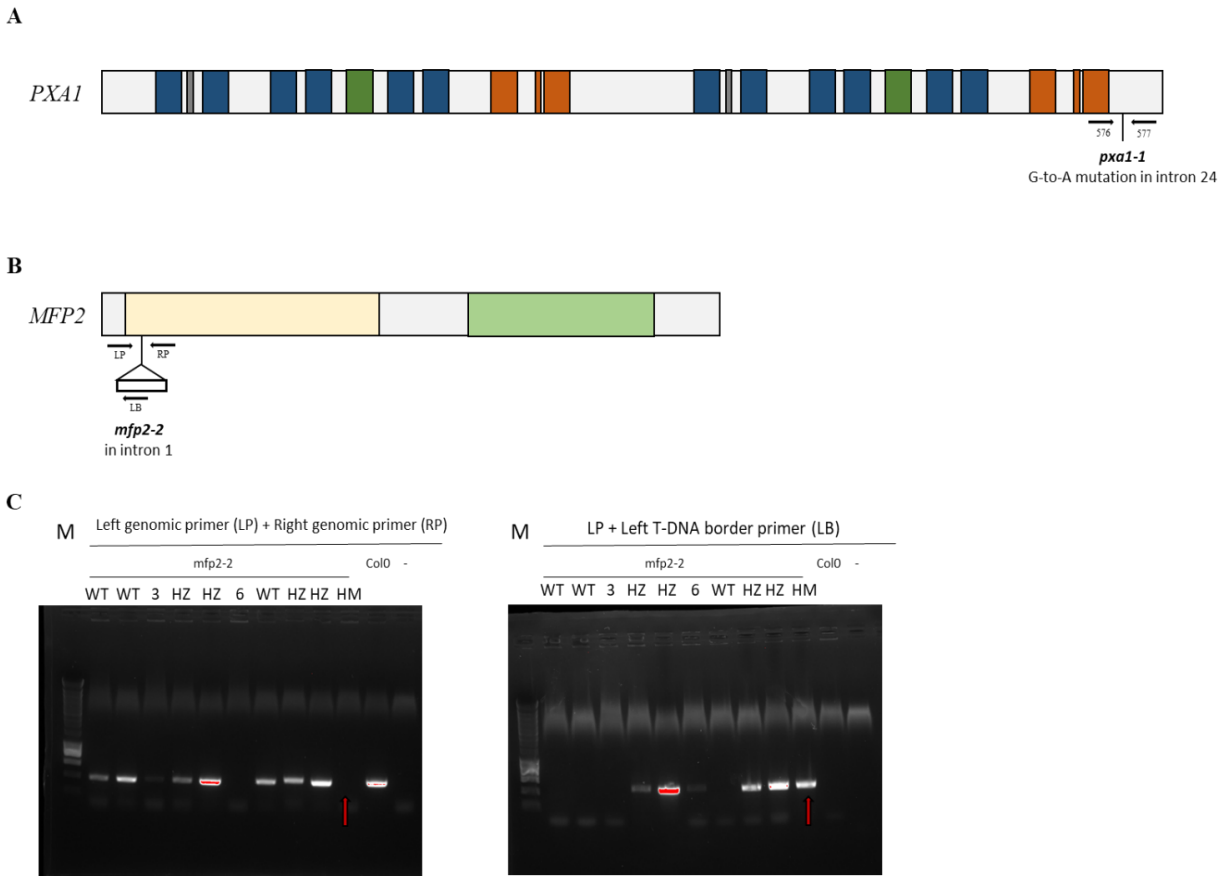


Figure 20. Isolation of *pxa1-1* and *mfp2-2* homozygous plant mutants. A. Point mutation site in *pxa1-1* mutant. *PXA1* gene encodes several conserved domains, including the TMD domains shown in blue, NBD domains in red, corresponding to PXA1 protein structure (**Figure 18**), respectively, and two EAA-like domains in green, which are conserved regions on the cytoplasmic face of the protein between TMD 4 and 5 and are thought to control substrate specificity by binding fatty acids. *pxa1-1* has a G-to-A mutation at position 5559 that disrupts the 5′-splice site of intron 24. Two oligonucleotides were used to sequence the *pxa1-1* mutant site. B. Position of T-DNA insertion site in *mfp2-2* mutant. *MFP2* gene encodes domains having ECH (in yellow), and HACD (in green) activities, corresponding to MFP2 protein structure (**Figure 19**), respectively. The *mfp2-2* mutant has a T-DNA in the first intron, 283 bp 3' from the initiator ATG. Three primers were designed, including a left genomic primer (LP), right genomic primer (RP), and left T-DNA border prime (LB), for SALK *mfp2-2* line genotyping. C. PCR results for HM *mfp2-2* mutant, shown with red arrows. homozygous lines, HM; heterozygous lines, HZ; wild type, WT.

The *mfp2-2* mutant has a T-DNA in the first intron, 283 bp 3' from the initiator ATG (**Figure 20B**; Rylott et al., 2006). To isolate homozygous (HM) lines of *mfp2-2* mutant, three primers were designed, including a left genomic primer (LP), right genomic primer (RP), and left T-DNA border primer (LB), to perform PCRs for SALK lines genotyping (**Figure 20B**). Wild type (WT) will generate PCR products from LP to RP, whereas HM lines will display a band from the LP of the vector to LB of insertion site, and heterozygous (HZ) lines will show both bands (**Figure 20C**). Thus, the PCR results revealed an examined plant that is HM line of *mfp2*-2 mutant (**Figure 20C**). Thereafter, the HM M_2 mutant population of *mfp2-2* mutant was harvested and stored for the subsequent analysis.

4.2 Phenotypic observations of *pxa1* and *mfp2* mutants under standard and Pi-starved conditions

4.2.1 Growth examination of Arabidopsis *pxa1* and *mfp2* calli

The germination defects observed in M_2 *pxa1-1* mutant seeds limited us to perform phenotypic analysis of seedling establishment under Pi-enriched and Pi-deprived conditions. Therefore, Arabidopsis calli of *pxa1-1* and *mfp2-2* mutant, hereafter referred to as the *pxa1* and *mfp2* mutant, respectively, were directly induced from the original seed batch received from NASC, and genotyped for the subsequent analyses.

During the calli subculturing, *pxa1* calli exhibited slower growth, compared to Col0 and *mfp2* calli. Thus, conducting a growth assay onto the generated calli of *pxa1*, with controls of Col0 and *mfp2* calli, in the presence or absence of Pi would be of significant interest.

Calli of the comparable size were thus placed on media with or without Pi, and their growth were followed every week (**Figure 21A**) and quantified by their areas using Fiji software with the ROI manager (**Figure 21B**). On the medium containing Pi, the growth of *mfp2* calli was similar to that of wild-type calli, whereas *pxa1* calli exhibited significantly slower growth (**Figure 21A & 21B**). In the absence of Pi, the growth of Arabidopsis wild-type calli was inhibited due to stress, and a similar growth inhibition was observed in *mfp2* calli (**Figure 21A & 21B**). Interestingly, when compared to the growth of *pxa1* calli in +Pi, no further growth inhibition was observed in Pi-starved *pxa1* calli (**Figure 21A & 21B**). These results indicated that, though *pxa1* calli exhibited a significant growth defect in Pi-replete condition, lack of Pi inhibited the growth of Col0 and *mfp2* calli, but did not significantly affect the growth of *pxa1* calli.

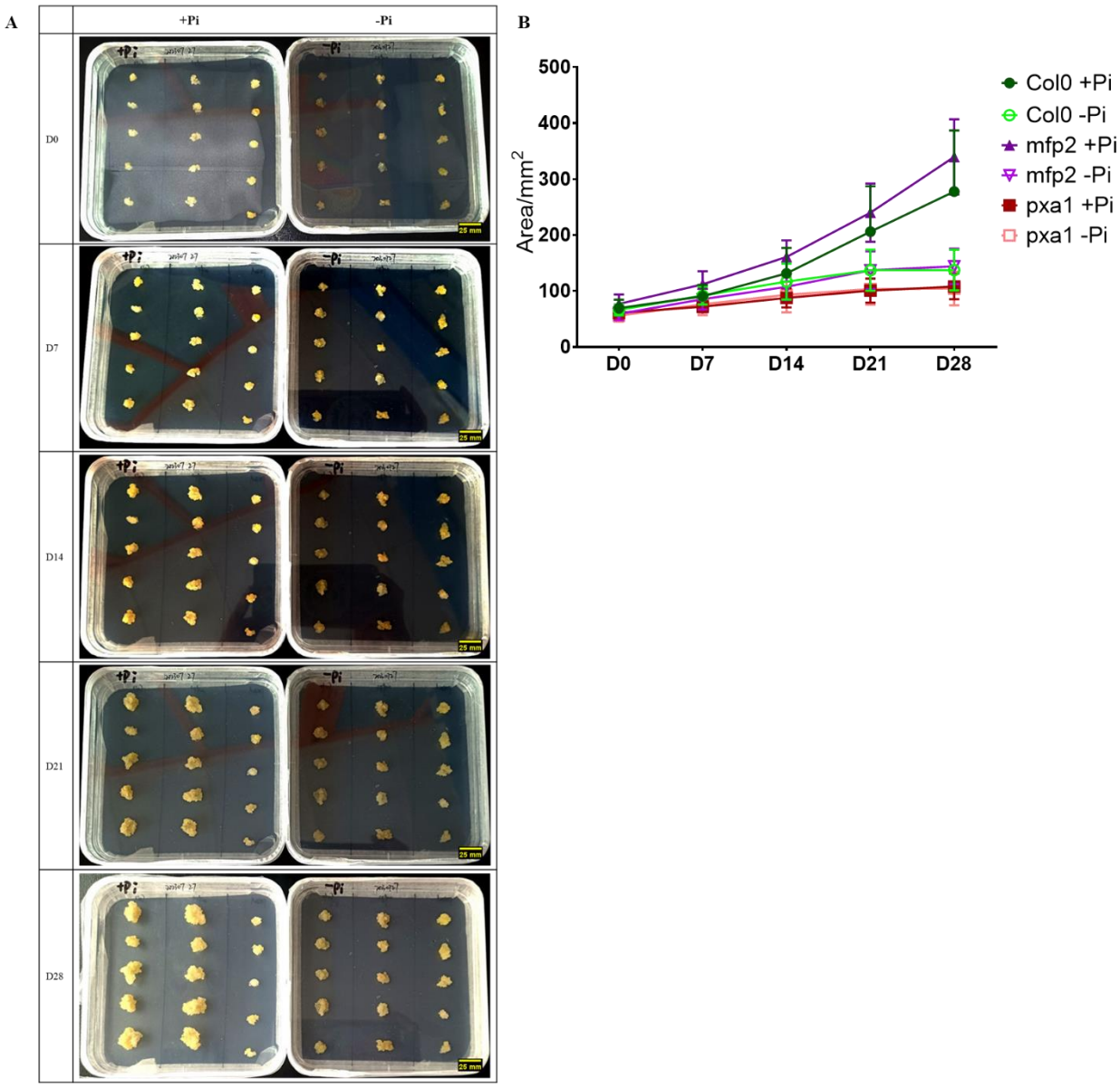


Figure 21. Growth rate of Arabidopsis wild type, *pxa1*, and *mfp2* calli under Pi-enriched (+Pi) and Pi-limited (-Pi) conditions. A. Photographs were taken at 0, 7, 14, 21, and 28 days of growth under both conditions. Scale bar = 25 mm. B. Experiments were performed in triplicates. Calli areas were quantified using Fiji software with the ROI manager. N=14-15.

4.2.2 Seedling establishment examination of *mfp2* mutant

Hereby, due to the limitations in *pxa1* germination defects, we primarily focused on Col0 and *mfp2* mutant to measure their primary root length, and thus to assess their abilities in adaptation to low Pi. Seedlings of Col0 and *mfp2* mutant were vertically grown with 1 mM Pi (+Pi) or 0.005 mM Pi (-Pi) for 7 days, in triplicates. **Fig. 22A** showed that under low Pi conditions, both Col0 and *mfp2* seedlings exhibited yellowish cotyledons in reduced size, indicating that the examined seedlings were Pi-starved. However, the Pi-starved root phenotypes reported by previous studies, such as the inhibition of primary root growth, increases in lateral root formation and growth, and enhanced production and elongation of root hairs (reviewed in Péret et al., 2011), were absent in Pi-deprived Col0 seedlings in our study. No obvious differences were observed between wild type and *mfp2* mutant under either conditions (**Figure 22A**).

Quantifications of the primary root length were subsequently performed by ImageJ software. The comparative analysis revealed no significant difference in primary root length between +Pi and -Pi

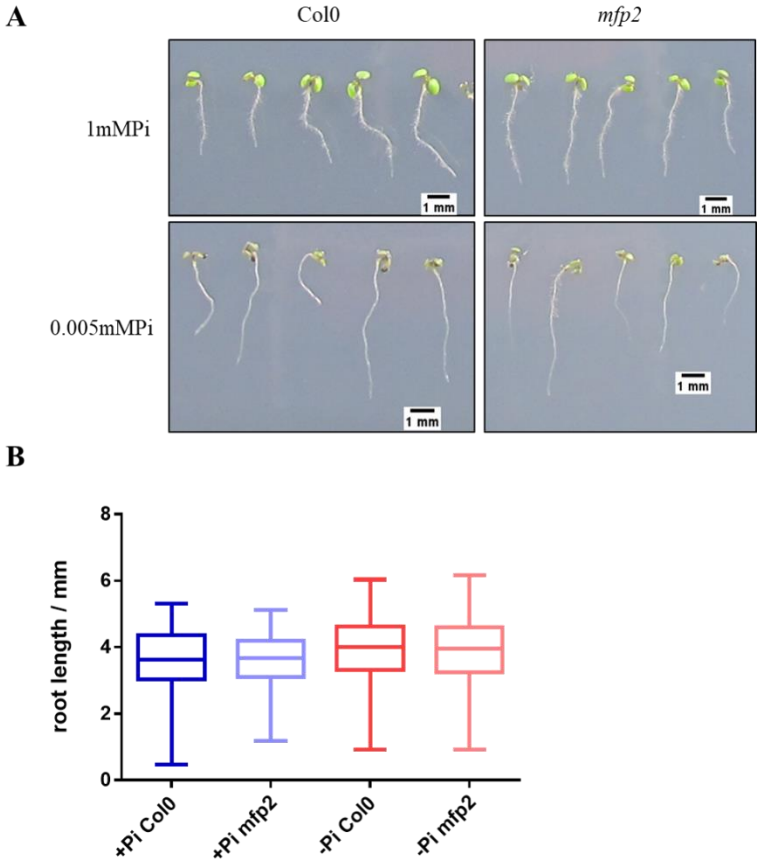


Figure 22. Root length of 7-day-old Arabidopsis wild-type, and *mfp2* seedlings under enriched Pi (1 mM Pi) and low Pi (0.005 mM Pi) conditions. A. Photographs were taken after 7 days of growth under both conditions. Scale bar = 1 mm. B. Experiments were performed in triplicates. Root length was manually quantified using ImageJ software. N=57-66.

conditions in both Col0 and *mfp2* mutant (**Figure 22B**), suggesting that the disruption of MFP2 gene does not affect primary root growth either under standard conditions, or in response to Pi starvation, and thus that the absence of MFP2 alone does not have physiological impact on plant's response to phosphate deprivation. This phenotype might be attributed to the compensatory ability of the second MFP2 homolog: AIM1.

4.3 Lipid analysis of the *pxa1* and *mfp2* mutants under standard and Pi-starved conditions

4.3.1 Preliminary data of lipid analysis of Col0 and *mfp2* seedling grown under standard and Pi-starved conditions

In order to further investigate whether *mfp2* mutant affects the ability of lipid remodeling during Pi starvation, samples of Col0 and *mfp2* seedlings grown under 1 mM Pi (High Pi) or 0.005 mM Pi (Low Pi) conditions were collected after 14 days and lipids were extracted by the standard Folch method, and subsequently quantified and analyzed by GC-FID and LC-MS/MS. However, because the plant phenotypes observed under -Pi conditions (including Col0) did not align with previous reports (reviewed in Péret et al., 2011), this experiment was conducted only once and was not repeated.

Under Pi-enriched conditions, there were no notable difference in both FA and lipid composition between Col0 and *mfp2* seedlings (**Figure 23A & 23B**, in dark or light blue). In the Pi-starved samples, both Col0 and *mfp2* mutant exhibited a general elevated level in 18:0 and decreased level in 18:2 (**Figure 23A**, in dark or light red). An increase in SQDG and DGDG with a corresponding decrease in phospholipids such as PG,

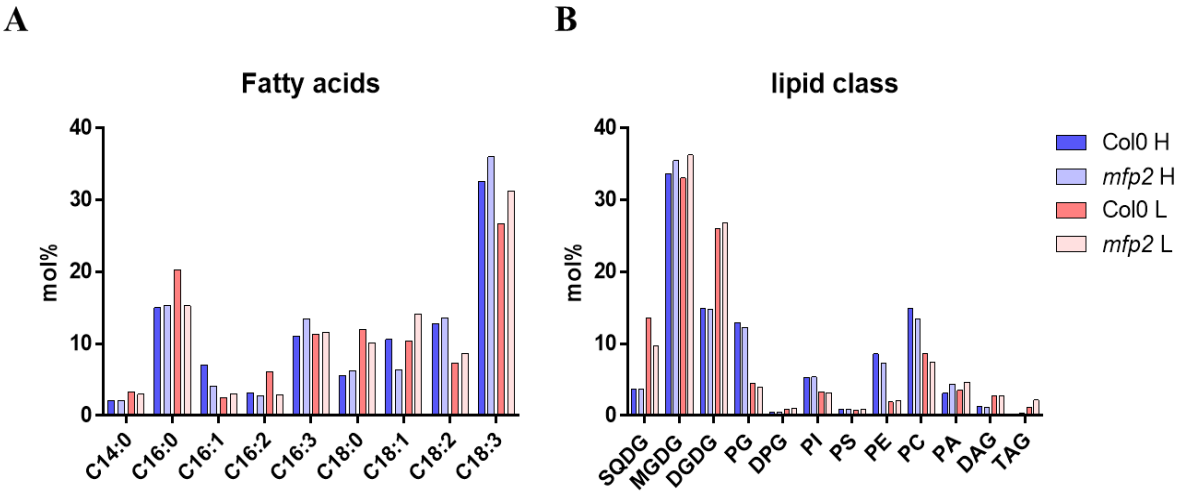


Figure 23. Lipid analysis of 14-day-old Arabidopsis wild-type, and *mfp2* seedlings under enriched Pi (1 mM Pi) and low Pi (0.005 mM Pi) conditions. A & B. Fatty acid and lipid composition of 14-day-old Col0 and *mfp2* seedlings grown under 1 mM Pi or 0.005 mM Pi conditions. "H" and "L" represented a sufficient level of Pi in 1 mM and a low level of Pi in 0.005 mM, respectively.

PI, PE, and PC, and a slight increase in DAG and TAG levels were observed in both Pi-starved Col0 and *mfp2* seedlings (**Figure 23B**, in dark or light red). Additionally, Pi-deprived *mfp2* seedlings displayed a possible accumulation of C18:1 compare to Pi-sufficient conditions, which was not observed in the wild type (**Figure 23A**). However, no significant differences in each lipid composition were observed between Col0 and *mfp2* mutant under both standard and Pi-starved conditions (**Figure 23B**), indicating that disruption of MFP2 did not significantly affect the seedling lipid content under standard conditions, nor influence lipid remodeling in response to phosphate starvation in seedlings.

4.3.2 Lipid analysis of Col0, *mfp2* and *pxa1* cell suspension cultures under standard and Pi-starved conditions

Calli of *A. thaliana* wild type Col0, homozygous *mfp2* and *pxa1* mutants were cultivated in cell suspension culture in the defined medium with (+Pi) and without Pi (-Pi). Samples from each line were collected after 2, 4, 6, and 8 days of cultivation under both conditions. Lipids from freeze-dried samples were extracted by the standard Folch method, and subsequently quantified and analyzed by GC-FID and LC-MS/MS.

Firstly, comparing the total lipid amount of calli in nmol of fatty acid methyl esters (FAMEs) per mg of fresh weight of calli at different time points, there was no significant difference between Col0, *mfp2* and

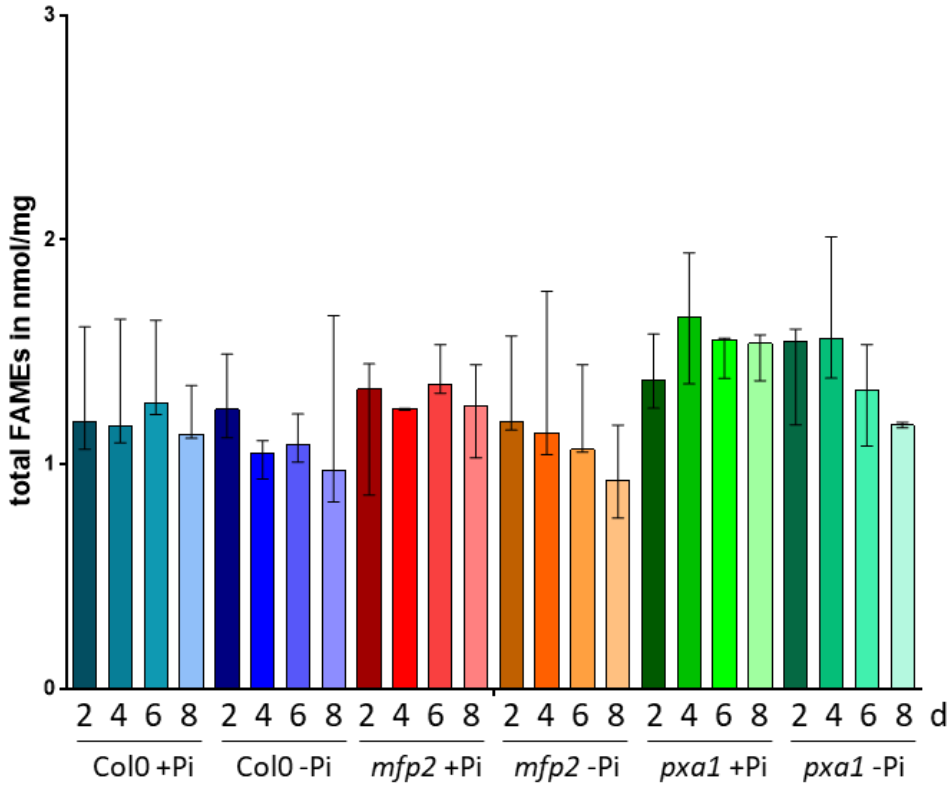


Figure 24. Total amount in nmol of fatty acid methyl esters (FAMEs) per mg of fresh weight from Col0, *mfp2* and *pxa1* calli grown under phosphate replete (+Pi) and deplete (-Pi) conditions at various time points. Data represented the means ± SD of five biological replicates for each condition.

pxa1 mutant in either normal or Pi-starved cultures (**Figure 24**). Under Pi-deprived conditions, as mentioned before, all cell lines exhibited a gradual decrease in total lipid content over time (**Figure 24**), likely reflecting a lipid degradation in response to Pi starvation, and indicating that complete or partial disruption of β-oxidation pathway did not affect this general lipid turnover.

Thereafter, the fatty acid composition (in mol%) of all the cell lines after 4, 6, and 8 days of Pi starvation was analyzed by GC-FID (**Figure 25**). Results showed a general higher level of 18:3 and lower level of 18:2 in *pxa1*, compared with Col0 and *mfp2*, under both standard and Pi-deprived conditions at various time points (**Figure 25**). The distinct unsaturation levels of 18C observed in *pxa1* calli may result from the slow growth pattern of *pxa1* (Meï et al., 2015). No significant differences were observed between Col0 and *mfp2* calli under either conditions at any time points (**Figure 25**). Under Pi-starved conditions, all cell lines exhibited the similar responses of the decreased 18:1 and increased 18:3 at different time points (**Figure 25**), as reported by Meï et al., 2015.

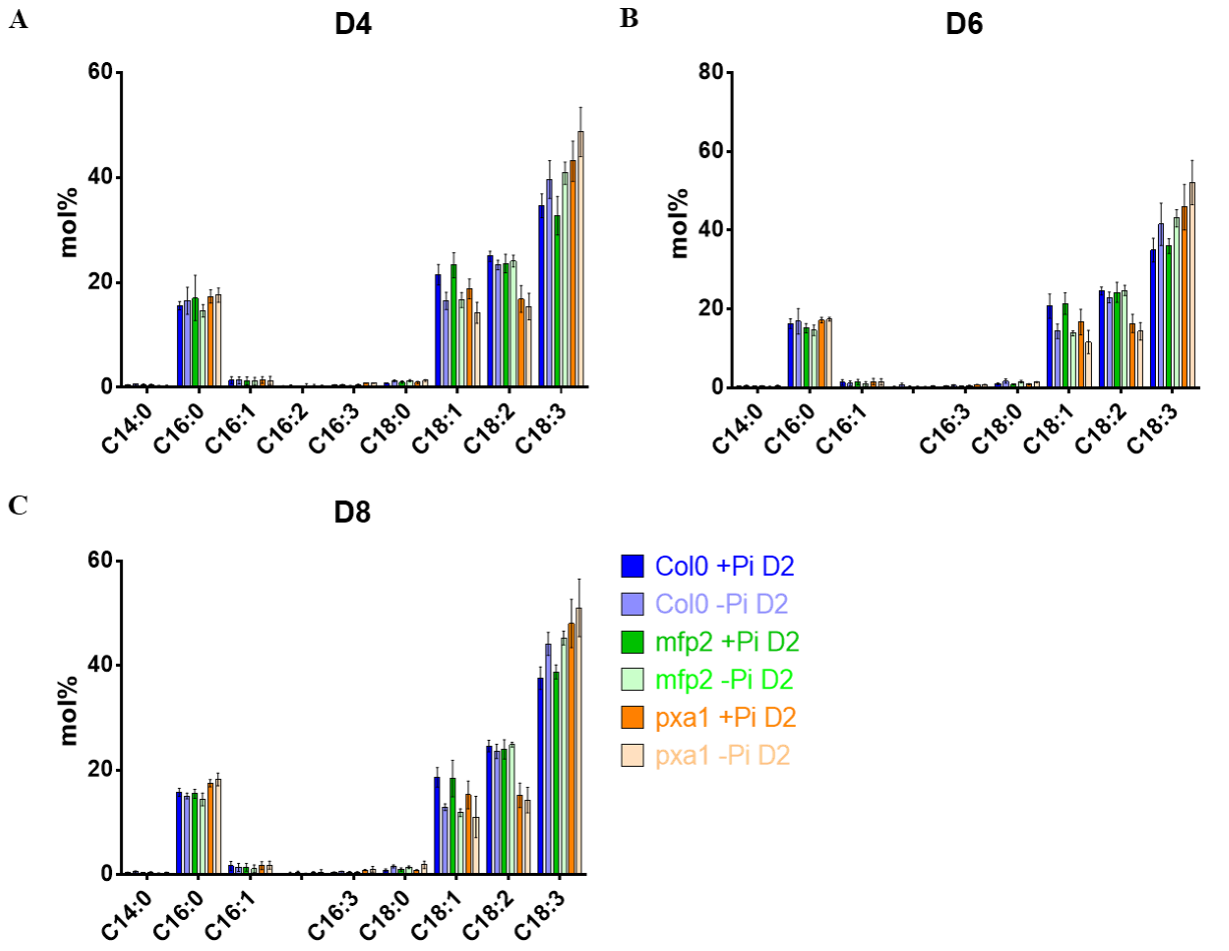


Figure 25. Fatty acid composition in mol% of Col0, *mfp2* and *pxa1* calli under Pi-enriched (+Pi) and Pi-deprived (-Pi) conditions at various time points. Data represented the means ± SD of five biological replicates for each condition.

Then each lipid class composition in nmol of each lipid class per mg of Col0, *mfp2*, and *pxa1* calli fresh weigh under Pi-enriched and Pi-starved conditions at 4, 6, and 8 days was analyzed using LC-MS/MS. Under standard conditions, higher levels of MGDG, DGDG and TAG were consistently observed in *pxa1* mutant after 4, 6 and 8 days of cultures, compared to wild type (**Figure 26**). A lower level of PC was also observed in 6-day-old *mfp2* and *pxa1* cultures grown in the presence of Pi (**Figure 26B**). In all Pi-starved cell lines, the lipid remodeling in response to phosphate starvation, specifically the PL-to-galactoglycerolipids replacement was observed in all cell lines at all time points (**Figure 26**), indicating that disruption of PXA1 or MFP2 did not affect lipid remodeling in response to phosphate starvation in Arabidopsis calli. The degradation of PE and PC, and the increase in DGDG content did not present significant differences in *mfp2* calli at all time points compared to Col0 (**Figure 26**). However, Pi-deprived *pxa1* calli exhibited a higher level of PE after 4 days of Pi starvation (**Figure 26A**), but not after 6 or 8 days (**Figure 26B & 26C**), suggesting a slight delay in the degradation of PE in *pxa1* mutant. In addition, similar to the observations in Pi-enriched *pxa1* cultures, a higher level of galactolipids (MGDG and DGDG) and TAG was observed in all Pi-starved *pxa1* cultures, compared to the wild-type (**Figure 26**). Furthermore, 4 and 8-day-old Pi-starved *pxa1* cells displayed a significant DAG accumulation, compared to Col0 (**Figure 26A & 26C**).

Subsequently, the fold change of the lipid quantity in –Pi versus +Pi was calculated using the Log_2 scale, which provides a logarithmic representation of the ratio between –Pi/+Pi (**Figure 27**). A positive Log_2 fold change indicates an increased amount of lipid class in –Pi compared to +Pi, while a negative value indicates a decrease in –Pi compared to +Pi. The magnitude of the Log_2 fold change reflects the degree of change, with larger values indicating a more substantial alteration. This analysis confirmed that the extent of lipid remodeling is similar between Col0 and these two β-oxidation mutants (**Figure 27**). In addition, it suggested a significant accumulation of DAG in 6-day-old Pi-starved *pxa1* mutant compared to Col0 (**Figure 27B**), and revealed an increase in TAG content in *mfp2* mutant after 8 days of Pi starvation (**Figure 27C**).

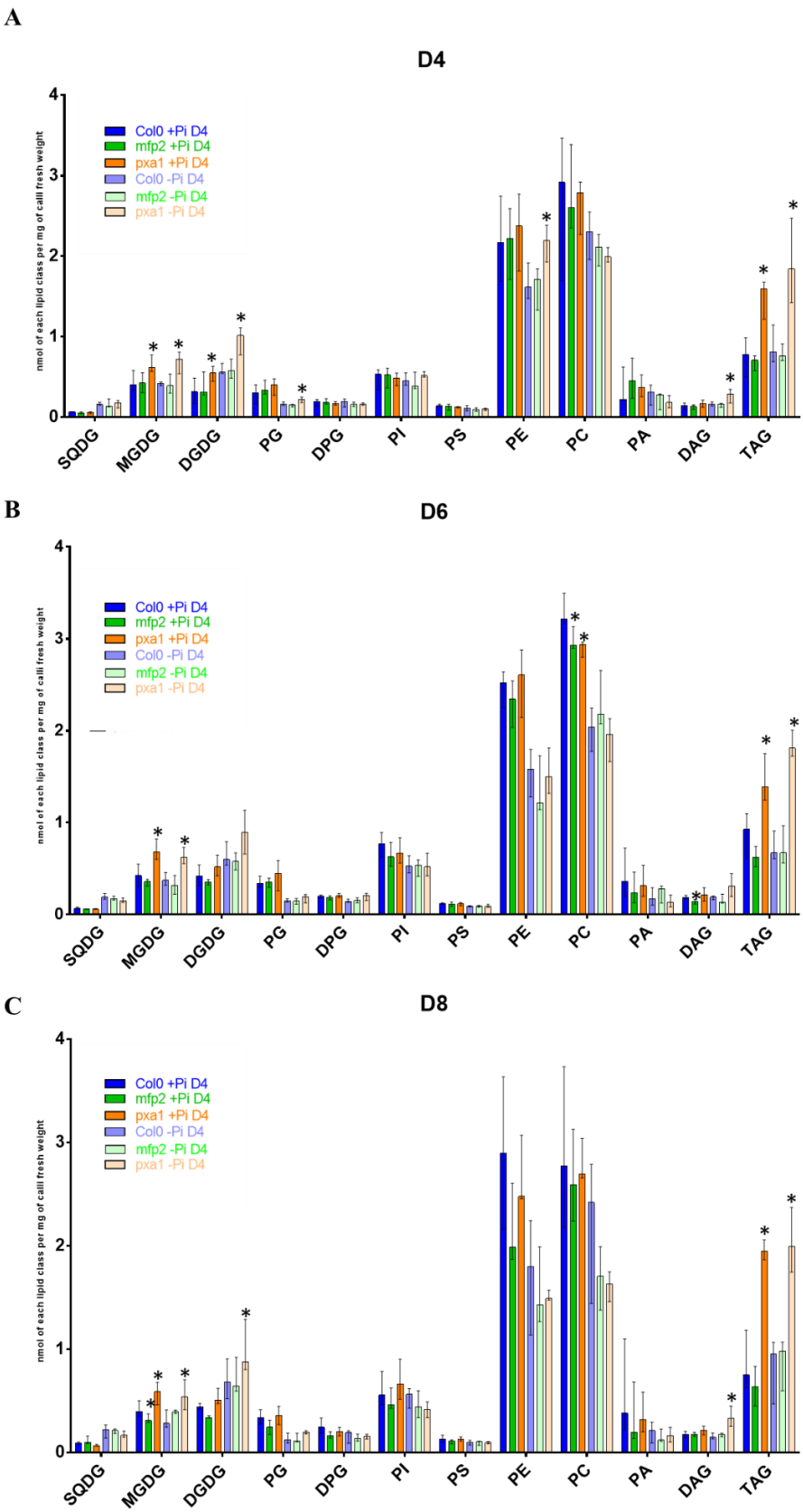


Figure 26. Lipid analysis of Arabidopsis wild type, *mfp2*, and *pxa1* calli grown with (+Pi) or without (−Pi) phosphate after 4, 6, and 8 days of incubation via LC-MS/MS . A, B & C. Data represented the means ± SD of five biological replicates for each condition, excluding outliers. Statistical significant differences ($P < 0.05$) were shown by asterisks and were calculated by a multiple t test using GraphPad Prism software: Col +Pi vs *mfp2* or *pxa1* +Pi, or Col -Pi vs *mfp2* or *pxa1* –Pi.

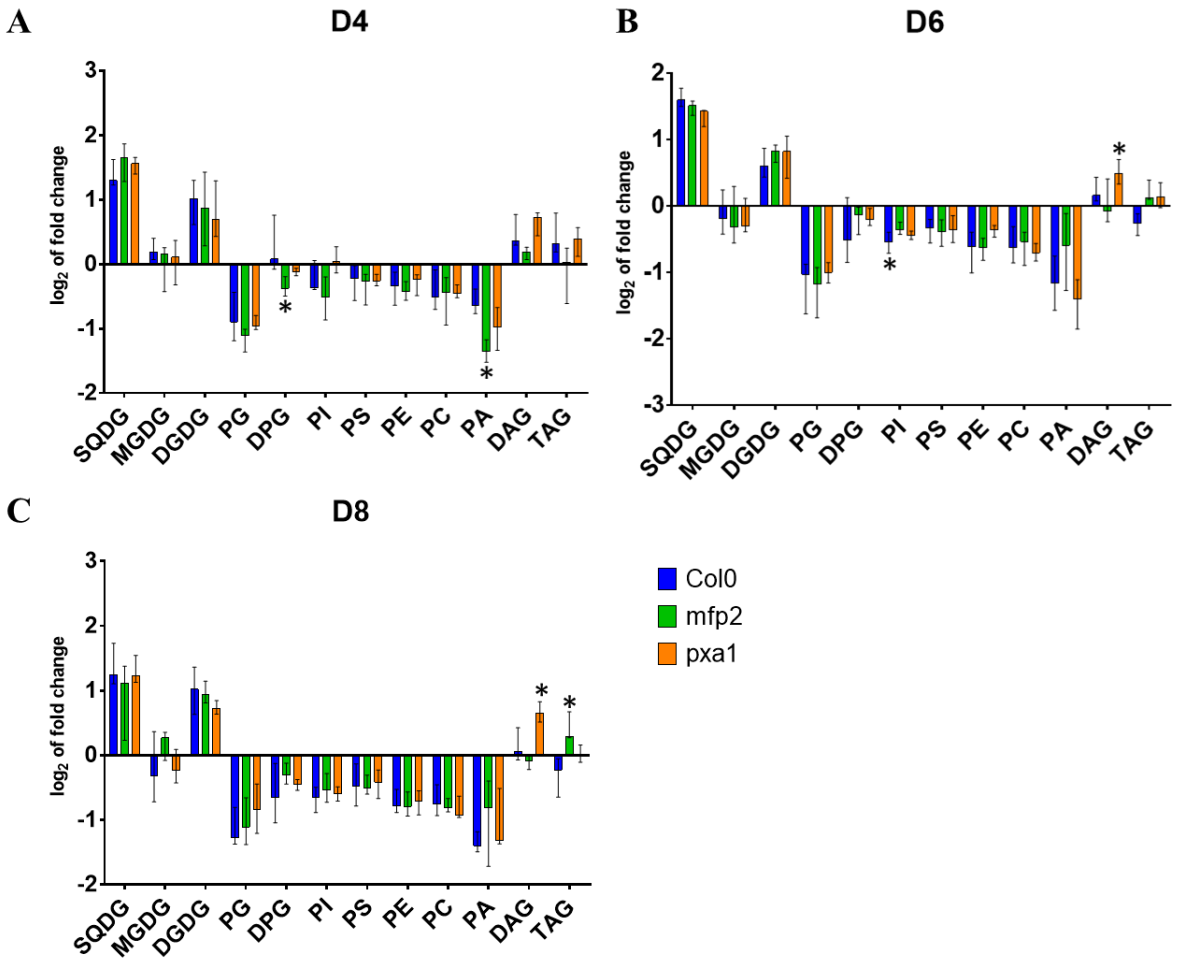


Figure 27. Log2 of fold change in lipid quantities of Arabidopsis wild type, *mfp2*, and *pxa1* calli between +Pi and -Pi conditions. Data represented the means ± SD of five biological replicates for each condition. Statistical significant differences ($P < 0.05$) were shown by asterisks and were calculated by a multiple t test using GraphPad Prism software: Col +Pi vs *mfp2* or *pxa1* +Pi, or Col -Pi vs *mfp2* or *pxa1* –Pi.

4.4 Preliminary data of electron microscopy observation of mitochondrial morphology in *mfp2* and *pxa1* mutant grown in cell suspension cultures under standard and Pi-starved condition

To assess the integrity and morphology of organelles within the two β-oxidation mutants under standard and Pi-stressed conditions, an electron microscopy (EM) survey was performed onto 4-day-old Arabidopsis wild type, *mfp2*, and *pxa1* cell suspensions. In Col0 cells subcultured in standard or Pi-starved media, numerous round mitochondria were observed (**Figure 28A**). Additionally, several other organelles, such as ER, Golgi, and plastids containing starch grains, were also identified within all cell lines (**Figure 28**); however, we failed to identify the peroxisomes.

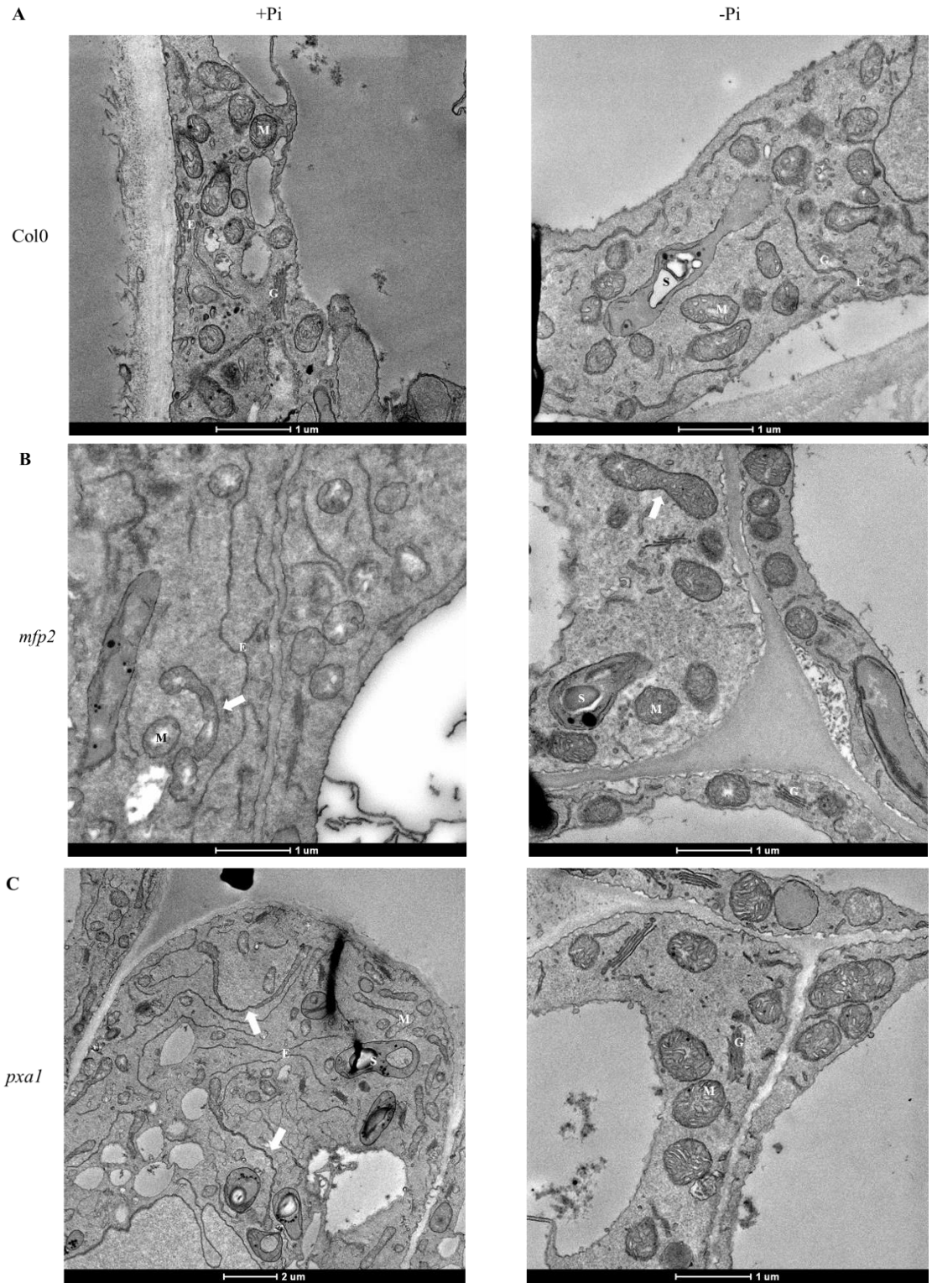


Figure 28. Electron microscopy observation in 4-day-old *A. thaliana* wild type, *mfp2*, and *pxa1* calli grown in suspension under Pi-enriched and Pi-deprived conditions. A. 4-day-old Arabidopsis Col0 cells in standard +Pi or -Pi medium. B. 4-day-old Arabidopsis *mfp2* cells in standard +Pi or -Pi medium. White arrows indicated elongated, dumbbell-shaped mitochondria, which were thicker at their ends and thinner in the middle. C. 4-day-old Arabidopsis *pxa1* cells in standard +Pi or -Pi medium. White arrows represented more pronounced dumbbell-shaped mitochondria, with longer and thinner middle sections. M, mitochondria; E, ER; G, Golgi; S, starch. Scale bars were indicated at the bottom of the photographs.

In *mfp2* cells, an elongated, dumbbell-shaped mitochondria, which was thicker at their ends and thinner in the middle, stretched, and curved, was frequently observed under both conditions (**Figure 28B**), although fewer were present under Pi-starved conditions (**Table 17**). In *pxa1* cells, this abnormal mitochondrial morphology was more pronounced, with longer and thinner middle sections, under standard conditions (**Figure 28C**); however, under Pi-limited conditions, this severe morphology was rarely observed, though a few elongated mitochondria were still present (**Table 14**). **Table 17** summarized the proportions of the elongated mitochondria within Arabidopsis wild type, *mfp2*, and *pxa1* cells grown in suspension cultures under Pi-enriched and Pi-deprived conditions. This abnormal mitochondrial morphology observed in *mfp2* and *pxa1* cells particularly under standard conditions may suggest a partially dysfunctional mitochondrial division due to the disruption of β-oxidation pathway; however, the reasons for the reduced frequency of abnormal mitochondria in Pi-starved mutants cells requires further investigation.

		Normal	Elongated	Total	Elongated%
Col0	**+Pi**	**115**	**10**	**125**	**8%**
	-Pi	**96**	**15**	**111**	**13.5%**
mfp2	**+Pi**	**86**	**29**	**115**	**25.2%**
	-Pi	**119**	**7**	**126**	**5.6%**
pxa1	**+Pi**	**76**	**45**	**121**	**37.2%**
	-Pi	**92**	**9**	**101**	**8.9%**

Table 17. Percentage of elongated mitochondria within Arabidopsis wild type, *mfp2*, and *pxa1* cells grown in suspension under Pi-enriched and Pi-deprived conditions.

Moreover, the perimeter length of mitochondria in Pi-sufficient and Pi-starved Col0 cells was measured using Fiji software with the ROI manager. Results indicated that Pi-starved Col0 cells displayed longer perimeter lengths (**Figure 29**), which suggested an increase in mitochondria size in response to Pi starvation. This finding was unexpected, as previous EM studies on heterotrophic cell cultures did not show any defect in mitochondria morphology (Jouhet et al., 2004). Of note, this increase in mitochondrial size was also observed in 6-day-old Pi-starved Col0 calli by another member in the team, Paul Montmayeul (data not shown). However, due to the abnormal mitochondrial morphology observed in *mfp2* and *pxa1* cells under standard conditions, it remains challenging to determine the mitochondrial perimeter length in the mutants.

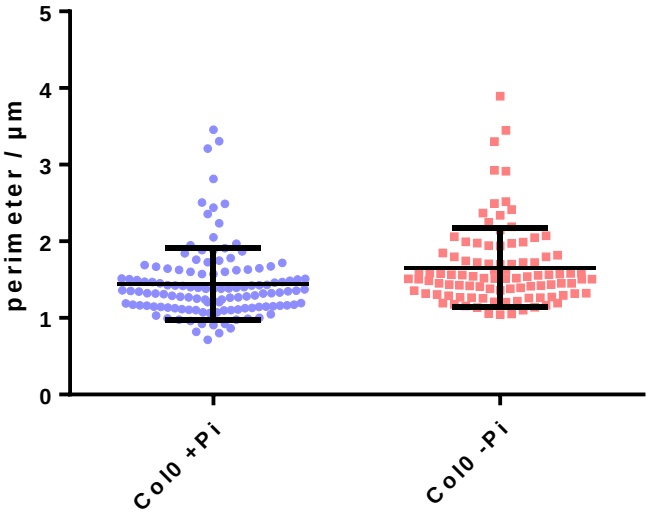


Figure 29. The perimeter length of mitochondria in Pi-enriched and Pi-starved Col0 calli. Values were measured using Fiji software with the ROI manager. N=97-125.

4.5 Preliminary measurements of β-oxidation activity in *A. thaliana* cell cultures under standard and Pi-starved conditions

The analyses of the changes in transcript levels, along with the phenotypic and lipidomic analyses of the relevant β-oxidation mutants in response to Pi deprivation, did not revealed a significant contribution of β-oxidation pathway in Pi starvation response. To further investigate the implication of β-oxidation in Pi-starvation response, we wandered whether the activity of this metabolic pathway was affected by Pi deprivation.

The β-oxidation activities under standard conditions and during Pi starvation were measured in total extracted proteins from Arabidopsis Col0 calli grown in the presence or absence of Pi over a period of 0 to 8 days, via assessing ACX activities, the first and limiting reaction of the β-oxidation process, using well-established protocols (Adham et al., 2005; Hooks et al., 1999). However, the β-oxidation levels detected in 4-day-old calli samples under both conditions were barely detectable (data not shown). Compared to the negative control, lacking any exogenous substrate in the reactions, no discernible distinction was evident (data not shown), indicating that the net rate of ACX enzyme activity in Arabidopsis calli was low to negligible, or that we were not able to measure ACX activity due to technical issues.

Given that β-oxidation plays a critical role in the breakdown of storage lipids to provide the energy in germinating seeds (see “General Introduction”; Graham & Eastmond, 2002), therefore, β-oxidation levels were measured in germinating seedlings grown in liquid culture in presence and absence of Pi. However,

due to unknown technical issues and the strong interference from the green color of the ground seedlings, the results were not able to be interpreted (data not shown).

5 Discussion and perspectives

5.1 The unexpected germination defect was found in M_2 *pxa1-1* mutants

The germination defect was reported in all *pxa1* alleles (Footitt et al., 2006; M. Hayashi et al., 2002; Zolman et al., 2001). However, the reason why newly generated batch of homozygous M_2 *pxa1-1* seeds in this study failed to germinate, unlike the *pxa1-1* seeds received from NASC that germinate well, remains to be elucidated. Several factors could influence seed germination, such as immature seeds, seed dormancy due to fresh or poor storage, etc. Footitt et al., 2006 analyzed the germination ability of several *pxa1* lines, including *pxa1-1*, alongside their corresponding WT lines, in different growth, harvesting, and storage conditions. They also observed a severe germination defect in the *pxa1-1* line, in contrast to the finding of Zolman et al. 2001. Therefore, our results are in agreement with the importance of the environmental factors (such as seeds maturation, drying, and storage conditions) for the efficient germination ability of *pxa1-1* seeds. Multiple strategies were employed to enhance the germination rate of the M_2 *pxa1-1* seeds, including longer storage periods, pre-chilled treatments, and the addition of exogenous gibberellin, propionate, or isobutyrate to the growth media, as reported by Russell et al., 2000, but none of them proved effective. Additionally, another M_3 batch from a few germinated M_2 *pxa1-1* seeds was generated, and exhibited the same germination defect.

In order to explain this observation, as mentioned in **section 2** regarding the "forever dormant" phenotype of *cts-1* mutant, the *CTS* gene, equivalent to the *PXA1*/*PED3* locus, is a target for loci that repress germination, and serves as a major control point between the removal of dormancy and germination (Footitt, 2002; Russell et al., 2000). Footitt, 2002 demonstrated that the expression of *CTS* is tightly associated with germination, and that *CTS* interacts genetically with several loci that repress germination, including *RDO2* and *ABI1*. Therefore, the weak alleles represented by *pxa1, ped3-2* and *ped3-4* are still able to conduct lipid breakdown and germinate, even in the absence of sucrose, possibly indicating that these weak alleles retain sufficient transport function at threshold levels (M. Hayashi et al., 2002; Zolman et al., 2001). Thus, in order to assess the ability of newly generated M_2 *pxa1-1* seeds, analyzing the *CTS* expression could be done to predict the germination potential, and to guide subsequent steps for the plant phenotypic analysis.

5.2 Lack of Pi inhibits the growth of Col0 and *mfp2* calli, but likely not affects growth of *pxa1* calli

Plant *Arabidopsis thaliana* has been shown to adapt its root system architectures to Pi deprivation by the inhibition of primary root growth, increases in lateral root formation and growth, and enhanced production

and elongation of root hairs, which could improve P uptake by increasing the root absorption surface and promoting foraging of topsoil where Pi accumulates (reviewed in Péret et al., 2011). However, in our study, the roots of Pi-starved Col0 displayed different phenotypes from those previously reported. Under low Pi conditions, neither the reduced length of primary roots, or the increased number of lateral root, nor changes in root hairs, were observed in either Col0 or *mfp2* (**Figure 22**), although they all exhibited yellowish cotyledons in reduced size, indicating that the examined seedlings were Pi-starved (**Figure 22**).

Natural variation in root length and growth in response to low Pi has been demonstrated in various contrasting studies (Chevalier et al., 2003; Reymond et al., 2006). In Reymond et al., 2006, Col0 exhibited a strong response to low Pi conditions (5 µm Pi), whereas in Chevalier et al., 2003 (1 µm Pi), the primary root length was only slightly inhibited. These discrepancies may arise from differences in seed germination and plant growth conditions, including variations in germination and growth medium, particularly the contained mineral solution (Godon et al., 2019; Wang et al., 2019; Ward et al., 2008), light sources, etc., thus possibly suggesting that the *A. thaliana* Col0 accession is sensitive to these specific aspects of growth conditions. This presents a significant challenge for our phenotypic analyses for the mutants in response to Pi deficiency.

Moreover, due to the germination defect observed in M_2 *pxa1-1* mutant seeds, we were unable to perform phenotypic analysis of *pxa1* seedling under Pi-enriched and Pi-deprived conditions. However, during the subculturing of Col0, *mfp2* and *pxa1* calli, *pxa1* calli exhibited slower growth, compared to Col0 and *mfp2* calli (**Figure 21**). Consequently, a growth assay onto the *pxa1* calli, with Col0 and *mfp2* calli as controls, in the presence or absence of Pi was performed. Results showed that lack of Pi inhibited the growth of Arabidopsis wild type and *mfp2* calli, whereas Pi-deprived *pxa1* calli appears to grow as similar as that in control condition (**Figure 21**).

Pi starvation typically inhibits plant growth and development due to the critical physiological and molecular roles of P within the plant cells (see "General Introduction"). However, this is not the case observed in *pxa1* calli (**Figure 21A & 21B**). One plausible explanation is that the loss of function in *pxa1* mutants, thus in FAs and hormone metabolism, may lead to an accumulation of specific metabolic intermediates that help plants to better manage energy and Pi homeostasis under Pi-starved conditions. This adaptive mechanism may provide the *pxa1* mutant with a growth advantage when Pi is scarce. Another hypothesis may be that due to the slow growth rate of *pxa1* calli, their demand for lipid synthesis and transport is lower than Col0 calli, consequently, *pxa1* calli can sustain the lipid requirements for cell division even in the absence of Pi. Certainly, further experimental studies are required to pinpoint the exact mechanism behind the differential growth response to Pi starvation in *pxa1* mutant. Furthermore, it is definitely essential to investigate the

phenotypic behaviors of *pxa1* plants in response to Pi starvation after resolving the *pxa1* seed germination defect and identifying optimal growth conditions for root growth.

5.3 β-oxidation pathway is not involved in the metabolic processes of lipid remodeling in response to Pi starvation in *A. thaliana* cell cultures

The progressively declining total lipid content observed in all cell lines (**Figure 24**) may indicate a general unknown lipid turnover to other compounds in response to Pi starvation. Another hypothesis may be that the amount of membrane (i.e. organelle content) per cells decreases under Pi-deprived conditions, which explains the global diminution of the total lipid content per mg of calli fresh weight. However, the complete or partial disruption of β-oxidation pathway did not affect this lipid turnover, suggesting that MFP2 and PXA1 protein, and thus β-oxidation pathway, are not essential for the downstream metabolic processes of lipid remodeling in response to Pi starvation in *A. thaliana* cell cultures. In addition, the lipid remodeling, characterized by the increased SQDG and DGDG and decreased phospholipids (PG, PE, PC and PA), occurs in all cell lines (**Figure 26**), sharing a similar tendency as the wild type. It suggests that the deficiency of MFP2 or PXA1 protein, thus the β-oxidation pathway, does not influence lipid remodeling during phosphate starvation. Consequently, it leads to the conclusion that β-oxidation is not crucial for lipid remodeling in plant adaptation to Pi starvation, and that β-oxidation pathway does not play an essential role in metabolic processes of FA recycling during lipid remodeling in response to Pi starvation (**Figure 30**).

The elevated level of unsaturated 18:3 observed in *pxa1* mutant in cell suspension cultures under both standard and Pi-starved conditions (**Figure 25**) could be explained by the variability of the unsaturation level of 18C relative to the growth rate discrepancies among these cell lines, as exploited by Meï et al., 2015. Furthermore, the slow growth rate of *pxa1* mutant may induce an increasing level of polyunsaturated fatty acids (PUFAs) in phospholipids, DAGs and TAGs, compared with Col0 and *mfp2* (data not shown).

In addition, higher quantities of MGDG and DGDG, synthesized within the chloroplasts, were observed in the *pxa1* mutant under both +Pi and –Pi conditions at different time points (**Figure 26**). Moreover, as illustrated in **Fig. 27**, the rise in galactolipids in response to Pi deprivation is consistent between Col0 and *pxa1*, and exhibited even slightly lower at D8 in Pi-starved *pxa1* mutant (**Figure 27C**), indicating that this galactolipid accumulation in *pxa1* mutant is not linked to Pi starvation. Unlike other lipids, MGDG and DGDG are not typically degraded for energy production or further metabolic processes of lipid remodeling. Instead, they play critical roles in the organization of chloroplast membranes and the efficient functioning of photosynthetic machinery. When other lipid classes undergo lipid degradation pathways, such as β-oxidation, MGDG and DGDG are generally conserved and not degraded in the same manner (Goss & Latowski, 2020). Thus, the observation of galactolipid accumulation in the context of PXA1 deficiency

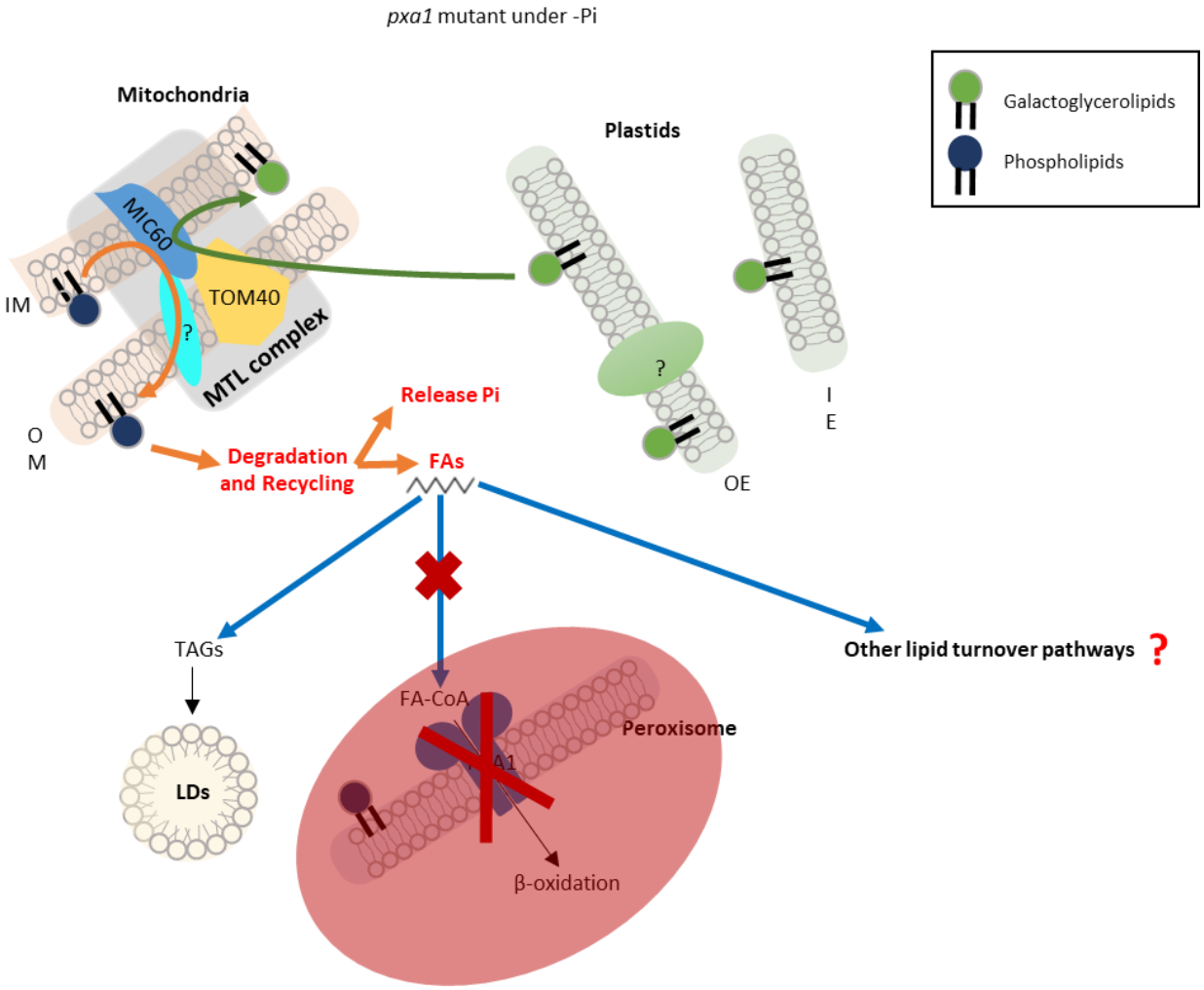


Figure 30. An updated model of lipid remodeling between organelles in *A. thaliana pxa1* mutant in cell suspension cultures under Pi-deprived conditions.

may imply an increased abundance of plastids, making an EM observation focusing on the amounts of chloroplasts in *pxa1* cells under both conditions of great interest. Alternatively, the number of plastids might remain stable, but they could contain more internal membrane structures similar to thylakoids.

Furthermore, a moderate reduction in PE degradation is noticeable in the 4-day-old Pi-starved *pxa1* mutant, compared to Col0 (**Figure 26A**). Given the resilient growth of *pxa1* mutant during Pi starvation (**Figure 21**), *pxa1* mutant may exhibit a delayed response of PL degradation to tolerate stress at the early period of Pi-starved treatments.

Additionally, a general increased TAG level was observed in *pxa1* mutant under both conditions, compared to Col0 and *mfp2* (**Figure 26**). In the β-oxidation *pxa1* mutant, the β-oxidation pathway responsible for FAs recycling is completely blocked, consequently, FAs would accumulate or preferentially follow alternative processes, for instance kept in TAG, which has been reported by Footitt, 2002. Moreover, TAG

accumulation is a known late response to severe Pi deprivation in higher plants and green algae, typically appearing after 13 days of Pi starvation in *A. thaliana* seedlings (Pant et al., 2015). However, in our study, this was observed at the early phase of Pi starvation in Col0 after 4 days, while this response varied in *pxa1* and *mfp2* at different time points (**Figure 27**). Certainly, further studies with extended periods of Pi starvation treatments in Arabidopsis cell cultures are required.

No significant differences in FAs and lipid composition were observed between the *mfp2* mutant and wild type under both conditions (**Figure 24, 25, 26 & 27**), indicating that the residual activity executed by AIM1 may counterbalance the functional deficiency of MFP2.

5.4 Other aspects of lipid metabolism may play metabolic roles in membrane lipid remodeling in response to Pi deficiency

Under Pi-deprived conditions, an increased level of another non-phosphorous anionic plant lipid class, glucuronosyldiacylglycerol (GlcADG), was identified in Arabidopsis and rice, suggesting its physiological significance in the protection of plants against Pi limitation stress (Okazaki et al., 2013). The GlcADG accumulation was found in a series of mutants deficient in the two first enzymes responsible for SQDG biosynthesis (i. e. synthesis of UDP-sulfoquinovose), but was impaired in *sqd2* mutant under Pi-depleted conditions. This leads to the hypothesis that GlcADG synthesis partially shares the pathway of SQDG synthesis and is mediated by SQD2, using DAG and a sugar donor, likely UDP-glucuronic acid (UDP-GlcA) instead of UDP-SQ for SQDG synthesis (Okazaki et al., 2013). The two other enzymes involved in SQDG synthesis, UGP3 and SQD1, are not involved in the synthesis of GlcADG (Okazaki et al., 2013).

The accumulation of this anionic glycolipid, GlcADG, was not quantified by our LC-MS/MS methods, thus potentially accounting for certain part of the observed discrepancy in total lipid content. However, since GlcADG is synthesized by SQD2 inside plastids, it is likely devoted primarily to plastidial lipid compensation rather than extraplastidial lipid remodeling. Nevertheless, further investigations would be of significant interest to determine the involvement of Pi-starved inducible GlcADG synthesis in the metabolic flow of lipid remodeling in response to Pi starvation.

Additionally, in Pi-starved *sqd2* mutants, the levels of certain phospholipids (PI and PE) and GlcADG are reciprocally maintained compared to wild type (Okazaki et al., 2013), similar to the maintenance of PE observed in the 4-day-old Pi-starved *pxa1* mutant in this study (**Figure 26A**). It may suggest that these phospholipids, that are also anionic, exhibit preference to maintain proper membrane properties in plants that are deficient in GlcADG biosynthesis or β-oxidation pathways under Pi-depleted conditions.

Sucrose has been mentioned as an eventual product of lipid turnover in plants (**Figure 6**, see "General Introduction"), thus it is also of great interest to conduct comparative analyses of the starch content in wild-

type and mutant calli between Pi-enriched and Pi-deprived conditions. Preliminary data from EM studies has shown the presence of plastids containing starch grains in all cell lines under both conditions (**Figure 28**); however, no discernible differences have been observed so far. Certainly, further investigations are required to quantify the starch quantities more accurately.

In addition, Pi starvation significantly induces PC degradation in both vegetative shoots and roots, with a portion converted to lyso-PC by a PLA, serving as the signaling molecule (Drissner et al., 2007). Hence, this may be another perspective to explain the reduced total lipid content under Pi-starved conditions, and may suggest a potential coordination between membrane lipid remodeling regulation with mycorrhizae and other plant–microbe interactions in the rhizosphere.

5.5 The abnormal mitochondrial morphology observed in β-oxidation mutants under standard conditions suggests a potential association with ROS accumulation

The morphology and respiration of plant mitochondria remained unaffected in 3-day-old Pi-deprived heterotrophic green cell cultures, as reported by Jouhet et al., 2004. However, based on the preliminary data in our study, the mitochondrial size was larger in 4-day-old Pi-starved wild-type calli (**Figure 29**), contrasting with their findings. Of note, this increase in mitochondrial size was also observed in 6-day-old Pi-starved Col0 calli (Montmayeul, data not shown). The formation of giant mitochondria have been observed in healthy etiolated seedlings triggered by stress (i.e., darkness) in the early stages to expand their surface area as a way to overcome stress (Fukushima et al., 2022). In our study, additional experiments are required to confirm our observations in both wild type and two β-oxidation mutants, and thereafter to elucidate the role of alternations in the lipid composition in mitochondrial structure and function under stress conditions.

Abnormal elongated mitochondrial morphology was found in two β-oxidation mutants, *pxa1* and *mfp2*, especially under normal growth conditions (**Figure 28B & 28C**, **Table 17**). This abnormal mitochondrial morphology has been documented in several studies associated with the elevated ROS levels and thus defects in mitochondrial inner membrane potential (Kritsiligkou et al., 2017), the dysfunction in mitochondrial fission (Nagaoka et al., 2017), or the interactions between mitochondria and autophagic vacuoles (Youn et al., 2021). We also attempted to verify this observation using confocal microscopy in the living cells stained with MitoTracker (data not shown); however, we were unable to optimize the protocol that would allow MitoTracker to effectively enter the cells and accurately visualize mitochondria in Arabidopsis calli. Future studies could focus on Arabidopsis young seedlings for further investigation.

Therefore, this abnormal mitochondrial morphology observed in β-oxidation mutants in our study may be explained by the hypothesis that disruption of MFP2 or PXA1 leads to an elevated ROS levels under

standard conditions. Additional studies could be conducted to assess the redox status of these two mutant calli under both standard and Pi-starved conditions, such as using redox status markers in conjunction with Western blot analyses, chemical probes that can lead to a colorimetric change or induce fluorescence, electron paramagnetic resonance (EPR) spectroscopy to detect unpaired electrons (including ROS and RNS) both *in vitro* and *in vivo*, or measuring the activities of ROS scavengers (ascorbate and glutathione) *in vivo* (Akter et al., 2021; Mattiazzi Ušaj et al., 2015).

Furthermore, the elongated tubular mitochondria, similar to those observed in *pxa1* calli under standard conditions (**Figure 28C**), have also been noted in etiolated cotyledons grown for 4 days in the dark (Fukushima et al., 2022). This phenomenon was suggested to attributed to an increased presence of mitochondrial nanotunnels, defined as a connecting structure across nonadjacent mitochondria, due to mitochondrial DNA defects (Vincent et al., 2019), or by mitochondrial outer membrane protrusions (MOPs) that form a bridge between two mitochondria after dark treatment (Yamashita et al., 2016a, 2016b), allowing for continued expansion of their surface area as a way to overcome stresses (Fukushima et al., 2022).

However, in our study, this elongated mitochondrial morphology in β-oxidation mutants was absent under Pi-stressed conditions (**Figure 28B & 28C**, **Table 17**). It may explained by that Pi starvation may trigger extensive adaptive metabolic reprogramming and induce the expression of antioxidant enzymes and other ROS-scavenging mechanisms to reduce the ROS production, as the oxidative symptoms have been reported during Pi starvation (Hernández & Munné-Bosch, 2015; Juszczuk et al., 2001). Moreover, another explanation could be related to technical issues in preparation of thin sections for EM studies. Some mitochondria that were recognized separately on the section might be actually connected, and the absence of elongated mitochondria under Pi-starved conditions in two β-oxidation mutants might result from the sliced section at the thicker ends of these structures. Therefore, larger number of samples and images, or an accurate 3D image are needed to be analyzed to draw conclusions more accurately.

Additionally, it has been reported that yeast PXA1 and PXA2 deletion mutants have morphologically intact peroxisomes (Zolman et al., 2001). Thus, we would like to evaluate the morphology of peroxisome in these β-oxidation mutants under both standard and stress conditions, compared to wild type. However, in our study, we failed to identify peroxisome in the EM observations. Although *mfp2* mutants was reported to have reduced number of enlarged peroxisomes (Hayashi et al., 2001; Rylott et al., 2006), the comparisons between *mfp2*, Col0 and *pxa1* mutant did not allow us to identify peroxisomes among all the single-membrane organelles, which appears to be clear with a thin boundary. Indeed, recognizing peroxisomes in EM observations of plant cells can be challenging due to their small size and similarity to other cellular organelles. Certain key features may help in their identification. For instance, some peroxisomes contain a

dense, crystalline core or nucleoid within the organelle (Just et al., 1989). However, this feature is not always present, and we did not observe it in our EM results. Additionally, peroxisomes are often located near other organelles such as mitochondria and chloroplasts in leaves (Shai et al., 2016). This proximity may help differentiate them from other organelles of similar size and shape. Furthermore, immunolabeling with antibodies against peroxisomal marker proteins (e.g., catalase or PEX14) may specifically highlight peroxisomes in EM preparations.

Chapter 3

Identification of interactions between peroxisomal PXA1 protein and mitochondrial TOM complex at peroxisome-mitochondria membrane contact sites

1 Peroxisome-mitochondria membrane contact sites (MCSs)

Membrane contact sites (MCSs) are specific regions formed by the close apposition between two membranes, typically at a distance less than 30 nm (for a review, Scorrano et al., 2019). These structures can be tethered and stabilized by protein-protein and/or protein-lipid interactions (Leterme & Michaud, 2022; Pérez-Sancho et al., 2016; Scorrano et al., 2019). MCSs play essential roles in various cellular processes, such as metabolite exchanges, cell signaling, organelle fission and fusion, and autophagy (Prin et al., 2020). MCSs have been extensively described in different eukaryotic organisms, principally in yeast and animals. In plants, MCSs are much less studied but they exhibit conserved functions (Pérez-Sancho et al., 2016).

Plant MCSs are highly dynamic structures in response to stresses (Bian et al., 2023; Michaud & Jouhet, 2019). During Pi starvation, the number of MCSs between plastids and mitochondria significantly increases, likely playing a role in stress-inducible lipid remodeling, and an involvement of a MTL complex has been identified for mitochondrial membrane lipid remodeling (Jouhet et al., 2004; Michaud, 2018; Michaud et al., 2016). As previously mentioned, in order to identify potential components of MTL complex outside mitochondria, co-IPs using a MTL member TOM40 protein at mitochondrial OM were performed (Michaud and Albrieux, unpublished data). Unexpectedly, we found several peroxisomal proteins involved in β-oxidation pathway, particularly PXA1 protein, as putative partners of TOM40. Therefore, confirming the interaction between mitochondrial TOM40 and peroxisomal PXA1 is of great interest, and it will provide new insights into the mechanism of peroxisome-mitochondria MCSs formation in plants as well as its putative role in lipid remodeling during Pi starvation.

Several studies have highlighted the importance of peroxisome-mitochondria connections in metabolic processes across species. In yeast, tight physical connections and close associations between these two organelles have been confirmed by detailed EM studies (Rosenberger et al., 2009). Cohen et al., 2014 uncovered that peroxisomes are closely adjacent to mitochondria through the pyruvate dehydrogenase (PDH) complex and the ERMES complex via fluorescence microscopy (FM) co-localization studies. In addition, ScPex11 has been shown to physically interact with the mitochondrial ERMES component Mdm34 (Mattiazzi Ušaj et al., 2015). ScPex34, a member of the ScPex11 protein family, functions as a peroxisome-mitochondria tether and mediates the transport of β-oxidation products from peroxisomes to mitochondria at the site of acetyl-CoA synthesis to feed the tricarboxylic (TCA) cycle and mitochondria respiration (Shai et al., 2018). However, the binding partner of ScPex34 on the mitochondrial membrane remains yet to be identified. Furthermore, the mitochondrial outer membrane protein ScFzo1 also acts as a peroxisome-mitochondria tether, though its exact roles remain unclear (Shai et al., 2018). In mammals, both peroxisomes and mitochondria possess separate β-oxidation pathways, which are different from yeast and

plants (Schrader et al., 2020). A close spatial association between peroxisome and mitochondrion was initially observed in the myocardium of rodents and primates in the 1970s (Hicks & Fahimi, 1977). Mammalian peroxisome-mitochondria MCSs are believed to play an important role in steroid hormone biosynthesis, a pathway involving enzymes located in both organelles (Fan et al., 2016). This study also demonstrated a tethering complex between these two organelles, including a splice isoform of an acyl-CoA binding domain-containing protein, and enoyl-CoA δ isomerase 2 (ACBD2/ECI2). Moreover, overexpression of mammalian PEX11β induces the formation of mitochondrion-interacting membrane protrusions, indicating the presence of an organelle interaction between peroxisomes and mitochondria in mammalian cells (Kustatscher et al., 2019). In plants, it has been shown that the proximity between chloroplasts, mitochondria and peroxisomes, as evidenced by EM studies, is increased during plant photorespiration (Mueller-Schuessele et al., 2024). However, the proteins that mediate these interactions and their roles between these organelles have not been conclusively determined in plants (Pan et al., 2020)

Collectively, these findings reinforce the importance of confirming the interaction between mitochondrial TOM40 and peroxisomal PXA1 in plants, and underscore the need for further investigations into peroxisomes-mitochondria MCSs, particularly in the context of metabolic changes induced by Pi starvation.

2 Methods for protein-protein interactions at MCSs

To date, it remains challenging to visualize and purify contact sites, thus making it difficult to confirm their presences, understand their functions, and study the effects of genetic perturbations on environmental stress responses. Given that the observations over years displayed transient nature or variable abundance and thus instability of results, any study wishing to characterize contact-site components or functions requires multiple approaches to obtain reliable outcomes. Various experimental approaches to study protein-protein interactions (PIPs) at MCSs have been documented with distinct pros and cons, including genetic (such as yeast two-hybrid, Y2H) and biochemical (such as co-IP) methods, diverse microscopy methods based on different principles (such as advanced high-resolution imaging, immunofluorescence, split fluorescence probes), cell fractionation techniques, and proximity labeling and ligation assays (Scorrano et al., 2019).

In this study, co-IP was firstly employed to identify PIPs of mitochondrial TOM40, and a peroxisomal candidate protein, PXA1, has been found as its putative partner. Thereafter, two additional strategies, based on the principles of *in vivo* visualization and proximity labeling, were selected to verify this interaction.

Immunoprecipitation (IP) is a method using a target protein-specific antibody coupled with protein A/G affinity beads, and is a widely used and effective tool to identify molecules that interact with specific proteins in living cells (Lin & Lai, 2017; Ransone, 1995). Co-IP experiments can detect proteins through direct or indirect interactions, or as part of a protein complex (Lin et al., 2024). Consequently, the identified

proteins may not directly bind to the protein of interest, but act as a third party playing a bridge role. Moreover, the time and cost for the preparation of a highly specific antibody are the other major drawbacks of this technique (Yang et al., 2014), but tagged version of the protein can be used to overcome this problem. Additionally, the transient protein-protein interactions may not be detected without cross-linking.

In addition, we have chosen a bimolecular fluorescence complementation (BiFC) technology, also referred to "split-fluorescent protein", to verify the *in vivo* interaction between PXA1 protein and plant TOM complex. BiFC is introduced in plants in recent decades to directly visualize *in vivo* protein-protein interactions by transient expression in *Nicotiana benthamiana* (Bracha-Drori et al., 2004; Horstman et al., 2014; Walter et al., 2004). In this technique, a yellow fluorescent protein (YFP) is divided into two non-fluorescent "halves", an N-terminal half (YFP^N) and a C-terminal half (YFP^C), which are then fused to the proteins of interest (P1 and P2), respectively. The YFP molecule is reconstituted upon interactions between P1 and P2, resulting in yellow fluorescence when the molecules are excited at the appropriate wavelength. Despite its widespread application, the BiFC method does have notable limitations. The two major drawbacks are 1) the so-called "self-assembly" ability of the two halves to reassemble without genuine protein-protein interactions, leading to a high background signal and a false-positive BiFC signal and 2) the irreversibility of the YFP assembly (Horstman et al., 2014), which is an important problem when studying dynamic structures such as MCSs. To address the problem of "self-assembly", the comparative analysis with negative controls was initially employed in our study. The cell lines utilized in this study were summarized in **Table 8** (see "Mat & Met").

An alternative strategy, the proximity biotin labeling (BioID), was also chosen not only to confirm the interaction between PXA1 and TOM40, but also to determine a wider range of partners for TOM40 and PXA1 in presence and absence of Pi. This recently developed tool allows to identify proteins in close proximity to the protein of interest or present within a region of approximately 10 nm diameter in the living cells (Mair et al., 2019; Zhang et al., 2019). BioID uses a modified biotin ligase, TurboID from *Escherichia coli*, which can catalyze the non-specific biotinylation of lysine residues of proteins located close to its active site (Mair et al., 2019; Zhang et al., 2019). The protein of interest, hereby TOM40, is fused with the TurboID biotin ligase, enabling the *in vivo* covalent biotinylation of proximal and interacting proteins in the presence of biotin. The biotinylated proteins can be then captured by streptavidin-based affinity purification, and identified via immunoblots or mass spectrometry (MS). Unlike the standard methods such as co-IP, BioID approach labels proteins in living cells within the native cellular environment (Zhang et al., 2019). In addition, the covalent biotin modification allows the isolation of partners in harsh conditions, without the necessity to maintain protein complexes. Furthermore, BioID enables the identification of weakly and transiently interacting proteins, which are typically lost during co-IP experiments (Mair et al.,

2019). Though BioID strategy is well-optimized in mammals (Branon et al., 2018), only few studies have applied it to plants (Mair et al., 2019; Zhang et al., 2019).

Therefore, during my master internship in our laboratory, the optimization of BioID strategy in our plant calli cell culture system was performed (Yan and Michaud, unpublished data). Two cell lines were utilized: one corresponding to *A. thaliana* Col0 plants stably transformed with a vector expressing TurboID fused at the C-terminal of TOM40; the other corresponding to *A. thaliana* Col0 plants stably transformed with a vector expressing TurboID alone, served as a control to detect non-specific labeling. Three critical parameters were highlighted to obtain an efficient labeling: protein expression level, biotin concentration, and labeling duration. We showed that efficient labeling required a substantially high expression of the protein, the addition of 1 mM biotin to the media, and a labeling duration of 3 hours. In addition, in order to determine partners of TOM40 located at other organelles, the fused TurboID ligase must be positioned on the cytosolic side of the mitochondrial OM. However, the orientation of the TOM40 N- and C-terminal ends in plants is unknown. Thus, it is of importance to ascertain the orientation of the fused TurboID. Thermolysin treatments, in which this aspecific protease can degrade proteins located at the surface of mitochondria, were conducted on isolated mitochondria to monitor the position of TurboID. However, results indicated that TurboID fused to TOM40 protein was localized in the IMS inside mitochondria, in accordance with the structural analysis of the TOM complex in yeast (Nussberger et al., 2024). Given that TOM40 is a multi-transmembrane protein, predicting the site for TurboID insertion without interfering TOM40 localization and function is challenging. Therefore, another candidate TOM20, a protein interacting with TOM40 within the mitochondrial TOM complex, was chosen for the subsequent analysis in this study. TOM20 is anchored to the mitochondrial outer membrane by a C-terminal hydrophobic segment and exposes a receptor domain to the cytosol. Moreover, we have confirmed the presence of TOM20 in the MTL complex by Western Blot (Michaud and Albrieux, unpublished data). Additionally, TOM20 in mammals has been implicated at mitochondria-peroxisome MCSs (Fan et al., 2016).

Therefore, for the subsequent investigations of peroxisomes-mitochondria MCSs, mitochondrial TOM20 and peroxisomal PXA1 were taken for studies.

3 Preliminary BiFC results to confirm PXA1-TOM complex interaction

The BiFC approach using split YFP was initially employed to verify the potential direct interaction between the mitochondrial TOM complex and peroxisomal PXA1, as suggested by the co-IPs results (Michaud and Albrieux, unpublished data).

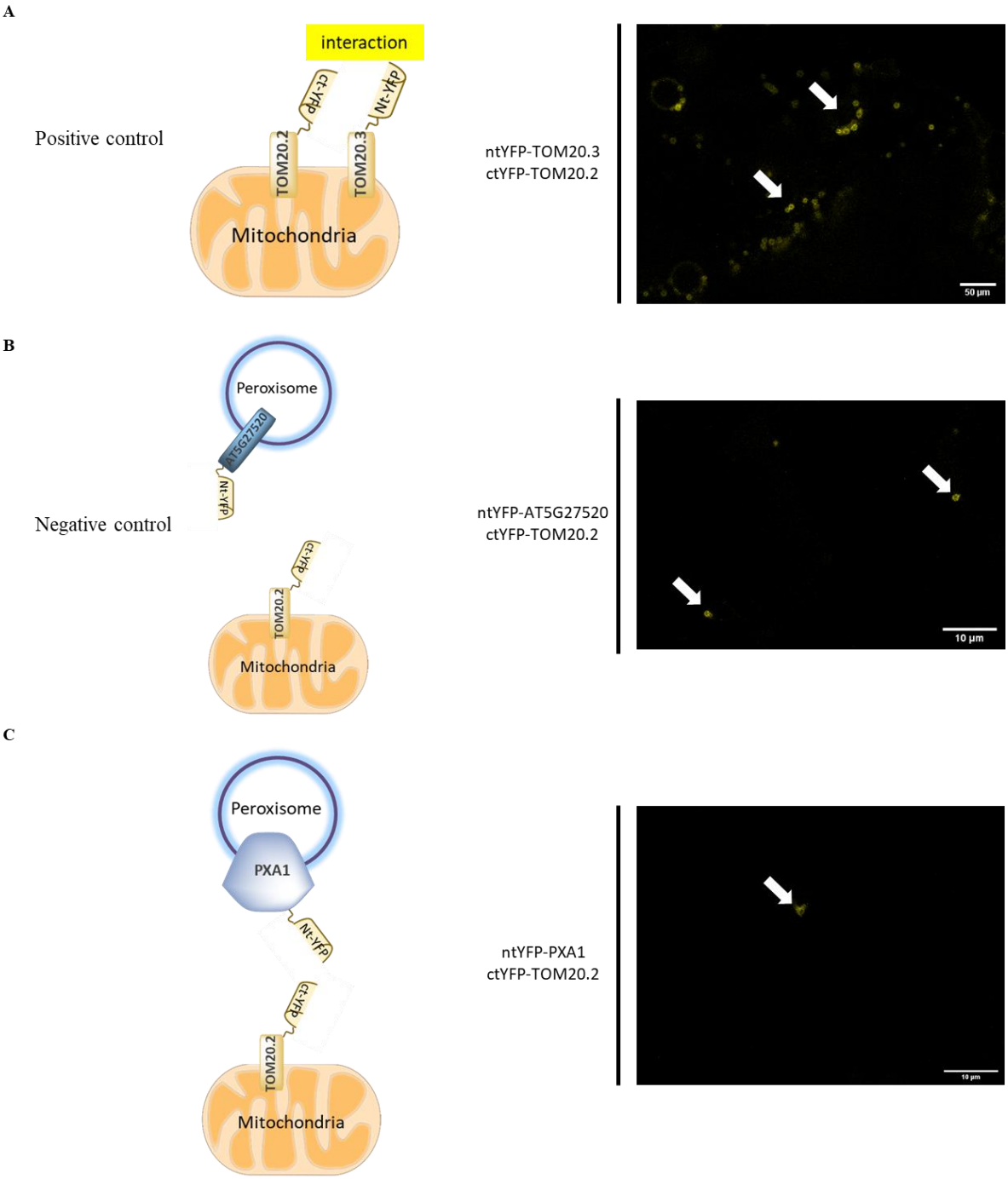


Figure 31. Classic BiFC results. A. Fluorescence confocal microscopy images of the positive control, expressing ntYFP-TOM20.3 and ctYFP-TOM20.2 constructs in *Nicotiana benthamiana* leaves. B. Fluorescence confocal microscopy images of the negative control, expressing ntYFP-AT5G27520 and ctYFP-TOM20.2 constructs in *Nicotiana benthamiana* leaves. C. Fluorescence confocal microscopy images, showing ntYFP-PXA1 and ctYFP-TOM20.2 constructs expressed in *Nicotiana benthamiana* leaves. White arrows represented the YFP signals. Scale bars were indicated at the bottom of the images.

The constructs of the TOM20.3 fused with the N-terminal end of the YFP protein and TOM20.2 fused with the C-terminal end of YFP were generated and expressed in the *Nicotiana benthamiana* leaves, serving as a positive control (**Figure 31A**), as they are subunits of the TOM complex (Lister et al., 2007). Multiple YFP signals were observed around the mitochondria (**Figure 31A**), suggesting that this technique functioned effectively in our system. A peroxisomal protein, AT5G27520, which was not found in the TOM40 co-IP results (Michaud and Albrieux, unpublished data), was taken as a potential negative control. This protein was fused with the N-terminal of YFP and co-expressed with ctYFP-TOM20.2 construct in the *Nicotiana benthamiana* leaves (**Figure 31B**). Few YFP signals were detected, and their frequency appeared to be lower compared to the positive control (**Figure 31B**). The expression of PXA1-ntYFP and ctYFP-TOM20.2 constructs in the *N. benthamiana* leaves was then carried out (**Figure 31C**). Few YFP signals were found in the results with a lower frequency compared to the positive control (**Figure 31C**). The transient expression levels of each construct in the agroinfiltrated *N. benthamiana* leaves were subsequently assessed using Western blot analyses. Results indicated that constructs of AT5G27520-TOM20.2 and PXA1-TOM20.2 exhibited significantly lower expression levels compared to TOM20.2-TOM20.3 (data not shown). This lower expression may explain the minimal YFP signals observed in **Fig. 31B & 31C**.

The YFP signals observed in cells expressing PXA1-ntYFP and ctYFP-TOM20.2 constructs were expected to co-localize at the interface between peroxisomes and mitochondria, thereby indicating the interaction between PXA1 and TOM20 at peroxisomes-mitochondria MCSs. Therefore, fluorescent organelle markers for peroxisomes and mitochondria, respectively, were co-infiltrated with PXA1-ntYFP and ctYFP-TOM20.2 constructs (**Figure 32**). However, results showed that YFP signals sometimes co-localized with both peroxisomes and mitochondria (**Figure 32A**), whereas mostly it is not the case (**Figure 32B**). In addition, several intense YFP signals were observed when peroxisomes were aggregating in the cells (**Figure 32C**), which might suggest that TOM20 was mistargeted to peroxisomes and thereafter interacted with PXA1.

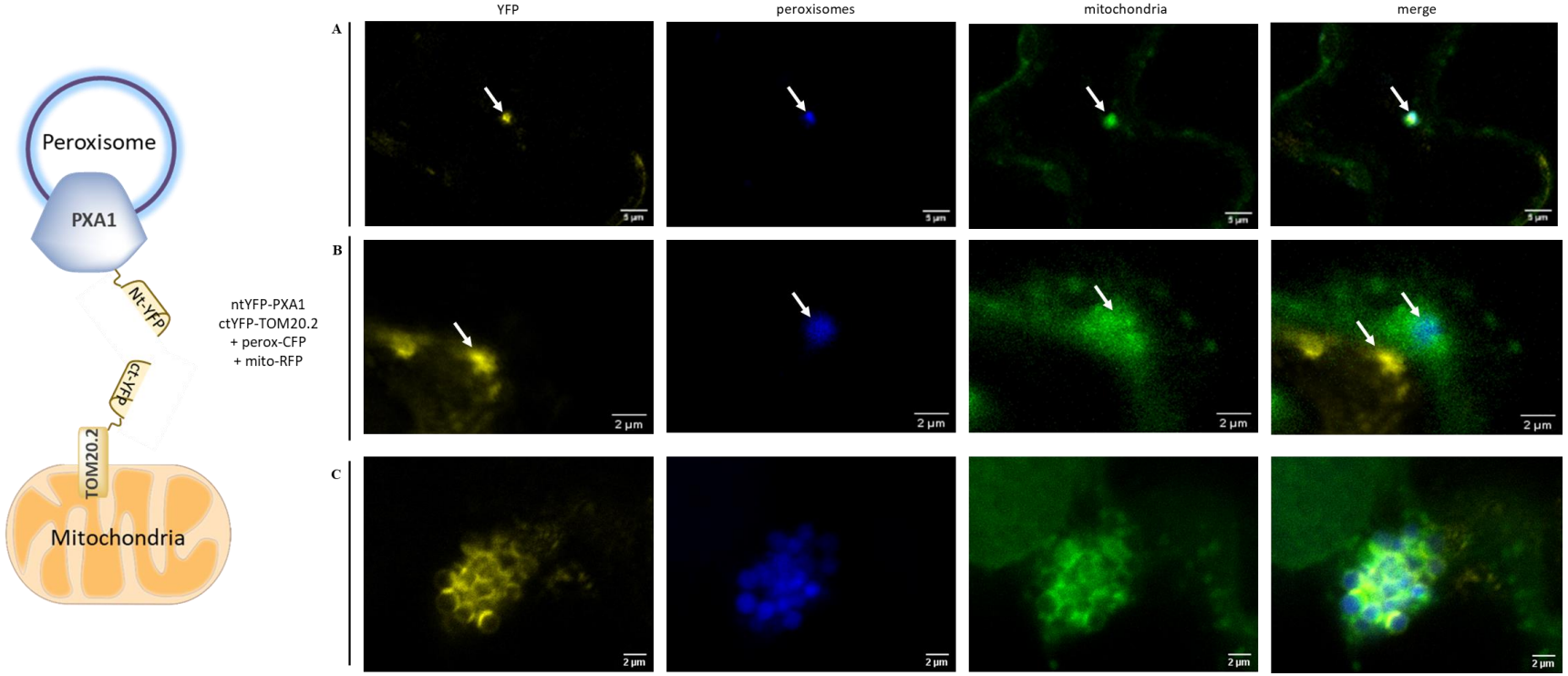


Figure 32. Classic BiFC results of ntYFP-PXA1 and ctYFP-TOM20.2 constructs co-expressed with organelle markers in *Nicotiana benthamiana* leaves. Perox-CFP and mito-RFP were used as peroxisomal and mitochondrial markers, respectively. Images were taken from one same leaf of a single plant agroinfiltrated on the same day. Scale bars were indicated at the bottom of the images. A. YFP signal co-localized at peroxisomes and mitochondria. White arrows represented the YFP signal, the localizations of peroxisome and mitochondria, and their co-localizations, respectively. B. YFP signals do not co-localize with either peroxisome or mitochondria. White arrows represented the YFP signal, the localizations of peroxisome and mitochondria. C. An aggregation of YFP signals surrounded peroxisomes and co-localized with mitochondria.

Additionally, PXA1 protein is known to be localized in peroxisomes in Arabidopsis (Cui et al., 2016; Footitt, 2002; Hayashi et al., 2002), however, several YFP signals were observed outside the peroxisomes (**Figure 32B**), suggesting that PXA1 might be mislocalized when overexpressed in *N. benthamiana* leaves. Hence, to investigate the subcellular localization of PXA1 protein in our overexpression system, a new construction of PXA1-GFP was generated. GFP signals were observed not only in peroxisomes (**Figure 33A**), but also in the ER network (**Figure 33A**), and at some unidentified locations when TOM40 was overexpressed in cells (**Figure 33B**).

Furthermore, results varied significantly from one experiment to another (data not shown), depending on the level of protein expression, the stage of plant development, the bacterial activity, the duration of agroinfiltration treatments, and certain unknown factors, thus suggesting the presence of methodological issues that needed to be resolved in this experiment.

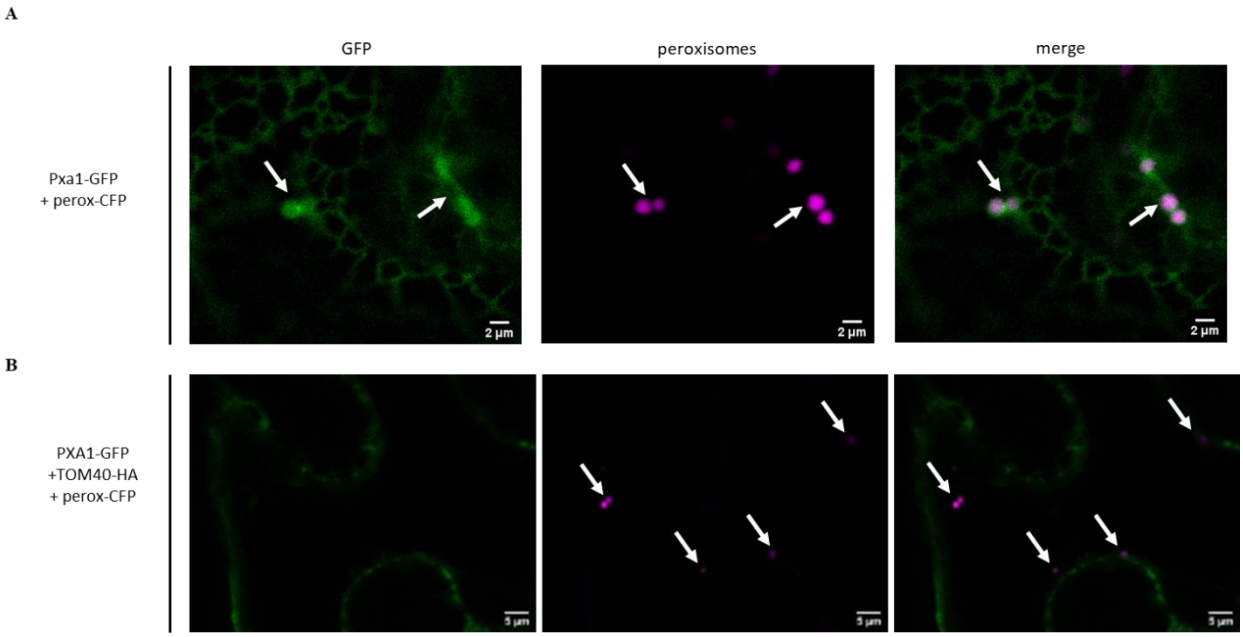


Figure 33. PXA1-GFP localization. Perox-CFP was used as peroxisomal marker. Scale bars were indicated at the bottom of the images. A shows co-localization signals of PXA1-GFP with peroxisomes, and PXA1-GFP signals located on ER network. White arrows represented the GFP signals, the localization of peroxisomes, and their co-localizations. B shows the mis-localization signals of PXA1-GFP with either peroxisomes or ER network. White arrows represented the localization of peroxisomes.

4 Conclusions and perspectives

4.1 There exists some methodological issues associated with split fluorescent protein and overexpression systems to confirm specific protein-protein interactions between organelles

The main challenges associated with the drawbacks of the BiFC technique include 1) high background signals observed in cells, 2) difficulties to distinguish real signals from the false positives, and 3) the non-reproducible results. To address the issues of high background and false-positive BiFC signals observed in our study, a myriad of technical modifications may prove effective, including changing the split position in eYFP or YFP Venus from AA155 to AA173 or AA210 (Schapire et al., 2008), introducing point mutations to suppress self-assembly of the two FP halves (Köker et al., 2018), and conducting comparative analyses using negative controls, such as the point-mutated versions of the proteins. To improve the reproducibility of BiFC results, several aspects could be considered, such as using quantitative methods to measure and normalize expression levels, assessing the transfection efficiency, and rigorously validating the specificity of the BiFC signals (Scorrano et al., 2019).

Additionally, the unsuccessful attempts to probe interactions at MCSs using split YFP can likely be attributed to the high dynamics of plant MCSs, where the maturation of the chromophore after YFP assembly may exceed the duration of organelle contacts. To avoid the step of chromophore maturation after reassembly, an alternative fluorescent protein, the self-assembly split-GFP protein (Xie et al., 2017), or the recently developed reversible system based on split FAST (Li et al., 2024), could potentially be facilitated to achieve the visualization of protein-protein interactions.

The mislocalization of PXA1 observed in this study may be due to protein misfolding or altered trafficking signals, since the addition of large BiFC fragments to the protein can create steric hindrance and cause incorrect assembly of the transmembrane domains, leading to retention in the ER or misrouting to other organelles. Additionally, overexpression can lead to protein aggregation, as observed in **Fig. 32C**. Alternative approaches to confirm PXA1-TOM complex interaction could be employed, such as yeast 2 hybrid (Y2H) or fluorescence resonance energy transfer (FRET); however, similar to BiFC, they may be not suitable for membrane protein with multiple transmembrane domains, such as PXA1.

4.2 BioID strategy is suitable to confirm PXA1-TOM complex interactions and to further identify potential partners in plant cells

During my master internship, this proximity-dependent labeling strategy has been demonstrated to be suitable for the identification of protein-protein interactions in our plant model system. However, it was

shown that TOM20, rather than TOM40, was the better candidate inside the TOM complex for the subsequent studies because of the localization of its soluble domain at the surface of mitochondria. Therefore, TurboID was fused to the soluble domain of TOM20 at the N-terminal end, with a longer and more flexible linker between them to achieve a larger and more encompassing labeling region. Moreover, constructs of TurboID fused to PXA1, along with the negative controls, were generated. The constructs for subsequent investigations using BioID strategy to confirm PXA1-TOM complex interactions were listed in **Table 8** (see "Mat & Met"). Additionally, conducting comparative analyses on TurboID-TOM20 line grown in presence and absence of Pi will be of great interest to identify specific components of MTL complex in response to Pi starvation. This will significantly enhance on our understanding of mitochondria-organelles MCSs formation and regulation in response to stress.

However, further analysis of the obtained stable transgenic lines for those constructions were not pursued, due to the high-risk nature of this project and the extensive work in the frame of Chapter one and two.

General conclusion and perspectives

Phosphate (Pi) starvation is a common abiotic stress encountered by plants in nature, significantly affecting plant growth and crop yield (Dissanayaka et al., 2021; Plaxton & Tran, 2011). To adapt to Pi starvation, plants activate various mechanisms to ensure their survival, including increasing Pi uptake from the soil and remobilizing intracellular phosphorus (P) reserves (López-Arredondo et al., 2013, 2014). Notably, during Pi starvation, phospholipids (PL) in extra-plastidial membranes are partially degraded to release Pi, while plastidial digalactosyldiacylglycerol (DGDG), a non-phosphorus plastid-synthesized lipid, is transferred to extra-plastidial organelles to replace PL, maintaining their integrity and functions (Andersson et al., 2003, 2005; Jouhet et al., 2004; Nakamura et al., 2005; Tjellström et al., 2008). Previous studies have shown that the diacylglycerol (DAG) backbone of newly formed DGDG originates from extra-plastidial PC, indicating that partially degraded PC is recycled to synthesize DGDG (for a review, Nakamura, 2013). To date, at least three pathways for this phospholipid-to-DAG catabolism, as well as a pathway for DAG-to-DGDG biosynthesis has been proposed (for a review, Nakamura, 2013).

However, certain emerging issues must be investigated. In our study, we observed a significant decrease in total lipid content under Pi deprivation, suggesting that not all phospholipids were converted into galactolipids and were likely degraded (**Figure 8B**). This led us to hypothesize a potential association with the β-oxidation, a lipid degradation pathway in peroxisomes. The finding of β-oxidation proteins in Tom40 co-IPs further supported this hypothesis. Consequently, using genetic, phenotypic, lipidomic, and cellular imaging analyses onto two Arabidopsis β-oxidation mutants, *pxa1* and *mfp2*, we attempted to investigate whether the β-oxidation pathway is crucial for recycling free fatty acids derived from partially degraded PL under Pi deprivation and, more broadly, by isolating peroxisomes from Arabidopsis suspension cells and analyzing peroxisomal lipidome and proteome, we aimed to elucidate whether peroxisomes are involved in lipid remodeling during Pi starvation. Indeed, several studies have reported that FAs β-oxidation activity increases upon nutrient deprivation, for instance, carbon starvation (Contento & Bassham, 2010), cold stress (Dong et al., 2009) and extended darkness (Kunz et al., 2009). Our study contributes to the investigation of the role of FAs β-oxidation pathway in response to Pi starvation.

However, the results showed that β-oxidation is not crucial for lipid remodeling in plant adaptation to Pi starvation, and that β-oxidation pathway does not play an essential role in metabolic flow of FA recycling during lipid remodeling in response to Pi starvation. Thus, other lipid metabolism pathways warrant further investigations to explain the reduced lipid content under Pi-deprived conditions, such as an accumulation of another non-phosphorous anionic plant lipid class, GlcADG (Okazaki et al., 2013), or examination of starch or lyso-PC content within cells (Drissner et al., 2007; C. Li et al., 2015). Moreover, another hypothesis could be that cells reduced their global membrane content (i. e. less organelles per cells) during

Pi starvation. Further quantitative studies could be utilized through biochemical assays (i. e. membrane protein extraction), various microscopy techniques, and flow cytometry.

Thereafter, because membrane lipid remodeling occurs in a wide variety of plants other than Arabidopsis and various model plants, it will be interesting to compare the regulation of this process in other plants (Yuzawa et al., 2012). A genome-wide gene-expression profiling of Pi-starved rice showed no changes in putative ABC transporters similar to *Arabidopsis thaliana* PXA1 protein (Li et al., 2010), suggesting that the non-involvement of PXA1 and possibly the β-oxidation pathway in response to Pi deficiency may be consistent across plants other than Arabidopsis.

We attempted to purify peroxisome from Arabidopsis calli grown under both Pi-enriched and Pi-deprived conditions using an adapted isolation protocol from previous studies (Taylor et al., 2014), to refine our understanding of peroxisomal lipid composition in *Arabidopsis thaliana* and to study its lipidomic and proteomic responses to Pi starvation. However, it remains challenging to isolate peroxisome with high purity from plants, due to their low abundance, high fragility and significant contamination from other organelles. Undoubtedly, using this optimized protocol, we enriched peroxisomes with satisfactory yields for analyses under both standard and stress conditions, and highlighted the major phospholipid composition of peroxisomal membranes, similar across various species (Reglinski et al., 2020; Rosenberger et al., 2009; Schneiter et al., 1999; Schrader et al., 2020; Tuller et al., 1999; Wriessnegger et al., 2007; Zinser et al., 1991). We also identified proteins related to oxidative stress response and nitrogen metabolism, which exhibit significant differences between normal growth conditions and Pi deficiency, thus suggesting a potential association between Pi starvation and oxidative stress. However, the proteomic results indicated that the purity of peroxisomes was not sufficient to assess the lipidomic and proteomic differences in response to Pi deficiency. This also suggests that future studies wishing to isolate organelles from plant cells should verify the purity combing with proteomic data, rather than relying solely on Western blot and lipidomic analyses.

Induced oxidative stress symptoms by phosphate deficiency have been studied across various species (such as bean, tobacco, bacteria and Arabidopsis), and in different tissue types (including roots and suspension cells; Juszczuk et al., 2001; Moreau et al., 2001; Shin et al., 2005; Shin & Schachtman, 2004; Sm et al., 2005; Tyburski et al., 2009). However, few genes were identified to be involved in this regulation (Chacón-López et al., 2011; Shukla et al., 2021). Our findings provide novel putative peroxisomal proteins that regulate ROS metabolism and exhibit changes in abundance during Pi starvation.

Moreover, elongated mitochondrial morphology observed in β-oxidation mutants, *pxa1* and *mfp2*, particularly under standard conditions, opened new perspectives on the relationship between these two β-

oxidation enzyme deficiency and oxidative stress in plants, since such morphological changes have been documented in several studies associated with the elevated ROS levels (Kritsiligkou et al., 2017) and stress responses (Fukushima et al., 2022). However, in our study, this phenomenon was absent under Pi-stressed conditions in these two mutants. Hence, additional studies will be conducted to assess the redox status of these two mutant calli under both Pi-sufficient and Pi-starved conditions using redox status markers in conjunction with Western blot analyses or other well-established methods (Akter et al., 2021; Mattiazzi Ušaj et al., 2015).

Furthermore, it would be of great interest to determine if the elongated mitochondria observed in our mutants are functional, considering that defective mitochondria in both structure and activity have been documented in several peroxisomal disorders in mammals (Baumgart et al., 2001; López-Erauskin et al., 2013), which was suggested due to increased oxidative stress induced probably by defective peroxisomal antioxidant mechanisms with an accumulation of lipid intermediates in peroxisomal β-oxidation system.

Additionally, increased oxidative stress and ROS levels during Pi deprivation can disrupt light energy utilization and shut down chloroplast metabolism (Shukla et al., 2021). Thus, the morphology and functionality of chloroplast in both wild type and two β-oxidation mutants also deserve further elucidation under standard and stress conditions.

In our study, the roots of Pi-starved Col0 displayed different phenotypes from those previously reported (reviewed in Péret et al., 2011). Under low Pi conditions, neither the reduced length of primary roots, or the increased number of lateral root, nor changes in root hairs, were observed in either Col0 or *mfp2* seedlings. The distinct Pi-starved phenotypes could be attributed to the different germination and growth conditions, particularly the influence of the mineral solution in the growth medium (Godon et al., 2019; Wang et al., 2019; Ward et al., 2008). Certainly, further studies are required to identify optimal growth conditions. Moreover, as elevated ROS levels in the elongation zone of the root are considered as an important factor for accelerating root growth (Liszkay et al., 2004), the reported reduced primary root length may result from the absence of ROS in the elongation zone affected by Pi deficiency treatment. This suggests a specific pattern of ROS distribution typical for the primary and lateral root growth of the growing seedlings during Pi deprivation. Hence, assessing ROS levels in Arabidopsis seedling roots under both standard and stress conditions would provide valuable insights into the status of plant adaptation to Pi starvation.

In addition, based on the distinctions between standard and Pi-stressed conditions, and between various environmental stresses (Reszczyńska & Hanaka, 2020), it suggests a role of lipids as biomarkers to identify the status of plants. While most findings so far come from researches on model Arabidopsis and rice plants,

it is also important to explore the complex mechanisms underlying membrane lipid remodeling in other plants. Given our current understanding of lipid metabolism in response to Pi starvation, artificially modified membranes can be targeted to re-organize structural and functional interactions, and mechanisms within cells to overcome stress for plants. Therefore, a better comprehension of plant lipid responses to stress from different disciplinary backgrounds will be required to unravel open issues in the coming decades for lipid manipulation in biochemistry and biotechnology, along with potential applications in diverse industrial sectors such as pharmacy, cosmetics and nutrition, ultimately benefiting humans.

In conclusion, our study revealed that peroxisomal β-oxidation pathway does not play a major role in the metabolic flow of phospholipid degradation in response to Pi starvation, and characterized notable cellular responses in β-oxidation mutants.

Title: Lipid Droplets degradation mechanisms from microalgae to mammals, a comparative overview.

Under the supervision of Juliette Salvaing, and in collaboration with Chems Amari, Marta Carletti, Morgane Michaud, we summarized current knowledge on the various lipid droplets (LD) degradation pathways across several main phyla of model organisms, including budding yeast, mammals, land plants and microalgae. My contribution focused on the section addressing LD degradation and lipolysis in plants. This review is currently under revision in *Biochimie*.

Manuscript Click here to view linked References

Title: Lipid Droplets degradation mechanisms from microalgae to mammals, a comparative overview.

Authors: Chems Amari[1,2], Marta Carletti[1], Siqi Yan[1], Morgane Michaud[1] and Juliette Salvaing[1*]

[1]Laboratoire de Physiologie Cellulaire et Végétale, Université Grenoble Alpes, Institut National de Recherche pour l'Agriculture, l'Alimentation et l'Environnement, Centre National de la Recherche Scientifique, Commissariat à l'Energie Atomique et aux Energies Alternatives,; IRIG, CEA-Grenoble, 17 rue des Martyrs; 38000 Grenoble, France
[2]Department of Chemistry, École Normale Supérieure, PSL University, Sorbonne Université, CNRS, Paris, France.

* Corresponding author : juliette.salvaing@cea.fr

Highlights

- LD degradation occurs through two main pathways: lipolysis and lipophagy
- The key core components and the initial steps of degradation appear conserved through evolution but many downstream differences are observed
- Lipolysis regulation strongly depends on the organism/tissue and conditions that trigger it
- Lipophagy pathways greatly differ among organisms
- Degradation mechanisms of LD condition the fate of LD components

Abstract:

Lipid droplets (LD) are organelles composed of a hydrophobic core (mostly triacylglycerol and steryl esters) delineated by a lipid monolayer and found throughout the tree of life. LD were seen for a long time as simple energy storage organelles but recent works highlighted their versatile roles in several fundamental cellular processes, particularly during stress response. LD biogenesis occurs in the ER and their number and size can be dynamically regulated depending on their function, *e.g.* during development or stress. Understanding their biogenesis and degradation mechanisms is thus essential to better apprehend their roles. LD degradation can occur in the cytosol by lipolysis or after their internalization into lytic compartments (*e. g.* vacuoles or lysosomes) using diverse mechanisms that depend on the considered organism, tissue, developmental stage or environmental condition. In this review, we summarize our current knowledge on the different LD degradation pathways in several main phyla of model organisms, unicellular or pluricellular, photosynthetic or not (budding yeast, mammals, land plants and microalgae). We highlight the conservation of the main degradation pathways throughout evolution, but also the differences between organisms, or inside an organism between different organs. Finally, we discuss how this comparison can help to shed light on relationships between LD degradation pathways and LD functions.

Keywords: Lipid droplets, lipolysis, lipophagy

Abbreviations :

AMPK: Adenosine monophosphate-activated protein kinase (AMPK); CE: cholesteryl ester; CMA: chaperone-mediated autophagy; DAG: diacylglycerol; ER: endoplasmic reticulum; ESCRT: endosomal sorting complex required for transport; FA: fatty acid; LD: Lipid droplet; MAG: monoacylglycerol; mTOR: mechanistic target of rapamycin; PtdIns(3)P: phosphatidylinositol 3-phosphate; PtdIns(4)P: phosphatidylinositol 4-phosphate; PRKA: protein kinase AMP-activated; TAG: triacylglycerol; SE: sterol ester; vCLIP: vacuole-LD contact site.

1. Introduction

Lipid droplets (LD) are found throughout the tree of life (Lundquist et al., 2020; Lupette and Maréchal, 2020; Murphy, 2012). They contain a hydrophobic core, mostly composed of triacylglycerols (TAG) and steryl esters (SE), surrounded by a monolayer of membrane glycerolipids. Many proteins are found at their surface, either embedded in the lipid monolayer or associated through protein-lipid or protein-protein interactions (Fujimoto and Parton, 2011; Tauchi-Sato et al., 2002). For a long time, LD were seen as simple storage organelles, used to absorb the excess of energy uptake (*e.g.* adipose tissues) or to provide energy to sustain developmental programs (*e.g.* plant seeds germination) (Graham, 2008; Huang, 1992). This view has been progressively expanded to account for their central role in lipid metabolism and actual knowledge highlights the wide diversity of LD functions. In particular, LD appear as essential in response to a multiple variety of stresses, of both abiotic and biotic origin, in algae and plants as well as in mammals and yeast (Guzha et al., 2023; Le Moigne et al., 2022; Mathiowetz and Olzmann, 2024; Olzmann and Carvalho, 2019). However, these functions can vary greatly depending on the considered organism, tissue, environmental condition or even between LD within the same cell.

In order to better understand LD functions it is essential to apprehend their life cycle, from biogenesis to degradation. LD biogenesis starts with the accumulation of neutral lipids between the two leaflets of the endoplasmic reticulum (ER) membrane; when their concentration increases, these neutral lipids coalesce into lenses and eventually bud from the ER, a process that can occur spontaneously but is promoted by proteins, in particular Seipin (reviewed in (Thiam and Ikonen, 2021; Walther et al., 2017)). The Seipin protein functions, controlling the ER-LD junction and the TAG flux from ER to LD, appear conserved in all eukaryotic cells (reviewed in (Klug et al., 2024)). Yet interactions of Seipin with other proteins emerge as potential important factors to modulate its activity and the composition of newly formed LD (Greer et al., 2020; Klug et al., 2024).

Following their biogenesis, LD fate can vary greatly. In storage tissues or organs, such as adipocytes or oleaginous seeds, LD are stable organelles. By contrast, in unicellular organisms, and in most tissues from plants and animals, LD can be very dynamic, and their number and size can quickly vary to respond to environmental cues (*e. g.* stress) or to developmental programs that trigger their formation or responsive remobilization. To answer these rapid LD turnover and their specific functions, two main degradation pathways have evolved in all eukaryotic groups: lipolysis, which allows selective degradation of the lipids contained in the

LD, and lipophagy, corresponding to the complete or partial degradation of LD inside the vacuoles or the lysosomes (Filali-Mouncef et al., 2022; Grabner et al., 2021; Guzha et al., 2023; Li-Beisson et al., 2021; Schepers and Behl, 2021). We will aim in the present review not to be exhaustive but to describe the different degradation pathways, highlighting their conservation throughout evolution, but also the differences between organisms, or inside an organism between different organs. Finally we will reflect on how LD degradation relates to the functions of LD. To this aim, we will focus on very different model organisms: the budding yeast *Saccharomyces cerevisiae*, mammals for animal models, angiosperms with the major model *Arabidopsis thaliana* and finally microalgae with two very different groups, green algae, in particular *Chlamydomonas reinhardtii*, and stramenopiles, with a focus on diatoms, in particular *Phaeodactylum tricornutum*.

2. LD degradation through lipolysis

The first way to degrade LD is to degrade their hydrophobic core through lipolysis (Grabner et al., 2021). As previously mentioned, this core is mainly composed of TAG and SE. Three main lipolysis steps are required for TAG degradation: to diacylglycerol (DAG), monoacylglycerol (MAG) and finally glycerol, with fatty acids (FA) released at each step (Figure 1).

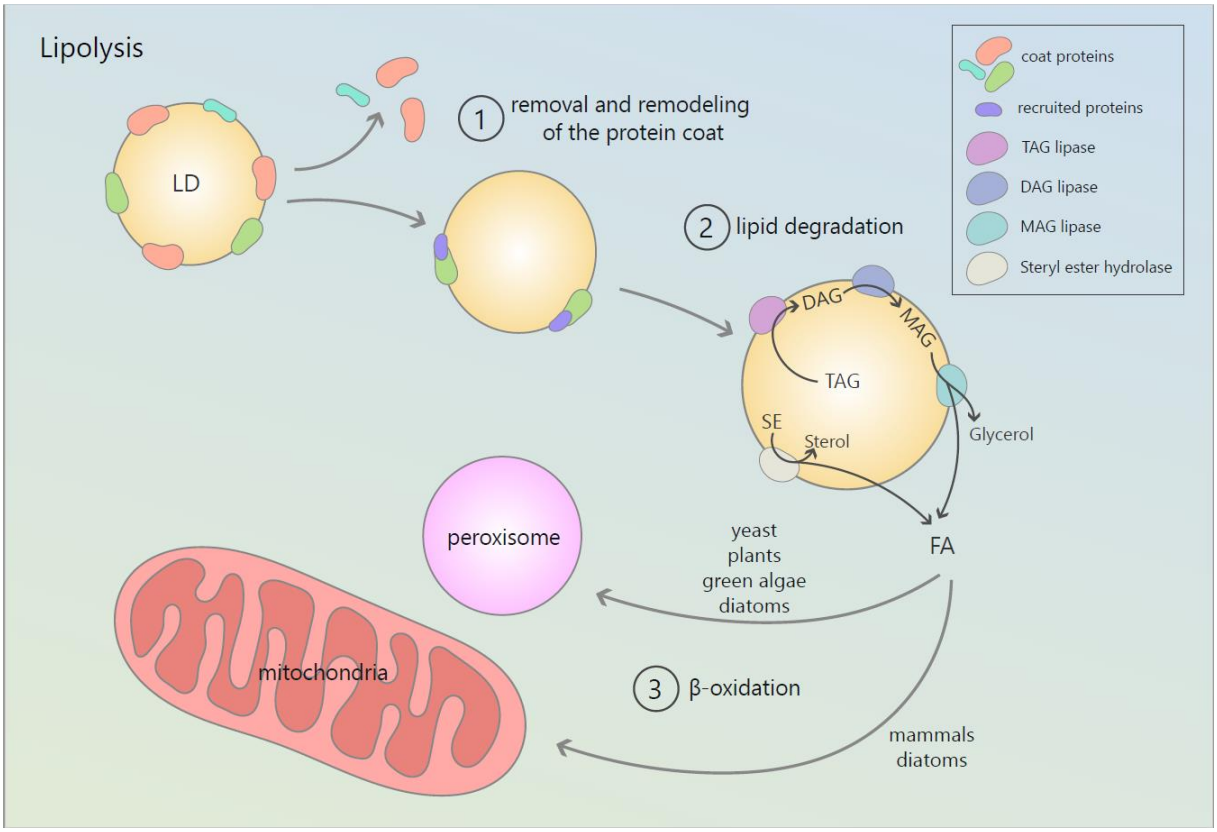


Figure 1: Schematic representation of lipolysis mechanism. 1) Remodeling of the protein coat surrounding the lipid droplet that can include removal of proteins (*e.g.* oleosins in seeds, Perilipin2 and 3 in mammals) or post-translational modifications (*e.g.* Perilipin1 and 5 in mammals). This remodeling can induce recruitment of additional factors to the LD; 2) Degradation of triacylglycerol (TAG) into diacylglycerol (DAG) and then monoacylglycerol (MAG) by membrane-localized enzymes, eventually leads to the release of glycerol and fatty acids (FA). A minor contribution is given by the degradation of steryl esters (SE). 3) FA can subsequently be degraded by β-oxidation, which can occur in the peroxisome, mitochondria or both depending on the considered organism.

In mammals, the primary step of TAG hydrolysis to DAG is catalyzed by the adipose triglyceride lipase (ATGL) (Zimmermann et al., 2004), encoded by the *PNPLA2* (*patatin-like phospholipase domain-containing protein 2*) gene in humans (Table 1). Knock out of ATGL in mice results in a drastic decrease of lipolysis both in whole-body and specific adipocytes (Haemmerle et al., 2006). Accordingly, human mutations that disrupt ATGL activity are associated with decreased rates of glycerol and fatty acid formation in response to lipolytic agents as well as with neutral lipid storage disease and myopathy (Fischer et al., 2007). Homologs of ATGL in other organisms have been widely identified and their function as major TAG lipases has also been demonstrated (Table 1). TGL4 is identified as the yeast ATGL homolog and is one of the main TAG lipase (Athenstaedt and Daum, 2005), although the major TAG lipase activity is ensured by another patatin domain containing lipase, TGL3 (Athenstaedt and Daum, 2003). In plants, the patatin-like lipase SUCROSE DEPENDENT1 (SDP1) was identified in *Arabidopsis thaliana* as the major lipase involved in TAG mobilization during seed germination (Eastmond, 2006), and a second homolog named SDP1-LIKE (SDP1L) was later identified (Kelly et al., 2011; Scherer et al., 2010). Together, SDP1 and SDP1L contribute to over 95% of TAG hydrolysis activity during seed germination (Kelly et al., 2011), and SDP1 also appears to be important for LD turnover in vegetative tissues, in particular roots and stems (Kelly et al., 2013). Identification of lipases in microalgae is more recent. LiSDP1 was identified in the LD proteome of the green alga *Lobosphera incisa* (Siegler et al., 2017). More recently, LIP4 was identified in the green alga *Chlamydomonas reinhardtii* as a homolog of SDP1, with which it shares 44% amino acid identity; LIP4 is involved in TAG remobilization during nitrogen starvation recovery as well as in TAG global homeostasis (Warakanont et al., 2019). Similarly, SDP1 homologs have been identified in secondary endosymbionts, but appear to have different importance in TAG breakdown. Indeed, while in the diatom *Phaeodactylum tricornutum,* TGL1 seems to play a major role, similar to ATGL or SDP1 (Barka et al., 2016), its role seems much more limited in *Fistulifera solaris* (Maeda et al., 2021); additionally, study of NoTGL1 and NoTGL2 in *Nannochloropsis oceanica* shows that these ER-localized

enzymes modulate TAG synthesis at the ER by degrading *de novo* synthesized TAG (Nobusawa et al., 2019).

	Name	Function	References
H. sapiens	ATGL	TAG lipase	(Zimmermann et al., 2004)
	HSL	Hormone-sensitive lipase recruited at LD surface upon cAMP stimulation, degrades preferentially DAG and cholesterol esters	(Strand et al., 1964)
	PNLPA3	TAG and DAG lipase	(He et al., 2010)
	MGL	MAG lipase	(Chon et al., 2007)
	CES1	TAG lipase and cholesteryl-esterase activities	(Ghosh et al., 2003; Zhao et al., 2005)
	PLIN1	LD coat protein removed through phosphorylation upon induction of LD degradation	(Kimmel and Sztalryd, 2016)
	PLIN2-3	LD coat proteins degraded through chaperone-mediated autophagy upon induction of LD degradation	(Kaushik and Cuervo, 2015)
	CGI-58	ATGL activator	(Lass et al., 2006)
S. cerevisiae	TGL4	TAG lipase	(Athenstaedt and Daum, 2005)
	TGL3	TAG and MAG lipase + acyltransferase (LPE) patatin-like domain	(Athenstaedt and Daum, 2003)
	TGL5	TAG lipase + acyltransferase (LPA) patatin-like domain	(Athenstaedt and Daum, 2005)
	Ldh1	TAG lipase, global lipid homeostasis	(Debelyy et al., 2011; Thoms et al., 2011)
	Ayr1	TAG lipase	(Ploier et al., 2013)
	Yju3	MAG lipase	(Heier et al., 2010)
	Yeh1 and 2	Sterol-esters hydrolases	(Köffel et al., 2005)
	Tgl1	Sterol-esters hydrolases	(Jandrositz et al., 2005; Köffel et al., 2005)
	Lct1	CGI-58 homolog	(Ghosh et al., 2008)
	Tld1	Negative regulator of Tgl3	(Speer et al., 2023)
A. thaliana	MIEL1	Ubiquitination of oleosin coat proteins to promote their removal from LD	(Traver and Bartel, 2023)
	PUX10	Binds to the ubiquitinated oleosins and recruits CDC48A	(Deruyffelaere et al., 2018; Kretzschmar et al., 2018)

	CDC48A	Segregase activity that promote oleosins removal from LD surface	(Deruyffelaere et al., 2018; Kretzschmar et al., 2018)
	VPS29	Regulates the translocation of SDP1 from peroxisomes to LD through the peroxisomal tubular extensions	(Thazar-Poulot et al., 2015)
	PEX11e	Stimulates peroxisomal tubule formation	(Huang et al., 2022)
	FREE1	Protein of the ESCRT complex that interacts with PEX11e and SDP1 and promote SDP1 transfer from peroxisomes to LD	(Huang et al., 2022)
	SDP1	TAG lipase, essential for seed germination	(Kelly et al., 2013)
	SDP1-LIKE (SDP1L)	TAG lipase that have overlapping function with SDP1 during seed germination, but not in the roots and leaves of mature plants	(Kelly et al., 2011)
	AtOBL1	TAG, DAG and MAG lipase located at LD surface and important for pollen tube growth	(Müller and Ischebeck, 2018)
	MAGL8	MAG lipase associated with LD in germinating seeds and leaves	(Kim et al., 2016)
	At4g18550/ATDSEL	DAG and MAG lipase acting at the *sn-1* position involved in the regulation of storage oil mobilization and the establishment of early seedlings	(Kim et al., 2011)
	LIDL1 and LIDL2	Putative sterol-esters hydrolases located at LD	(Kretzschmar et al., 2020)
	LOX	Involves in TAG degradation by the hydroperoxidation of either linoleic or linolenic acid acyl chains	(Viswanath et al., 2020)
	CGI-58	Regulates TAG breakdown and interacts with PXA1 at peroxisome surface	(Park et al., 2013)
C. reinhardtii	LIP4	TAG lipase	(Warakanont et al., 2019)
	LIP1	DAG lipase	(Li et al., 2012)
	CHT7	Major regulator of TAG remobilization during quiescence exit upon nitrogen resupply	(Tsai et al., 2014)
	MLDP	LD coat protein, possible role in control of lypolysis	(Moellering and Benning, 2010)
P. tricornutum	TGL1	TAG lipase	(Barka et al., 2016)
	PtLDP1/StLDP	Structural protein, possible role in control of lypolysis	(Taparia et al., 2022)
	CGI-58	Located to mitochondria and promotes de novo fatty acid synthesis and TAG degradation through mitochondrial β-oxidation	(Shu et al., 2023)

Table 1: Summary of the proteins shown to play a role in lipid droplet degradation by lipolysis in *Homo sapiens*, *Saccharomyces cerevisiae*, *Arabidopsis thaliana*, *Chlamydomonas reinhardtii* and *Phaeodactylum tricornutum*

Subsequent steps including DAG hydrolysis to MAG and MAG hydrolysis to glycerol and FFA have been less well characterized. In mammals, the hormone-sensitive lipase (HSL, encoded by the *LIPE* gene) is the major DAG lipase but it also has a high activity in the hydrolysis of cholesteryl-esters, and a lower one towards TAG, MAG, retinyl esters and short-chain acyl esters ((Vaughan et al., 1964), reviewed in (Recazens et al., 2021)). Consistently, whole-body deficiency in HSL leads to DAG accumulation in the adipose tissue as well as decreased lipolysis in mice (Haemmerle et al., 2002) and human (Bezaire et al., 2009). Monoglyceride lipase (MGL) then catalyzes the hydrolysis of monoacylglycerol, and can use both *sn-1* MAG and *sn-2* MAG, in which FAs are esterified to the terminal or middle hydroxyl group of the glycerol backbone, respectively, as substrates (Fredrikson et al., 1986; Tornqvist and Belfrage, 1976). In yeast, Yju3 has been identified as the functional ortholog of MGL (Heier et al., 2010). In higher plants, several enzymes with DAG/MAG lipase activities have been identified, with different specificities (Kim et al., 2011, 2016; Müller and Ischebeck, 2018; Yu et al., 2023). Finally in microalgae, few reports of DAG or MAG lipases exist, apart from non-selective DAG lipase CrLIP1 in *C. reinhardtii* (Li et al., 2012).

In addition to TAG, LD can contain high amounts of SE. Several enzymes involved in SE degradation have been identified in yeast, namely Tgl1, Yeh1, and Yeh2, but their study suggests that SE degradation is mainly important for sterol homeostasis with little impact on the global dynamics of LD ((Köffel et al., 2005; Köffel and Schneiter, 2006; Müllner et al., 2005; Wagner et al., 2009), reviewed in (Wang, 2015)). Enzymes involved in the breakdown of plant SE are still unknown, although the LD-ASSOCIATED LIPASE (LIDL) 1 and 2, identified by quantitative proteomic analysis of LD-enriched fractions derived from *Arabidopsis* seedlings, are homologs of Tgl1 and have been hypothesized to function as sterol esterases (Kretzschmar et al., 2020). In mammals, SE exist as cholesteryl-esters (CE) and specific enzymes involved in their breakdown have been identified. Ghosh et al. (Ghosh et al., 2003) described a neutral cholesteryl ester hydrolase (CEH) in human macrophages named CES1, that is located at the surface of LD and mobilizes LD-contained CE (Zhao et al., 2005). CES1 overexpression results in an increased rate of cholesterol efflux to ApoA1, HDL and serum (Zhao et al., 2007), suggesting that CES1 can regulate both the CE content of LD and the cholesterol efflux. KIAA1363/NCEH1/AADACL1 has also been identified as a CE hydrolase as its KO in mice results in a decreased CE activity (Sekiya et al., 2009), while its

overexpression in macrophages markedly decreases the CE content (Igarashi et al., 2010). However, its implication in macrophage CE metabolism is debated, and yet unidentified other CEH may exist (Buchebner et al., 2010). In general, the importance of CE hydrolases in LD degradation remains controversial (reviewed in (Grabner et al., 2021)).

3. Lipolysis regulation

Lipolysis allows tight control of LD degradation. It can be regulated in many different ways, that are related to the global functions of LD or to the environmental conditions in which it is formed. In this part, we will overview these mechanisms and their biological significance, focusing on TAG breakdown.

Temporal control

The primary regulation of LD lipolysis is the control of LD breakdown timing. In plant seeds, LD are very important to ensure proper germination and the establishment of the developing seedling. Plant seed LD are covered by specific proteins called oleosins (Huang, 1992; Jolivet et al., 2004), which can protect stored TAGs from lipolytic enzymes (Jacquier et al., 2013; Winichayakul et al., 2013) and are absent from LD in vegetative tissues. The removal of oleosins is tightly regulated through initial ubiquitination and subsequent proteasome degradation (Deruyffelaere et al., 2015; Sharma et al., 2016). It involves the sequential recruitment of MYB30-interacting E3 ligase 1 (MIEL1), plant ubiquitin regulatory X (UBX) domain-containing protein10 (PUX10) and cell division cycle 48A (CDC48A) ATPase (Deruyffelaere et al., 2018; Kretzschmar et al., 2018; Traver and Bartel, 2023) (Table 1). However, protection of TAG by oleosins is not tight-proofed (Beisson et al., 2001) and additional mechanisms are require to regulate lipolysis. Interestingly, the main lipase SDP1 is initially localized on peroxisomes. Its relocalization to LD requires the formation of peroxisomal tubulations called peroxules (Cui et al., 2016; Thazar-Poulot et al., 2015). Recent advances have shown involvement of the endosomal sorting complex required for transport (ESCRT) machinery and PEROXIN 11e (PEX11e) in the formation of these tubules (Huang et al., 2022) but the triggering mechanisms remain elusive.

In mammals, hormonal signals control LD lipolysis through different mechanisms (reviewed in (Grabner et al., 2021)). Both ATGL and HSL are regulated at the transcriptional level and can be upregulated in response to endocrine, paracrine or autocrine factors including hormones, cytokines and neurotransmitters. Peroxisome proliferator-activated receptor γ (PPAR) in particular can promote lipase expression in response to starvation (Roy et al., 2017;

Yogosawa et al., 2013). HSL expression can also be activated by sterol regulatory element binding proteins (SREBPs) (Gambo et al., 2016). In addition to this transcriptional regulation, the activity of lipases is regulated post-translationally, both directly and indirectly through cyclic Adenosyl MonoPhosphate (cAMP) signaling. Indeed, protein kinase A (PKA), which is activated by cAMP in response to β-adrenergic stimulation, can phosphorylate both HSL and perilipin 1 (PLIN1), a LD coat protein (reviewed in (Kimmel and Sztalryd, 2016)). This phosphorylation triggers the relocation of HSL to LD but also the dissociation of PLIN1 and Comparative gene identification-58 (CGI-58), which is a major activator of ATGL ((Lass et al., 2006) reviewed in (Yu et al., 2020)). Thus, similarly to oleosins, Perilipins (PLIN), the major proteins found at the surface of LD (Londos et al., 1999) in mammals, participate in lipolysis regulation ((Brasaemle et al., 2000), reviewed in (Griseti et al., 2024)). This is the case in white adipocytes where PLIN1 is predominant, and in oxidative tissues (heart, skeletal muscle, liver, brown adipose tissue) where PLIN5 performs a similar function ((Granneman et al., 2011; Keenan et al., 2021; Pollak et al., 2015), reviewed in (Griseti et al., 2024)). Another degradation mechanism called chaperone-mediated autophagy (CMA) has been described for PLIN2 and 3: *in vivo* studies revealed that CMA degradation of both proteins is increased during starvation, and that their degradation enhances LD degradation through lipolysis, but also through macroautophagy (see section 4) (Kaushik and Cuervo, 2015) (Table 1).

In unicellular organisms, cell cycle appears as a major regulator of metabolism and particularly of lipolysis. Indeed, in budding yeast, the TAG synthesis enzymes Pah1 is inhibited (O'Hara et al., 2006; Santos-Rosa et al., 2005) while the TAG lipase TGL4 is activated (Kurat et al., 2009) by Cdk1/Cdc28 during log phase. This regulation is consistent with the central role of TAG in lipid metabolism, as a source of building blocks for membrane lipids (Rajakumari et al., 2010). In photosynthetic microorganisms, light is another essential growth factor and circadian rhythms play important roles in the regulation of the cell cycle and of energy metabolism. This has been well shown in the diatom *Phaeodactylum tricornutum* (Chauton et al., 2013; Huysman et al., 2015, 2013; Zhang et al., 2022), where lipid droplets form during the day and are degraded during the night when cell division occurs. Yet this coordination does not imply direct regulation of TAG degradation by cell-cycle dependent mechanisms. Such regulation has only been shown so far in the green alga *Chlamydomonas reinhardtii*, in which the regulatory protein COMPROMISED IN TAG HYDROLYSIS7 (CHT7) (Tsai et al., 2014), involved in the exit of quiescence following nitrogen resupply, appears as a major regulator of TAG remobilization, linking the resumption of cell cycle and TAG hydrolysis.

Spatial control

The regulatory mechanisms we have described above allow coordination of TAG hydrolysis with the cell or organisms needs on a broad level. But lipolysis also allows finer regulation of TAG breakdown, enabling the release of specific fatty acids or the degradation of specific populations of lipid droplets. Indeed, while we have focused in part 2 on the "canonical" TAG breakdown enzymes, every organism contains a great variety of TAG, DAG or MAG lipases (Table 1).

These enzymes can exhibit different substrates specificities. In budding yeast, the major TAG lipase TGL3 shows unspecific activity towards TAG or even DAG (Athenstaedt and Daum, 2003). TGL4 on the other hand shows a preference for TAG containing C14 and C16 acyl-chains, while TGL5 is involved in the breakdown of TAG containing very long chain fatty acids C26 (Athenstaedt and Daum, 2005). Both TGL3 and TGL5 also exhibit acyl-transferase activity, respectively towards lyso-phosphatidylethanolamine (LPE) and lyso-phosphatidic acid (LPA) (Rajakumari and Daum, 2010). In *Arabidopsis*, a cytosolic member of the DAD1-like acyl-hydrolase family encoded by At4g18550 demonstrates a specific ability to hydrolyze DAG and MAG at the *sn*-1 position and is crucial in the establishment of early seedlings (Kim et al., 2011). AtMAGL8 plays an important role in seeds and exhibits a notable substrate preference for MAG containing C20:1 fatty acids (Kim et al., 2016). Such substrates specificities have not yet been shown in microalgae, but the development of bioinformatics tools has allowed the identification of many new potential lipases that remain to be investigated (Ali et al., 2021; Murison et al., 2023b).

In multicellular organisms, the role of lipases can vary from one tissue to another. In land plants, studies on LD were primarily focused on seeds germination but such interest has since expanded to other tissues, in particular the pollen tube, where LD are essential, and leaves, where LD play roles in response to various abiotic and biotic stresses (for review: (Bouchnak et al., 2023; Le Moigne et al., 2022)). Oil body lipase 1 (AtOBL1 in *Arabidopsis*) has been identified as a TAG lipase, but can also degrade DAG and MAG with no obvious substrate specificity. Its role in seeds is very minor, but it is essential in pollen tubes (Müller and Ischebeck, 2018). We have previously mentioned the importance of oleosins in seeds; Lipid droplet associated protein (LDAP) and LDAP-interacting protein (LDIP) are the major lipid droplets proteins in vegetative tissues, where they play important roles for LD homeostasis (Gidda et al., 2016, 2013; Pyc et al., 2017) but their potential involvement in LD degradation

remains to investigate. Finally, a homolog of CGI-58 has been identified in *Arabidopsis*; its function in TAG breakdown is conserved (James et al., 2010; Kelly et al., 2011) but unlike its mammalian counterparts, it localizes to peroxisomes and its mechanism of action appears very different (Park et al., 2013). Yet, while it seems to play only a minor role in seeds LD breakdown, the loss of CGI-58 causes a major effect in plant leaves (James et al., 2010). In mammals, the canonical pathway through ATGL and HSL accounts for over 90% of TAG degradation in adipocytes (Schweiger et al., 2006). Many other lipases have been identified, but their importance even in other tissues remains poorly evaluated (reviewed in (Grabner et al., 2021)). For instance, PNLPA3, a close relative of ATGL that can hydrolyze TAG and DAG (He et al., 2010), is expressed in both white and brown adipose tissue in mice, is highly abundant in human hepatocytes and is associated with liver diseases; however, PNLPA3 KO has little impact and deleterious effects are observed as results of dominant negative mutations that increase its association with CGI-58 to the detriment of ATGL association (Dong, 2019; McHenry and Davidson, 2019; Wilson et al., 2006). We have mentioned above the different distribution of PLIN proteins between different tissues. It is therefore possible that regulation of lipolysis in different tissues is more dependent on the protein equipment of LD and their regulation of the lipolytic enzymes rather than on the presence of different lipolysis enzymes (see (Griseti et al., 2024)). This type of regulation moreover allows differential treatment of individual LD within the same cell. Such a mechanism has recently been shown in budding yeast, where TG-associated LD protein 1 (Tld1) protein localizes specifically to LD containing TAG but not SE and can specifically inhibit their degradation by TGL3 (Speer et al., 2023).

Association with co-factors and other regulations

We have previously introduced the function of CGI-58, a regulator of lipolysis, in mammals and plants. Homologs of CGI-58 also exist in yeast (Ghosh et al., 2008) and microalgae (Shu et al., 2023; Trentacoste et al., 2013). Surprisingly, while reduction of CGI-58 homolog levels in the diatom *Thalassiosira pseudonana* has the expected effect of reducing TAG hydrolysis (Trentacoste et al., 2013), the overexpression of the *Phaeodactylum tricornutum* homolog also leads to an overaccumulation of TAG; moreover, CGI-58 is reported to be localized to mitochondria and the authors suggests that it plays a role in promoting *de novo* fatty acids synthesis as well as TAG degradation through mitochondrial β-oxidation (Shu et al., 2023).

LD degradation pathways can determine fatty acids fate. In addition to the classical degradation pathway presented in part 2, a LD-specific lipoxygenase (LOX)-dependent pathway for lipid mobilization during seed germination has been proposed in various plant species, such as Arabidopsis, watermelon, cucumber, wheat, barley, potato, tomato, sunflower and tobacco. This pathway allows direct coupling of TAG degradation with the generation of oxylipins, involved in signaling, or phytoalexins (Feussner et al., 2001; Viswanath et al., 2020).

4. Lipophagy

Autophagy is a general process to target the degradation of specific organelles or compounds (for review: (Gatica et al., 2018; Mizushima, 2018)). Initially described in yeast and mammals, autophagy core components are well conserved in plants (for reviews, see (Avin-Wittenberg et al., 2012; Gomez et al., 2021; Lin et al., 2021)) and algae (for review (Pérez-Pérez et al., 2021)). In plants, autophagy plays an important role in response to biotic and abiotic stresses. In agreement, plants having a decrease in autophagy flux usually present a higher sensitivity to many stresses including heat, drought and nutrient stresses, likely due to the role of this process in cell compounds recycling and damaged or unwanted organelles removal under harsh environment (for reviews, see (Gomez et al., 2021; Yagyu and Yoshimoto, 2023)). The link between autophagy and LD is complex as autophagy can be involved in both LD biogenesis and degradtion and LD can also play a role in autophagy by providing lipids for autophagosome biogenesis (for review: (Xu and Fan, 2022)). Here we will focus on the role of autophagy in LD degradation.

Regulation of lipid metabolism through autophagy, also known as lipophagy, has only been shown quite recently (Liu and Czaja, 2013; Singh et al., 2009). Several autophagy, and subsequently lipophagy, pathways can be distinguished. Macroautophagy has been known for a long time (Duve and Wattiaux, 1966). It involves the formation of an autophagosome, that will engulf the targeted organelle, and fuse with lysosomes in mammals or vacuoles in other organisms to direct their degradation. By contrast, microautophagy involves direct contact of the targeted organelle with lysosomes or lytic vacuoles and their subsequent engulfment in these lytic compartments. The use of these two pathways for LD degradation differs between organisms. While macrolipophagy seems to be a major process in mammalian cells, LD degradation by different microlipophagy processes has been described in yeast, plants and microalgae. It should be however noted that lipophagy processes only start to be studied in some organisms and that the current view is probably still very partial.

Macrolipophagy in mammals

In mammals, macrolipophagy, also known as lysosome-mediated acid lipolysis, has been well described in the liver, where it is important to control intracellular lipid storage, free lipids and energy homeostasis (Figure 2A) (for review: (Feng et al., 2023)). It involves the Lysosomal acid lipase (LAL) (Mahadevan and Tappel, 1968), encoded by the *Lipa* gene. While it is ubiquitously expressed, its highest expression is in macrophages and hepatocytes. LAL can degrade most components of LD, including TAG and DAG but also steryl and retinyl esters ((Grumet et al., 2016; Sheriff et al., 1995; Warner et al., 1981) reviewed in (Grabner et al., 2021)). LD degradation by LAL follows targeting of LD to lysosomes through the classical macroautophagy route, that relies on the evolutionarily conserved autophagy-related genes Atg (Mizushima et al., 2011). It is triggered in response to starvation via several signaling pathway, including repression of the mTOR (mechanistic target of rapamycin kinase) complex 1 (MTORC1) (Hosokawa et al., 2009; Soto-Avellaneda and Morrison, 2020), and activation of protein kinase AMP-activated catalytic subunit (PRKA)/adenosine monophosphate-activated protein kinase (AMPK) (Tamargo-Gómez and Mariño, 2018; Zhu et al., 2014). These in turn activate the ULK1/Atg1 (unc-51 like autophagy activating kinase 1) kinase complex (Jung et al., 2009; Wong et al., 2013), leading to the formation of a phagophore, which will evolve in forming the nascent autophagosome (Roberts and Ktistakis, 2013). Specifically, the ULK1 complex phosphorylates and activates the class III phosphatidylinositol 3-kinase (PtdIns3K) complex, composed of Beclin-1/Vps30/Atg6, PIK3R4/VPS15, Atg14, PIK3C3/VPS34, AMBRA1 and NRBF2 (He and Levine, 2010). Recruitment of this complex and production of a pool of phosphatidylinositol 3-phosphate (PtdIns(3)P) at ER extensions called omegasomes promotes the recruitment of PtdIns3P-binding proteins, such as ZFYVE1/DFCP1 (zinc finger FYVE-type containing 1/double FYVE domain – containing protein 1) (Axe et al., 2008) and WIPI2 (WD repeat domain, phosphoinositide interacting) protein (Polson et al., 2010). WIPI2/Atg18 will then recruit and promote the assembly of the Atgl12-5-16L1 complex (Dooley et al., 2014) which acts as an E3-like ligase and recruits the E2-like protein Atg3 for the conjugation of the members of the MAP1LC3/LC3 (microtubule associated protein 1 light chain 3), also called Atg8, protein family to phosphatidylethanolamine (PE) (Sakoh-Nakatogawa et al., 2013). LC3 proteins are important for autophagic cargo selection, phagophore elongation and closure. Last, autophagosomes appear to traffic along microtubules in higher eukaryotes, eventually targeting and fusing with lysosomes following a SNARE mechanism (Nair et al., 2011).

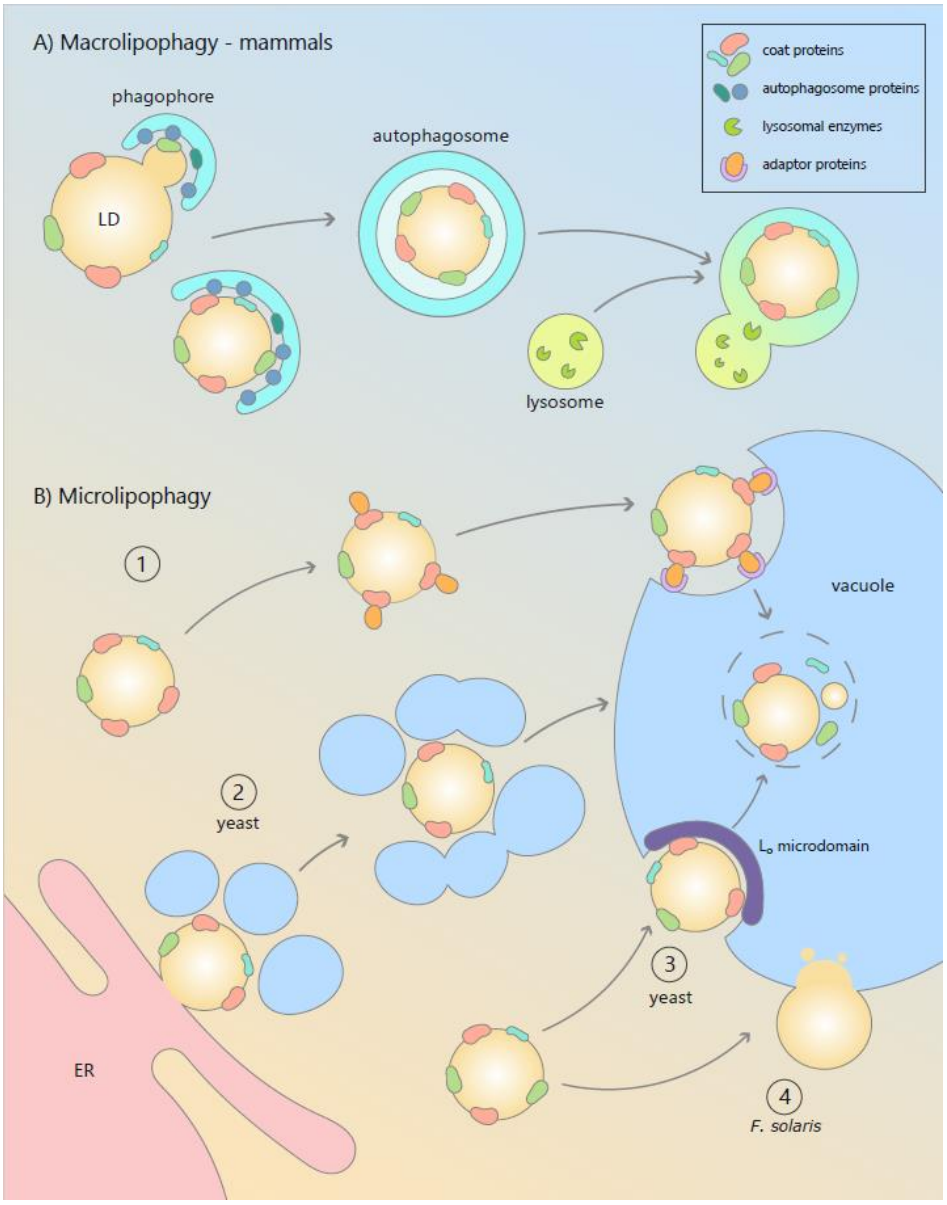


Figure 2: Overview of lipophagy mechanisms in differents organisms. A) Macrolipophagy has been described in mammals: after the formation of the phagophore, the autophagosome completely surrounds the LD and eventually fuses with lysosomes. B) Microlipophagy has been observed in several eukaryotic organisms, however several mechanisms have been described 1) Specific proteins bind to the LD coat proteins and direct it to the lytic compartment where it is recognized by specific receptors. This broad and simple description matches what has been described in *A. thaliana*, where the coat protein CLO1 appears to regulate addressing to the vacuole, possibly interacting with Atg8 and in yeast, where the LD proteins Ldo16 and Ldo45 can directly bind to the vacuolar protein Vac8 to trigger microlipophagy. 2) In yeast, in response to endoplasmic reticulum (ER) stress, the vacuole fragments into smaller vesicles that organize around the LD, envelope them and form invagination which release the LD into the vacuolar lumen following membrane scission; 3) In yeast, during nutrient starvation, LD can be recruited to the vacuole thanks to specific microdomains (L_O microdomains) for efficient internalization. 4) In *Fistulifera solaris*, a direct fusion of vacuoles and LDs have been observed without the complete absorption of the LD, suggesting a novel type of microlipophagy.

The recognition of LD for macrolipophagy degradation can involve several proteins, including the adaptator SQSTM1/p62 (Wang et al., 2017) and several members of the Rab GTPase family, in particular Rab7 (Schroeder et al., 2015), but also Rab10, 25 and 32 (reviewed

in (Feng et al., 2023)) (Table 2). Perilipins also appear to play central roles in regulating lipophagy. Indeed, PLIN 2 protects LD from lipophagy (Tsai et al., 2017) and the degradation of PLIN2 and 3 by chaperone mediated autophagy can promote both association of ATGL (as described in section 3) and LC3 proteins at the surface of LD (Kaushik and Cuervo, 2015; Sztalryd and Brasaemle, 2017). PLIN1 colocalizes with p32 (Wang et al., 2017) and its phosphorylation is necessary to allow Rab7 docking (Lizaso et al., 2013).

Microlipophagy in mammals and yeast

The prevalence of macrolipophagy appears specific to mammals as in all other organisms, lipophagy mainly occurs through pathways related to microautophagy.

Microlipophagy was thought to be absent from mammalian cells, but some recent evidences have shown that this pathway plays a significant role in LD degradation in mammal liver hepatocytes (Schulze et al., 2020). Indeed, in those cells LD and lysosomes can form transient contacts that usually last 30 to 60 s and that do not depend on the canonical macroautophagic machinery pathway, both in presence or absence of nutrients.

In budding yeast, actors and mechanisms involved depend on the condition or stress promoting microlipophagy (Table 2). Microlipophagy was observed in response 1) to nutrients starvation triggered by cells entry into stationary phase or by acute nitrogen or glucose depletion (Kang et al., 2024; Seo et al., 2017; Tsuji et al., 2017; van Zutphen et al., 2014; Wang et al., 2014); 2) to ER stress mediated by lipid imbalance in a strain with a deficiency in phosphatidylcholine (PC) synthesis, or by the addition of dithiothreitol (DTT) or tunicamycin (TUN), an inhibitor of ER protein glycosylation (Garcia et al., 2021; Liao et al., 2021; Vevea et al., 2015) or 3) to diauxic shift triggered by yeast transfer from a fermentative to a respiratory media (Oku et al., 2017).

Microlipophagy requires the targeting of LD and attachment to the vacuole membrane, followed by the engulfment of the LD by an inward invagination of the vacuolar membrane in the lumen (Figure 2B-1). After scission of the vacuole membrane, the LD is released in the vacuole lumen surrounded by the vacuolar membrane and is then degraded (Fairman and Ouimet, 2022; Liao and Pon, 2022).

During microlipophagy induced by nutrient starvation, LD were shown to be recruited at specific microdomains formed in the vacuolar membrane, the liquid-ordered (L_o) microdomains, before their inward budding to promote LD internalization. L_o domain

formation is essential for efficient internalization of LD into vacuoles under nutrient stress and lipid imbalance (Figure 2B-3) (Liao et al., 2021; Wang et al., 2014). Many proteins required for the formation of these microdomains were identified and their deletion negatively impacts microlipophagy (Table 2) (Kang et al., 2024; Murley et al., 2015; Toulmay and Prinz, 2013; Wang et al., 2014). L_o microdomains are enriched in sterols, contain sphingolipids, that are important for their formation (Kim and Budin, 2024; Liao et al., 2021; Lingwood and Simons, 2010; Toulmay and Prinz, 2013; Wang et al., 2014) and also PtdIns(3)P and phosphatidylinositol-4-phosphate (PtdIns(4)P) located in the cytosolic leaflet (Kurokawa et al., 2020; Tsuji et al., 2017). Vacuolar membrane are usually poorly enriched in sterols and sphingolipids implying that these lipids have to be transported to the vacuole membrane when required to form L_o microdomains (Kim and Budin, 2024; Tsuji and Fujimoto, 2018). Several lipid sources and transport mechanisms were proposed : 1) transport from the lumen of sterols coming from the degradation of intraluminal vesicles (ILV) originating from the fusion of sterol-enriched multivesicular bodies (MVB) or from the degradation of LD after their internalization by two vacuolar sterol transporters, Npc2 and Ncr1 (Liao et al., 2021; Tsuji et al., 2017; Winkler et al., 2019); 2) transport through non-vesicular pathway, as exemplified by Lam6, a sterol transporter located at the nucleo-vacuolar junction and involved in L_o microdomains formation (Murley et al., 2015); 3) transport to the vacuole by autophagy, as autophagosomes that fused with the vacuole membrane could be a source of sphingolipids and sterols (Seo et al., 2017; Tsuji and Fujimoto, 2018; van Zutphen et al., 2014; Wang et al., 2014). The involved mechanisms depend on the condition used to induce microlipophagy. Recently, the LD surface proteins Ldo16 and Ldo45, also named LDOs for LD organization, were shown to interact with the vacuolar protein Vac8 and to promote vacuole-LD contact site (vCLIP) formation (Álvarez-Guerra et al., 2024; Diep et al., 2024). LDOs are also involved in LD biogenesis as they are associated to the Seipin complex during logarithmic phase (Teixeira et al., 2018) and their progressive dephosphorylation when yeasts enter the stationary phase promotes vCLIP formation and lipophagy induction (Diep et al., 2024). Therefore, LDOs localization and function could be regulated by phosphorylation dependent on the metabolic status of the cells, connecting LD synthesis to LD degradation.

	Name	Function	References
S. cerevisiae	Ncr1 and Npc2	Formation and expansion of L_o microdomains in vacuole membrane by transferring sterols from the vacuole lumen to the vacuolar membrane	(Tsuji et al., 2017; Vevea et al., 2015)

Pik4 and Stt4	PtdIns(4) kinases required for local synthesis of PtdIns(4)P into vacuolar L_o microdomains and lipophagy under nitrogen starvation	(Kurokawa et al., 2020)
Lam6	Sterol transporter located at nucleo-vacuolar junction andpromoting L_o microdomain formation	(Murley et al., 2015)
Fab1	Phopshatidylinositides biosynthesis, required for L_o microdomains formation	(Toulmay and Prinz, 2013; Wang et al., 2014)
Nem	Phospholipid biosynthesis, required for L_o microdomains formation	(Toulmay and Prinz, 2013; Wang et al., 2014)
Vps4	AAA-ATPase, component of ESCRT complex involved in MVB synthesis, required for L_o microdomains formation	(Kang et al., 2024; Toulmay and Prinz, 2013; Vevea et al., 2015; Wang et al., 2014)
Sec18	Involved in vesicular trafficking, required for Lo microdomains formation	(Toulmay and Prinz, 2013)
Pep4	Vacuolar protease, required for L_o microdomains formation	(Kang et al., 2024; Vevea et al., 2015; Wang et al., 2014)
Are1/2	Synthesis of ergosteryl esters, required for L_o domain formation	(Wang et al., 2014)
ATG15	Vacuolar TAG lipase, degradation of LD TAG in the vacuole after internalization, required for L_o microdomains formation	(Kang et al., 2024; Robichaud et al., 2021)
Snf1/4	Subunits of the AMP-activated protein kinase complex, activate lipophagy during accute glucose reduction by assisting the relocalization of Atg14 to the vacuolar membrane	(Seo et al., 2017)
Atg6/14	Part of the phosphatidyl-inositol 3-kinase complex I that produces PtdIns(3)P. Could play a role in production or tageting of PtdIns(3)P to the vacuole for the formation of L_o microdomains	(Kang et al., 2024; Maeda et al., 2015; Seo et al., 2017)
ESCRT complex	Might assist LD internalization by promoting vacuole membrane invagination and membrane scission in lipophagy induced by diauxic shift from glcolysis to respiration or ER stress.	(Garcia et al., 2021; Oku et al., 2017; Vevea et al., 2015)
Ldo16, Ldo45 and Vac8	Triggers LD attachment to vacuole via interaction of the LD protein Ldo45 and Ldo16 with the vacuolar membrane protein Vac8	(Álvarez-Guerra et al., 2024; Diep et al., 2024)
Core autophagy proteins	Important for LD internalization into vacuole and for vacuole microdomain maintenance under nutrient starvation	(Kang et al., 2024; Seo et al., 2017; Tsuji et al., 2017; van Zutphen et al., 2014; Wang et al., 2014)
ATG39/ESM1	Involved in lipophagy under ER-stress triggers by PC imbalance	(Vevea et al., 2015)

	Vam3, Ypt7 and Vps33	Proteins involved in vacuolar membrane fusion and playing a role in lipophagy during ER-stress induced by DTT	(Garcia et al., 2021)
A. thaliana	ATG2/ATG5/ATG7	Involved in microautophagy to promote TAG degradation under starvation induced by extended darkness	(Fan et al., 2019)
		Regulation of lipid homeostasis in dark-induced senescence	(Barros et al., 2021)
		TAG degradation under carbon starvation in etiolated seedlings	(Avin-Wittenberg et al., 2015)
	CLO1	LD coat protein interacting with ATG8f to promote LD internalization into vacuole during lipophagy in germinating seeds	(Miklaszewska et al., 2023)
H. sapiens	SQSTM1/p62	LD recognition for macrolipophagy	(Wang et al., 2017)
	Rab7, Rab10, Rab25 and Rab32	LD recognition for macrolipophagy	(Feng et al., 2023; Schroeder et al., 2015)
	Core autophagy components	Target LD into vacuole by macrolipophagy	(Mizushima et al., 2011)
	LC3	Autophagic cargo selection, phagophore elongation and closure	(Schaaf et al., 2016)
	mTOR	Regulator of autophagy, is activated in presence of nutrients	(Soto-Avellaneda and Morrison, 2020)
	PRKA/AMPK	Regulator of autophagy	(Feng et al., 2023)
	Atg1	Initiator of the phagophore formation	(Wong et al., 2013)
	LAL/Lipa	Lysozomal lipase involved in LD lipids degradation after internalization by lipophagy	(Grumet et al., 2016; Sheriff et al., 1995; Warner et al., 1981)
Cr.	Core autophagy components	Promote TAG accumulation or LD formation upon nitrogen or phosphate starvation	(Couso et al., 2018)
	ATG8	LD degradation by microautophagy during nitrogen resupply	(Kajikawa et al., 2019)
Pt.	StLDP	Putative interaction with Atg8	(Leyland et al., 2020; Taparia et al., 2022)
	ACBP	Regulation of *Atg5*?	(Leyland et al., 2024)

Table 2. Summary of the proteins shown to play a role in lipid droplet degradation by lipophagy in *Homo sapiens*, *Saccharomyces cerevisiae*, *Arabidopsis thaliana*, *Chlamydomonas reinhardtii* (*Cr.*) and *Phaeodactylum tricornutum* (*Pt*).

The mechanisms involved in microlipophagy during ER stress under induction by DTT or TUN present significant differences compared to the ones occurring under nutrient stress. First of all, neither the core autophagy components nor the formation of L_o microdomains are required (Liao et al., 2021; Vevea et al., 2015). In addition, both stresses trigger vacuolar membrane fragmentation; LD internalization is then mediated by the remodeling of membrane

vacuoles that organize around LD, envelope them and form invaginations that release LD in the vacuolar lumen after membrane scission (Figure 2B-2) (Garcia et al., 2021). The formation of invaginations and the release of LD in this situation was proposed to be facilitated respectively by the action of the ESCRT complex and of proteins involved in vacuole fusion rather than by the property of the L_o microdomains as demonstrated under nutrient stress (Garcia et al., 2021; Liao et al., 2021; Wang et al., 2014). An intermediate situation is observed during lipid imbalance as both the ESCRT complex and the L_o microdomains formation mediated by Npc2 and Ncr1 are required (Liao et al., 2021), demonstrating the co-existence of different pathways mediating LD microlipophagy.

Once in the vacuoles, degradation of LD proteins and lipids could imply the protease Pep4 and the Atg15 lipase, that are located in the vacuole lumen and play a role in microlipophagy under both nutrient starvation and ER stress (Robichaud et al., 2021; Seo et al., 2017; Vevea et al., 2015). More recently, as for PLIN2 and PLIN3 in mammals (see section 3), autophagy was shown to be required for the removal of LD surface proteins prior to their internalization into vacuole under nutrient stress (Kang et al., 2024), shedding light on the poorly understood role of general autophagy in microautophagy. However, protein removal is not a pre-requisite for LD entry in the vacuole suggesting that LD protein removal and LD entry in the vacuole for lipolysis are two independent processes (Kang et al., 2024).

Microlipophagy-like processes in plants and algae

In plants, the number of studies investigating the involvement of autophagy core components in LD degradation are limited and results are variable depending on the species, the developmental stage, the tissue and/or the stress analyzed. During seed germination, TAG are mainly degraded by the cytosolic TAG lipases SDP1 and SDPL1 that are essential for seed germination in absence of carbon source in the media (see section 2). However, degradation of LD by a process similar to microlipophagy was also observed in *A. thaliana* where a subset of LD were located in the vacuoles 36 to 48h after germination (Miklaszewska et al., 2023; Poxleitner et al., 2006). In addition, autophagy inhibition by concanamycin A negatively impacts seedling growth after germination and leads to a high accumulation of LD in cotyledons, likely due to a lower level of degradation compared to WT seedlings (Miklaszewska et al., 2023).LD accumulation into vacuoles was also observed in other plant tissues including in tapetum cells during pollen development in rice as well as under dark-induced starvation in *A. thaliana* leaves (Fan et al., 2019; Kurusu et al., 2014), suggesting that microlipophagy could

be an important process involved in plant development and stress response. Microlipophagy in plants involves core components of the autophagy machinery as absence of ATG7 in rice, or ATG2 and ATG5 in *A. thaliana* significantly reduce the accumulation of LD into vacuoles (Fan et al., 2019; Kurusu et al., 2014). In addition, ATG8e and b, key autophagy proteins involved in cargo selection and autophagosome biogenesis, were co-localized with LD in leaves under dark stress and seedlings during germination, respectively (Fan et al., 2019; Miklaszewska et al., 2023). During germination, the seed specific LD coat protein of the caleosin family CLO1 is also a key player in microlipophagy as CLO1 seems to regulate the entry of LDs into the vacuole during germination but the exact mechanism remain to be investigated (Miklaszewska et al., 2023; Poxleitner et al., 2006). CLO1 could regulate LD-vacuole interaction and/or promote membrane fusion. In other plant tissues or stress conditions, mutations of autophagy core components can lead to a reduction of TAG and/or LD degradation. This is the case in tobacco pollen and maize leaves, as well as in *A. thaliana* seedlings under carbon starvation or leaves under dark-induced senescence (Avin-Wittenberg et al., 2015; Fan et al., 2019; McLoughlin et al., 2020; Zhao et al., 2020). However, the involvement of lipophagy in plants is not limited to lipids degradation but seems to play a more central role in lipids metabolism and homeostasis. Indeed, in leaves upon dark-induced senescence, ATG proteins were also shown to be involved in TAG synthesis and the authors propose that autophagy promotes TAG synthesis from membrane lipid turnover in specific tissues or developmental stages, while it is involved in TAG degradation in other tissues, such as pollen or seedlings, or under different stresses (Barros et al., 2021; Fan et al., 2019). A similar view has been proposed in the green alga *Chlamydomonas reinhardtii*, where inhibition of the autophagic flux prevents TAG accumulation and LD formation upon nitrogen or phosphate starvation (Couso et al., 2018).

Studies of lipophagy in microalgae are only emerging, but more and more evidence of a role of this process in LD degradation are reported in the literature. Inclusion of LD in vacuoles were initially observed in the green alga *Auxenochlorella protothecoides*, during heterotrophy to autotrophy transition (Zhao et al., 2014). Similarly, LD are found in the vacuolar lumen of *Parachlorella kessleri* following salt stress (You et al., 2019) and in *Chlamydomonas reinhardtii*, microphagy-like interactions of LD and vacuoles were observed during nitrogen resupply following starvation (Tsai et al., 2018). Like in plants, ATG8 is involved in lipophagy processes in *C. reinhardtii*. Indeed, LDs directly interact with ATG8-labeled structure under nitrogen starvation (Tran et al., 2019) and TAG degradation during nitrogen resupply is delayed in CrATG8 mutants (Kajikawa et al., 2019). While most lipophagy mechanisms in green

microalgae are described as “microphagy-like”, the involvement of ATG8, a protein involved in autophagosomes formation, and the description of autophagosome-like vesicles in both *C. reinhardtii* (Tran et al., 2019) and *Micrasterias denticulata* (Schwarz et al., 2017) suggests that macroautophagy processes can also be involved. The articulation between micro- and macro-autophagy processes remains unclear. Microphagy-like degradation of LD and involvement of ATG8 are also observed in Stramenopiles. In *Nannochloropsis oceanica*, microphagy-like degradation of LD during nitrogen resupply and interactions between NoATG8 and NoLSDP, the major LD protein in *N. oceanica*, have been observed (Zienkiewicz et al., 2020). An ATG8-interacting motif has also been identified in the Stramenopile lipid droplet protein (StLDP), the major protein at the surface of LD in the diatom *P. tricornutum* (Leyland et al., 2020; Yoneda et al., 2016), whose mutants show an overaccumulation of TAG and impaired LD degradation following nitrogen replenishment (Taparia et al., 2022). Similarly, a recent study has highlighted the importance of an acyl-binding protein (ACBP) in LD degradation and showed that impaired LD degradation in the ACBP KO could be linked to autophagy defects as *atg5* expression was repressed in these mutants (Leyland et al., 2024). Yet, the exact role of ACBP remains elusive and the role of lipophagy in LD degradation in *P. tricornutum* remains hypothetical. However, lipophagy has been shown to play a role in lipid degradation in another diatom, *Fistulifera solaris* (Tanaka et al., 2024). Electron microscopy images suggested that in *F. solaris*, LD monolayer could directly fuse with the vacuole membrane, leading to the delivery of their lipid content directly in the vacuole lumen without complete LD internalization (Figure 2B-4), suggesting that a microlipophagy pathway different from what is described in yeast could also exist in algae (Tanaka et al., 2024).

5. Conclusion

The degradation of LD follows similar general pathways in all organisms considered in this review, and some key core components, involved in the initial steps of LD degradation, appear conserved. This is the case for the main TAG lipases, that orchestrate hydrolysis of TAG to DAG (Table 1) and for the general autophagy machinery. However, the following steps show a great diversity, depending on organisms but also tissue/organ within the same organism, and subsequent fate of released fatty acids. CGI-58 is an interesting example in the lipolysis process. Indeed, while the protein is conserved at the sequence level and has been identified in all considered phyla, its localization and function vary (*cf.* section 3). In plants, CGI-58 is localized at the surface at peroxisomes and interacts with PXA1 (Park et al., 2013), likely to regulate FA entry into β-oxidation following TAG degradation (see Figure 1) and the subsequent use of

these FA as hormone precursors of the jasmonate and auxin biosynthetic pathways, particularly in vegetative tissues (Park et al., 2013). By contrast, localization at the surface of LD in mammals allows a wider range of fates of released FA (Yu et al., 2020), and association of CGI-58 with mitochondria in microalgae can serve to balance the fate of FA between degradation and recycling (Shu et al., 2023).

Lipophagy, and in particular microlipophagy, shows an even broader diversity of routes and players (Figure 2 and Table 2), suggesting that it has evolved differently in the considered phyla. However, it is important to note that knowledge regarding lipophagy is only recent and partial, as illustrated by the recent discovery of microlipophagy in human (Schulze et al., 2020). Our vision may thus be biased by research focus that differs between phyla. Indeed, in mammals, defects in LD formation or degradation are associated with many diseases, including metabolic diseases but also central nervous system diseases (for review (Zadoorian et al., 2023)). Metabolic diseases and the associated tissues (adipose tissue and liver) have consequently been a major focus of LD research. In plants, studies have for a long time focused on oleaginous seeds and germination, leaving aside other tissues or processes where LD seem much less prominent but play essential roles. Finally, in microalgae, a lot of research is turned towards the increase or alteration of TAG content for biotechnological applications. It is therefore possible that the differences in lipophagy, and more generally LD degradation pathways relate to the physiology and/or functions of studied LD in the considered tissue/condition of one organism. An interesting example of lipophagy-specific function has been shown in response to ER stress in yeast, where microlipophagy was suggested to contribute to ER quality control promoting cell survival through the removal of damaged proteins from the ER, as well as through the removal of lipid excess observed during lipid imbalance (Garcia et al., 2021; Vevea et al., 2015). Indeed, several cargo proteins, some being polyubiquitinated, are associated to LD under stress and are internalized into vacuole with LD for degradation, demonstrating the role of microlipophagy in proteostasis under ER stress (Garcia et al., 2021; Vevea et al., 2015). Investigating similar mechanisms in other organisms would be very interesting, especially in other unicellular organism as some very interesting common points can be drawn. We have highlighted in part 3 the relationship between cell cycle and LD degradation in unicellular organisms, that relates to their life cycle. Another very interesting feature is the close link between LD biogenesis and degradation that seem to exist within these organisms. Indeed, while in mammals and plants, described functions of LD coat proteins are related to protection against LD degradation (*cf.* part 3), the major LD proteins of two distant stramenopiles, *N. oceanica* and *P. tricornutum*, are involved in LD degradation,

probably through lipophagy (*cf.* part 4, (Taparia et al., 2022; Zienkiewicz et al., 2020)). In yeast, the LDO proteins are both involved in the Seipin complex and in LD degradation through microlipophagy (*cf.* part 4, (Álvarez-Guerra et al., 2024; Diep et al., 2024)). Thus, in these organisms, they need to quickly respond to environmental changes, LD seem to be primed for degradation during their biogenesis. It would be interesting to see if this is the case in some tissues of pluricellular organisms, especially plant leaves as the LD coat protein LDIP also interacts with Seipin and seems to be functionally homologous to LDO45 (Pyc et al., 2021).

Finally, in the present work we have presented lipolysis and lipophagy separately, but the degradation of large LD highlights the integration of both main routes, and its possible conservation. In the green microalga *Auxenochlorella protothecoides,* it has been suggested that large LD are first broken down by lipolysis to reduce their size, which allows their subsequent degradation by lipophagy (Zhao et al., 2014). Observations of LD dynamics following nitrogen replenishment in *Phaeodactylum tricornutum* suggest that a similar mechanism could be at play, as two phases are observed: a first one during which the number of LD increases while their size decreases, and a second where the number and size of LD decrease (Murison et al., 2023a). Finally, the existence of non-essential lipophagy to degrade LD in plant seeds (Miklaszewska et al., 2023; Poxleitner et al., 2006) and adipocytes (Lizaso et al., 2013) suggests that similar cooperation of lipolysis and lipophagy could facilitate the degradation of large LD in these tissues.

Funding:

All authors are supported by the French National Research Agency (GRAL Labex ANR-10-LABEX-04, EUR CBS ANR-17-EURE-0003, PEPR Algadvance A-22-PEBB-0002), CA is supported by a grant from the Ecole Normale Supérieure (ENS) of Paris, SY is supported by the French National Research Agency in the framework of the "Investissements d'avenir" program (ANR-15-IDEX-02). CA and JS are supported by the French National Research Agency (ANR-22-CE44-0036-02 CONTROLD) and MC and JS are supported by IDEX Université Grenoble-Alpes (DefiCO2 Cross-disciplinary Program Grant ANR-15-IDEX-02) and INRAE BAP division (S-PHAEO project).

Declaration of competing interest

The authors declare that they have no conflict of interest.

Bibliography

Ali, S., Liu, X., Sen, L., Lan, D., Wang, J., Hassan, Md.I., Wang, Y., 2021. Sequence and structure-based method to predict diacylglycerol lipases in protein sequence. International Journal of Biological Macromolecules 182, 455–463. https://doi.org/10.1016/j.ijbiomac.2021.04.011

Athenstaedt, K., Daum, G., 2005. Tgl4p and Tgl5p, Two Triacylglycerol Lipases of the Yeast Saccharomyces cerevisiae Are Localized to Lipid Particles. The Journal of Biological Chemistry 280, 37301–37309.

Athenstaedt, K., Daum, G., 2003. YMR313c/TGL3 Encodes a Novel Triacylglycerol Lipase Located in Lipid Particles of Saccharomyces cerevisiae. The Journal of Biological Chemistry 278, 23317–23323.

Barka, F., Angstenberger, M., Ahrendt, T., Lorenzen, W., Bode, H.B., Büchel, C., 2016. Identification of a triacylglycerol lipase in the diatom Phaeodactylum tricornutum. Biochimica et Biophysica Acta (BBA) - Molecular and Cell Biology of Lipids 1861, 239–248. https://doi.org/10.1016/j.bbalip.2015.12.023

Beisson, F., Ferté, N., Bruley, S., Voultoury, R., Verger, R., Arondel, V., 2001. Oil-bodies as substrates for lipolytic enzymes. Biochimica et Biophysica Acta (BBA) - Molecular and Cell Biology of Lipids 1531, 47–58. https://doi.org/10.1016/S1388-1981(01)00086-5

Bezaire, V., Mairal, A., Ribet, C., Lefort, C., Girousse, A., Jocken, J., Laurencikiene, J., Anesia, R., Rodriguez, A.-M., Ryden, M., Stenson, B.M., Dani, C., Ailhaud, G., Arner, P., Langin, D., 2009. Contribution of Adipose Triglyceride Lipase and Hormone-sensitive Lipase to Lipolysis in hMADS Adipocytes. J Biol Chem 284, 18282–18291. https://doi.org/10.1074/jbc.M109.008631

Brasaemle, D.L., Rubin, B., Harten, I.A., Gruia-Gray, J., Kimmel, A.R., Londos, C., 2000. Perilipin A Increases Triacylglycerol Storage by Decreasing the Rate of Triacylglycerol Hydrolysis*. Journal of Biological Chemistry 275, 38486–38493. https://doi.org/10.1074/jbc.M007322200

Chauton, M.S., Winge, P., Brembu, T., Vadstein, O., Bones, A.M., 2013. Gene Regulation of Carbon Fixation, Storage, and Utilization in the Diatom Phaeodactylum tricornutum Acclimated to Light/Dark Cycles1[C][W][OA]. Plant Physiol 161, 1034–1048. https://doi.org/10.1104/pp.112.206177

Cui, S., Hayashi, Y., Otomo, M., Mano, S., Oikawa, K., Hayashi, M., Nishimura, M., 2016. Sucrose Production Mediated by Lipid Metabolism Suppresses the Physical Interaction of Peroxisomes and Oil Bodies during Germination of Arabidopsis thaliana*. Journal of Biological Chemistry 291, 19734–19745. https://doi.org/10.1074/jbc.M116.748814

Deruyffelaere, C., Bouchez, I., Morin, H., Guillot, A., Miquel, M., Froissard, M., Chardot, T., D'Andrea, S., 2015. Ubiquitin-Mediated Proteasomal Degradation of Oleosins is Involved in Oil Body Mobilization During Post-Germinative Seedling Growth in Arabidopsis. Plant Cell Physiol 56, 1374–1387. https://doi.org/10.1093/pcp/pcv056

Deruyffelaere, C., Purkrtova, Z., Bouchez, I., Collet, B., Cacas, J.-L., Chardot, T., Gallois, J.-L., D'Andrea, S., 2018. PUX10 Is a CDC48A Adaptor Protein That Regulates the Extraction of Ubiquitinated Oleosins from Seed Lipid Droplets in Arabidopsis. Plant Cell 30, 2116–2136. https://doi.org/10.1105/tpc.18.00275

Dong, X.C., 2019. PNPLA3—A Potential Therapeutic Target for Personalized Treatment of Chronic Liver Disease. Front. Med. 6. https://doi.org/10.3389/fmed.2019.00304

Eastmond, P.J., 2006. *SUGAR-DEPENDENT1* Encodes a Patatin Domain Triacylglycerol Lipase That Initiates Storage Oil Breakdown in Germinating *Arabidopsis* Seeds. The Plant Cell 18, 665–675. https://doi.org/10.1105/tpc.105.040543

Feussner, I., Kühn, H., Wasternack, C., 2001. Lipoxygenase-dependent degradation of storage lipids. Trends in Plant Science 6, 268–273. https://doi.org/10.1016/S1360-1385(01)01950-1

Fischer, J., Lefèvre, C., Morava, E., Mussini, J.-M., Laforêt, P., Negre-Salvayre, A., Lathrop, M., Salvayre, R., 2007. The gene encoding adipose triglyceride lipase (PNPLA2) is mutated in neutral lipid storage disease with myopathy. Nat Genet 39, 28–30. https://doi.org/10.1038/ng1951

Fredrikson, G., Tornqvist, H., Belfrage, P., 1986. Hormone-sensitive lipase and monoacylglycerol lipase are both required for complete degradation of adipocyte triacylglycerol. Biochimica et Biophysica Acta (BBA) - Lipids and Lipid Metabolism 876, 288–293. https://doi.org/10.1016/0005-2760(86)90286-9

Fujimoto, T., Parton, R.G., 2011. Not Just Fat: The Structure and Function of the Lipid Droplet. Cold Spring Harb Perspect Biol 3, a004838. https://doi.org/10.1101/cshperspect.a004838

Gambo, Y., Matsumura, M., Fujimori, K., 2016. Triiodothyronine enhances accumulation of intracellular lipids in adipocytes through thyroid hormone receptor α via direct and indirect mechanisms. Molecular and Cellular Endocrinology 431, 1–11. https://doi.org/10.1016/j.mce.2016.04.023

Ghosh, A.K., Ramakrishnan, G., Chandramohan, C., Rajasekharan, R., 2008. CGI-58, the causative gene for Chanarin-Dorfman syndrome, mediates acylation of lysophosphatidic acid. The Journal of biological chemistry 283, 24525–33. https://doi.org/10.1074/jbc.M801783200

Ghosh, S., St. Clair, R.W., Rudel, L.L., 2003. Mobilization of cytoplasmic CE droplets by overexpression of human macrophage cholesteryl ester hydrolase. Journal of Lipid Research 44, 1833–1840. https://doi.org/10.1194/jlr.M300162-JLR200

Gidda, S.K., Park, S., Pyc, M., Yurchenko, O., Cai, Y., Wu, P., Andrews, D.W., Chapman, K.D., Dyer, J.M., Mullen, R.T., 2016. Lipid Droplet-Associated Proteins (LDAPs) Are Required for the Dynamic Regulation of Neutral Lipid Compartmentation in Plant Cells. Plant physiology 170, 2052–71. https://doi.org/10.1104/pp.15.01977

Gidda, S.K., Watt, S.C., Collins-Silva, J., Kilaru, A., Arondel, V., Yurchenko, O., Horn, P.J., James, C.N., Shintani, D., Ohlrogge, J.B., Chapman, K.D., Mullen, R.T., Dyer, J.M., 2013. Lipid droplet-associated proteins (LDAPs) are involved in the compartmentalization of lipophilic compounds in plant cells. Plant Signaling & Behavior 8, e27141. https://doi.org/10.4161/psb.27141

Grabner, G.F., Xie, H., Schweiger, M., Zechner, R., 2021. Lipolysis: cellular mechanisms for lipid mobilization from fat stores. Nat Metab 3, 1445–1465. https://doi.org/10.1038/s42255-021-00493-6

Graham, I.A., 2008. Seed Storage Oil Mobilization. Annual Review of Plant Biology 59, 115–142. https://doi.org/10.1146/annurev.arplant.59.032607.092938

Granneman, J.G., Moore, H.-P.H., Mottillo, E.P., Zhu, Z., Zhou, L., 2011. Interactions of Perilipin-5 (Plin5) with Adipose Triglyceride Lipase*. Journal of Biological Chemistry 286, 5126–5135. https://doi.org/10.1074/jbc.M110.180711

Greer, M.S., Cai, Y., Gidda, S.K., Esnay, N., Kretzschmar, F.K., Seay, D., McClinchie, E., Ischebeck, T., Mullen, R.T., Dyer, J.M., Chapman, K.D., 2020. SEIPIN Isoforms Interact with the Membrane-Tethering Protein VAP27-1 for Lipid Droplet Formation. Plant Cell 32, 2932–2950. https://doi.org/10.1105/tpc.19.00771

Griseti, E., Bello, A.A., Bieth, E., Sabbagh, B., Iacovoni, J.S., Bigay, J., Laurell, H., Čopič, A., 2024. Molecular mechanisms of perilipin protein function in lipid droplet metabolism. FEBS Letters 598, 1170–1198. https://doi.org/10.1002/1873-3468.14792

Guzha, A., Whitehead, P., Ischebeck, T., Chapman, K.D., 2023. Lipid Droplets: Packing Hydrophobic Molecules Within the Aqueous Cytoplasm. Annual Review of Plant Biology 74, 195–223. https://doi.org/10.1146/annurev-arplant-070122- 021752

Haemmerle, G., Lass, A., Zimmermann, R., Gorkiewicz, G., Meyer, C., Rozman, J., Heldmaier, G., Maier, R., Theussl, C., Eder, S., Kratky, D., Wagner, E.F., Klingenspor, M., Hoefler, G., Zechner, R., 2006. Defective Lipolysis and Altered Energy Metabolism in Mice Lacking Adipose Triglyceride Lipase. Science 312, 734–737. https://doi.org/10.1126/science.1123965

Haemmerle, G., Zimmermann, R., Hayn, M., Theussl, C., Waeg, G., Wagner, E., Sattler, W., Magin, T.M., Wagner, E.F., Zechner, R., 2002. Hormone-sensitive Lipase Deficiency in Mice Causes Diglyceride Accumulation in Adipose Tissue, Muscle, and Testis. The Journal of Biological Chemistry 277, 4806–4815. https://doi.org/10.1074/jbc.M110355200

He, S., McPhaul, C., Li, J.Z., Garuti, R., Kinch, L., Grishin, N.V., Cohen, J.C., Hobbs, H.H., 2010. A Sequence Variation (I148M) in PNPLA3 Associated with Nonalcoholic Fatty Liver Disease Disrupts Triglyceride Hydrolysis*. Journal of Biological Chemistry 285, 6706–6715. https://doi.org/10.1074/jbc.M109.064501

Heier, C., Taschler, U., Rengachari, S., Oberer, M., Wolinski, H., Natter, K., Kohlwein, S.D., Leber, R., Zimmermann, R., 2010. Identification of Yju3p as functional orthologue of mammalian monoglyceride lipase in the yeast Saccharomycescerevisiae. Biochim Biophys Acta 1801, 1063–1071. https://doi.org/10.1016/j.bbalip.2010.06.001

Huang, A.H.C., 1992. Oil Bodies and Oleosins in Seeds. Annual Review of Plant Physiology and Plant Molecular Biology 43, 177–200. https://doi.org/10.1146/annurev.pp.43.060192.001141

Huang, S., Liu, Z., Cao, W., Li, H., Zhang, W., Cui, Y., Hu, S., Luo, M., Zhu, Y., Zhao, Q., Xie, L., Gao, C., Xiao, S., Jiang, L., 2022. The plant ESCRT component FREE1 regulates peroxisome-mediated turnover of lipid droplets in germinating Arabidopsis seedlings. The Plant Cell koac195. https://doi.org/10.1093/plcell/koac195

Huysman, M.J., Tanaka, A., Bowler, C., Vyverman, W., De Veylder, L., 2015. Functional characterization of the diatom cyclin-dependent kinase A2 as a mitotic regulator reveals plant-like properties in a non-green lineage. BMC Plant Biology 15, 86. https://doi.org/10.1186/s12870-015-0469-6

Huysman, M.J.J., Fortunato, A.E., Matthijs, M., Costa, B.S., Vanderhaeghen, R., Van den Daele, H., Sachse, M., Inzé, D., Bowler, C., Kroth, P.G., Wilhelm, C., Falciatore, A., Vyverman, W., De Veylder, L., 2013. AUREOCHROME1a-Mediated Induction of the Diatom-Specific Cyclin dsCYC2 Controls the Onset of Cell Division in Diatoms (Phaeodactylum tricornutum). The Plant Cell 25, 215–228. https://doi.org/10.1105/tpc.112.106377

Jacquier, N., Mishra, S., Choudhary, V., Schneiter, R., 2013. Expression of oleosin and perilipins in yeast promotes formation of lipid droplets from the endoplasmic reticulum. Journal of Cell Science 126, 5198–5209. https://doi.org/10.1242/jcs.131896

James, C.N., Horn, P.J., Case, C.R., Gidda, S.K., Zhang, D., Mullen, R.T., Dyer, J.M., Anderson, R.G., Chapman, K.D., 2010. Disruption of the Arabidopsis CGI-58 homologue produces Chanarin-Dorfman-like lipid droplet accumulation in plants. Proceedings of the National Academy of Sciences of the United States of America 107, 17833–8. https://doi.org/10.1073/pnas.0911359107

Jolivet, P., Roux, E., D'Andrea, S., Davanture, M., Negroni, L., Zivy, M., Chardot, T., 2004. Protein composition of oil bodies in Arabidopsis thaliana ecotype WS. Plant physiology and biochemistry : PPB 42, 501–9. https://doi.org/10.1016/j.plaphy.2004.04.006

Keenan, S.N., De Nardo, W., Lou, J., Schittenhelm, R.B., Montgomery, M.K., Granneman, J.G., Hinde, E., Watt, M.J., 2021. Perilipin 5 S155 phosphorylation by PKA is required for the control of hepatic lipid metabolism and glycemic control. Journal of Lipid Research 62, 100016. https://doi.org/10.1194/jlr.RA120001126

Kelly, A.A., Quettier, A.-L., Shaw, E., Eastmond, P.J., 2011. Seed Storage Oil Mobilization Is Important But Not Essential for Germination or Seedling Establishment in Arabidopsis. Plant Physiology 157, 866–875. https://doi.org/10.1104/pp.111.181784

Kelly, A.A., van Erp, H., Quettier, A.-L., Shaw, E., Menard, G., Kurup, S., Eastmond, P.J., 2013. The SUGAR-DEPENDENT1 Lipase Limits Triacylglycerol Accumulation in Vegetative Tissues of Arabidopsis1[W]. Plant Physiol 162, 1282–1289. https://doi.org/10.1104/pp.113.219840

Kim, E.Y., Seo, Y.S., Kim, W.T., 2011. AtDSEL, an *Arabidopsis* cytosolic DAD1-like acylhydrolase, is involved in negative regulation of storage oil mobilization during seedling establishment. Journal of Plant Physiology 168, 1705–1709. https://doi.org/10.1016/j.jplph.2011.03.004

Kim, R.J., Kim, H.J., Shim, D., Suh, M.C., 2016. Molecular and biochemical characterizations of the monoacylglycerol lipase gene family of Arabidopsis thaliana. The Plant Journal 85, 758–771. https://doi.org/10.1111/tpj.13146

Kimmel, A.R., Sztalryd, C., 2016. The Perilipins: Major Cytosolic Lipid Droplet–Associated Proteins and Their Roles in Cellular Lipid Storage, Mobilization, and Systemic Homeostasis*. Annual Review of Nutrition 36, 471–509. https://doi.org/10.1146/annurev-nutr-071813-105410

Klug, Y.A., Ferreira, J.V., Carvalho, P., 2024. A unifying mechanism for seipin-mediated lipid droplet formation. FEBS Letters 598, 1116–1126. https://doi.org/10.1002/1873-3468.14825

Köffel, R., Schneiter, R., 2006. Yeh1 Constitutes the Major Steryl Ester Hydrolase under Heme-Deficient Conditions in Saccharomyces cerevisiae. Eukaryotic Cell 5, 1018–1025. https://doi.org/10.1128/ec.00002-06

Köffel, R., Tiwari, R., Falquet, L., Schneiter, R., 2005. The Saccharomyces cerevisiae YLL012/YEH1, YLR020/YEH2, and TGL1 Genes Encode a Novel Family of Membrane-Anchored Lipases That Are Required for Steryl Ester Hydrolysis. Molecular and Cellular Biology 25, 1655. https://doi.org/10.1128/MCB.25.5.1655-1668.2005

Kretzschmar, F.K., Doner, N.M., Krawczyk, H.E., Scholz, P., Schmitt, K., Valerius, O., Braus, G.H., Mullen, R.T., Ischebeck, T., 2020. Identification of Low-Abundance Lipid Droplet Proteins in Seeds and Seedlings. Plant physiology 182, 1326–1345. https://doi.org/10.1104/pp.19.01255

Kretzschmar, F.K., Mengel, L.A., Müller, A.O., Schmitt, K., Blersch, K.F., Valerius, O., Braus, G.H., Ischebeck, T., 2018. PUX10 Is a Lipid Droplet-Localized Scaffold Protein That Interacts with CELL DIVISION CYCLE48 and Is Involved in the Degradation of Lipid Droplet Proteins. Plant Cell 30, 2137–2160. https://doi.org/10.1105/tpc.18.00276

Kurat, C.F., Wolinski, H., Petschnigg, J., Kaluarachchi, S., Andrews, B., Natter, K., Kohlwein, S.D., 2009. Cdk1/Cdc28-Dependent Activation of the Major Triacylglycerol Lipase Tgl4 in Yeast Links Lipolysis to Cell-Cycle Progression. Molecular Cell 33, 53–63. https://doi.org/10.1016/j.molcel.2008.12.019

Lass, A., Zimmermann, R., Haemmerle, G., Riederer, M., Schoiswohl, G., Schweiger, M., Kienesberger, P., Strauss, J.G., Gorkiewicz, G., Zechner, R., 2006. Adipose triglyceride lipase-mediated lipolysis of cellular fat stores is activated by CGI-58 and

defective in Chanarin-Dorfman Syndrome. Cell metabolism 3, 309–19. https://doi.org/10.1016/j.cmet.2006.03.005

Le Moigne, D., Guéguen, N., Salvaing, J., 2022. Lipid droplets in plants: More than a simple fat storage, in: Lipids in Plants and Algae: From Fundamental Science to Industrial Applications, Advances in Botanical Research. Academic Press, pp. 191–223. https://doi.org/10.1016/bs.abr.2021.07.004

Li, X., Benning, C., Kuo, M.-H., 2012. Rapid Triacylglycerol Turnover in Chlamydomonas reinhardtii Requires a Lipase with Broad Substrate Specificity. Eukaryot Cell 11, 1451–1462. https://doi.org/10.1128/EC.00268-12

Li-Beisson, Y., Kong, F., Wang, P., Lee, Y., Kang, B.-H., 2021. The disassembly of lipid droplets in Chlamydomonas. New Phytologist 231, 1359–1364. https://doi.org/10.1111/nph.17505

Londos, C., Brasaemle, D.L., Schultz, C.J., Segrest, J.P., Kimmel, A.R., 1999. Perilipins, ADRP, and other proteins that associate with intracellular neutral lipid droplets in animal cells. Seminars in Cell & Developmental Biology 10, 51–58. https://doi.org/10.1006/scdb.1998.0275

Lundquist, P.K., Shivaiah, K.-K., Espinoza-Corral, R., 2020. Lipid droplets throughout the evolutionary tree. Progress in Lipid Research 78, 101029. https://doi.org/10.1016/j.plipres.2020.101029

Lupette, J., Maréchal, E., 2020. The Puzzling Conservation and Diversification of Lipid Droplets from Bacteria to Eukaryotes, in: Kloc, M. (Ed.), Symbiosis: Cellular, Molecular, Medical and Evolutionary Aspects, Results and Problems in Cell Differentiation. Springer International Publishing, Cham, pp. 281–334. https://doi.org/10.1007/978-3-030-51849-3_11

Maeda, Y., Watanabe, K., Kaha, M., Yabu, Y., Yoshino, T., Matsumoto, M., Tanaka, T., 2021. Assessment on the oil accumulation by knockdown of triacylglycerol lipase in the oleaginous diatom Fistulifera solaris. Sci Rep 11, 20905. https://doi.org/10.1038/s41598-021-00453-w

Mathiowetz, A.J., Olzmann, J.A., 2024. Lipid droplets and cellular lipid flux. Nat Cell Biol 26, 331–345. https://doi.org/10.1038/s41556-024-01364-4

McHenry, S., Davidson, N.O., 2019. Missense mutant PNPLA3 alters lipid droplet turnover in partnership with CGI-58. Hepatology 69, 2323–2325. https://doi.org/10.1002/hep.30620

Müller, A.O., Ischebeck, T., 2018. Characterization of the enzymatic activity and physiological function of the lipid droplet-associated triacylglycerol lipase AtOBL1. New Phytologist 217, 1062–1076. https://doi.org/10.1111/nph.14902

Müllner, H., Deutsch, G., Leitner, E., Ingolic, E., Daum, G., 2005. *YEH2/YLR020c* Encodes a Novel Steryl Ester Hydrolase of the Yeast *Saccharomyces cerevisiae**. Journal of Biological Chemistry 280, 13321–13328. https://doi.org/10.1074/jbc.M409914200

Murison, V., Hérault, J., Schoefs, B., Marchand, J., Ulmann, L., 2023b. Marine Drugs | Free Full-Text | Bioinformatics-Based Screening Approach for the Identification and Characterization of Lipolytic Enzymes from the Marine Diatom Phaeodactylum tricornutum. Marine Drugs 125.

Murison V, Hérault J, Côme M, Guinio S, Lebon A, Chamot C, Bénard M, Galas L, Schoefs B, Marchand J, Bardor M and Ulmann L, 2023a. Comparison of two Phaeodactylum tricornutum ecotypes under nitrogen starvation and resupply reveals distinct lipid accumulation strategies but a common degradation process. Front. Plant Sci. 14:1257500. doi: 10.3389/fpls.2023.1257500

Murphy, D.J., 2012. The dynamic roles of intracellular lipid droplets: from archaea to mammals. Protoplasma 249, 541–585. https://doi.org/10.1007/s00709-011-0329-7

Nobusawa, T., Yamakawa-Ayukawa, K., Saito, F., Nomura, S., Takami, A., Ohta, H., 2019. A homolog of Arabidopsis SDP1 lipase in Nannochloropsis is involved in degradation of de novo-synthesized triacylglycerols in the endoplasmic reticulum. Biochimica et Biophysica Acta (BBA) - Molecular and Cell Biology of Lipids 1864, 1185–1193. https://doi.org/10.1016/j.bbalip.2019.05.013

O'Hara, L., Han, G.-S., Sew, P.-C., Grimsey, N., Carman, G.M., Siniossoglou, S., 2006. Control of phospholipid synthesis by phosphorylation of the yeast lipin Pah1p/Smp2p Mg2+-dependent phosphatidate phosphatase. Journal of Biological Chemistry 281, 34537–34548. https://doi.org/10.1074/jbc.M606654200

Olzmann, J.A., Carvalho, P., 2019. Dynamics and functions of lipid droplets. Nature reviews. Molecular cell biology 20, 137–155. https://doi.org/10.1038/s41580-018-0085-z

Park, S., Gidda, S.K., James, C.N., Horn, P.J., Khuu, N., Seay, D.C., Keereetaweep, J., Chapman, K.D., Mullen, R.T., Dyer, J.M., 2013. The α/β Hydrolase CGI-58 and Peroxisomal Transport Protein PXA1 Coregulate Lipid Homeostasis and Signaling in Arabidopsis[W]. Plant Cell 25, 1726–1739. https://doi.org/10.1105/tpc.113.111898

Pollak, N.M., Jaeger, D., Kolleritsch, S., Zimmermann, R., Zechner, R., Lass, A., Haemmerle, G., 2015. The Interplay of Protein Kinase A and Perilipin 5 Regulates Cardiac Lipolysis. J. Biol. Chem. 290, 1295–1306. https://doi.org/10.1074/jbc.M114.604744

Pyc, M., Cai, Y., Gidda, S.K., Yurchenko, O., Park, S., Kretzschmar, F.K., Ischebeck, T., Valerius, O., Braus, G.H., Chapman, K.D., Dyer, J.M., Mullen, R.T., 2017. Arabidopsis lipid droplet-associated protein (LDAP) - interacting protein (LDIP) influences lipid droplet size and neutral lipid homeostasis in both leaves and seeds. The Plant journal : for cell and molecular biology 92, 1182–1201. https://doi.org/10.1111/tpj.13754

Rajakumari, S., Daum, G., 2010. Janus-faced Enzymes Yeast Tgl3p and Tgl5p Catalyze Lipase and Acyltransferase Reactions. Mol Biol Cell 21, 501–510. https://doi.org/10.1091/mbc.E09-09-0775

Rajakumari, S., Rajasekharan, R., Daum, G., 2010. Triacylglycerol lipolysis is linked to sphingolipid and phospholipid metabolism of the yeast *Saccharomyces cerevisiae*. Biochimica et Biophysica Acta (BBA) - Molecular and Cell Biology of Lipids 1801, 1314–1322. https://doi.org/10.1016/j.bbalip.2010.08.004

Recazens, E., Mouisel, E., Langin, D., 2021. Hormone-sensitive lipase: sixty years later - ScienceDirect. Progress in Lipid Research 82. https://doi.org/10.1016/j.plipres.2020.101084

Roy, D., Farabaugh, K.T., Wu, J., Charrier, A., Smas, C., Hatzoglou, M., Thirumurugan, K., Buchner, D.A., 2017. Coordinated transcriptional control of adipocyte triglyceride lipase (*Atgl*) by transcription factors Sp1 and peroxisome proliferator–activated receptor γ (PPARγ) during adipocyte differentiation. Journal of Biological Chemistry 292, 14827–14835. https://doi.org/10.1074/jbc.M117.783043

Santos-Rosa, H., Leung, J., Grimsey, N., Peak-Chew, S., Siniossoglou, S., 2005. The yeast lipin Smp2 couples phospholipid biosynthesis to nuclear membrane growth. The EMBO Journal 24, 1931–1941. https://doi.org/10.1038/sj.emboj.7600672

Scherer, G.F.E., Ryu, S.B., Wang, X., Matos, A.R., Heitz, T., 2010. Patatin-related phospholipase A: nomenclature, subfamilies and functions in plants. Trends in Plant Science 15, 693–700. https://doi.org/10.1016/j.tplants.2010.09.005

Schweiger, M., Schreiber, R., Haemmerle, G., Lass, A., Fledelius, C., Jacobsen, P., Tornqvist, H., Zechner, R., Zimmermann, R., 2006. Adipose Triglyceride Lipase and Hormone-sensitive Lipase Are the Major Enzymes in Adipose Tissue Triacylglycerol Catabolism*. Journal of Biological Chemistry 281, 40236–40241. https://doi.org/10.1074/jbc.M608048200

Sharma, B., Joshi, D., Yadav, P.K., Gupta, A.K., Bhatt, T.K., 2016. Role of Ubiquitin-Mediated Degradation System in Plant Biology. Front. Plant Sci. 7. https://doi.org/10.3389/fpls.2016.00806

Shu, Q., Pan, Y., Hu, H., 2023. CGI-58 Protein Acts as a Positive Regulator of Triacylglycerol Accumulation in Phaeodactylum tricornutum. J Microbiol Biotechnol 33, 242–250. https://doi.org/10.4014/jmb.2209.09029

Siegler, H., Valerius, O., Ischebeck, T., Popko, J., Tourasse, N.J., Vallon, O., Khozin-Goldberg, I., Braus, G.H., Feussner, I., 2017. Analysis of the lipid body proteome of the oleaginous alga Lobosphaera incisa. BMC Plant Biol 17, 98. https://doi.org/10.1186/s12870-017-1042-2

Speer, N.O., Braun, R.J., Reynolds, E.G., Brudnicka, A., Swanson, J.M.J., Henne, W.M., 2023. Tld1 is a regulator of triglyceride lipolysis that demarcates a lipid droplet subpopulation. J Cell Biol 223, e202303026. https://doi.org/10.1083/jcb.202303026

Tauchi-Sato, K., Ozeki, S., Houjou, T., Taguchi, R., Fujimoto, T., 2002. The Surface of Lipid Droplets Is a Phospholipid Monolayer with a Unique Fatty Acid Composition. Journal of Biological Chemistry 277, 44507–44512. https://doi.org/10.1074/jbc.M207712200

Thazar-Poulot, N., Miquel, M., Fobis-Loisy, I., Gaude, T., 2015. Peroxisome extensions deliver the Arabidopsis SDP1 lipase to oil bodies. Proceedings of the National Academy of Sciences 112, 4158–4163. https://doi.org/10.1073/pnas.1403322112

Thiam, A.R., Ikonen, E., 2021. Lipid Droplet Nucleation. Trends in Cell Biology 31, 108–118. https://doi.org/10.1016/j.tcb.2020.11.006

Tornqvist, H., Belfrage, P., 1976. PURIFICATION AND SOME PROPERTIES OF A MONOACYLGLYCEROL-HYDROLYZING ENZYME OF RAT ADIPOSE-TISSUE. JOURNAL OF BIOLOGICAL CHEMISTRY 251, 813–819.

Traver, M.S., Bartel, B., 2023. The ubiquitin-protein ligase MIEL1 localizes to peroxisomes to promote seedling oleosin degradation and lipid droplet mobilization. Proc. Natl. Acad. Sci. U.S.A. 120, e2304870120. https://doi.org/10.1073/pnas.2304870120

Trentacoste, E.M., Shrestha, R.P., Smith, S.R., Glé, C., Hartmann, A.C., Hildebrand, M., Gerwick, W.H., 2013. Metabolic engineering of lipid catabolism increases microalgal lipid accumulation without compromising growth. Proceedings of the National Academy of Sciences 110, 19748–19753. https://doi.org/10.1073/pnas.1309299110

Tsai, C.H., Warakanont, J., Takeuchi, T., Sears, B.B., Moellering, E.R., Benning, C., 2014. The protein Compromised Hydrolysis of Triacylglycerols 7 (CHT7) acts as a repressor of cellular quiescence in Chlamydomonas. Proceedings of the National Academy of Sciences of the United States of America 111, 15833–8. https://doi.org/10.1073/pnas.1414567111

Vaughan, M., Berger, J., Steinberg, D., 1964. HORMONE-SENSITIVE LIPASE + MONOGLYCERIDE LIPASE ACTIVITIES IN ADIPOSE TISSUE. JOURNAL OF BIOLOGICAL CHEMISTRY 239, 401-+.

Viswanath, K.K., Varakumar, P., Pamuru, R.R., Basha, S.J., Mehta, S., Rao, A.D., 2020. Plant Lipoxygenases and Their Role in Plant Physiology. J. Plant Biol. 63, 83–95. https://doi.org/10.1007/s12374-020-09241-x

Wagner, A., Grillitsch, K., Leitner, E., Daum, G., 2009. Mobilization of steryl esters from lipid particles of the yeast *Saccharomyces cerevisiae*. Biochimica et Biophysica Acta (BBA) - Molecular and Cell Biology of Lipids 1791, 118–124. https://doi.org/10.1016/j.bbalip.2008.11.004

Walther, T.C., Chung, J., Farese, R.V., 2017. Lipid Droplet Biogenesis. Annual Review of Cell and Developmental Biology 33, 491–510. https://doi.org/10.1146/annurev-cellbio-100616060608

Wang, C.-W., 2015. Lipid droplet dynamics in budding yeast. Cell Mol Life Sci 72, 2677–2695. https://doi.org/10.1007/s00018-015-1903-5

Warakanont, J., Li-Beisson, Y., Benning, C., 2019. LIP4 Is Involved in Triacylglycerol Degradation in Chlamydomonas reinhardtii. Plant and Cell Physiology 60, 1250–1259. https://doi.org/10.1093/pcp/pcz037

Wilson, P.A., Gardner, S.D., Lambie, N.M., Commans, S.A., Crowther, D.J., 2006. Characterization of the human patatin-like phospholipase family. Journal of Lipid Research 47, 1940–1949. https://doi.org/10.1194/jlr.M600185-JLR200

Winichayakul, S., Scott, R.W., Roldan, M., Hatier, J.-H.B., Livingston, S., Cookson, R., Curran, A.C., Roberts, N.J., 2013. In Vivo Packaging of Triacylglycerols Enhances Arabidopsis Leaf Biomass and Energy Density. Plant Physiology 162, 626–639. https://doi.org/10.1104/pp.113.216820

Yogosawa, S., Mizutani, S., Ogawa, Y., Izumi, T., 2013. Activin Receptor-Like Kinase 7 Suppresses Lipolysis to Accumulate Fat in Obesity Through Downregulation of Peroxisome Proliferator–Activated Receptor g and C/EBPa. Diabetes 62, 115–123.

Yu, L., Li, Y., Grisé, A., Wang, H., 2020. CGI-58: Versatile Regulator of Intracellular Lipid Droplet Homeostasis, in: Jiang, X.-C. (Ed.), Lipid Transfer in Lipoprotein Metabolism and Cardiovascular Disease. Springer, Singapore, pp. 197–222. https://doi.org/10.1007/978-981-15-6082-8_13

Yu, L., Shen, W., Fan, J., Sah, S.K., Mavraganis, I., Wang, L., Gao, P., Gao, J., Zheng, Q., Meesapyodsuk, D., Yang, H., Li, Q., Zou, J., Xu, C., 2023. A chloroplast diacylglycerol lipase modulates glycerolipid pathway balance in Arabidopsis. The Plant Journal 115, 335–350. https://doi.org/10.1111/tpj.16228

Zhang, T., Huang, J., Zhang, Z., Lv, J., Zhang, D., Qing, R., Lan, L., 2022. Flow cytometry and 5-ethynyl-2′-deoxyuridine (EdU) labeling to detect the cell cycle dynamics of Phaeodactylum tricornutum under light. Journal of Phycology 58, 555–567. https://doi.org/10.1111/jpy.13250

Zhao, B., Fisher, B.J., Clair, R.W.St., Rudel, L.L., Ghosh, S., 2005. Redistribution of macrophage cholesteryl ester hydrolase from cytoplasm to lipid droplets upon lipid loading1. Journal of Lipid Research 46, 2114–2121. https://doi.org/10.1194/jlr.M500207-JLR200

Zimmermann, R., Strauss, J.G., Haemmerle, G., Schoiswohl, G., Birner-Gruenberger, R., Riederer, M., Lass, A., Neuberger, G., Eisenhaber, F., Hermetter, A., Zechner, R., 2004. Fat Mobilization in Adipose Tissue Is Promoted by Adipose Triglyceride Lipase. Science 306, 1383–1386. https://doi.org/10.1126/science.1100747

References

Abel, S., Ticconi, C. A., & Delatorre, C. A. (2002). Phosphate sensing in higher plants. *Physiologia Plantarum*, *115*(1), 1–8. https://doi.org/10.1034/j.1399-3054.2002.1150101.x

Adeyo, O., Horn, P. J., Lee, S., Binns, D. D., Chandrahas, A., Chapman, K. D., & Goodman, J. M. (2011). The yeast lipin orthologue Pah1p is important for biogenesis of lipid droplets. *Journal of Cell Biology*, *192*(6), 1043–1055. https://doi.org/10.1083/jcb.201010111

Adham, A. R., Zolman, B. K., Millius, A., & Bartel, B. (2005). Mutations in Arabidopsis acyl-CoA oxidase genes reveal distinct and overlapping roles in beta-oxidation. *The Plant Journal: For Cell and Molecular Biology*, *41*(6), 859–874. https://doi.org/10.1111/j.1365-313X.2005.02343.x

Agrimi, G., Russo, A., Pierri, C. L., & Palmieri, F. (2012). The peroxisomal NAD+ carrier of Arabidopsis thaliana transports coenzyme A and its derivatives. *Journal of Bioenergetics and Biomembranes*, *44*(3), 333–340. https://doi.org/10.1007/s10863-012-9445-0

Ahmed, S., Shah, P., & Ahmed, O. (2024). Biochemistry, Lipids. In *StatPearls*. StatPearls Publishing. http://www.ncbi.nlm.nih.gov/books/NBK525952/

Aktas, M., Danne, L., Möller, P., & Narberhaus, F. (2014). Membrane lipids in Agrobacterium tumefaciens: Biosynthetic pathways and importance for pathogenesis. *Frontiers in Plant Science*, *5*, 109. https://doi.org/10.3389/fpls.2014.00109

Akter, S., Shahneawz Khan, M., N. Smith, E., & Flashman, E. (2021). Measuring ROS and redox markers in plant cells. *RSC Chemical Biology*, *2*(5), 1384–1401. https://doi.org/10.1039/D1CB00071C

Ali, U., Lu, S., Fadlalla, T., Iqbal, S., Yue, H., Yang, B., Hong, Y., Wang, X., & Guo, L. (2022). The functions of phospholipases and their hydrolysis products in plant growth, development and stress responses. *Progress in Lipid Research*, *86*, 101158. https://doi.org/10.1016/j.plipres.2022.101158

Andersson, M. X., & Dörmann, P. (n.d.). *Chloroplast Membrane Lipid Biosynthesis and Transport* (pp. 1–34). Springer. https://doi.org/10.1007/7089_2008_18

Andersson, M. X., Goksör, M., & Sandelius, A. S. (2007). Optical manipulation reveals strong attracting forces at membrane contact sites between endoplasmic reticulum and chloroplasts. *The Journal of Biological Chemistry*, *282*(2), 1170–1174. https://doi.org/10.1074/jbc.M608124200

Andersson, M. X., Larsson, K. E., Tjellström, H., Liljenberg, C., & Sandelius, A. S. (2005). Phosphate-limited oat. The plasma membrane and the tonoplast as major targets for phospholipid-to-glycolipid replacement and stimulation of phospholipases in the plasma membrane. *The Journal of Biological Chemistry*, *280*(30), 27578–27586. https://doi.org/10.1074/jbc.M503273200

Andersson, M. X., Stridh, M. H., Larsson, K. E., Liljenberg, C., & Sandelius, A. S. (2003). Phosphate-deficient oat replaces a major portion of the plasma membrane phospholipids with the galactolipid digalactosyldiacylglycerol. *FEBS Letters*, *537*(1–3), 128–132. https://doi.org/10.1016/s0014-5793(03)00109-1

Angkawijaya, A. E., & Nakamura, Y. (2017). Arabidopsis *PECP1* and *PS2* are phosphate starvation-inducible phosphocholine phosphatases. *Biochemical and Biophysical Research Communications*, *494*(1), 397–401. https://doi.org/10.1016/j.bbrc.2017.09.094

Angkawijaya, A. E., Nguyen, V. C., & Nakamura, Y. (2019). LYSOPHOSPHATIDIC ACID ACYLTRANSFERASES 4 and 5 are involved in glycerolipid metabolism and nitrogen starvation response in Arabidopsis. *New Phytologist*, *224*(1), 336–351. https://doi.org/10.1111/nph.16000

Arabidopsis Genome Initiative. (2000). Analysis of the genome sequence of the flowering plant Arabidopsis thaliana. *Nature*, *408*(6814), 796–815. https://doi.org/10.1038/35048692

Arai, Y., Hayashi, M., & Nishimura, M. (2008). Proteomic identification and characterization of a novel peroxisomal adenine nucleotide transporter supplying ATP for fatty acid beta-oxidation in soybean and Arabidopsis. *The Plant Cell*, *20*(12), 3227–3240. https://doi.org/10.1105/tpc.108.062877

Arent, S., Christensen, C. E., Pye, V. E., Nørgaard, A., & Henriksen, A. (2010a). The Multifunctional Protein in Peroxisomal β-Oxidation. *The Journal of Biological Chemistry*, *285*(31), 24066–24077. https://doi.org/10.1074/jbc.M110.106005

Arent, S., Christensen, C. E., Pye, V. E., Nørgaard, A., & Henriksen, A. (2010b). The Multifunctional Protein in Peroxisomal β-Oxidation: STRUCTURE AND SUBSTRATE SPECIFICITY OF THE ARABIDOPSIS THALIANA PROTEIN MFP2 *. *Journal of Biological Chemistry*, *285*(31), 24066–24077. https://doi.org/10.1074/jbc.M110.106005

Awai, K., Maréchal, E., Block, M. A., Brun, D., Masuda, T., Shimada, H., Takamiya, K., Ohta, H., & Joyard, J. (2001). Two types of MGDG synthase genes, found widely in both 16:3 and 18:3 plants, differentially mediate galactolipid syntheses in photosynthetic and nonphotosynthetic tissues in Arabidopsis thaliana. *Proceedings of the National Academy of Sciences of the United States of America*, *98*(19), 10960–10965. https://doi.org/10.1073/pnas.181331498

Aymé, L., Arragain, S., Canonge, M., Baud, S., Touati, N., Bimai, O., Jagic, F., Louis-Mondésir, C., Briozzo, P., Fontecave, M., & Chardot, T. (2018). Arabidopsis thaliana DGAT3 is a [2Fe-2S] protein involved in TAG biosynthesis. *Scientific Reports*, *8*, 17254. https://doi.org/10.1038/s41598-018-35545-7

Bacher, A., Eberhardt, S., Fischer, M., Kis, K., & Richter, G. (2000). Biosynthesis of vitamin b2 (riboflavin). *Annual Review of Nutrition*, *20*, 153–167. https://doi.org/10.1146/annurev.nutr.20.1.153

Bai, Y., Shen, Y., Zhang, Z., Jia, Q., Xu, M., Zhang, T., Fang, H., Yu, X., Li, L., Liu, D., Qi, X., Chen, Z., Wu, S., Zhang, Q., & Liang, C. (2021). A GPAT1 Mutation in Arabidopsis Enhances Plant Height but Impairs Seed Oil Biosynthesis. *International Journal of Molecular Sciences*, *22*(2), 785. https://doi.org/10.3390/ijms22020785

Baker, A., Carrier, D. J., Schaedler, T., Waterham, H. R., van Roermund, C. W., & Theodoulou, F. L. (2015). Peroxisomal ABC transporters: Functions and mechanism. *Biochemical Society Transactions*, *43*(5), 959–965. https://doi.org/10.1042/BST20150127

Banaś, A., Dahlqvist, A., Ståhl, U., Lenman, M., & Stymne, S. (2000). The involvement of phospholipid:diacylglycerol acyltransferases in triacylglycerol production. *Biochemical Society Transactions*, *28*(6), 703–705.

Bankaitis, V. A., Malehorn, D. E., Emr, S. D., & Greene, R. (1989). The Saccharomyces cerevisiae SEC14 gene encodes a cytosolic factor that is required for transport of secretory proteins from the yeast Golgi complex. *Journal of Cell Biology*, *108*(4), 1271–1281. https://doi.org/10.1083/jcb.108.4.1271

Bao, X., Shorrosh, B. S., & Ohlrogge, J. B. (1997). Isolation and characterization of an Arabidopsis biotin carboxylase gene and its promoter. *Plant Molecular Biology*, *35*(5), 539–550. https://doi.org/10.1023/a:1005881006620

Bari, R., Datt Pant, B., Stitt, M., & Scheible, W.-R. (2006). PHO2, MicroRNA399, and PHR1 Define a Phosphate-Signaling Pathway in Plants. *Plant Physiology*, *141*(3), 988–999. https://doi.org/10.1104/pp.106.079707

Bariola, P. A., Howard, C. J., Taylor, C. B., Verburg, M. T., Jaglan, V. D., & Green, P. J. (1994). The Arabidopsis ribonuclease gene RNS1 is tightly controlled in response to phosphate limitation. *The Plant Journal*, *6*(5), 673–685. https://doi.org/10.1046/j.1365-313X.1994.6050673.x

Barton, K. A., Mathur, N., & Mathur, J. (2013). Simultaneous live-imaging of peroxisomes and the ER in plant cells suggests contiguity but no luminal continuity between the two organelles. *Frontiers in Physiology*, *4*. https://doi.org/10.3389/fphys.2013.00196

Bates, P. D., Ohlrogge, J. B., & Pollard, M. (2007). Incorporation of newly synthesized fatty acids into cytosolic glycerolipids in pea leaves occurs via acyl editing. *The Journal of Biological Chemistry*, *282*(43), 31206–31216. https://doi.org/10.1074/jbc.M705447200

Bates, T. R., & Lynch, J. P. (2001). Root hairs confer a competitive advantage under low phosphorus availability. *Plant and Soil*, *236*(2), 243–250. https://doi.org/10.1023/A:1012791706800

Baud, S., Guyon, V., Kronenberger, J., Wuillème, S., Miquel, M., Caboche, M., Lepiniec, L., & Rochat, C. (2003). Multifunctional acetyl-CoA carboxylase 1 is essential for very long chain fatty acid elongation and embryo development in Arabidopsis. *The Plant Journal: For Cell and Molecular Biology*, *33*(1), 75–86. https://doi.org/10.1046/j.1365-313x.2003.016010.x

Baumgart, E., Vanhorebeek, I., Grabenbauer, M., Borgers, M., Declercq, P. E., Fahimi, H. D., & Baes, M. (2001). Mitochondrial alterations caused by defective peroxisomal biogenesis in a mouse model for Zellweger syndrome (PEX5 knockout mouse). *The American Journal of Pathology*, *159*(4), 1477–1494. https://doi.org/10.1016/S0002-9440(10)62534-5

Beenakkers, A. M. T., Van der Horst, D. J., & Van Marrewijk, W. J. A. (1981). Role of Lipids in Energy Metabolism. In R. G. H. Downer (Ed.), *Energy Metabolism in Insects* (pp. 53–100). Springer US. https://doi.org/10.1007/978-1-4615-9221-1_3

Beisson, F., Ferté, N., Bruley, S., Voultoury, R., Verger, R., & Arondel, V. (2001). Oil-bodies as substrates for lipolytic enzymes. *Biochimica Et Biophysica Acta*, *1531*(1–2), 47–58. https://doi.org/10.1016/s1388-1981(01)00086-5

Ben Hamed, K., Ben Youssef, N., Ranieri, A., Zarrouk, M., & Abdelly, C. (2005). Changes in content and fatty acid profiles of total lipids and sulfolipids in the halophyte Crithmum maritimum under salt stress. *Journal of Plant Physiology*, *162*(5), 599–602. https://doi.org/10.1016/j.jplph.2004.11.010

Benning, C. (1998). BIOSYNTHESIS AND FUNCTION OF THE SULFOLIPID SULFOQUINOVOSYL DIACYLGLYCEROL. *Annual Review of Plant Physiology and Plant Molecular Biology*, *49*, 53–75. https://doi.org/10.1146/annurev.arplant.49.1.53

Benning, C. (2008). A role for lipid trafficking in chloroplast biogenesis. *Progress in Lipid Research*, *47*(5), 381–389. https://doi.org/10.1016/j.plipres.2008.04.001

Benning, C., Xu, C., & Awai, K. (2006). Non-vesicular and vesicular lipid trafficking involving plastids. *Current Opinion in Plant Biology*, *9*(3), 241–247. https://doi.org/10.1016/j.pbi.2006.03.012

Bergkemper, F., Schöler, A., Engel, M., Lang, F., Krüger, J., Schloter, M., & Schulz, S. (2016). Phosphorus depletion in forest soils shapes bacterial communities towards phosphorus recycling systems. *Environmental Microbiology*, *18*(6), 1988–2000. https://doi.org/10.1111/1462-2920.13188

Bessoule, J. J., Testet, E., & Cassagne, C. (1995). Synthesis of phosphatidylcholine in the chloroplast envelope after import of lysophosphatidylcholine from endoplasmic reticulum membranes. *European Journal of Biochemistry*, *228*(2), 490–497.

Bian, J., Su, X., Yuan, X., Zhang, Y., Lin, J., & Li, X. (2023). Endoplasmic reticulum membrane contact sites: Cross-talk between membrane-bound organelles in plant cells. *Journal of Experimental Botany*, *74*(10), 2956–2967. https://doi.org/10.1093/jxb/erad068

Biochemistry and Molecular Biology of Plants, 2nd Edition | Wiley. (n.d.). Wiley.Com. Retrieved February 27, 2024, from https://www.wiley.com/en-us/Biochemistry+and+Molecular+Biology+of+Plants%2C+2nd+Edition-p-9780470714218

Block, A., Widhalm, J. R., Fatihi, A., Cahoon, R. E., Wamboldt, Y., Elowsky, C., Mackenzie, S. A., Cahoon, E. B., Chapple, C., Dudareva, N., & Basset, G. J. (2014). The Origin and Biosynthesis of the Benzenoid Moiety of Ubiquinone (Coenzyme Q) in Arabidopsis[W]. *The Plant Cell*, *26*(5), 1938–1948. https://doi.org/10.1105/tpc.114.125807

Block, M. A., Douce, R., Joyard, J., & Rolland, N. (2007). Chloroplast envelope membranes: A dynamic interface between plastids and the cytosol. *Photosynthesis Research*, *92*(2), 225–244. https://doi.org/10.1007/s11120-007-9195-8

Böhme, K., Li, Y., Charlot, F., Grierson, C., Marrocco, K., Okada, K., Laloue, M., & Nogué, F. (2004). The Arabidopsis COW1 gene encodes a phosphatidylinositol transfer protein essential for root hair tip growth. *The Plant Journal*, *40*(5), 686–698. https://doi.org/10.1111/j.1365-313X.2004.02245.x

Bolik, S., Albrieux, C., Schneck, E., Demé, B., & Jouhet, J. (2022). Sulfoquinovosyldiacylglycerol and phosphatidylglycerol bilayers share biophysical properties and are good mutual substitutes in photosynthetic membranes. *Biochimica Et Biophysica Acta. Biomembranes*, *1864*(12), 184037. https://doi.org/10.1016/j.bbamem.2022.184037

Borner, G. H. H., Sherrier, D. J., Weimar, T., Michaelson, L. V., Hawkins, N. D., MacAskill, A., Napier, J. A., Beale, M. H., Lilley, K. S., & Dupree, P. (2005). Analysis of Detergent-Resistant Membranes in Arabidopsis. Evidence for Plasma Membrane Lipid Rafts. *Plant Physiology*, *137*(1), 104–116. https://doi.org/10.1104/pp.104.053041

Botella, C., Sautron, E., Boudiere, L., Michaud, M., Dubots, E., Yamaryo-Botté, Y., Albrieux, C., Marechal, E., Block, M. A., & Jouhet, J. (2016). ALA10, a Phospholipid Flippase, Controls FAD2/FAD3 Desaturation of Phosphatidylcholine in the ER and Affects Chloroplast Lipid Composition in Arabidopsis thaliana1. *Plant Physiology*, *170*(3), 1300–1314. https://doi.org/10.1104/pp.15.01557

Boussardon, C., Przybyla-Toscano, J., Carrie, C., & Keech, O. (2020). Tissue-specific isolation of Arabidopsis/plant mitochondria—IMTACT (isolation of mitochondria tagged in specific cell types). *The Plant Journal: For Cell and Molecular Biology*, *103*(1), 459–473. https://doi.org/10.1111/tpj.14723

Bracha-Drori, K., Shichrur, K., Katz, A., Oliva, M., Angelovici, R., Yalovsky, S., & Ohad, N. (2004). Detection of protein-protein interactions in plants using bimolecular fluorescence complementation. *The Plant Journal: For Cell and Molecular Biology*, *40*(3), 419–427. https://doi.org/10.1111/j.1365-313X.2004.02206.x

Bradford, M. M. (1976). A rapid and sensitive method for the quantitation of microgram quantities of protein utilizing the principle of protein-dye binding. *Analytical Biochemistry*, *72*, 248–254. https://doi.org/10.1006/abio.1976.9999

Branon, T. C., Bosch, J. A., Sanchez, A. D., Udeshi, N. D., Svinkina, T., Carr, S. A., Feldman, J. L., Perrimon, N., & Ting, A. Y. (2018). Efficient proximity labeling in living cells and organisms with TurboID. *Nature Biotechnology*, *36*(9), 880–887. https://doi.org/10.1038/nbt.4201

Brash, A. R. (1999). Lipoxygenases: Occurrence, Functions, Catalysis, and Acquisition of Substrate *. *Journal of Biological Chemistry*, *274*(34), 23679–23682. https://doi.org/10.1074/jbc.274.34.23679

Bretagnolle, F., Matejicek, A., Gregoire, S., Reboud, X., & Gaba, S. (2016). Determination of fatty acids content, global antioxidant activity and energy value of weed seeds from agricultural fields in France. *Weed Research*, *56*(1), 78–95. https://doi.org/10.1111/wre.12188

Brinch-Pedersen, H., Sørensen, L. D., & Holm, P. B. (2002). Engineering crop plants: Getting a handle on phosphate. *Trends in Plant Science*, *7*(3), 118–125. https://doi.org/10.1016/s1360-1385(01)02222-1

Brown, A. P., Affleck, V., Fawcett, T., & Slabas, A. R. (2006). Tandem affinity purification tagging of fatty acid biosynthetic enzymes in Synechocystis sp. PCC6803 and Arabidopsis thaliana. *Journal of Experimental Botany*, *57*(7), 1563–1571. https://doi.org/10.1093/jxb/erj150

Brown, J. M., Betters, J. L., Lord, C., Ma, Y., Han, X., Yang, K., Alger, H. M., Melchior, J., Sawyer, J., Shah, R., Wilson, M. D., Liu, X., Graham, M. J., Lee, R., Crooke, R., Shulman, G. I., Xue, B., Shi, H., & Yu, L. (2010). CGI-58 knockdown in mice causes hepatic steatosis but prevents diet-induced obesity and glucose intolerance. *Journal of Lipid Research*, *51*(11), 3306–3315. https://doi.org/10.1194/jlr.M010256

Browse: Glycerolipids—Google 学术搜索. (n.d.). Retrieved May 30, 2024, from https://scholar.google.com/scholar_lookup?title=Glycerolipids.&publication_year=1994&pages=881-936

Browse, J., McConn, M., James, D., & Miquel, M. (1993). Mutants of Arabidopsis deficient in the synthesis of alpha-linolenate. Biochemical and genetic characterization of the endoplasmic reticulum linoleoyl desaturase. *Journal of Biological Chemistry*, *268*(22), 16345–16351. https://doi.org/10.1016/S0021-9258(19)85427-3

Bryant, N., Lloyd, J., Sweeney, C., Myouga, F., & Meinke, D. (2011). Identification of nuclear genes encoding chloroplast-localized proteins required for embryo development in Arabidopsis. *Plant Physiology*, *155*(4), 1678–1689. https://doi.org/10.1104/pp.110.168120

Buchanan-Wollaston, V., Page, T., Harrison, E., Breeze, E., Lim, P. O., Nam, H. G., Lin, J.-F., Wu, S.-H., Swidzinski, J., Ishizaki, K., & Leaver, C. J. (2005). Comparative transcriptome analysis reveals significant differences in gene expression and signalling pathways between developmental and dark/starvation-induced senescence in Arabidopsis. *The Plant Journal*, *42*(4), 567–585. https://doi.org/10.1111/j.1365-313X.2005.02399.x

Burgal, J., Shockey, J., Lu, C., Dyer, J., Larson, T., Graham, I., & Browse, J. (2008). Metabolic engineering of hydroxy fatty acid production in plants: RcDGAT2 drives dramatic increases in ricinoleate levels in seed oil. *Plant Biotechnology Journal*, *6*(8), 819–831. https://doi.org/10.1111/j.1467-7652.2008.00361.x

Burger, K. N. (2000). Greasing membrane fusion and fission machineries. *Traffic (Copenhagen, Denmark)*, *1*(8), 605–613. https://doi.org/10.1034/j.1600-0854.2000.010804.x

Bussell, J. D., Behrens, C., Ecke, W., & Eubel, H. (2013). Arabidopsis peroxisome proteomics. *Frontiers in Plant Science*, *4*, 101. https://doi.org/10.3389/fpls.2013.00101

Bussell, J. D., Reichelt, M., Wiszniewski, A. A. G., Gershenzon, J., & Smith, S. M. (2014a). Peroxisomal ATP-Binding Cassette Transporter COMATOSE and the Multifunctional Protein ABNORMAL INFLORESCENCE MERISTEM Are Required for the Production of Benzoylated Metabolites in Arabidopsis Seeds1[W]. *Plant Physiology*, *164*(1), 48–54. https://doi.org/10.1104/pp.113.229807

Bussell, J. D., Reichelt, M., Wiszniewski, A. A. G., Gershenzon, J., & Smith, S. M. (2014b). Peroxisomal ATP-Binding Cassette Transporter COMATOSE and the Multifunctional Protein ABNORMAL INFLORESCENCE MERISTEM Are Required for the Production of Benzoylated Metabolites in Arabidopsis Seeds1[W]. *Plant Physiology*, *164*(1), 48–54. https://doi.org/10.1104/pp.113.229807

Caiveau, O., Fortune, D., Cantrel, C., Zachowski, A., & Moreau, F. (2001). Consequences of ω-6-Oleate Desaturase Deficiency on Lipid Dynamics and Functional Properties of Mitochondrial Membranes ofArabidopsis thaliana *. *Journal of Biological Chemistry*, *276*(8), 5788–5794. https://doi.org/10.1074/jbc.M006231200

Carrie, C., Murcha, M. W., Millar, A. H., Smith, S. M., & Whelan, J. (2007). Nine 3-ketoacyl-CoA thiolases (KATs) and acetoacetyl-CoA thiolases (ACATs) encoded by five genes in Arabidopsis thaliana are targeted either to peroxisomes or cytosol but not to mitochondria. *Plant Molecular Biology*, *63*(1), 97–108. https://doi.org/10.1007/s11103-006-9075-1

Carrier, D. J., van Roermund, C. W. T., Schaedler, T. A., Rong, H. L., IJlst, L., Wanders, R. J. A., Baldwin, S. A., Waterham, H. R., Theodoulou, F. L., & Baker, A. (2019). Mutagenesis separates ATPase and thioesterase activities of the peroxisomal ABC transporter, Comatose. *Scientific Reports*, *9*(1), 10502. https://doi.org/10.1038/s41598-019-46685-9

Castro, L. F. C., Tocher, D. R., & Monroig, O. (2016). Long-chain polyunsaturated fatty acid biosynthesis in chordates: Insights into the evolution of Fads and Elovl gene repertoire. *Progress in Lipid Research*, *62*, 25–40. https://doi.org/10.1016/j.plipres.2016.01.001

Cateni, F., Bonivento, P., Procida, G., Zacchigna, M., Favretto, L. G., Scialino, G., & Banfi, E. (2008). Chemoenzymatic synthesis and antimicrobial activity evaluation of monogalactosyl diglycerides. *European Journal of Medicinal Chemistry*, *43*(1), 210–221. https://doi.org/10.1016/j.ejmech.2007.03.012

Cevher-Keskin, B. (2020). Endomembrane Trafficking in Plants. In *Electrodialysis*. IntechOpen. https://doi.org/10.5772/intechopen.91642

Chacón-López, A., Ibarra-Laclette, E., Sánchez-Calderón, L., Gutiérrez-Alanis, D., & Herrera-Estrella, L. (2011). Global expression pattern comparison between low phosphorus insensitive 4 and WT Arabidopsis reveals an important role of reactive oxygen species and jasmonic acid in the root tip response to phosphate starvation. *Plant Signaling & Behavior*, *6*(3), 382–392. https://doi.org/10.4161/psb.6.3.14160

Chandrika, N. N. P., Sundaravelpandian, K., Yu, S.-M., & Schmidt, W. (2013). ALFIN-LIKE 6 is involved in root hair elongation during phosphate deficiency in Arabidopsis. *The New Phytologist*, *198*(3), 709–720. https://doi.org/10.1111/nph.12194

Chang, C.-L., & Liou, J. (2015). Phosphatidylinositol 4,5-Bisphosphate Homeostasis Regulated by Nir2 and Nir3 Proteins at Endoplasmic Reticulum-Plasma Membrane Junctions *. *Journal of Biological Chemistry*, *290*(23), 14289–14301. https://doi.org/10.1074/jbc.M114.621375

Chapman, K. D., Dyer, J. M., & Mullen, R. T. (2012). Biogenesis and functions of lipid droplets in plants: Thematic Review Series: Lipid Droplet Synthesis and Metabolism: from Yeast to Man. *Journal of Lipid Research*, *53*(2), 215–226. https://doi.org/10.1194/jlr.R021436

Chapman, K. D., & Ohlrogge, J. B. (2012a). Compartmentation of triacylglycerol accumulation in plants. *The Journal of Biological Chemistry*, *287*(4), 2288–2294. https://doi.org/10.1074/jbc.R111.290072

Chapman, K. D., & Ohlrogge, J. B. (2012b). Compartmentation of Triacylglycerol Accumulation in Plants. *The Journal of Biological Chemistry*, *287*(4), 2288–2294. https://doi.org/10.1074/jbc.R111.290072

Chapman, K. D., & Trelease, R. N. (1991). Acquisition of membrane lipids by differentiating glyoxysomes: Role of lipid bodies. *The Journal of Cell Biology*, *115*(4), 995–1007. https://doi.org/10.1083/jcb.115.4.995

Chen, D. L., Delatorre, C. A., Bakker, A., & Abel, S. (2000). Conditional identification of phosphate-starvation-response mutants in Arabidopsis thaliana. *Planta*, *211*(1), 13–22. https://doi.org/10.1007/s004250000271

Chen, J., Burke, J. J., Xin, Z., Xu, C., & Velten, J. (2006). Characterization of the Arabidopsis thermosensitive mutant atts02 reveals an important role for galactolipids in thermotolerance. *Plant, Cell & Environment*, *29*(7), 1437–1448. https://doi.org/10.1111/j.1365-3040.2006.01527.x

Chen, X., Snyder, C. L., Truksa, M., Shah, S., & Weselake, R. J. (2011). Sn-Glycerol-3-phosphate acyltransferases in plants. *Plant Signaling & Behavior*, *6*(11), 1695–1699. https://doi.org/10.4161/psb.6.11.17777

Cheng, L., Bucciarelli, B., Liu, J., Zinn, K., Miller, S., Patton-Vogt, J., Allan, D., Shen, J., & Vance, C. P. (2011). White Lupin Cluster Root Acclimation to Phosphorus Deficiency and Root Hair Development Involve Unique Glycerophosphodiester Phosphodiesterases. *Plant Physiology*, *156*(3), 1131–1148. https://doi.org/10.1104/pp.111.173724

Cheng, Y., Zhou, W., El sheery, N. I., Peters, C., Li, M., Wang, X., & Huang, J. (2011). Characterization of the Arabidopsis glycerophosphodiester phosphodiesterase (GDPD) family reveals a role of the plastid-localized AtGDPD1 in maintaining cellular phosphate homeostasis under phosphate starvation. *The Plant Journal*, *66*(5), 781–795. https://doi.org/10.1111/j.1365-313X.2011.04538.x

Chevalier, F., Pata, M., Nacry, P., Doumas, P., & Rossignol, M. (2003). Effects of phosphate availability on the root system architecture: Large-scale analysis of the natural variation between Arabidopsis accessions. *Plant, Cell & Environment*, *26*(11), 1839–1850. https://doi.org/10.1046/j.1365-3040.2003.01100.x

Choi, J. K., Yu, F., Wurtele, E. S., & Nikolau, B. J. (1995). Molecular cloning and characterization of the cDNA coding for the biotin-containing subunit of the chloroplastic acetyl-coenzyme A carboxylase. *Plant Physiology*, *109*(2), 619–625.

Choi, Y. J., Zaikova, K., Yeom, S.-J., Kim, Y.-S., & Lee, D. W. (2022). Biogenesis and Lipase-Mediated Mobilization of Lipid Droplets in Plants. *Plants*, *11*(9), 9. https://doi.org/10.3390/plants11091243

Chum, P. Y., Haimes, J. D., André, C. P., Kuusisto, P. K., & Kelley, M. L. (2012). Genotyping of Plant and Animal Samples without Prior DNA Purification. *Journal of Visualized Experiments : JoVE*, *67*, 3844. https://doi.org/10.3791/3844

Cohen, Y., Klug, Y. A., Dimitrov, L., Erez, Z., Chuartzman, S. G., Elinger, D., Yofe, I., Soliman, K., Gärtner, J., Thoms, S., Schekman, R., Elbaz-Alon, Y., Zalckvar, E., & Schuldiner, M. (2014). Peroxisomes are juxtaposed to strategic sites on mitochondria. *Molecular BioSystems*, *10*(7), 1742–1748. https://doi.org/10.1039/c4mb00001c

Contento, A. L., & Bassham, D. C. (2010). Increase in catalase-3 activity as a response to use of alternative catabolic substrates during sucrose starvation. *Plant Physiology and Biochemistry: PPB*, *48*(4), 232–238. https://doi.org/10.1016/j.plaphy.2010.01.004

Cornah, J. E., Germain, V., Ward, J. L., Beale, M. H., & Smith, S. M. (2004). Lipid utilization, gluconeogenesis, and seedling growth in Arabidopsis mutants lacking the glyoxylate cycle enzyme malate synthase. *The Journal of Biological Chemistry*, *279*(41), 42916–42923. https://doi.org/10.1074/jbc.M407380200

Corpas, F. J., Barroso, J. B., Palma, J. M., & Rodriguez-Ruiz, M. (2017). Plant peroxisomes: A nitro-oxidative cocktail. *Redox Biology*, *11*, 535–542. https://doi.org/10.1016/j.redox.2016.12.033

Cross, L. L., Ebeed, H. T., & Baker, A. (2016). Peroxisome biogenesis, protein targeting mechanisms and PEX gene functions in plants. *Biochimica Et Biophysica Acta*, *1863*(5), 850–862. https://doi.org/10.1016/j.bbamcr.2015.09.027

Cui, S., Fukao, Y., Mano, S., Yamada, K., Hayashi, M., & Nishimura, M. (2013). Proteomic analysis reveals that the Rab GTPase RabE1c is involved in the degradation of the peroxisomal protein receptor PEX7 (peroxin 7). *The Journal of Biological Chemistry*, *288*(8), 6014–6023. https://doi.org/10.1074/jbc.M112.438143

Cui, S., Hayashi, Y., Otomo, M., Mano, S., Oikawa, K., Hayashi, M., & Nishimura, M. (2016). Sucrose Production Mediated by Lipid Metabolism Suppresses the Physical Interaction of Peroxisomes and Oil Bodies during Germination of Arabidopsis thaliana. *The Journal of Biological Chemistry*, *291*(38), 19734–19745. https://doi.org/10.1074/jbc.M116.748814

Cutler, S. R., Ehrhardt, D. W., Griffitts, J. S., & Somerville, C. R. (2000). Random GFP::cDNA fusions enable visualization of subcellular structures in cells of Arabidopsis at a high frequency. *Proceedings of the National Academy of Sciences of the United States of America*, *97*(7), 3718–3723. https://doi.org/10.1073/pnas.97.7.3718

Dahlqvist, A., Stahl, U., Lenman, M., Banas, A., Lee, M., Sandager, L., Ronne, H., & Stymne, S. (2000). Phospholipid:diacylglycerol acyltransferase: An enzyme that catalyzes the acyl-CoA-independent formation of triacylglycerol in yeast and plants. *Proceedings of the National Academy of Sciences of the United States of America*, *97*(12), 6487–6492. https://doi.org/10.1073/pnas.120067297

Dall'Armi, C., Devereaux, K. A., & Di Paolo, G. (2013). The role of lipids in the control of autophagy. *Current Biology: CB*, *23*(1), R33-45. https://doi.org/10.1016/j.cub.2012.10.041

Damodaran, S., & Strader, L. C. (2019). Indole 3-Butyric Acid Metabolism and Transport in Arabidopsis thaliana. *Frontiers in Plant Science*, *10*, 851. https://doi.org/10.3389/fpls.2019.00851

Dancer, J., Neuhaus, H. E., & Stitt, M. (1990). Subcellular compartmentation of uridine nucleotides and nucleoside-5' -diphosphate kinase in leaves. *Plant Physiology*, *92*(3), 637–641. https://doi.org/10.1104/pp.92.3.637

Dave, A., Hernández, M. L., He, Z., Andriotis, V. M. E., Vaistij, F. E., Larson, T. R., & Graham, I. A. (2011). 12-Oxo-Phytodienoic Acid Accumulation during Seed Development Represses Seed Germination in Arabidopsis[C][W][OA]. *The Plant Cell*, *23*(2), 583–599. https://doi.org/10.1105/tpc.110.081489

De Bellis, L., Luvisi, A., & Alpi, A. (2020). Aconitase: To Be or not to Be Inside Plant Glyoxysomes, That Is the Question. *Biology*, *9*(7), 162. https://doi.org/10.3390/biology9070162

De Marcos Lousa, C., van Roermund, C. W. T., Postis, V. L. G., Dietrich, D., Kerr, I. D., Wanders, R. J. A., Baldwin, S. A., Baker, A., & Theodoulou, F. L. (2013). Intrinsic acyl-CoA thioesterase activity of a peroxisomal ATP binding cassette transporter is required for transport and metabolism of fatty acids. *Proceedings of the National Academy of Sciences*, *110*(4), 1279–1284. https://doi.org/10.1073/pnas.1218034110

De Palma, M., Grillo, S., Massarelli, I., Costa, A., Balogh, G., Vigh, L., & Leone, A. (2008). Regulation of desaturase gene expression, changes in membrane lipid composition and freezing tolerance in potato plants. *Molecular Breeding*, *21*(1), 15–26. https://doi.org/10.1007/s11032-007-9105-y

de Silva, K., Laska, B., Brown, C., Sederoff, H. W., & Khodakovskaya, M. (2011). Arabidopsis thaliana calcium-dependent lipid-binding protein (AtCLB): A novel repressor of abiotic stress response. *Journal of Experimental Botany*, *62*(8), 2679–2689. https://doi.org/10.1093/jxb/erq468

Dean, M., Rzhetsky, A., & Allikmets, R. (2001). The Human ATP-Binding Cassette (ABC) Transporter Superfamily. *Genome Research*, *11*(7), 1156–1166. https://doi.org/10.1101/gr.184901

del Pozo, J. C., Allona, I., Rubio, V., Leyva, A., de la Peña, A., Aragoncillo, C., & Paz-Ares, J. (1999a). A type 5 acid phosphatase gene from Arabidopsis thaliana is induced by phosphate starvation and by some other types of phosphate mobilising/oxidative stress conditions. *The Plant Journal: For Cell and Molecular Biology*, *19*(5), 579–589. https://doi.org/10.1046/j.1365-313x.1999.00562.x

del Pozo, J. C., Allona, I., Rubio, V., Leyva, A., de la Peña, A., Aragoncillo, C., & Paz-Ares, J. (1999b). A type 5 acid phosphatase gene from Arabidopsis thaliana is induced by phosphate starvation and by some other types of phosphate mobilising/oxidative stress conditions. *The Plant Journal: For Cell and Molecular Biology*, *19*(5), 579–589. https://doi.org/10.1046/j.1365-313x.1999.00562.x

Delhaize, E., & Randall, P. J. (1995). Characterization of a Phosphate-Accumulator Mutant of Arabidopsis thaliana. *Plant Physiology*, *107*(1), 207–213.

Dellaporta, S. L., Wood, J., & Hicks, J. B. (1983). A plant DNA minipreparation: Version II. *Plant Molecular Biology Reporter*, *1*(4), 19–21. https://doi.org/10.1007/BF02712670

Deruyffelaere, C., Bouchez, I., Morin, H., Guillot, A., Miquel, M., Froissard, M., Chardot, T., & D'Andrea, S. (2015). Ubiquitin-Mediated Proteasomal Degradation of Oleosins is Involved in Oil Body Mobilization During Post-Germinative Seedling Growth in Arabidopsis. *Plant & Cell Physiology*, *56*(7), 1374–1387. https://doi.org/10.1093/pcp/pcv056

Deruyffelaere, C., Purkrtova, Z., Bouchez, I., Collet, B., Cacas, J.-L., Chardot, T., Gallois, J.-L., & D'Andrea, S. (2018). PUX10 Is a CDC48A Adaptor Protein That Regulates the Extraction of Ubiquitinated Oleosins from Seed Lipid Droplets in Arabidopsis. *The Plant Cell*, *30*(9), 2116–2136. https://doi.org/10.1105/tpc.18.00275

Desai, M., & Hu, J. (2008). Light Induces Peroxisome Proliferation in Arabidopsis Seedlings through the Photoreceptor Phytochrome A, the Transcription Factor HY5 HOMOLOG, and the Peroxisomal Protein PEROXIN11b. *Plant Physiology*, *146*(3), 1117–1127. https://doi.org/10.1104/pp.107.113555

Di Paolo, G., & De Camilli, P. (2006). Phosphoinositides in cell regulation and membrane dynamics. *Nature*, *443*(7112), 651–657. https://doi.org/10.1038/nature05185

Dietrich, D., Schmuths, H., Lousa, C. D. M., Baldwin, J. M., Baldwin, S. A., Baker, A., Theodoulou, F. L., & Holdsworth, M. J. (2009). Mutations in the Arabidopsis Peroxisomal ABC Transporter COMATOSE Allow Differentiation between Multiple Functions In Planta: Insights from an Allelic Series. *Molecular Biology of the Cell*, *20*(1), 530–543. https://doi.org/10.1091/mbc.E08-07-0745

Dissanayaka, D. M. S. B., Ghahremani, M., Siebers, M., Wasaki, J., & Plaxton, W. C. (2021). Recent insights into the metabolic adaptations of phosphorus-deprived plants. *Journal of Experimental Botany*, *72*(2), 199–223. https://doi.org/10.1093/jxb/eraa482

Dixon, D. P., Hawkins, T., Hussey, P. J., & Edwards, R. (2009). Enzyme activities and subcellular localization of members of the Arabidopsis glutathione transferase superfamily. *Journal of Experimental Botany*, *60*(4), 1207–1218. https://doi.org/10.1093/jxb/ern365

Dlouhý, O., Kurasová, I., Karlický, V., Javornik, U., Šket, P., Petrova, N. Z., Krumova, S. B., Plavec, J., Ughy, B., Špunda, V., & Garab, G. (2020). Modulation of non-bilayer lipid phases and the structure and functions of thylakoid membranes: Effects on the water-soluble enzyme violaxanthin de-epoxidase. *Scientific Reports*, *10*(1), 11959. https://doi.org/10.1038/s41598-020-68854-x

Donaldson, R. P., & Beevers, H. (1977). Lipid composition of organelles from germinating castor bean endosperm. *Plant Physiology*, *59*(2), 259–263. https://doi.org/10.1104/pp.59.2.259

Dong, C.-H., Zolman, B. K., Bartel, B., Lee, B., Stevenson, B., Agarwal, M., & Zhu, J.-K. (2009). Disruption of Arabidopsis CHY1 Reveals an Important Role of Metabolic Status in Plant Cold Stress Signaling. *Molecular Plant*, *2*(1), 59–72. https://doi.org/10.1093/mp/ssn063

Dörmann, P., & Benning, C. (2002). Galactolipids rule in seed plants. *Trends in Plant Science*, *7*(3), 112–118. https://doi.org/10.1016/S1360-1385(01)02216-6

Dowhan, W., & Bogdanov, M. (2002). Chapter 1 Functional roles of lipids in membranes. In *New Comprehensive Biochemistry* (Vol. 36, pp. 1–35). Elsevier. https://doi.org/10.1016/S0167-7306(02)36003-4

Drissner, D., Kunze, G., Callewaert, N., Gehrig, P., Tamasloukht, M., Boller, T., Felix, G., Amrhein, N., & Bucher, M. (2007). Lyso-Phosphatidylcholine Is a Signal in the Arbuscular Mycorrhizal Symbiosis. *Science*, *318*(5848), 265–268. https://doi.org/10.1126/science.1146487

Du, Y.-Y., Wang, P.-C., Chen, J., & Song, C.-P. (2008). Comprehensive functional analysis of the catalase gene family in Arabidopsis thaliana. *Journal of Integrative Plant Biology*, *50*(10), 1318–1326. https://doi.org/10.1111/j.1744-7909.2008.00741.x

Duan, K., Yi, K., Dang, L., Huang, H., Wu, W., & Wu, P. (2008). Characterization of a sub-family of Arabidopsis genes with the SPX domain reveals their diverse functions in plant tolerance to phosphorus starvation. *The Plant Journal: For Cell and Molecular Biology*, *54*(6), 965–975. https://doi.org/10.1111/j.1365-313X.2008.03460.x

Duarte, B., Martins, I., Rosa, R., Matos, A. R., Roleda, M. Y., Reusch, T. B. H., Engelen, A. H., Serrão, E. A., Pearson, G. A., Marques, J. C., Caçador, I., Duarte, C. M., & Jueterbock, A. (2018). Climate Change Impacts on Seagrass Meadows and Macroalgal Forests: An Integrative Perspective on Acclimation and Adaptation Potential. *Frontiers in Marine Science*, *5*. https://doi.org/10.3389/fmars.2018.00190

Duarte, B., Matos, A. R., Marques, J. C., & Caçador, I. (2018). Leaf fatty acid remodeling in the salt-excreting halophytic grass Spartina patens along a salinity gradient. *Plant Physiology and Biochemistry: PPB*, *124*, 112–116. https://doi.org/10.1016/j.plaphy.2018.01.007

Dufourc, E. J. (2008). Sterols and membrane dynamics. *Journal of Chemical Biology*, *1*(1–4), 63–77. https://doi.org/10.1007/s12154-008-0010-6

Eastmond, P. J. (2004). Cloning and characterization of the acid lipase from castor beans. *The Journal of Biological Chemistry*, *279*(44), 45540–45545. https://doi.org/10.1074/jbc.M408686200

Eastmond, P. J. (2006). SUGAR-DEPENDENT1 Encodes a Patatin Domain Triacylglycerol Lipase That Initiates Storage Oil Breakdown in Germinating Arabidopsis Seeds. *The Plant Cell*, *18*(3), 665–675. https://doi.org/10.1105/tpc.105.040543

Eastmond, P. J. (2007). MONODEHYROASCORBATE REDUCTASE4 Is Required for Seed Storage Oil Hydrolysis and Postgerminative Growth in Arabidopsis. *The Plant Cell*, *19*(4), 1376–1387. https://doi.org/10.1105/tpc.106.043992

Eastmond, P. J., Germain, V., Lange, P. R., Bryce, J. H., Smith, S. M., & Graham, I. A. (2000). Postgerminative growth and lipid catabolism in oilseeds lacking the glyoxylate cycle. *Proceedings of the National Academy of Sciences of the United States of America*, *97*(10), 5669–5674.

Eastmond, P. J., & Graham, I. A. (2000). The multifunctional protein At MFP2 is co-ordinately expressed with other genes of fatty acid β-oxidation during seed germination in Arabidopsis thaliana (L.) Heynh. *Biochemical Society Transactions*, *28*(2), 95–99. https://doi.org/10.1042/bst0280095

Eastmond, P. J., & Graham, I. A. (2001). Re-examining the role of the glyoxylate cycle in oilseeds. *Trends in Plant Science*, *6*(2), 72–78. https://doi.org/10.1016/s1360-1385(00)01835-5

Eastmond, P. J., Hooks, M., & Graham, I. A. (2000). The Arabidopsis acyl-CoA oxidase gene family. *Biochemical Society Transactions*, *28*(6), 755–757.

Eastmond, P. J., Quettier, A.-L., Kroon, J. T. M., Craddock, C., Adams, N., & Slabas, A. R. (2010). Phosphatidic acid phosphohydrolase 1 and 2 regulate phospholipid synthesis at the endoplasmic reticulum in Arabidopsis. *The Plant Cell*, *22*(8), 2796–2811. https://doi.org/10.1105/tpc.109.071423

El-Kouhen, K., Blangy, S., Ortiz, E., Gardies, A.-M., Ferté, N., & Arondel, V. (2005). Identification and characterization of a triacylglycerol lipase in Arabidopsis homologous to mammalian acid lipases. *FEBS Letters*, *579*(27), 6067–6073. https://doi.org/10.1016/j.febslet.2005.09.072

eMaatta, S., eScheu, B., Roth, M. R., eTamura, P., eLi, M., Williams, T. D., eWang, X., & eWelti, R. (2012). *Levels of Arabidopsis thaliana leaf phosphatidic acids, phosphatidylserines, and most trienoate-containing polar lipid molecular species increase during the dark period of the diurnal cycle*. https://agris.fao.org/search/en/providers/122436/records/64747f7637abb250f4f5a149

Essigmann, B., Güler, S., Narang, R. A., Linke, D., & Benning, C. (1998). Phosphate availability affects the thylakoid lipid composition and the expression of SQD1, a gene required for sulfolipid biosynthesis in Arabidopsis thaliana. *Proceedings of the National Academy of Sciences*, *95*(4), 1950–1955. https://doi.org/10.1073/pnas.95.4.1950

Eubel, H., Meyer, E. H., Taylor, N. L., Bussell, J. D., O'Toole, N., Heazlewood, J. L., Castleden, I., Small, I. D., Smith, S. M., & Millar, A. H. (2008). Novel Proteins, Putative Membrane Transporters, and an Integrated Metabolic Network Are Revealed by Quantitative Proteomic Analysis of Arabidopsis Cell Culture Peroxisomes. *Plant Physiology*, *148*(4), 1809–1829. https://doi.org/10.1104/pp.108.129999

Falsone, G., Zilic, J., Bonivento, P., Zacchigna, M., Žigon, D., & Altinier, G. (2004). Glyceroglycolipids from Euphorbia nicaeensis All. With antiinflamatory activity. *Arkivoc*, *2004*, 54–65.

Fan, J., Li, X., Issop, L., Culty, M., & Papadopoulos, V. (2016). ACBD2/ECI2-Mediated Peroxisome-Mitochondria Interactions in Leydig Cell Steroid Biosynthesis. *Molecular Endocrinology*, *30*(7), 763–782. https://doi.org/10.1210/me.2016-1008

Fan, J., Yan, C., Roston, R., Shanklin, J., & Xu, C. (2014). *Arabidopsis* Lipins, PDAT1 Acyltransferase, and SDP1 Triacylglycerol Lipase Synergistically Direct Fatty Acids toward β-Oxidation, Thereby Maintaining Membrane Lipid Homeostasis. *The Plant Cell*, *26*(10), 4119–4134. https://doi.org/10.1105/tpc.114.130377

Fan, J., Zhai, Z., Yan, C., & Xu, C. (2015). Arabidopsis TRIGALACTOSYLDIACYLGLYCEROL5 Interacts with TGD1, TGD2, and TGD4 to Facilitate Lipid Transfer from the Endoplasmic Reticulum to Plastids. *The Plant Cell*, *27*(10), 2941–2955. https://doi.org/10.1105/tpc.15.00394

Farré, J., Mahalingam, S. S., Proietto, M., & Subramani, S. (2019). Peroxisome biogenesis, membrane contact sites, and quality control. *EMBO Reports*, *20*(1), e46864. https://doi.org/10.15252/embr.201846864

Ferreira, A. R., Marques, M., Ramos, B., Kagan, J. C., & Ribeiro, D. (2022). Emerging roles of peroxisomes in viral infections. *Trends in Cell Biology*, *32*(2), 124–139. https://doi.org/10.1016/j.tcb.2021.09.010

Feussner, I., Kühn, H., & Wasternack, C. (2001). Lipoxygenase-dependent degradation of storage lipids. *Trends in Plant Science*, *6*(6), 268–273. https://doi.org/10.1016/s1360-1385(01)01950-1

Feussner, I., Wasternack, C., Kindl, H., & Kühn, H. (1995). Lipoxygenase-catalyzed oxygenation of storage lipids is implicated in lipid mobilization during germination. *Proceedings of the National Academy of Sciences*, *92*(25), 11849–11853. https://doi.org/10.1073/pnas.92.25.11849

Folch, J., Lees, M., & Sloane Stanley, G. H. (1957). A simple method for the isolation and purification of total lipides from animal tissues. *The Journal of Biological Chemistry*, *226*(1), 497–509.

Footitt, S. (2002). Control of germination and lipid mobilization by COMATOSE, the Arabidopsis homologue of human ALDP. *The EMBO Journal*, *21*(12), 2912–2922. https://doi.org/10.1093/emboj/cdf300

Footitt, S., Cornah, J. E., Pracharoenwattana, I., Bryce, J. H., & Smith, S. M. (2007). The Arabidopsis 3-ketoacyl-CoA thiolase-2 (kat2-1) mutant exhibits increased flowering but reduced reproductive success. *Journal of Experimental Botany*, *58*(11), 2959–2968. https://doi.org/10.1093/jxb/erm146

Footitt, S., Marquez, J., Schmuths, H., Baker, A., Theodoulou, F. L., & Holdsworth, M. (2006). Analysis of the role of COMATOSE and peroxisomal beta-oxidation in the determination of germination potential in Arabidopsis. *Journal of Experimental Botany*, *57*(11), 2805–2814. https://doi.org/10.1093/jxb/erl045

Footitt, S., Slocombe, S. P., Larner, V., Kurup, S., Wu, Y., Larson, T., Graham, I., Baker, A., & Holdsworth, M. (2002). Control of germination and lipid mobilization by COMATOSE, the Arabidopsis homologue of human ALDP. *The EMBO Journal*, *21*(12), 2912–2922. https://doi.org/10.1093/emboj/cdf300

Frederick, S. E., & Newcomb, E. H. (1969). CYTOCHEMICAL LOCALIZATION OF CATALASE IN LEAF MICROBODIES (PEROXISOMES). *Journal of Cell Biology*, *43*(2), 343–353. https://doi.org/10.1083/jcb.43.2.343

Froman, B. E., Edwards, P. C., Bursch, A. G., & Dehesh, K. (2000). ACX3, a Novel Medium-Chain Acyl-Coenzyme A Oxidase from Arabidopsis. *Plant Physiology*, *123*(2), 733–742. https://doi.org/10.1104/pp.123.2.733

Fukao, Y., Hayashi, M., Hara-Nishimura, I., & Nishimura, M. (2003). Novel glyoxysomal protein kinase, GPK1, identified by proteomic analysis of glyoxysomes in etiolated cotyledons of Arabidopsis thaliana. *Plant & Cell Physiology*, *44*(10), 1002–1012. https://doi.org/10.1093/pcp/pcg145

Fukao, Y., Hayashi, M., & Nishimura, M. (2002). Proteomic analysis of leaf peroxisomal proteins in greening cotyledons of Arabidopsis thaliana. *Plant & Cell Physiology*, *43*(7), 689–696. https://doi.org/10.1093/pcp/pcf101

Fukushima, S., Akita, K., Takagi, T., Kobayashi, K., Moritoki, N., Sugaya, H., Arimura, S., Kuroiwa, H., Kuroiwa, T., & Nagata, N. (2022). Existence of giant mitochondria-containing sheet structures lacking cristae and matrix in the etiolated cotyledon of Arabidopsis thaliana. *Protoplasma*, *259*(3), 731–742. https://doi.org/10.1007/s00709-021-01696-0

Fulda, M., Schnurr, J., Abbadi, A., Heinz, E., & Browse, J. (2004). Peroxisomal Acyl-CoA Synthetase Activity Is Essential for Seedling Development in Arabidopsis thaliana. *The Plant Cell*, *16*(2), 394–405. https://doi.org/10.1105/tpc.019646

Fulda, M., Shockey, J., Werber, M., Wolter, F. P., & Heinz, E. (2002). Two long-chain acyl-CoA synthetases from Arabidopsis thaliana involved in peroxisomal fatty acid beta-oxidation. *The Plant Journal: For Cell and Molecular Biology*, *32*(1), 93–103. https://doi.org/10.1046/j.1365-313x.2002.01405.x

Furse, S., & de Kroon, A. I. P. M. (2015). Phosphatidylcholine's functions beyond that of a membrane brick. *Molecular Membrane Biology*, *32*(4), 117–119. https://doi.org/10.3109/09687688.2015.1066894

Galmes, R., Houcine, A., van Vliet, A. R., Agostinis, P., Jackson, C. L., & Giordano, F. (2016). ORP5/ORP8 localize to endoplasmic reticulum–mitochondria contacts and are involved in mitochondrial function. *EMBO Reports*, *17*(6), 800–810. https://doi.org/10.15252/embr.201541108

Gao, C., Luo, M., Zhao, Q., Yang, R., Cui, Y., Zeng, Y., Xia, J., & Jiang, L. (2014). A unique plant ESCRT component, FREE1, regulates multivesicular body protein sorting and plant growth. *Current Biology: CB*, *24*(21), 2556–2563. https://doi.org/10.1016/j.cub.2014.09.014

Gao, J., Ajjawi, I., Manoli, A., Sawin, A., Xu, C., Froehlich, J. E., Last, R. L., & Benning, C. (2009). FATTY ACID DESATURASE4 of Arabidopsis encodes a protein distinct from characterized fatty acid desaturases. *The Plant Journal*, *60*(5), 832–839. https://doi.org/10.1111/j.1365-313X.2009.04001.x

Garstka, M., Venema, J. H., Rumak, I., Gieczewska, K., Rosiak, M., Koziol-Lipinska, J., Kierdaszuk, B., Vredenberg, W. J., & Mostowska, A. (2007). Contrasting effect of dark-chilling on chloroplast structure and arrangement of chlorophyll-protein complexes in pea and tomato: Plants with a different susceptibility to non-freezing temperature. *Planta*, *226*(5), 1165–1181. https://doi.org/10.1007/s00425-007-0562-7

Gaude, N., Nakamura, Y., Scheible, W.-R., Ohta, H., & Dörmann, P. (2008). Phospholipase C5 (NPC5) is involved in galactolipid accumulation during phosphate limitation in leaves of Arabidopsis. *The Plant Journal*, *56*(1), 28–39. https://doi.org/10.1111/j.1365-313X.2008.03582.x

Gaude, N., Tippmann, H., Flemetakis, E., Katinakis, P., Udvardi, M., & Dörmann, P. (2004). The galactolipid digalactosyldiacylglycerol accumulates in the peribacteroid membrane of nitrogen-fixing nodules of soybean and Lotus. *The Journal of Biological Chemistry*, *279*(33), 34624–34630. https://doi.org/10.1074/jbc.M404098200

Gerhardt, B., Fischer, K., Balkenhohl, T. J., Pohnert, G., Kühn, H., Wasternack, C., & Feussner, I. (2005). Lipoxygenase-mediated metabolism of storage lipids in germinating sunflower cotyledons and beta-oxidation of (9Z,11E,13S)-13-hydroxy-octadeca-9,11-dienoic acid by the cotyledonary glyoxysomes. *Planta*, *220*(6), 919–930. https://doi.org/10.1007/s00425-004-1408-1

Germain, V., Rylott, E. L., Larson, T. R., Sherson, S. M., Bechtold, N., Carde, J. P., Bryce, J. H., Graham, I. A., & Smith, S. M. (2001). Requirement for 3-ketoacyl-CoA thiolase-2 in peroxisome development, fatty acid beta-oxidation and breakdown of triacylglycerol in lipid bodies of Arabidopsis seedlings. *The Plant Journal: For Cell and Molecular Biology*, *28*(1), 1–12. https://doi.org/10.1046/j.1365-313x.2001.01095.x

Ghosh, A. K., Chauhan, N., Rajakumari, S., Daum, G., & Rajasekharan, R. (2009). At4g24160, a Soluble Acyl-Coenzyme A-Dependent Lysophosphatidic Acid Acyltransferase. *Plant Physiology*, *151*(2), 869–881. https://doi.org/10.1104/pp.109.144261

Ghosh, A. K., Ramakrishnan, G., Chandramohan, C., & Rajasekharan, R. (2008). CGI-58, the causative gene for Chanarin-Dorfman syndrome, mediates acylation of lysophosphatidic acid. *The Journal of Biological Chemistry*, *283*(36), 24525–24533. https://doi.org/10.1074/jbc.M801783200

Gibson, D. G., Young, L., Chuang, R.-Y., Venter, J. C., Hutchison, C. A., & Smith, H. O. (2009). Enzymatic assembly of DNA molecules up to several hundred kilobases. *Nature Methods*, *6*(5), 343–345. https://doi.org/10.1038/nmeth.1318

Gidda, S. K., Shockey, J. M., Rothstein, S. J., Dyer, J. M., & Mullen, R. T. (2009). Arabidopsis thaliana GPAT8 and GPAT9 are localized to the ER and possess distinct ER retrieval signals: Functional divergence of the dilysine ER retrieval motif in plant cells. *Plant Physiology and Biochemistry: PPB*, *47*(10), 867–879. https://doi.org/10.1016/j.plaphy.2009.05.008

Godon, C., Mercier, C., Wang, X., David, P., Richaud, P., Nussaume, L., Liu, D., & Desnos, T. (2019). Under phosphate starvation conditions, Fe and Al trigger accumulation of the transcription factor STOP1 in the nucleus of Arabidopsis root cells. *The Plant Journal: For Cell and Molecular Biology*, *99*(5), 937–949. https://doi.org/10.1111/tpj.14374

Goepfert, S., Hiltunen, J. K., & Poirier, Y. (2006). Identification and Functional Characterization of a Monofunctional Peroxisomal Enoyl-CoA Hydratase 2 That Participates in the Degradation of Even cis-Unsaturated Fatty Acids in Arabidopsis thaliana*. *Journal of Biological Chemistry*, *281*(47), 35894–35903. https://doi.org/10.1074/jbc.M606383200

Goepfert, S., Vidoudez, C., Tellgren-Roth, C., Delessert, S., Hiltunen, J. K., & Poirier, Y. (2008). Peroxisomal Δ3,Δ2-enoyl CoA isomerases and evolution of cytosolic paralogues in embryophytes. *The Plant Journal*, *56*(5), 728–742. https://doi.org/10.1111/j.1365-313X.2008.03635.x

Gomès, E., Jakobsen, M. K., Axelsen, K. B., Geisler, M., & Palmgren, M. G. (2000). Chilling Tolerance in Arabidopsis Involves ALA1, a Member of a New Family of Putative Aminophospholipid Translocases. *The Plant Cell*, *12*(12), 2441–2453. https://doi.org/10.1105/tpc.12.12.2441

Goode, J. H., & Dewey, R. E. (1999). Characterization of aminoalcoholphosphotransferases from Arabidopsis thaliana and soybean. *Plant Physiology and Biochemistry*, *37*(6), 445–457. https://doi.org/10.1016/S0981-9428(99)80049-7

Goss, R., & Latowski, D. (2020). Lipid Dependence of Xanthophyll Cycling in Higher Plants and Algae. *Frontiers in Plant Science*, *11*. https://doi.org/10.3389/fpls.2020.00455

Goss, R., Wilhelm, C., & Garab, G. (2000). Organization of the pigment molecules in the chlorophyll a/b/c containing alga Mantoniella squamata (Prasinophyceae) studied by means of absorption, circular and linear dichroism spectroscopy. *Biochimica Et Biophysica Acta*, *1457*(3), 190–199. https://doi.org/10.1016/s0005-2728(00)00101-8

Graham, I. A. (2008). Seed Storage Oil Mobilization. *Annual Review of Plant Biology*, *59*(1), 115–142. https://doi.org/10.1146/annurev.arplant.59.032607.092938

Graham, I. A., & Eastmond, P. J. (2002). Pathways of straight and branched chain fatty acid catabolism in higher plants. *Progress in Lipid Research*, *41*(2), 156–181. https://doi.org/10.1016/S0163-7827(01)00022-4

Graham, I. A., Li, Y., & Larson, T. R. (2002). Acyl-CoA measurements in plants suggest a role in regulating various cellular processes. *Biochemical Society Transactions*, *30*(Pt 6), 1095–1099. https://doi.org/10.1042/bst0301095

Grosjean, K., Mongrand, S., Beney, L., Simon-Plas, F., & Gerbeau-Pissot, P. (2015). Differential Effect of Plant Lipids on Membrane Organization. *The Journal of Biological Chemistry*, *290*(9), 5810–5825. https://doi.org/10.1074/jbc.M114.598805

Gu, Y., He, L., Zhao, C., Wang, F., Yan, B., Gao, Y., Li, Z., Yang, K., & Xu, J. (2017). Biochemical and Transcriptional Regulation of Membrane Lipid Metabolism in Maize Leaves under Low Temperature. *Frontiers in Plant Science*, *8*. https://www.frontiersin.org/journals/plant-science/articles/10.3389/fpls.2017.02053

Guimarães, C. P., Sá-Miranda, C., & Azevedo, J. E. (2005). Probing substrate-induced conformational alterations in adrenoleukodystrophy protein by proteolysis. *Journal of Human Genetics*, *50*(2), 99–105. https://doi.org/10.1007/s10038-004-0226-4

Gupta, A., & Bhatla, S. C. (2007). Preferential phospholipase A2 activity on the oil bodies in cotyledons during seed germination in *Helianthus annuus* L. cv. Morden. *Plant Science*, *172*(3), 535–543. https://doi.org/10.1016/j.plantsci.2006.11.008

Hammond, J. P., Bennett, M. J., Bowen, H. C., Broadley, M. R., Eastwood, D. C., May, S. T., Rahn, C., Swarup, R., Woolaway, K. E., & White, P. J. (2003). Changes in gene expression in Arabidopsis shoots during phosphate starvation and the potential for developing smart plants. *Plant Physiology*, *132*(2), 578–596. https://doi.org/10.1104/pp.103.020941

Han, G.-S., Wu, W.-I., & Carman, G. M. (2006). The Saccharomyces cerevisiae Lipin Homolog Is a Mg2+-dependent Phosphatidate Phosphatase Enzyme *♦. *Journal of Biological Chemistry*, *281*(14), 9210–9218. https://doi.org/10.1074/jbc.M600425200

Hanchi, M., Thibaud, M.-C., Légeret, B., Kuwata, K., Pochon, N., Beisson, F., Cao, A., Cuyas, L., David, P., Doerner, P., Ferjani, A., Lai, F., Li-Beisson, Y., Mutterer, J., Philibert, M., Raghothama, K. G., Rivasseau, C., Secco, D., Whelan, J., … Javot, H. (2018). The Phosphate Fast-Responsive Genes PECP1 and PPsPase1 Affect Phosphocholine and Phosphoethanolamine Content1[OPEN]. *Plant Physiology*, *176*(4), 2943–2962. https://doi.org/10.1104/pp.17.01246

Hardeman, D., Zomer, H. W., Schutgens, R. B., Tager, J. M., & van den Bosch, H. (1990). Effect of peroxisome proliferation on ether phospholipid biosynthesizing enzymes in rat liver. *The International Journal of Biochemistry*, *22*(12), 1413–1418. https://doi.org/10.1016/0020-711x(90)90231-q

Härtel, H., Dormann, P., & Benning, C. (2000). DGD1-independent biosynthesis of extraplastidic galactolipids after phosphate deprivation in Arabidopsis. *Proceedings of the National Academy of Sciences of the United States of America*, *97*(19), 10649–10654. https://doi.org/10.1073/pnas.180320497

Harwood, J. L., & Okanenko, A. A. (2003). Sulphoquinovosyl Diacylglycerol (SQDG)—The Sulpholipid of Higher Plants. In Y. P. Abrol & A. Ahmad (Eds.), *Sulphur in Plants* (pp. 189–219). Springer Netherlands. https://doi.org/10.1007/978-94-017-0289-8_11

Hashimoto, K., Igarashi, H., Mano, S., Takenaka, C., Shiina, T., Yamaguchi, M., Demura, T., Nishimura, M., Shimmen, T., & Yokota, E. (2008). An isoform of Arabidopsis myosin XI interacts with small GTPases in its C-terminal tail region. *Journal of Experimental Botany*, *59*(13), 3523–3531. https://doi.org/10.1093/jxb/ern202

Hasslacher, M., Ivessa, A. S., Paltauf, F., & Kohlwein, S. D. (1993). Acetyl-CoA carboxylase from yeast is an essential enzyme and is regulated by factors that control phospholipid metabolism. *The Journal of Biological Chemistry*, *268*(15), 10946–10952.

Hatzig, S. V., Nuppenau, J.-N., Snowdon, R. J., & Schießl, S. V. (2018). Drought stress has transgenerational effects on seeds and seedlings in winter oilseed rape (Brassica napus L.). *BMC Plant Biology*, *18*(1), 297. https://doi.org/10.1186/s12870-018-1531-y

Hause, B., Weichert, H., Höhne, M., Kindl, H., & Feussner, I. (2000). Expression of cucumber lipid-body lipoxygenase in transgenic tobacco: Lipid-body lipoxygenase is correctly targeted to seed lipid bodies. *Planta*, *210*(5), 708–714. https://doi.org/10.1007/s004250050671

Hayashi, M., Nito, K., Takei-Hoshi, R., Yagi, M., Kondo, M., Suenaga, A., Yamaya, T., & Nishimura, M. (2002). Ped3p is a Peroxisomal ATP-Binding Cassette Transporter that might Supply Substrates for Fatty Acid β-Oxidation. *Plant and Cell Physiology*, *43*(1), 1–11. https://doi.org/10.1093/pcp/pcf023

Hayashi, M., Toriyama, K., Kondo, M., & Nishimura, M. (1998a). 2,4-Dichlorophenoxybutyric acid-resistant mutants of Arabidopsis have defects in glyoxysomal fatty acid beta-oxidation. *The Plant Cell*, *10*(2), 183–195. https://doi.org/10.1105/tpc.10.2.183

Hayashi, M., Toriyama, K., Kondo, M., & Nishimura, M. (1998b). 2,4-Dichlorophenoxybutyric acid-resistant mutants of Arabidopsis have defects in glyoxysomal fatty acid beta-oxidation. *The Plant Cell*, *10*(2), 183–195.

Hayashi, Y., Hayashi, M., Hayashi, H., Hara-Nishimura, I., & Nishimura, M. (2001). Direct interaction between glyoxysomes and lipid bodies in cotyledons of the Arabidopsis thaliana ped1 mutant. *Protoplasma*, *218*(1–2), 83–94. https://doi.org/10.1007/BF01288364

He, Y., & Gan, S. (2002). A gene encoding an acyl hydrolase is involved in leaf senescence in Arabidopsis. *The Plant Cell*, *14*(4), 805–815. https://doi.org/10.1105/tpc.010422

Heinz, E. (1977). Enzymatic Reactions in Galactolipid Biosynthesis. In M. Tevini & H. K. Lichtenthaler (Eds.), *Lipids and Lipid Polymers in Higher Plants* (pp. 102–120). Springer. https://doi.org/10.1007/978-3-642-66632-2_6

Hellgren, L. I., & Sandelius, A. S. (2001). Age-dependent variation in membrane lipid synthesis in leaves of garden pea (Pisum sativum L.). *Journal of Experimental Botany*, *52*(365), 2275–2282. https://doi.org/10.1093/jexbot/52.365.2275

Hernández, I., & Munné-Bosch, S. (2015). Linking phosphorus availability with photo-oxidative stress in plants. *Journal of Experimental Botany*, *66*(10), 2889–2900. https://doi.org/10.1093/jxb/erv056

Hettema, E. H., van Roermund, C. W., Distel, B., van den Berg, M., Vilela, C., Rodrigues-Pousada, C., Wanders, R. J., & Tabak, H. F. (1996). The ABC transporter proteins Pat1 and Pat2 are required for import of long-chain fatty acids into peroxisomes of Saccharomyces cerevisiae. *The EMBO Journal*, *15*(15), 3813–3822. https://doi.org/10.1002/j.1460-2075.1996.tb00755.x

Hewitt, M. M., Carr, J. M., Williamson, C. L., & Slocum, R. D. (2005). Effects of phosphate limitation on expression of genes involved in pyrimidine synthesis and salvaging in Arabidopsis. *Plant Physiology and Biochemistry: PPB*, *43*(2), 91–99. https://doi.org/10.1016/j.plaphy.2005.01.003

Hicks, L., & Fahimi, H. D. (1977). Peroxisomes (microbodies) in the myocardium of rodents and primates. A comparative Ultrastructural cytochemical study. *Cell and Tissue Research*, *175*(4), 467–481. https://doi.org/10.1007/BF00222413

Hirabayashi, Y., Kwon, S.-K., Paek, H., Pernice, W. M., Paul, M. A., Lee, J., Erfani, P., Raczkowski, A., Petrey, D. S., Pon, L. A., & Polleux, F. (2017). ER-mitochondria tethering by PDZD8 regulates Ca2+ dynamics in mammalian neurons. *Science (New York, N.Y.)*, *358*(6363), 623–630. https://doi.org/10.1126/science.aan6009

Höhne, M., Nellen, A., Schwennesen, K., & Kindl, H. (1996). Lipid Body Lipoxygenase Characterized by Protein Fragmentation, cDNA Sequence and very early Expression of the Enzyme during Germination of Cucumber Seeds. *European Journal of Biochemistry*, *241*(1), 6–11. https://doi.org/10.1111/j.1432-1033.1996.0006t.x

Holthuis, J. C. M., & Levine, T. P. (2005). Lipid traffic: Floppy drives and a superhighway. *Nature Reviews. Molecular Cell Biology*, *6*(3), 209–220. https://doi.org/10.1038/nrm1591

Hölzl, G., & Dörmann, P. (2019). Chloroplast Lipids and Their Biosynthesis. *Annual Review of Plant Biology*, *70*, 51–81. https://doi.org/10.1146/annurev-arplant-050718-100202

Holzmeister, C., Gaupels, F., Geerlof, A., Sarioglu, H., Sattler, M., Durner, J., & Lindermayr, C. (2015). Differential inhibition of Arabidopsis superoxide dismutases by peroxynitrite-mediated tyrosine nitration. *Journal of Experimental Botany*, *66*(3), 989–999. https://doi.org/10.1093/jxb/eru458

Hooks, M. A., Turner, J. E., Murphy, E. C., Johnston, K. A., Burr, S., & Jarosławski, S. (2007). The Arabidopsis ALDP protein homologue COMATOSE is instrumental in peroxisomal acetate metabolism. *The Biochemical Journal*, *406*(3), 399–406. https://doi.org/10.1042/BJ20070258

Horibata, Y., Ando, H., Zhang, P., Vergnes, L., Aoyama, C., Itoh, M., Reue, K., & Sugimoto, H. (2016). StarD7 Protein Deficiency Adversely Affects the Phosphatidylcholine Composition, Respiratory Activity, and Cristae Structure of Mitochondria *. *Journal of Biological Chemistry*, *291*(48), 24880–24891. https://doi.org/10.1074/jbc.M116.736793

Horstman, A., Tonaco, I. A. N., Boutilier, K., & Immink, R. G. H. (2014). A Cautionary Note on the Use of Split-YFP/BiFC in Plant Protein-Protein Interaction Studies. *International Journal of Molecular Sciences*, *15*(6), 6. https://doi.org/10.3390/ijms15069628

Hsiao, E. S. L., & Tzen, J. T. C. (2011). Ubiquitination of oleosin-H and caleosin in sesame oil bodies after seed germination. *Plant Physiology and Biochemistry: PPB*, *49*(1), 77–81. https://doi.org/10.1016/j.plaphy.2010.10.001

Hu, J., Baker, A., Bartel, B., Linka, N., Mullen, R. T., Reumann, S., & Zolman, B. K. (2012). Plant Peroxisomes: Biogenesis and Function. *The Plant Cell*, *24*(6), 2279–2303. https://doi.org/10.1105/tpc.112.096586

Hua, R., Cheng, D., Coyaud, É., Freeman, S., Di Pietro, E., Wang, Y., Vissa, A., Yip, C. M., Fairn, G. D., Braverman, N., Brumell, J. H., Trimble, W. S., Raught, B., & Kim, P. K. (2017). VAPs and ACBD5 tether peroxisomes to the ER for peroxisome maintenance and lipid homeostasis. *Journal of Cell Biology*, *216*(2), 367–377. https://doi.org/10.1083/jcb.201608128

Huang, C.-H., Kuo, W.-Y., Weiss, C., & Jinn, T.-L. (2012). Copper Chaperone-Dependent and -Independent Activation of Three Copper-Zinc Superoxide Dismutase Homologs Localized in Different Cellular Compartments in Arabidopsis1[W][OA]. *Plant Physiology*, *158*(2), 737–746. https://doi.org/10.1104/pp.111.190223

Huang, S., Jiang, L., & Zhuang, X. (2019). Possible Roles of Membrane Trafficking Components for Lipid Droplet Dynamics in Higher Plants and Green Algae. *Frontiers in Plant Science*, *10*, 207. https://doi.org/10.3389/fpls.2019.00207

Huang, S., Liu, Z., Cao, W., Li, H., Zhang, W., Cui, Y., Hu, S., Luo, M., Zhu, Y., Zhao, Q., Xie, L., Gao, C., Xiao, S., & Jiang, L. (2022). The plant ESCRT component FREE1 regulates peroxisome-mediated turnover of lipid droplets in germinating Arabidopsis seedlings. *The Plant Cell*, *34*(11), 4255–4273. https://doi.org/10.1093/plcell/koac195

Hurry, V., Strand, A., Furbank, R., & Stitt, M. (2000). The role of inorganic phosphate in the development of freezing tolerance and the acclimatization of photosynthesis to low temperature is revealed by the pho mutants of Arabidopsis thaliana. *The Plant Journal: For Cell and Molecular Biology*, *24*(3), 383–396. https://doi.org/10.1046/j.1365-313x.2000.00888.x

Igal, R. A., & Coleman, R. A. (1996). Acylglycerol recycling from triacylglycerol to phospholipid, not lipase activity, is defective in neutral lipid storage disease fibroblasts. *The Journal of Biological Chemistry*, *271*(28), 16644–16651. https://doi.org/10.1074/jbc.271.28.16644

Ishikawa, K., Tamura, K., Fukao, Y., & Shimada, T. (2020). Structural and functional relationships between plasmodesmata and plant endoplasmic reticulum–plasma membrane contact sites consisting of three synaptotagmins. *New Phytologist*, *226*(3), 798–808. https://doi.org/10.1111/nph.16391

Iskandarov, U., Silva, J. E., Kim, H. J., Andersson, M., Cahoon, R. E., Mockaitis, K., & Cahoon, E. B. (2017). A Specialized Diacylglycerol Acyltransferase Contributes to the Extreme Medium-Chain Fatty Acid Content of Cuphea Seed Oil. *Plant Physiology*, *174*(1), 97–109. https://doi.org/10.1104/pp.16.01894

J, W., Cr, M., J, L., H, W., T, K., Ma, H., Xj, W., Vb, B., & Nh, C. (2012). The response and recovery of the Arabidopsis thaliana transcriptome to phosphate starvation. *BMC Plant Biology*, *12*. https://doi.org/10.1186/1471-2229-12-62

Jacquier, N., Mishra, S., Choudhary, V., & Schneiter, R. (2013). Expression of oleosin and perilipins in yeast promotes formation of lipid droplets from the endoplasmic reticulum. *Journal of Cell Science*, *126*(Pt 22), 5198–5209. https://doi.org/10.1242/jcs.131896

James, C. N., Horn, P. J., Case, C. R., Gidda, S. K., Zhang, D., Mullen, R. T., Dyer, J. M., Anderson, R. G. W., & Chapman, K. D. (2010). Disruption of the Arabidopsis CGI-58 homologue produces Chanarin-Dorfman-like lipid droplet accumulation in plants. *Proceedings of the National Academy of Sciences of the United States of America*, *107*(41), 17833–17838. https://doi.org/10.1073/pnas.0911359107

Jandrositz, A., Petschnigg, J., Zimmermann, R., Natter, K., Scholze, H., Hermetter, A., Kohlwein, S. D., & Leber, R. (2005). The lipid droplet enzyme Tgl1p hydrolyzes both steryl esters and triglycerides in the yeast, Saccharomyces cerevisiae. *Biochimica Et Biophysica Acta*, *1735*(1), 50–58. https://doi.org/10.1016/j.bbalip.2005.04.005

Jansen, R. L. M., Santana-Molina, C., van den Noort, M., Devos, D. P., & van der Klei, I. J. (2021). Comparative Genomics of Peroxisome Biogenesis Proteins: Making Sense of the PEX Proteins. *Frontiers in Cell and Developmental Biology*, *9*. https://doi.org/10.3389/fcell.2021.654163

Jarvis, P., Dörmann, P., Peto, C. A., Lutes, J., Benning, C., & Chory, J. (2000). Galactolipid deficiency and abnormal chloroplast development in the Arabidopsis MGD synthase 1 mutant. *Proceedings of the National Academy of Sciences of the United States of America*, *97*(14), 8175–8179. https://doi.org/10.1073/pnas.100132197

Jayawardhane, K. N., Singer, S. D., Weselake, R. J., & Chen, G. (2018). Plant sn-Glycerol-3-Phosphate Acyltransferases: Biocatalysts Involved in the Biosynthesis of Intracellular and Extracellular Lipids. *Lipids*, *53*(5), 469–480. https://doi.org/10.1002/lipd.12049

Jennings, W., & Epand, R. M. (2020). CDP-diacylglycerol, a critical intermediate in lipid metabolism. *Chemistry and Physics of Lipids*, *230*, 104914. https://doi.org/10.1016/j.chemphyslip.2020.104914

Jessen, D., Roth, C., Wiermer, M., & Fulda, M. (2015). Two activities of long-chain acyl-coenzyme A synthetase are involved in lipid trafficking between the endoplasmic reticulum and the plastid in Arabidopsis. *Plant Physiology*, *167*(2), 351–366. https://doi.org/10.1104/pp.114.250365

Jia, Y., & Li, W. (2018). Phospholipase D antagonist 1-butanol inhibited the mobilization of triacylglycerol during seed germination in Arabidopsis. *Plant Diversity*, *40*(6), 292–298. https://doi.org/10.1016/j.pld.2018.11.002

Jiménez, J., Bru, S., Ribeiro, M. P., & Clotet, J. (2016). Phosphate: From stardust to eukaryotic cell cycle control. *International Microbiology: The Official Journal of the Spanish Society for Microbiology*, *19*(3), 133–141. https://doi.org/10.2436/20.1501.01.271

Jin, H., Song, Z., & Nikolau, B. J. (2012). Reverse genetic characterization of two paralogous acetoacetyl CoA thiolase genes in Arabidopsis reveals their importance in plant growth and development. *The Plant Journal*, *70*(6), 1015–1032. https://doi.org/10.1111/j.1365-313X.2012.04942.x

Johnston, M. L., Luethy, M. H., Miernyk, J. A., & Randall, D. D. (1997). Cloning and molecular analyses of the *Arabidopsis thaliana* plastid pyruvate dehydrogenase subunits1. *Biochimica et Biophysica Acta (BBA) - Bioenergetics*, *1321*(3), 200–206. https://doi.org/10.1016/S0005-2728(97)00059-5

Jolivet, P., Roux, E., D'Andrea, S., Davanture, M., Negroni, L., Zivy, M., & Chardot, T. (2004). Protein composition of oil bodies in Arabidopsis thaliana ecotype WS. *Plant Physiology and Biochemistry: PPB*, *42*(6), 501–509. https://doi.org/10.1016/j.plaphy.2004.04.006

José A. Trujillo-Hernandez, Laetitia Bariat, Lucia C. Strader, Jean-Philippe Reichheld, & Christophe Belin. (2019). IBA endogenous auxin regulates Arabidopsis root system development in a glutathione-dependent way and is important for adaptation to phosphate deprivation. *BioRxiv*, 818344. https://doi.org/10.1101/818344

Jouhet, J. (2013). Importance of the hexagonal lipid phase in biological membrane organization. *Frontiers in Plant Science*, *4*. https://doi.org/10.3389/fpls.2013.00494

Jouhet, J., Maréchal, E., Baldan, B., Bligny, R., Joyard, J., & Block, M. A. (2004). Phosphate deprivation induces transfer of DGDG galactolipid from chloroplast to mitochondria. *Journal of Cell Biology*, *167*(5), 863–874. https://doi.org/10.1083/jcb.200407022

Jouhet, J., Maréchal, E., Bligny, R., Joyard, J., & Block, M. A. (2003). Transient increase of phosphatidylcholine in plant cells in response to phosphate deprivation. *FEBS Letters*, *544*(1), 63–68. https://doi.org/10.1016/S0014-5793(03)00477-0

Jouhet, J., Maréchal, E., & Block, M. A. (2007). Glycerolipid transfer for the building of membranes in plant cells. *Progress in Lipid Research*, *46*(1), 37–55. https://doi.org/10.1016/j.plipres.2006.06.002

Joyard, J., Douce, R., Siebertz, H. P., & Heinz, E. (1980). Distribution of Radioactive Lipids between Envelopes and Thylakoids from Chloroplasts Labelled in vivo. *European Journal of Biochemistry*, *108*(1), 171–176. https://doi.org/10.1111/j.1432-1033.1980.tb04709.x

Jp, H., Mj, B., Hc, B., Mr, B., Dc, E., St, M., C, R., R, S., Ke, W., & Pj, W. (2003). Changes in gene expression in Arabidopsis shoots during phosphate starvation and the potential for developing smart plants. *Plant Physiology*, *132*(2). https://doi.org/10.1104/pp.103.020941

Jung, S. H., Kim, R. J., Kim, K. J., Lee, D. H., & Suh, M. C. (2019). Plastidial and Mitochondrial Malonyl CoA-ACP Malonyltransferase is Essential for Cell Division and Its Overexpression Increases Storage Oil Content. *Plant and Cell Physiology*, *60*(6), 1239–1249. https://doi.org/10.1093/pcp/pcz032

Just, W. W., Gorgas, K., Hartl, F. U., Heinemann, P., Salzer, M., & Schimassek, H. (1989). Biochemical effects and zonal heterogeneity of peroxisome proliferation induced by perfluorocarboxylic acids in rat liver. *Hepatology (Baltimore, Md.)*, *9*(4), 570–581. https://doi.org/10.1002/hep.1840090411

Juszczuk, I., Malusà, E., & Rychter, A. M. (2001). Oxidative stress during phosphate deficiency in roots of bean plants (*Phaseolus vulgaris* L.). *Journal of Plant Physiology*, *158*(10), 1299–1305. https://doi.org/10.1078/0176-1617-00541

Kader, J.-C. (1996). LIPID-TRANSFER PROTEINS IN PLANTS. *Annual Review of Plant Biology*, *47*(Volume 47, 1996), 627–654. https://doi.org/10.1146/annurev.arplant.47.1.627

Kamp, F., & Hamilton, J. A. (2006). How fatty acids of different chain length enter and leave cells by free diffusion. *Prostaglandins, Leukotrienes and Essential Fatty Acids*, *75*(3), 149–159. https://doi.org/10.1016/j.plefa.2006.05.003

Kang, H., Jia, C., Liu, N., Aboagla, A. A. A., Chen, W., Gong, W., Tang, S., & Hong, Y. (2020). Plastid Glycerol-3-phosphate Acyltransferase Enhanced Plant Growth and Prokaryotic Glycerolipid Synthesis in Brassica napus. *International Journal of Molecular Sciences*, *21*(15), 5325. https://doi.org/10.3390/ijms21155325

Kao, Y.-T., Gonzalez, K. L., & Bartel, B. (2018). Peroxisome Function, Biogenesis, and Dynamics in Plants. *Plant Physiology*, *176*(1), 162–177. https://doi.org/10.1104/pp.17.01050

Kaplan, M. R., & Simoni, R. D. (1985). Intracellular transport of phosphatidylcholine to the plasma membrane. *Journal of Cell Biology*, *101*(2), 441–445. https://doi.org/10.1083/jcb.101.2.441

Karki, N., Johnson, B. S., & Bates, P. D. (2019). Metabolically Distinct Pools of Phosphatidylcholine Are Involved in Trafficking of Fatty Acids out of and into the Chloroplast for Membrane Production. *The Plant Cell*, *31*(11), 2768–2788. https://doi.org/10.1105/tpc.19.00121

Kaup, M. T., Froese, C. D., & Thompson, J. E. (2002). A Role for Diacylglycerol Acyltransferase during Leaf Senescence. *Plant Physiology*, *129*(4), 1616–1626. https://doi.org/10.1104/pp.003087

Ke, J., Wen, T.-N., Nikolau, B. J., & Wurtele, E. S. (2000). Coordinate Regulation of the Nuclear and Plastidic Genes Coding for the Subunits of the Heteromeric Acetyl-Coenzyme A Carboxylase. *Plant Physiology*, *122*(4), 1057–1072.

Kelly, A. A., & Dörmann, P. (2002). DGD2, an Arabidopsis Gene Encoding a UDP-Galactose-dependent Digalactosyldiacylglycerol Synthase Is Expressed during Growth under Phosphate-limiting Conditions *. *Journal of Biological Chemistry*, *277*(2), 1166–1173. https://doi.org/10.1074/jbc.M110066200

Kelly, A. A., & Dörmann, P. (2004). Green light for galactolipid trafficking. *Current Opinion in Plant Biology*, *7*(3), 262–269. https://doi.org/10.1016/j.pbi.2004.03.009

Kelly, A. A., Froehlich, J. E., & Dörmann, P. (2003). Disruption of the two digalactosyldiacylglycerol synthase genes DGD1 and DGD2 in Arabidopsis reveals the existence of an additional enzyme of galactolipid synthesis. *The Plant Cell*, *15*(11), 2694–2706. https://doi.org/10.1105/tpc.016675

Kelly, A. A., Kalisch, B., Hölzl, G., Schulze, S., Thiele, J., Melzer, M., Roston, R. L., Benning, C., & Dörmann, P. (2016). Synthesis and transfer of galactolipids in the chloroplast envelope membranes of Arabidopsis thaliana. *Proceedings of the National Academy of Sciences of the United States of America*, *113*(38), 10714–10719. https://doi.org/10.1073/pnas.1609184113

Kelly, A. A., Quettier, A.-L., Shaw, E., & Eastmond, P. J. (2011). Seed storage oil mobilization is important but not essential for germination or seedling establishment in Arabidopsis. *Plant Physiology*, *157*(2), 866–875. https://doi.org/10.1104/pp.111.181784

Kelly, A. A., van Erp, H., Quettier, A.-L., Shaw, E., Menard, G., Kurup, S., & Eastmond, P. J. (2013). The sugar-dependent1 lipase limits triacylglycerol accumulation in vegetative tissues of Arabidopsis. *Plant Physiology*, *162*(3), 1282–1289. https://doi.org/10.1104/pp.113.219840

Kennedy, E. P. (1961). Biosynthesis of complex lipids. *Federation Proceedings*, *20*, 934–940.

Keogh, M. R., Courtney, P. D., Kinney, A. J., & Dewey, R. E. (2009). Functional Characterization of Phospholipid N-Methyltransferases from Arabidopsis and Soybean *. *Journal of Biological Chemistry*, *284*(23), 15439–15447. https://doi.org/10.1074/jbc.M109.005991

Khan, B. R., Adham, A. R., & Zolman, B. K. (2012). Peroxisomal Acyl-CoA oxidase 4 activity differs between Arabidopsis accessions. *Plant Molecular Biology*, *78*(1), 45–58. https://doi.org/10.1007/s11103-011-9843-4

Kikuchi, M., Hatano, N., Yokota, S., Shimozawa, N., Imanaka, T., & Taniguchi, H. (2004). Proteomic analysis of rat liver peroxisome: Presence of peroxisome-specific isozyme of Lon protease. *The Journal of Biological Chemistry*, *279*(1), 421–428. https://doi.org/10.1074/jbc.M305623200

Kim, E. Y., Seo, Y. S., & Kim, W. T. (2011). AtDSEL, an Arabidopsis cytosolic DAD1-like acylhydrolase, is involved in negative regulation of storage oil mobilization during seedling establishment. *Journal of Plant Physiology*, *168*(14), 1705–1709. https://doi.org/10.1016/j.jplph.2011.03.004

Kim, H. U., Hsieh, K., Ratnayake, C., & Huang, A. H. C. (2002). A Novel Group of Oleosins Is Present Inside the Pollen ofArabidopsis *. *Journal of Biological Chemistry*, *277*(25), 22677–22684. https://doi.org/10.1074/jbc.M109298200

Kim, H. U., & Huang, A. H. C. (2004). Plastid lysophosphatidyl acyltransferase is essential for embryo development in Arabidopsis. *Plant Physiology*, *134*(3), 1206–1216. https://doi.org/10.1104/pp.103.035832

Kim, H. U., Li, Y., & Huang, A. H. C. (2005). Ubiquitous and endoplasmic reticulum-located lysophosphatidyl acyltransferase, LPAT2, is essential for female but not male gametophyte development in Arabidopsis. *The Plant Cell*, *17*(4), 1073–1089. https://doi.org/10.1105/tpc.104.030403

Kim, R. J., Kim, H. J., Shim, D., & Suh, M. C. (2016). Molecular and biochemical characterizations of the monoacylglycerol lipase gene family of Arabidopsis thaliana. *The Plant Journal: For Cell and Molecular Biology*, *85*(6), 758–771. https://doi.org/10.1111/tpj.13146

Kirchhoff, H. (2008). Molecular crowding and order in photosynthetic membranes. *Trends in Plant Science*, *13*(5), 201–207. https://doi.org/10.1016/j.tplants.2008.03.001

Kirchhoff, H. (2018). Structure-function relationships in photosynthetic membranes: Challenges and emerging fields. *Plant Science: An International Journal of Experimental Plant Biology*, *266*, 76–82. https://doi.org/10.1016/j.plantsci.2017.09.021

Klaus, D., Härtel, H., Fitzpatrick, L. M., Froehlich, J. E., Hubert, J., Benning, C., & Dörmann, P. (2002). Digalactosyldiacylglycerol Synthesis in Chloroplasts of the Arabidopsis dgd1 Mutant. *Plant Physiology*, *128*(3), 885–895. https://doi.org/10.1104/pp.010780

Kliebenstein, D. J., Monde, R. A., & Last, R. L. (1998). Superoxide dismutase in Arabidopsis: An eclectic enzyme family with disparate regulation and protein localization. *Plant Physiology*, *118*(2), 637–650. https://doi.org/10.1104/pp.118.2.637

Kobayashi, K., Awai, K., Nakamura, M., Nagatani, A., Masuda, T., & Ohta, H. (2009). Type-B monogalactosyldiacylglycerol synthases are involved in phosphate starvation-induced lipid remodeling, and are crucial for low-phosphate adaptation. *The Plant Journal*, *57*(2), 322–331. https://doi.org/10.1111/j.1365-313X.2008.03692.x

Kobayashi, K., Awai, K., Takamiya, K., & Ohta, H. (2004). Arabidopsis Type B Monogalactosyldiacylglycerol Synthase Genes Are Expressed during Pollen Tube Growth and Induced by Phosphate Starvation. *Plant Physiology*, *134*(2), 640–648. https://doi.org/10.1104/pp.103.032656

Kobayashi, K., Kondo, M., Fukuda, H., Nishimura, M., & Ohta, H. (2007). Galactolipid synthesis in chloroplast inner envelope is essential for proper thylakoid biogenesis, photosynthesis, and embryogenesis. *Proceedings of the National Academy of Sciences of the United States of America*, *104*(43), 17216–17221. https://doi.org/10.1073/pnas.0704680104

Kodama, H., Horiguchi, G., Nishiuchi, T., Nishimura, M., & Iba, K. (1995). Fatty Acid Desaturation during Chilling Acclimation Is One of the Factors Involved in Conferring Low-Temperature Tolerance to Young Tobacco Leaves. *Plant Physiology*, *107*(4), 1177–1185. https://doi.org/10.1104/pp.107.4.1177

Kode, V., Mudd, E. A., Iamtham, S., & Day, A. (2005). The tobacco plastid accD gene is essential and is required for leaf development. *The Plant Journal: For Cell and Molecular Biology*, *44*(2), 237–244. https://doi.org/10.1111/j.1365-313X.2005.02533.x

Köker, T., Fernandez, A., & Pinaud, F. (2018). Characterization of Split Fluorescent Protein Variants and Quantitative Analyses of Their Self-Assembly Process. *Scientific Reports*, *8*(1), 5344. https://doi.org/10.1038/s41598-018-23625-7

Kol, M. A., de Kruijff, B., & de Kroon, A. I. P. M. (2002). Phospholipid flip-flop in biogenic membranes: What is needed to connect opposite sides. *Seminars in Cell & Developmental Biology*, *13*(3), 163–170. https://doi.org/10.1016/S1084-9521(02)00044-7

Koo, A. J. K., Chung, H. S., Kobayashi, Y., & Howe, G. A. (2006). Identification of a peroxisomal acyl-activating enzyme involved in the biosynthesis of jasmonic acid in Arabidopsis. *The Journal of Biological Chemistry*, *281*(44), 33511–33520. https://doi.org/10.1074/jbc.M607854200

Koo, A. J. K., Ohlrogge, J. B., & Pollard, M. (2004). On the Export of Fatty Acids from the Chloroplast *. *Journal of Biological Chemistry*, *279*(16), 16101–16110. https://doi.org/10.1074/jbc.M311305200

Kopriva, S., & Rennenberg, H. (2004). Control of sulphate assimilation and glutathione synthesis: Interaction with N and C metabolism. *Journal of Experimental Botany*, *55*(404), 1831–1842. https://doi.org/10.1093/jxb/erh203

Korn, E. D. (1966). Structure of biological membranes. *Science (New York, N.Y.)*, *153*(3743), 1491–1498. https://doi.org/10.1126/science.153.3743.1491

Kornmann, B., Currie, E., Collins, S. R., Schuldiner, M., Nunnari, J., Weissman, J. S., & Walter, P. (2009). An ER-Mitochondria Tethering Complex Revealed by a Synthetic Biology Screen. *Science*, *325*(5939), 477–481. https://doi.org/10.1126/science.1175088

Krapp, A., Saliba-Colombani, V., & Daniel-Vedele, F. (2005). Analysis of C and N metabolisms and of C/N interactions using quantitative genetics. *Photosynthesis Research*, *83*(2), 251–263. https://doi.org/10.1007/s11120-004-3196-7

Kretzschmar, F. K., Doner, N. M., Krawczyk, H. E., Scholz, P., Schmitt, K., Valerius, O., Braus, G. H., Mullen, R. T., & Ischebeck, T. (2020). Identification of Low-Abundance Lipid Droplet Proteins in Seeds and Seedlings1[OPEN]. *Plant Physiology*, *182*(3), 1326–1345. https://doi.org/10.1104/pp.19.01255

Kretzschmar, F. K., Mengel, L. A., Müller, A. O., Schmitt, K., Blersch, K. F., Valerius, O., Braus, G. H., & Ischebeck, T. (2018). PUX10 Is a Lipid Droplet-Localized Scaffold Protein That Interacts with CELL DIVISION CYCLE48 and Is

Involved in the Degradation of Lipid Droplet Proteins. *The Plant Cell*, *30*(9), 2137–2160. https://doi.org/10.1105/tpc.18.00276

Kritsiligkou, P., Chatzi, A., Charalampous, G., Mironov, A., Grant, C. M., & Tokatlidis, K. (2017). Unconventional Targeting of a Thiol Peroxidase to the Mitochondrial Intermembrane Space Facilitates Oxidative Protein Folding. *Cell Reports*, *18*(11), 2729–2741. https://doi.org/10.1016/j.celrep.2017.02.053

Kruft, V., Eubel, H., Jänsch, L., Werhahn, W., & Braun, H. P. (2001). Proteomic approach to identify novel mitochondrial proteins in Arabidopsis. *Plant Physiology*, *127*(4), 1694–1710.

Kunst, L., Browse, J., & Somerville, C. (1989a). A mutant of Arabidopsis deficient in desaturation of palmitic Acid in leaf lipids. *Plant Physiology*, *90*(3), 943–947. https://doi.org/10.1104/pp.90.3.943

Kunst, L., Browse, J., & Somerville, C. (1989b). Enhanced thermal tolerance in a mutant of Arabidopsis deficient in palmitic Acid unsaturation. *Plant Physiology*, *91*(1), 401–408. https://doi.org/10.1104/pp.91.1.401

Kunz, H.-H., Scharnewski, M., Feussner, K., Feussner, I., Flügge, U.-I., Fulda, M., & Gierth, M. (2009). The ABC Transporter PXA1 and Peroxisomal β-Oxidation Are Vital for Metabolism in Mature Leaves of Arabidopsis during Extended Darkness. *The Plant Cell*, *21*(9), 2733–2749. https://doi.org/10.1105/tpc.108.064857

Kustatscher, G., Grabowski, P., Schrader, T. A., Passmore, J. B., Schrader, M., & Rappsilber, J. (2019). Co-regulation map of the human proteome enables identification of protein functions. *Nature Biotechnology*, *37*(11), 1361–1371. https://doi.org/10.1038/s41587-019-0298-5

Kwon, Y., Yu, S., Lee, H., Yim, J. H., Zhu, J.-K., & Lee, B. (2012). Arabidopsis Serine Decarboxylase Mutants Implicate the Roles of Ethanolamine in Plant Growth and Development. *International Journal of Molecular Sciences*, *13*(3), 3. https://doi.org/10.3390/ijms13033176

LaBrant, E., Barnes, A. C., & Roston, R. L. (2018a). Lipid transport required to make lipids of photosynthetic membranes. *Photosynthesis Research*, *138*(3), 345–360. https://doi.org/10.1007/s11120-018-0545-5

LaBrant, E., Barnes, A. C., & Roston, R. L. (2018b). Lipid transport required to make lipids of photosynthetic membranes. *Photosynthesis Research*, *138*(3), 345–360. https://doi.org/10.1007/s11120-018-0545-5

Lahiri, S., Chao, J. T., Tavassoli, S., Wong, A. K. O., Choudhary, V., Young, B. P., Loewen, C. J. R., & Prinz, W. A. (2014). A Conserved Endoplasmic Reticulum Membrane Protein Complex (EMC) Facilitates Phospholipid Transfer from the ER to Mitochondria. *PLoS Biology*, *12*(10), e1001969. https://doi.org/10.1371/journal.pbio.1001969

Lambers, H. (2022). Phosphorus Acquisition and Utilization in Plants. *Annual Review of Plant Biology*, *73*(1), 17–42. https://doi.org/10.1146/annurev-arplant-102720-125738

Larsson, K. E., Kjellberg, J. M., Tjellström, H., & Sandelius, A. S. (2007). LysoPC acyltransferase/PC transacylase activities in plant plasma membrane and plasma membrane-associated endoplasmic reticulum. *BMC Plant Biology*, *7*, 64. https://doi.org/10.1186/1471-2229-7-64

Lass, A., Zimmermann, R., Haemmerle, G., Riederer, M., Schoiswohl, G., Schweiger, M., Kienesberger, P., Strauss, J. G., Gorkiewicz, G., & Zechner, R. (2006). Adipose triglyceride lipase-mediated lipolysis of cellular fat stores is activated by CGI-58 and defective in Chanarin-Dorfman Syndrome. *Cell Metabolism*, *3*(5), 309–319. https://doi.org/10.1016/j.cmet.2006.03.005

Lazarow, P. B. (2022). The Peroxisome. In R. A. Bradshaw, G. W. Hart, & P. D. Stahl (Eds.), *Encyclopedia of Cell Biology (Second Edition)* (pp. 298–341). Academic Press. https://doi.org/10.1016/B978-0-12-821618-7.00127-9

Lazarow, P. B., & Fujiki, Y. (1985). Biogenesis of peroxisomes. *Annual Review of Cell Biology*, *1*, 489–530. https://doi.org/10.1146/annurev.cb.01.110185.002421

Lee, E., Santana, B. V. N., Samuels, E., Benitez-Fuente, F., Corsi, E., Botella, M. A., Perez-Sancho, J., Vanneste, S., Friml, J., Macho, A., Azevedo, A. A., & Rosado, A. (2020). Rare earth elements induce cytoskeleton-dependent and PI4P-associated rearrangement of SYT1/SYT5 endoplasmic reticulum–plasma membrane contact site complexes in Arabidopsis. *Journal of Experimental Botany*, *71*(14), 3986–3998. https://doi.org/10.1093/jxb/eraa138

Lee, H. G., Kim, H., Suh, M. C., Kim, H. U., & Seo, P. J. (2018). The MYB96 Transcription Factor Regulates Triacylglycerol Accumulation by Activating DGAT1 and PDAT1 Expression in Arabidopsis Seeds. *Plant & Cell Physiology*, *59*(7), 1432–1442. https://doi.org/10.1093/pcp/pcy073

Lee, H. G., & Seo, P. J. (2018). Interaction of DGAT1 and PDAT1 to enhance TAG assembly in Arabidopsis. *Plant Signaling & Behavior*, *14*(1), 1554467. https://doi.org/10.1080/15592324.2018.1554467

Lefèvre, C., Jobard, F., Caux, F., Bouadjar, B., Karaduman, A., Heilig, R., Lakhdar, H., Wollenberg, A., Verret, J. L., Weissenbach, J., Ozgüc, M., Lathrop, M., Prud'homme, J. F., & Fischer, J. (2001). Mutations in CGI-58, the gene encoding a new protein of the esterase/lipase/thioesterase subfamily, in Chanarin-Dorfman syndrome. *American Journal of Human Genetics*, *69*(5), 1002–1012. https://doi.org/10.1086/324121

Lenburg, M. E., & O'Shea, E. K. (1996). Signaling phosphate starvation. *Trends in Biochemical Sciences*, *21*(10), 383–387. https://doi.org/10.1016/S0968-0004(96)10048-7

Leterme, S., & Michaud, M. (2022). Chapter Four—Non-vesicular glycerolipids transport in plant cells. In F. Rébeillé & E. Maréchal (Eds.), *Advances in Botanical Research* (Vol. 101, pp. 121–189). Academic Press. https://doi.org/10.1016/bs.abr.2021.07.001

Leterme, S., Michaud, M., & Jouhet, J. (2021). Isolation of mitochondria for lipid analysis. In D. Bartels & P. Dörmann (Eds.), *Plant Lipids -Methods and Protocols* (Vol. 2295, pp. 337–349). Humana Press, New York, NY. https://doi.org/10.1007/978-1-0716-1362-7_18

Li, C., Cheng, X., Jia, Q., Song, H., Liu, X., Wang, K., Zhao, C., Zhang, Y., Ohlrogge, J., & Zhang, M. (2017). Investigation of Plant Species with Identified Seed Oil Fatty Acids in Chinese Literature and Analysis of Five Unsurveyed Chinese Endemic Species. *Frontiers in Plant Science*, *8*, 224. https://doi.org/10.3389/fpls.2017.00224

Li, C., Duckney, P., Zhang, T., Fu, Y., Li, X., Kroon, J., De Jaeger, G., Cheng, Y., Hussey, P. J., & Wang, P. (2022). TraB family proteins are components of ER-mitochondrial contact sites and regulate ER-mitochondrial interactions and mitophagy. *Nature Communications*, *13*, 5658. https://doi.org/10.1038/s41467-022-33402-w

Li, C., Liu, G., Liu, Q., Godwin, I. D., & Gilbert, R. G. (2015). Characterization of the time evolution of starch structure from rice callus. *Carbohydrate Polymers*, *127*, 116–123. https://doi.org/10.1016/j.carbpol.2015.03.046

Li, D., Zhu, H., Liu, K., Liu, X., Leggewie, G., Udvardi, M., & Wang, D. (2002a). Purple acid phosphatases of Arabidopsis thaliana. Comparative analysis and differential regulation by phosphate deprivation. *The Journal of Biological Chemistry*, *277*(31), 27772–27781. https://doi.org/10.1074/jbc.M204183200

Li, D., Zhu, H., Liu, K., Liu, X., Leggewie, G., Udvardi, M., & Wang, D. (2002b). Purple acid phosphatases of Arabidopsis thaliana. Comparative analysis and differential regulation by phosphate deprivation. *The Journal of Biological Chemistry*, *277*(31), 27772–27781. https://doi.org/10.1074/jbc.M204183200

Li, L., Liu, C., & Lian, X. (2010). Gene expression profiles in rice roots under low phosphorus stress. *Plant Molecular Biology*, *72*(4), 423–432. https://doi.org/10.1007/s11103-009-9580-0

Li, M., Qin, C., Welti, R., & Wang, X. (2006). Double knockouts of phospholipases Dzeta1 and Dzeta2 in Arabidopsis affect root elongation during phosphate-limited growth but do not affect root hair patterning. *Plant Physiology*, *140*(2), 761–770. https://doi.org/10.1104/pp.105.070995

Li, M., Welti, R., & Wang, X. (2006). Quantitative profiling of Arabidopsis polar glycerolipids in response to phosphorus starvation. Roles of phospholipases D zeta1 and D zeta2 in phosphatidylcholine hydrolysis and digalactosyldiacylglycerol accumulation in phosphorus-starved plants. *Plant Physiology*, *142*(2), 750–761. https://doi.org/10.1104/pp.106.085647

Li, S. J., & Cronan, J. E. (1992). The genes encoding the two carboxyltransferase subunits of Escherichia coli acetyl-CoA carboxylase. *The Journal of Biological Chemistry*, *267*(24), 16841–16847.

Li, W., Li, M., Zhang, W., Welti, R., & Wang, X. (2004). The plasma membrane-bound phospholipase Ddelta enhances freezing tolerance in Arabidopsis thaliana. *Nature Biotechnology*, *22*(4), 427–433. https://doi.org/10.1038/nbt949

Li, X., Gamuyao, R., Wu, M.-L., Cho, W. J., King, S. V., Petersen, R. A., Stabley, D. R., Lindow, C., Climer, L. K., Shirinifard, A., Ferrara, F., Throm, R. E., Robinson, C. G., Zhou, Y., Carisey, A. F., Tebo, A. G., & Chang, C.-L. (2024). A fluorogenic complementation tool kit for interrogating lipid droplet-organelle interaction. *The Journal of Cell Biology*, *223*(9), e202311126. https://doi.org/10.1083/jcb.202311126

Liavonchanka, A., & Feussner, I. (2006). Lipoxygenases: Occurrence, functions and catalysis. *Journal of Plant Physiology*, *163*(3), 348–357. https://doi.org/10.1016/j.jplph.2005.11.006

Li-Beisson, Y., Shorrosh, B., Beisson, F., Andersson, M. X., Arondel, V., Bates, P. D., Baud, S., Bird, D., DeBono, A., Durrett, T. P., Franke, R. B., Graham, I. A., Katayama, K., Kelly, A. A., Larson, T., Markham, J. E., Miquel, M., Molina, I., Nishida, I., … Ohlrogge, J. (2013). Acyl-Lipid Metabolism. *The Arabidopsis Book*, *11*, e0161. https://doi.org/10.1199/tab.0161

Li-Beisson, Y., & Wada, H. (2019). Plant and algal lipids set sail for new horizons. *Plant and Cell Physiology*, *60*(6), 1161. https://doi.org/10.1093/pcp/pcz092/5489916

Lin, J.-S., Ali, J., & Lai, E.-M. (2024). Protein-Protein Interactions: Co-immunoprecipitation. *Methods in Molecular Biology (Clifton, N.J.)*, *2715*, 273–283. https://doi.org/10.1007/978-1-0716-3445-5_18

Lin, J.-S., & Lai, E.-M. (2017). Protein-Protein Interactions: Co-Immunoprecipitation. *Methods in Molecular Biology (Clifton, N.J.)*, *1615*, 211–219. https://doi.org/10.1007/978-1-4939-7033-9_17

Lin, Y.-C., Kobayashi, K., Hung, C.-H., Wada, H., & Nakamura, Y. (2016). Arabidopsis phosphatidylglycerophosphate phosphatase 1 involved in phosphatidylglycerol biosynthesis and photosynthetic function. *The Plant Journal: For Cell and Molecular Biology*, *88*(6), 1022–1037. https://doi.org/10.1111/tpj.13311

Lindquist, E., & Aronsson, H. (2018). Chloroplast vesicle transport. *Photosynthesis Research*, *138*(3), 361–371. https://doi.org/10.1007/s11120-018-0566-0

Linka, N., Theodoulou, F. L., Haslam, R. P., Linka, M., Napier, J. A., Neuhaus, H. E., & Weber, A. P. M. (2008). Peroxisomal ATP import is essential for seedling development in Arabidopsis thaliana. *The Plant Cell*, *20*(12), 3241–3257. https://doi.org/10.1105/tpc.108.062042

Lipp, N.-F., Ikhlef, S., Milanini, J., & Drin, G. (2020). Lipid Exchangers: Cellular Functions and Mechanistic Links With Phosphoinositide Metabolism. *Frontiers in Cell and Developmental Biology*, *8*, 663. https://doi.org/10.3389/fcell.2020.00663

Lisenbee, C. S., Lingard, M. J., & Trelease, R. N. (2005). Arabidopsis peroxisomes possess functionally redundant membrane and matrix isoforms of monodehydroascorbate reductase. *The Plant Journal: For Cell and Molecular Biology*, *43*(6), 900–914. https://doi.org/10.1111/j.1365-313X.2005.02503.x

Lister, R., Carrie, C., Duncan, O., Ho, L. H. M., Howell, K. A., Murcha, M. W., & Whelan, J. (2007). Functional Definition of Outer Membrane Proteins Involved in Preprotein Import into Mitochondria. *The Plant Cell*, *19*(11), 3739–3759. https://doi.org/10.1105/tpc.107.050534

Liszkay, A., van der Zalm, E., & Schopfer, P. (2004). Production of Reactive Oxygen Intermediates (O2 ˙−, H2O2, and ˙OH) by Maize Roots and Their Role in Wall Loosening and Elongation Growth. *Plant Physiology*, *136*(2), 3114–3123. https://doi.org/10.1104/pp.104.044784

Liu, Y., Wang, G., & Wang, X. (2015). Role of Aminoalcoholphosphotransferases 1 and 2 in Phospholipid Homeostasis in Arabidopsis. *The Plant Cell*, *27*(5), 1512–1528. https://doi.org/10.1105/tpc.15.00180

Liu, Y., Wu, G., Ke, X., Zheng, Z., & Zheng, Y. (2023). Loss-of-Function of ATS1 Enhances Arabidopsis Salt Tolerance. *Plants*, *12*(14), 14. https://doi.org/10.3390/plants12142646

Lodhi, I. J., & Semenkovich, C. F. (2014). Peroxisomes: A Nexus for Lipid Metabolism and Cellular Signaling. *Cell Metabolism*, *19*(3), 380–392. https://doi.org/10.1016/j.cmet.2014.01.002

Löfke, C., Ischebeck, T., König, S., Freitag, S., & Heilmann, I. (2008). Alternative metabolic fates of phosphatidylinositol produced by phosphatidylinositol synthase isoforms in Arabidopsis thaliana. *The Biochemical Journal*, *413*(1), 115–124. https://doi.org/10.1042/BJ20071371

López-Arredondo, D. L., Leyva-González, M. A., Alatorre-Cobos, F., & Herrera-Estrella, L. (2013). Biotechnology of nutrient uptake and assimilation in plants. *The International Journal of Developmental Biology*, *57*(6-7–8), 6-7–8. https://doi.org/10.1387/ijdb.130268lh

López-Arredondo, D. L., Leyva-González, M. A., González-Morales, S. I., López-Bucio, J., & Herrera-Estrella, L. (2014). Phosphate Nutrition: Improving Low-Phosphate Tolerance in Crops. *Annual Review of Plant Biology*, *65*(1), 95–123. https://doi.org/10.1146/annurev-arplant-050213-035949

López-Bucio, J., Hernández-Abreu, E., Sánchez-Calderón, L., Nieto-Jacobo, M. F., Simpson, J., & Herrera-Estrella, L. (2002). Phosphate availability alters architecture and causes changes in hormone sensitivity in the Arabidopsis root system. *Plant Physiology*, *129*(1), 244–256. https://doi.org/10.1104/pp.010934

López-Casillas, F., Bai, D. H., Luo, X. C., Kong, I. S., Hermodson, M. A., & Kim, K. H. (1988). Structure of the coding sequence and primary amino acid sequence of acetyl-coenzyme A carboxylase. *Proceedings of the National Academy of Sciences of the United States of America*, *85*(16), 5784–5788.

López-Erauskin, J., Galino, J., Ruiz, M., Cuezva, J. M., Fabregat, I., Cacabelos, D., Boada, J., Martínez, J., Ferrer, I., Pamplona, R., Villarroya, F., Portero-Otín, M., Fourcade, S., & Pujol, A. (2013). Impaired mitochondrial oxidative phosphorylation in the peroxisomal disease X-linked adrenoleukodystrophy. *Human Molecular Genetics*, *22*(16), 3296–3305. https://doi.org/10.1093/hmg/ddt186

Lord, C. C., Betters, J. L., Ivanova, P. T., Milne, S. B., Myers, D. S., Madenspacher, J., Thomas, G., Chung, S., Liu, M., Davis, M. A., Lee, R. G., Crooke, R. M., Graham, M. J., Parks, J. S., Brasaemle, D. L., Fessler, M. B., Brown, H. A., & Brown, J. M. (2012). CGI-58/ABHD5-derived signaling lipids regulate systemic inflammation and insulin action. *Diabetes*, *61*(2), 355–363. https://doi.org/10.2337/db11-0994

Lou, H. Q., Fan, W., Xu, J. M., Gong, Y. L., Jin, J. F., Chen, W. W., Liu, L. Y., Hai, M. R., Yang, J. L., & Zheng, S. J. (2016). An Oxalyl-CoA Synthetase Is Involved in Oxalate Degradation and Aluminum Tolerance. *Plant Physiology*, *172*(3), 1679–1690. https://doi.org/10.1104/pp.16.01106

Lu, C., Xin, Z., Ren, Z., Miquel, M., & Browse, J. (2009). An enzyme regulating triacylglycerol composition is encoded by the ROD1 gene of Arabidopsis. *Proceedings of the National Academy of Sciences of the United States of America*, *106*(44), 18837–18842. https://doi.org/10.1073/pnas.0908848106

Lü, S., Song, T., Kosma, D. K., Parsons, E. P., Rowland, O., & Jenks, M. A. (2009). Arabidopsis CER8 encodes LONG-CHAIN ACYL-COA SYNTHETASE 1 (LACS1) that has overlapping functions with LACS2 in plant wax and cutin synthesis. *The Plant Journal: For Cell and Molecular Biology*, *59*(4), 553–564. https://doi.org/10.1111/j.1365-313X.2009.03892.x

Lynch, D. V., & Dunn, T. M. (2004). An introduction to plant sphingolipids and a review of recent advances in understanding their metabolism and function. *New Phytologist*, *161*(3), 677–702. https://doi.org/10.1111/j.1469-8137.2004.00992.x

Lynch, J. (1995). Root Architecture and Plant Productivity. *Plant Physiology*, *109*(1), 7–13.
Ma, X.-F., Wright, E., Ge, Y., Bell, J., Xi, Y., Bouton, J. H., & Wang, Z.-Y. (2009). Improving phosphorus acquisition of white clover (Trifolium repens L.) by transgenic expression of plant-derived phytase and acid phosphatase genes. *Plant Science: An International Journal of Experimental Plant Biology*, *176*(4), 479–488. https://doi.org/10.1016/j.plantsci.2009.01.001
Maatta, S., Scheu, B., Li, M., Wang, X., & Welti, R. (2012). Levels of Arabidopsis thaliana Leaf Phosphatidic Acids, Phosphatidylserines, and Most Trienoate-Containing Polar Lipid Molecular Species Increase during the Dark Period of the Diurnal Cycle. *Frontiers in Plant Science*, *3*. https://doi.org/10.3389/fpls.2012.00049
Mackender, R. O., & Leech, R. M. (1974). The Galactolipid, Phospholipid, and Fatty Acid Composition of the Chloroplast Envelope Membranes of Vicia faba. L. *Plant Physiology*, *53*(3), 496–502. https://doi.org/10.1104/pp.53.3.496
Maeda, N., Kokai, Y., Ohtani, S., Sahara, H., Kumamoto-Yonezawa, Y., Kuriyama, I., Hada, T., Sato, N., Yoshida, H., & Mizushina, Y. (2008). Anti-tumor effect of orally administered spinach glycolipid fraction on implanted cancer cells, colon-26, in mice. *Lipids*, *43*(8), 741–748. https://doi.org/10.1007/s11745-008-3202-5
Mair, A., Xu, S.-L., Branon, T. C., Ting, A. Y., & Bergmann, D. C. (2019). Proximity labeling of protein complexes and cell-type-specific organellar proteomes in Arabidopsis enabled by TurboID. *ELife*, *8*, e47864. https://doi.org/10.7554/eLife.47864
Mansfeld, J., Schöpfel, M., Lorenz, J., Trutschel, T., Heilmann, I., Brandt, W., & Ulbrich-Hofmann, R. (2014). Probing selected structural regions in the secreted phospholipase A_2 from Arabidopsis thaliana for their impact on stability and activity. *Biochimie*, *101*, 60–66. https://doi.org/10.1016/j.biochi.2013.12.015
Marschner: Mechanisms of regulation of mineral nutrition... - Google 学术搜索. (n.d.). Retrieved March 11, 2024, from https://scholar.google.com/scholar_lookup?title=Mineral%20Nutrition%20of%20Higher%20Plants&publication_year=1995&author=H.%20Marschner
Martinoia, E., Klein, M., Geisler, M., Bovet, L., Forestier, C., Kolukisaoglu, Ü., Müller-Röber, B., & Schulz, B. (2002). Multifunctionality of plant ABC transporters – more than just detoxifiers. *Planta*, *214*(3), 345–355. https://doi.org/10.1007/s004250100661
Mashima, R., & Okuyama, T. (2015). The role of lipoxygenases in pathophysiology; new insights and future perspectives. *Redox Biology*, *6*, 297–310. https://doi.org/10.1016/j.redox.2015.08.006
Matthus, E., Doddrell, N. H., Guillaume, G., Mohammad-Sidik, A. B., Wilkins, K. A., Swarbreck, S. M., & Davies, J. M. (2020). Phosphate Deprivation Can Impair Mechano-Stimulated Cytosolic Free Calcium Elevation in Arabidopsis Roots. *Plants*, *9*(9), 9. https://doi.org/10.3390/plants9091205
Mattiazzi Ušaj, M., Brložnik, M., Kaferle, P., Žitnik, M., Wolinski, H., Leitner, F., Kohlwein, S. D., Zupan, B., & Petrovič, U. (2015). Genome-Wide Localization Study of Yeast Pex11 Identifies Peroxisome-Mitochondria Interactions through the ERMES Complex. *Journal of Molecular Biology*, *427*(11), 2072–2087. https://doi.org/10.1016/j.jmb.2015.03.004
May, A., Spinka, M., & Köck, M. (2012). Arabidopsis thaliana PECP1: Enzymatic characterization and structural organization of the first plant phosphoethanolamine/phosphocholine phosphatase. *Biochimica Et Biophysica Acta*, *1824*(2), 319–325. https://doi.org/10.1016/j.bbapap.2011.10.003
May, C., Preisig-Müller, R., Höhne, M., Gnau, P., & Kindl, H. (1998). A phospholipase A2 is transiently synthesized during seed germination and localized to lipid bodies. *Biochimica Et Biophysica Acta*, *1393*(2–3), 267–276. https://doi.org/10.1016/s0005-2760(98)00081-2
Mazur, R., Mostowska, A., Szach, J., Gieczewska, K., Wójtowicz, J., Bednarska, K., Garstka, M., & Kowalewska, Ł. (2019). Galactolipid deficiency disturbs spatial arrangement of the thylakoid network in Arabidopsis thaliana plants. *Journal of Experimental Botany*, *70*(18), 4689–4704. https://doi.org/10.1093/jxb/erz219
Mbuyane, L. L., Bauer, F. F., & Divol, B. (2021). The metabolism of lipids in yeasts and applications in oenology. *Food Research International*, *141*, 110142. https://doi.org/10.1016/j.foodres.2021.110142
McCammon, M. T., Dowds, C. A., Orth, K., Moomaw, C. R., Slaughter, C. A., & Goodman, J. M. (1990). Sorting of peroxisomal membrane protein PMP47 from Candida boidinii into peroxisomal membranes of Saccharomyces cerevisiae. *The Journal of Biological Chemistry*, *265*(33), 20098–20105.
McFarlane, H. E., Lee, E. K., van Bezouwen, L. S., Ross, B., Rosado, A., & Samuels, A. L. (2017). Multiscale Structural Analysis of Plant ER-PM Contact Sites. *Plant & Cell Physiology*, *58*(3), 478–484. https://doi.org/10.1093/pcp/pcw224
Meï, C., Michaud, M., Cussac, M., Albrieux, C., Gros, V., Maréchal, E., Block, M. A., Jouhet, J., & Rébeillé, F. (2015). Levels of polyunsaturated fatty acids correlate with growth rate in plant cell cultures. *Scientific Reports*, *5*, 15207. https://doi.org/10.1038/srep15207

Mhaske, V., Beldjilali, K., Ohlrogge, J., & Pollard, M. (2005). Isolation and characterization of an *Arabidopsis thaliana* knockout line for phospholipid: Diacylglycerol transacylase gene (At5g13640). *Plant Physiology and Biochemistry*, *43*(4), 413–417. https://doi.org/10.1016/j.plaphy.2005.01.013

Michaud, M. (2018). Analysis of the MTL Supercomplex at Contact Sites Between Mitochondria and Plastids. *Methods in Molecular Biology (Clifton, N.J.)*, *1829*, 173–188. https://doi.org/10.1007/978-1-4939-8654-5_12

Michaud, M. (2024). Analysis of a Super-Complex at Contact Sites Between Mitochondria and Plastids. In E. Maréchal (Ed.), *Plastids: Methods and Protocols* (pp. 161–176). Springer US. https://doi.org/10.1007/978-1-0716-3726-5_9

Michaud, M., Gros, V., Tardif, M., Brugière, S., Ferro, M., Prinz, W. A., Toulmay, A., Mathur, J., Wozny, M., Falconet, D., Maréchal, E., Block, M. A., & Jouhet, J. (2016). AtMic60 Is Involved in Plant Mitochondria Lipid Trafficking and Is Part of a Large Complex. *Current Biology*, *26*(5), 627–639. https://doi.org/10.1016/j.cub.2016.01.011

Michaud, M., & Jouhet, J. (2019). Lipid Trafficking at Membrane Contact Sites During Plant Development and Stress Response. *Frontiers in Plant Science*, *10*, 2. https://doi.org/10.3389/fpls.2019.00002

Michaud, M., Prinz, W. A., & Jouhet, J. (2017). Glycerolipid synthesis and lipid trafficking in plant mitochondria. *The FEBS Journal*, *284*(3), 376–390. https://doi.org/10.1111/febs.13812

Michels, P. A. M., Moyersoen, J., Krazy, H., Galland, N., Herman, M., & Hannaert, V. (2005). Peroxisomes, glyoxysomes and glycosomes (review). *Molecular Membrane Biology*, *22*(1–2), 133–145. https://doi.org/10.1080/09687860400024186

Miliara, X., Tatsuta, T., Berry, J.-L., Rouse, S. L., Solak, K., Chorev, D. S., Wu, D., Robinson, C. V., Matthews, S., & Langer, T. (2019). Structural determinants of lipid specificity within Ups/PRELI lipid transfer proteins. *Nature Communications*, *10*, 1130. https://doi.org/10.1038/s41467-019-09089-x

Millar, A. H., & Heazlewood, J. L. (2003). Genomic and Proteomic Analysis of Mitochondrial Carrier Proteins in Arabidopsis. *Plant Physiology*, *131*(2), 443–453. https://doi.org/10.1104/pp.009985

Millar, A. H., Sweetlove, L. J., Giegé, P., & Leaver, C. J. (2001). Analysis of the Arabidopsis mitochondrial proteome. *Plant Physiology*, *127*(4), 1711–1727.

Milligan, S. C., Alb, J. G., Jr., Elagina, R. B., Bankaitis, V. A., & Hyde, D. R. (1997). The Phosphatidylinositol Transfer Protein Domain of Drosophila Retinal Degeneration B Protein Is Essential for Photoreceptor Cell Survival and Recovery from Light Stimulation. *Journal of Cell Biology*, *139*(2), 351–363. https://doi.org/10.1083/jcb.139.2.351

Minnikin, D. E., Abdolrahimzadeh, H., & Baddiley, J. (1974). Replacement of acidic phosphates by acidic glycolipids in Pseudomonas diminuta. *Nature*, *249*(454), 268–269. https://doi.org/10.1038/249268a0

Miquel, M., & Browse, J. (1992). Arabidopsis mutants deficient in polyunsaturated fatty acid synthesis. Biochemical and genetic characterization of a plant oleoyl-phosphatidylcholine desaturase. *The Journal of Biological Chemistry*, *267*(3), 1502–1509.

Mishra, P. K., Singh, N., Ahmad, G., Dube, A., & Maurya, R. (2005). Glycolipids and other constituents from Desmodium gangeticum with antileishmanial and immunomodulatory activities. *Bioorganic & Medicinal Chemistry Letters*, *15*(20), 4543–4546. https://doi.org/10.1016/j.bmcl.2005.07.020

Misson, J., Raghothama, K. G., Jain, A., Jouhet, J., Block, M. A., Bligny, R., Ortet, P., Creff, A., Somerville, S., Rolland, N., Doumas, P., Nacry, P., Herrerra-Estrella, L., Nussaume, L., & Thibaud, M.-C. (2005). A genome-wide transcriptional analysis using Arabidopsis thaliana Affymetrix gene chips determined plant responses to phosphate deprivation. *Proceedings of the National Academy of Sciences of the United States of America*, *102*(33), 11934–11939. https://doi.org/10.1073/pnas.0505266102

Miura, K., Lee, J., Gong, Q., Ma, S., Jin, J. B., Yoo, C. Y., Miura, T., Sato, A., Bohnert, H. J., & Hasegawa, P. M. (2011). SIZ1 regulation of phosphate starvation-induced root architecture remodeling involves the control of auxin accumulation. *Plant Physiology*, *155*(2), 1000–1012. https://doi.org/10.1104/pp.110.165191

Moellering, E. R., Muthan, B., & Benning, C. (2010). Freezing tolerance in plants requires lipid remodeling at the outer chloroplast membrane. *Science (New York, N.Y.)*, *330*(6001), 226–228. https://doi.org/10.1126/science.1191803

Mongrand, S., Bessoule, J.-J., Cabantous, F., & Cassagne, C. (1998). The C16:3C18:3 fatty acid balance in photosynthetic tissues from 468 plant species. *Phytochemistry*, *49*, 1049–1064. https://doi.org/10.1016/S0031-9422(98)00243-X

Mongrand, S., Cassagne, C., & Bessoule, J.-J. (2000). Import of Lyso-Phosphatidylcholine into Chloroplasts Likely at the Origin of Eukaryotic Plastidial Lipids. *Plant Physiology*, *122*(3), 845–852.

Mongrand, S., Morel, J., Laroche, J., Claverol, S., Carde, J.-P., Hartmann, M.-A., Bonneu, M., Simon-Plas, F., Lessire, R., & Bessoule, J.-J. (2004). Lipid Rafts in Higher Plant Cells: PURIFICATION AND CHARACTERIZATION OF TRITON X-100-INSOLUBLE MICRODOMAINS FROM TOBACCO PLASMA MEMBRANE*. *Journal of Biological Chemistry*, *279*(35), 36277–36286. https://doi.org/10.1074/jbc.M403440200

Mongrand, S., Stanislas, T., Bayer, E. M. F., Lherminier, J., & Simon-Plas, F. (2010). Membrane rafts in plant cells. *Trends in Plant Science*, *15*(12), 656–663. https://doi.org/10.1016/j.tplants.2010.09.003

Montero-Moran, G., Caviglia, J. M., McMahon, D., Rothenberg, A., Subramanian, V., Xu, Z., Lara-Gonzalez, S., Storch, J., Carman, G. M., & Brasaemle, D. L. (2010). CGI-58/ABHD5 is a coenzyme A-dependent lysophosphatidic acid acyltransferase. *Journal of Lipid Research*, *51*(4), 709–719. https://doi.org/10.1194/jlr.M001917

Morcuende, R., Bari, R., Gibon, Y., Zheng, W., Pant, B. D., Bläsing, O., Usadel, B., Czechowski, T., Udvardi, M. K., Stitt, M., & Scheible, W.-R. (2007). Genome-wide reprogramming of metabolism and regulatory networks of Arabidopsis in response to phosphorus. *Plant, Cell & Environment*, *30*(1), 85–112. https://doi.org/10.1111/j.1365-3040.2006.01608.x

Moreau, P., Bessoule, J. J., Mongrand, S., Testet, E., Vincent, P., & Cassagne, C. (1998). Lipid trafficking in plant cells. *Progress in Lipid Research*, *37*(6), 371–391. https://doi.org/10.1016/S0163-7827(98)00016-2

Moreau, P. L., Gérard, F., Lutz, N. W., & Cozzone, P. (2001). Non-growing Escherichia coli cells starved for glucose or phosphate use different mechanisms to survive oxidative stress. *Molecular Microbiology*, *39*(4), 1048–1060. https://doi.org/10.1046/j.1365-2958.2001.02303.x

Moreau, P., Rodriguez, M., Cassagne, C., Morré, D. M., & Morré, D. J. (1991). Trafficking of lipids from the endoplasmic reticulum to the Golgi apparatus in a cell-free system from rat liver. *The Journal of Biological Chemistry*, *266*(7), 4322–4328.

Motley, A. M., Galvin, P. C., Ekal, L., Nuttall, J. M., & Hettema, E. H. (2015). Reevaluation of the role of Pex1 and dynamin-related proteins in peroxisome membrane biogenesis. *The Journal of Cell Biology*, *211*(5), 1041–1056. https://doi.org/10.1083/jcb.201412066

Mou, Z., He, Y., Dai, Y., Liu, X., & Li, J. (2000). Deficiency in fatty acid synthase leads to premature cell death and dramatic alterations in plant morphology. *The Plant Cell*, *12*(3), 405–418. https://doi.org/10.1105/tpc.12.3.405

Mudge, S. R., Rae, A. L., Diatloff, E., & Smith, F. W. (2002). Expression analysis suggests novel roles for members of the Pht1 family of phosphate transporters in Arabidopsis. *The Plant Journal: For Cell and Molecular Biology*, *31*(3), 341–353. https://doi.org/10.1046/j.1365-313x.2002.01356.x

Mueller, S. P., Unger, M., Guender, L., Fekete, A., & Mueller, M. J. (2017). Phospholipid:Diacylglycerol Acyltransferase-Mediated Triacylglyerol Synthesis Augments Basal Thermotolerance. *Plant Physiology*, *175*(1), 486–497. https://doi.org/10.1104/pp.17.00861

Mueller-Schuessele, S. J., Leterme, S., & Michaud, M. (2024a). Plastid Transient and Stable Interactions with Other Cell Compartments. In E. Maréchal (Ed.), *Plastids: Methods and Protocols* (pp. 107–134). Springer US. https://doi.org/10.1007/978-1-0716-3726-5_6

Mueller-Schuessele, S. J., Leterme, S., & Michaud, M. (2024b). Plastid Transient and Stable Interactions with Other Cell Compartments. *Methods in Molecular Biology (Clifton, N.J.)*, *2776*, 107–134. https://doi.org/10.1007/978-1-0716-3726-5_6

Mueller-Schuessele, S. J., Leterme, S., & Michaud, M. (2024c). Plastid Transient and Stable Interactions with Other Cell Compartments. *Methods in Molecular Biology (Clifton, N.J.)*, *2776*, 107–134. https://doi.org/10.1007/978-1-0716-3726-5_6

Mukherjee, I., Ghosh, M., & Meinecke, M. (2021). MICOS and the mitochondrial inner membrane morphology—When things get out of shape. *FEBS Letters*, *595*(8), 1159–1183. https://doi.org/10.1002/1873-3468.14089

Mullen, R. T., Lisenbee, C. S., Miernyk, J. A., & Trelease, R. N. (1999). Peroxisomal Membrane Ascorbate Peroxidase Is Sorted to a Membranous Network That Resembles a Subdomain of the Endoplasmic Reticulum. *The Plant Cell*, *11*(11), 2167–2185. https://doi.org/10.1105/tpc.11.11.2167

Müller, A. O., & Ischebeck, T. (2018). Characterization of the enzymatic activity and physiological function of the lipid droplet-associated triacylglycerol lipase AtOBL1. *The New Phytologist*, *217*(3), 1062–1076. https://doi.org/10.1111/nph.14902

Murcha, M. W., Wang, Y., Narsai, R., & Whelan, J. (2014). The plant mitochondrial protein import apparatus—The differences make it interesting. *Biochimica et Biophysica Acta (BBA) - General Subjects*, *1840*(4), 1233–1245. https://doi.org/10.1016/j.bbagen.2013.09.026

Muro, E., Atilla-Gokcumen, G. E., & Eggert, U. S. (2014). Lipids in cell biology: How can we understand them better? *Molecular Biology of the Cell*, *25*(12), 1819–1823. https://doi.org/10.1091/mbc.E13-09-0516

Murphy, S. E., & Levine, T. P. (2016). VAP, a Versatile Access Point for the Endoplasmic Reticulum: Review and analysis of FFAT-like motifs in the VAPome. *Biochimica et Biophysica Acta (BBA) - Molecular and Cell Biology of Lipids*, *1861*(8, Part B), 952–961. https://doi.org/10.1016/j.bbalip.2016.02.009

Nagaoka, N., Yamashita, A., Kurisu, R., Watari, Y., Ishizuna, F., Tsutsumi, N., Ishizaki, K., Kohchi, T., & Arimura, S. (2017). DRP3 and ELM1 are required for mitochondrial fission in the liverwort Marchantia polymorpha. *Scientific Reports*, *7*(1), 4600. https://doi.org/10.1038/s41598-017-04886-0

Nakamura, Y. (2013). Phosphate starvation and membrane lipid remodeling in seed plants. *Progress in Lipid Research*, *52*(1), 43–50. https://doi.org/10.1016/j.plipres.2012.07.002

Nakamura, Y. (2017). Plant Phospholipid Diversity: Emerging Functions in Metabolism and Protein-Lipid Interactions. *Trends in Plant Science*, *22*(12), 1027–1040. https://doi.org/10.1016/j.tplants.2017.09.002

Nakamura, Y., Awai, K., Masuda, T., Yoshioka, Y., Takamiya, K., & Ohta, H. (2005). A novel phosphatidylcholine-hydrolyzing phospholipase C induced by phosphate starvation in Arabidopsis. *The Journal of Biological Chemistry*, *280*(9), 7469–7476. https://doi.org/10.1074/jbc.M408799200

Nakamura, Y., Koizumi, R., Shui, G., Shimojima, M., Wenk, M. R., Ito, T., & Ohta, H. (2009). Arabidopsis lipins mediate eukaryotic pathway of lipid metabolism and cope critically with phosphate starvation. *Proceedings of the National Academy of Sciences of the United States of America*, *106*(49), 20978–20983. https://doi.org/10.1073/pnas.0907173106

Narendra, S., Venkataramani, S., Shen, G., Wang, J., Pasapula, V., Lin, Y., Kornyeyev, D., Holaday, A. S., & Zhang, H. (2006). The Arabidopsis ascorbate peroxidase 3 is a peroxisomal membrane-bound antioxidant enzyme and is dispensable for Arabidopsis growth and development. *Journal of Experimental Botany*, *57*(12), 3033–3042. https://doi.org/10.1093/jxb/erl060

Negi, J., Munemasa, S., Song, B., Tadakuma, R., Fujita, M., Azoulay-Shemer, T., Engineer, C. B., Kusumi, K., Nishida, I., Schroeder, J. I., & Iba, K. (2018). Eukaryotic lipid metabolic pathway is essential for functional chloroplasts and CO2 and light responses in Arabidopsis guard cells. *Proceedings of the National Academy of Sciences of the United States of America*, *115*(36), 9038–9043. https://doi.org/10.1073/pnas.1810458115

Nilsson, L., Müller, R., & Nielsen, T. H. (2007). Increased expression of the MYB-related transcription factor, PHR1, leads to enhanced phosphate uptake in Arabidopsis thaliana. *Plant, Cell & Environment*, *30*(12), 1499–1512. https://doi.org/10.1111/j.1365-3040.2007.01734.x

Nito, K., Kamigaki, A., Kondo, M., Hayashi, M., & Nishimura, M. (2007). Functional classification of Arabidopsis peroxisome biogenesis factors proposed from analyses of knockdown mutants. *Plant & Cell Physiology*, *48*(6), 763–774. https://doi.org/10.1093/pcp/pcm053

Noblet, A., Leymarie, J., & Bailly, C. (2017). Chilling temperature remodels phospholipidome of Zea mays seeds during imbibition. *Scientific Reports*, *7*(1), 1. https://doi.org/10.1038/s41598-017-08904-z

Noll, F., May, C., & Kindl, H. (2000). Phospholipid monolayer of plant lipid bodies attacked by phospholipase A2 shows 80 nm holes analyzed by atomic force microscopy. *Biophysical Chemistry*, *86*(1), 29–35. https://doi.org/10.1016/s0301-4622(00)00156-3

Noshi, M., Yamada, H., Hatanaka, R., Tanabe, N., Tamoi, M., & Shigeoka, S. (2017). Arabidopsis dehydroascorbate reductase 1 and 2 modulate redox states of ascorbate-glutathione cycle in the cytosol in response to photooxidative stress. *Bioscience, Biotechnology, and Biochemistry*, *81*(3), 523–533. https://doi.org/10.1080/09168451.2016.1256759

Nussaume, L., Kanno, S., Javot, H., Marin, E., & Thibaud, M.-C. (2011). Phosphate Import in Plants: Focus on the PHT1 Transporters. *Frontiers in Plant Science*, *2*. https://doi.org/10.3389/fpls.2011.00083

Nussberger, S., Ghosh, R., & Wang, S. (2024). New insights into the structure and dynamics of the TOM complex in mitochondria. *Biochemical Society Transactions*, *52*(2), 911–922. https://doi.org/10.1042/BST20231236

Nyathi, Y., De Marcos Lousa, C., van Roermund, C. W., Wanders, R. J. A., Johnson, B., Baldwin, S. A., Theodoulou, F. L., & Baker, A. (2010). The *Arabidopsis* Peroxisomal ABC Transporter, Comatose, Complements the *Saccharomyces cerevisiae pxa1 pxa2*Δ Mutant for Metabolism of Long-chain Fatty Acids and Exhibits Fatty Acyl-CoA-stimulated ATPase Activity*. *Journal of Biological Chemistry*, *285*(39), 29892–29902. https://doi.org/10.1074/jbc.M110.151225

Nyathi, Y., Lousa, C. D. M., Roermund, C. W. van, Wanders, R. J. A., Johnson, B., Baldwin, S. A., Theodoulou, F. L., & Baker, A. (2010). The Arabidopsis Peroxisomal ABC Transporter, Comatose, Complements the Saccharomyces cerevisiae pxa1 pxa2Δ Mutant for Metabolism of Long-chain Fatty Acids and Exhibits Fatty Acyl-CoA-stimulated ATPase Activity *. *Journal of Biological Chemistry*, *285*(39), 29892–29902. https://doi.org/10.1074/jbc.M110.151225

Ohlrogge, J. B., & Jaworski, J. G. (1997). REGULATION OF FATTY ACID SYNTHESIS. *Annual Review of Plant Physiology and Plant Molecular Biology*, *48*, 109–136. https://doi.org/10.1146/annurev.arplant.48.1.109

Ohlrogge, J., & Browse, J. (1995). Lipid biosynthesis. *The Plant Cell*, *7*(7), 957–970. https://doi.org/10.1105/tpc.7.7.957

Okazaki, Y., Otsuki, H., Narisawa, T., Kobayashi, M., Sawai, S., Kamide, Y., Kusano, M., Aoki, T., Hirai, M. Y., & Saito, K. (2013). A new class of plant lipid is essential for protection against phosphorus depletion. *Nature Communications*, *4*, 1510. https://doi.org/10.1038/ncomms2512

Okazaki, Y., Shimojima, M., Sawada, Y., Toyooka, K., Narisawa, T., Mochida, K., Tanaka, H., Matsuda, F., Hirai, A., Hirai, M. Y., Ohta, H., & Saito, K. (2009). A chloroplastic UDP-glucose pyrophosphorylase from Arabidopsis is the committed enzyme for the first step of sulfolipid biosynthesis. *The Plant Cell*, *21*(3), 892–909. https://doi.org/10.1105/tpc.108.063925

Okuley, J., Lightner, J., Feldmann, K., Yadav, N., Lark, E., & Browse, J. (1994). Arabidopsis FAD2 gene encodes the enzyme that is essential for polyunsaturated lipid synthesis. *The Plant Cell*, *6*(1), 147–158. https://doi.org/10.1105/tpc.6.1.147

O'Neill, E. M., Kaffman, A., Jolly, E. R., & O'Shea, E. K. (1996). Regulation of PHO4 nuclear localization by the PHO80-PHO85 cyclin-CDK complex. *Science (New York, N.Y.)*, *271*(5246), 209–212. https://doi.org/10.1126/science.271.5246.209

O'Quin, J. B., Bourassa, L., Zhang, D., Shockey, J. M., Gidda, S. K., Fosnot, S., Chapman, K. D., Mullen, R. T., & Dyer, J. M. (2010). Temperature-sensitive post-translational regulation of plant omega-3 fatty-acid desaturases is mediated by the endoplasmic reticulum-associated degradation pathway. *The Journal of Biological Chemistry*, *285*(28), 21781–21796. https://doi.org/10.1074/jbc.M110.135236

Orth, T., Reumann, S., Zhang, X., Fan, J., Wenzel, D., Quan, S., & Hu, J. (2007a). The PEROXIN11 Protein Family Controls Peroxisome Proliferation in Arabidopsis. *The Plant Cell*, *19*(1), 333–350. https://doi.org/10.1105/tpc.106.045831

Orth, T., Reumann, S., Zhang, X., Fan, J., Wenzel, D., Quan, S., & Hu, J. (2007b). The PEROXIN11 Protein Family Controls Peroxisome Proliferation in Arabidopsis. *The Plant Cell*, *19*(1), 333–350. https://doi.org/10.1105/tpc.106.045831

Osuna, D., Usadel, B., Morcuende, R., Gibon, Y., Bläsing, O. E., Höhne, M., Günter, M., Kamlage, B., Trethewey, R., Scheible, W.-R., & Stitt, M. (2007). Temporal responses of transcripts, enzyme activities and metabolites after adding sucrose to carbon-deprived Arabidopsis seedlings. *The Plant Journal*, *49*(3), 463–491. https://doi.org/10.1111/j.1365-313X.2006.02979.x

Padham, A. K., Hopkins, M. T., Wang, T.-W., McNamara, L. M., Lo, M., Richardson, L. G. L., Smith, M. D., Taylor, C. A., & Thompson, J. E. (2007). Characterization of a plastid triacylglycerol lipase from Arabidopsis. *Plant Physiology*, *143*(3), 1372–1384. https://doi.org/10.1104/pp.106.090811

Palma, J. M., Corpas, F. J., & del Río, L. A. (2009). Proteome of plant peroxisomes: New perspectives on the role of these organelles in cell biology. *Proteomics*, *9*(9), 2301–2312. https://doi.org/10.1002/pmic.200700732

Pan, R., Liu, J., Wang, S., & Hu, J. (2020). Peroxisomes: Versatile organelles with diverse roles in plants. *New Phytologist*, *225*(4), 1410–1427. https://doi.org/10.1111/nph.16134

Pant, B. D., Burgos, A., Pant, P., Cuadros-Inostroza, A., Willmitzer, L., & Scheible, W.-R. (2015a). The transcription factor PHR1 regulates lipid remodeling and triacylglycerol accumulation in Arabidopsis thaliana during phosphorus starvation. *Journal of Experimental Botany*, *66*(7), 1907–1918. https://doi.org/10.1093/jxb/eru535

Pant, B. D., Burgos, A., Pant, P., Cuadros-Inostroza, A., Willmitzer, L., & Scheible, W.-R. (2015b). The transcription factor PHR1 regulates lipid remodeling and triacylglycerol accumulation in Arabidopsis thaliana during phosphorus starvation. *Journal of Experimental Botany*, *66*(7), 1907–1918. https://doi.org/10.1093/jxb/eru535

Park, S., Gidda, S. K., James, C. N., Horn, P. J., Khuu, N., Seay, D. C., Keereetaweep, J., Chapman, K. D., Mullen, R. T., & Dyer, J. M. (2013). The α/β Hydrolase CGI-58 and Peroxisomal Transport Protein PXA1 Coregulate Lipid Homeostasis and Signaling in Arabidopsis. *The Plant Cell*, *25*(5), 1726–1739. https://doi.org/10.1105/tpc.113.111898

Paungfoo-Lonhienne, C., Lonhienne, T. G. A., Mudge, S. R., Schenk, P. M., Christie, M., Carroll, B. J., & Schmidt, S. (2010). DNA Is Taken Up by Root Hairs and Pollen, and Stimulates Root and Pollen Tube Growth. *Plant Physiology*, *153*(2), 799–805. https://doi.org/10.1104/pp.110.154963

Payne, G., Lad, M., Foster, T., Khosla, A., & Gray, D. (2014). Composition and properties of the surface of oil bodies recovered from Echium plantagineum. *Colloids and Surfaces. B, Biointerfaces*, *116*, 88–92. https://doi.org/10.1016/j.colsurfb.2013.11.043

Peng, Z., Ruan, J., Tian, H., Shan, L., Meng, J., Guo, F., Zhang, Z., Ding, H., Wan, S., & Li, X. (2020). The Family of Peanut Fatty Acid Desaturase Genes and a Functional Analysis of Four ω-3 AhFAD3 Members. *Plant Molecular Biology Reporter*, *38*(2), 209–221. https://doi.org/10.1007/s11105-019-01191-0

Péret, B., Clément, M., Nussaume, L., & Desnos, T. (2011). Root developmental adaptation to phosphate starvation: Better safe than sorry. *Trends in Plant Science*, *16*(8), 442–450. https://doi.org/10.1016/j.tplants.2011.05.006

Pérez-Sancho, J., Tilsner, J., Samuels, A. L., Botella, M. A., Bayer, E. M., & Rosado, A. (2016). Stitching Organelles: Organization and Function of Specialized Membrane Contact Sites in Plants. *Trends in Cell Biology*, *26*(9), 705–717. https://doi.org/10.1016/j.tcb.2016.05.007

Péterfy, M., Phan, J., Xu, P., & Reue, K. (2001). Lipodystrophy in the fld mouse results from mutation of a new gene encoding a nuclear protein, lipin. *Nature Genetics*, *27*(1), 121–124. https://doi.org/10.1038/83685

Pfanner, N., van der Laan, M., Amati, P., Capaldi, R. A., Caudy, A. A., Chacinska, A., Darshi, M., Deckers, M., Hoppins, S., Icho, T., Jakobs, S., Ji, J., Kozjak-Pavlovic, V., Meisinger, C., Odgren, P. R., Park, S. K., Rehling, P., Reichert, A. S., Sheikh, M. S., … Nunnari, J. (2014). Uniform nomenclature for the mitochondrial contact site and cristae organizing system. *The Journal of Cell Biology*, *204*(7), 1083–1086. https://doi.org/10.1083/jcb.201401006

Pidkowich, M. S., Nguyen, H. T., Heilmann, I., Ischebeck, T., & Shanklin, J. (2007). Modulating seed β-ketoacyl-acyl carrier protein synthase II level converts the composition of a temperate seed oil to that of a palm-like tropical oil. *Proceedings of the National Academy of Sciences*, *104*(11), 4742–4747. https://doi.org/10.1073/pnas.0611141104

Pike, L. J. (2003). Lipid rafts: Bringing order to chaos. *Journal of Lipid Research*, *44*(4), 655–667. https://doi.org/10.1194/jlr.R200021-JLR200

Pinfield-Wells, H., Rylott, E. L., Gilday, A. D., Graham, S., Job, K., Larson, T. R., & Graham, I. A. (2005). Sucrose rescues seedling establishment but not germination of Arabidopsis mutants disrupted in peroxisomal fatty acid catabolism. *The Plant Journal*, *43*(6), 861–872. https://doi.org/10.1111/j.1365-313X.2005.02498.x

Plaxton, W. C., & Tran, H. T. (2011). Metabolic adaptations of phosphate-starved plants. *Plant Physiology*, *156*(3), 1006–1015. https://doi.org/10.1104/pp.111.175281

Poirier, Y., Antonenkov, V. D., Glumoff, T., & Hiltunen, J. K. (2006). Peroxisomal β-oxidation—A metabolic pathway with multiple functions. *Biochimica et Biophysica Acta (BBA) - Molecular Cell Research*, *1763*(12), 1413–1426. https://doi.org/10.1016/j.bbamcr.2006.08.034

Poirier, Y., Thoma, S., Somerville, C., & Schiefelbein, J. (1991). Mutant of Arabidopsis deficient in xylem loading of phosphate. *Plant Physiology*, *97*(3), 1087–1093. https://doi.org/10.1104/pp.97.3.1087

Popov, V. N., Antipina, O. V., Pchelkin, V. P., & Tsydendambaev, V. D. (2017). Changes in fatty acid composition of lipids in chloroplast membranes of tobacco plants during cold hardening. *Russian Journal of Plant Physiology*, *64*(2), 156–161. https://doi.org/10.1134/S1021443717010137

Poulsen, L. R., López-Marqués, R. L., Pedas, P. R., McDowell, S. C., Brown, E., Kunze, R., Harper, J. F., Pomorski, T. G., & Palmgren, M. (2015). A phospholipid uptake system in the model plant Arabidopsis thaliana. *Nature Communications*, *6*(1), 7649. https://doi.org/10.1038/ncomms8649

Pracharoenwattana, I., Cornah, J. E., & Smith, S. M. (2007). Arabidopsis peroxisomal malate dehydrogenase functions in β-oxidation but not in the glyoxylate cycle: Peroxisomal malate dehydrogenase function. *The Plant Journal*, *50*(3), 381–390. https://doi.org/10.1111/j.1365-313X.2007.03055.x

Prathap, V., Kumar, S., Meena, N. L., Maheshwari, C., Dalal, M., & Tyagi, A. (2023). Phosphorus Starvation Tolerance in Rice Through Combined Physiological, Biochemical, and Proteome Analyses. *Rice Science*, *30*(6), 613–631. https://doi.org/10.1016/j.rsci.2023.04.007

Preuss, C. P., Huang, C. Y., & Tyerman, S. D. (2011). Proton-coupled high-affinity phosphate transport revealed from heterologous characterization in Xenopus of barley-root plasma membrane transporter, HvPHT1;1. *Plant, Cell & Environment*, *34*(4), 681–689. https://doi.org/10.1111/j.1365-3040.2010.02272.x

Prin, W. A., Toulmay, A., & Balla, T. (2020). The functional universe of membrane contact sites. *Nature Reviews. Molecular Cell Biology*, *21*(1), 7–24. https://doi.org/10.1038/s41580-019-0180-9

Pugh, C. E., Roy, A. B., Hawkes, T., & Harwood, J. L. (1995). A new pathway for the synthesis of the plant sulpholipid, sulphoquinovosyldiacylglycerol. *The Biochemical Journal*, *309 (Pt 2)*(Pt 2), 513–519. https://doi.org/10.1042/bj3090513

Pye, V. E., Christensen, C. E., Dyer, J. H., Arent, S., & Henriksen, A. (2010). Peroxisomal Plant 3-Ketoacyl-CoA Thiolase Structure and Activity Are Regulated by a Sensitive Redox Switch *. *Journal of Biological Chemistry*, *285*(31), 24078–24088. https://doi.org/10.1074/jbc.M110.106013

Qian, T., Li, C., Liu, F., Xu, K., Wan, C., Liu, Y., & Yu, H. (2022). Arabidopsis synaptotagmin 1 mediates lipid transport in a lipid composition-dependent manner. *Traffic*, *23*(6), 346–356. https://doi.org/10.1111/tra.12844

Qin, C., & Wang, X. (2002). The Arabidopsis Phospholipase D Family. Characterization of a Calcium-Independent and Phosphatidylcholine-Selective PLDζ1 with Distinct Regulatory Domains. *Plant Physiology*, *128*(3), 1057–1068. https://doi.org/10.1104/pp.010928

Qin, Z., Wang, T., Zhao, Y., Ma, C., & Shao, Q. (2023). Molecular Machinery of Lipid Droplet Degradation and Turnover in Plants. *International Journal of Molecular Sciences*, *24*(22), 16039. https://doi.org/10.3390/ijms242216039

Quettier, A.-L., & Eastmond, P. J. (2009). Storage oil hydrolysis during early seedling growth. *Plant Physiology and Biochemistry: PPB*, *47*(6), 485–490. https://doi.org/10.1016/j.plaphy.2008.12.005

Radetzky, R., & Langheinrich, U. (1994). Induction of accumulation and degradation of the 18.4-kDa oleosin in a triacylglycerol-storing cell culture of anise (Pimpinella anisum L.). *Planta*, *194*(1), 1–8. https://doi.org/10.1007/BF00201027

Radner, F. P. W., Grond, S., Lass, A., & Zechner, R. (2011). Fat in the skin. *Dermato-Endocrinology*, *3*(2), 77–83. https://doi.org/10.4161/derm.3.2.15472

Raghothama, K. G. (1999). PHOSPHATE ACQUISITION. *Annual Review of Plant Physiology and Plant Molecular Biology*, *50*, 665–693. https://doi.org/10.1146/annurev.arplant.50.1.665

Ransone, L. J. (1995). [32] Detection of protein-protein interactions by coimmunoprecipitation and dimerization. In *Methods in Enzymology* (Vol. 254, pp. 491–497). Academic Press. https://doi.org/10.1016/0076-6879(95)54034-2

Rawyler, A., Meylan-Bettex, M., & Siegenthaler, P. A. (1995). (Galacto) lipid export from envelope to thylakoid membranes in intact chloroplasts. II. A general process with a key role for the envelope in the establishment of lipid asymmetry in thylakoid membranes. *Biochimica et Biophysica Acta (BBA) - Biomembranes*, *1233*(2), 123–133. https://doi.org/10.1016/0005-2736(94)00248-N

Rawyler, A., Unitt, M. D., Giroud, C., Davies, H., Mayor, J. P., Harwood, J. L., & Siegenthaler, P.-A. (1987). The transmembrane distribution of galactolipids in chloroplast thylakoids is universal in a wide variety of temperate climate plants. *Photosynthesis Research*, *11*(1), 3–13. https://doi.org/10.1007/BF00117669

Reglinski, K., Steinfort-Effelsberg, L., Sezgin, E., Klose, C., Platta, H. W., Girzalsky, W., Eggeling, C., & Erdmann, R. (2020). Fluidity and Lipid Composition of Membranes of Peroxisomes, Mitochondria and the ER From Oleic Acid-Induced Saccharomyces cerevisiae. *Frontiers in Cell and Developmental Biology*, *8*. https://doi.org/10.3389/fcell.2020.574363

Remy, E., Cabrito, T. R., Batista, R. A., Teixeira, M. C., Sá-Correia, I., & Duque, P. (2012). The Pht1;9 and Pht1;8 transporters mediate inorganic phosphate acquisition by the Arabidopsis thaliana root during phosphorus starvation. *The New Phytologist*, *195*(2), 356–371. https://doi.org/10.1111/j.1469-8137.2012.04167.x

Ren, F., Guo, Q.-Q., Chang, L.-L., Chen, L., Zhao, C.-Z., Zhong, H., & Li, X.-B. (2012). Brassica napus PHR1 gene encoding a MYB-like protein functions in response to phosphate starvation. *PloS One*, *7*(8), e44005. https://doi.org/10.1371/journal.pone.0044005

Reszczyńska, E., & Hanaka, A. (2020). Lipids Composition in Plant Membranes. *Cell Biochemistry and Biophysics*, *78*(4), 401–414. https://doi.org/10.1007/s12013-020-00947-w

Reumann, S. (2011). Toward a definition of the complete proteome of plant peroxisomes: Where experimental proteomics must be complemented by bioinformatics. *Proteomics*, *11*(9), 1764–1779. https://doi.org/10.1002/pmic.201000681

Reumann, S., Babujee, L., Ma, C., Wienkoop, S., Siemsen, T., Antonicelli, G. E., Rasche, N., Lüder, F., Weckwerth, W., & Jahn, O. (2007). Proteome analysis of Arabidopsis leaf peroxisomes reveals novel targeting peptides, metabolic pathways, and defense mechanisms. *The Plant Cell*, *19*(10), 3170–3193. https://doi.org/10.1105/tpc.107.050989

Reumann, S., & Bartel, B. (2016). Plant peroxisomes: Recent discoveries in functional complexity, organelle homeostasis, and morphological dynamics. *Current Opinion in Plant Biology*, *34*, 17–26. https://doi.org/10.1016/j.pbi.2016.07.008

Reumann, S., Ma, C., Lemke, S., & Babujee, L. (2004). AraPerox. A Database of Putative Arabidopsis Proteins from Plant Peroxisomes. *Plant Physiology*, *136*(1), 2587–2608. https://doi.org/10.1104/pp.104.043695

Reumann, S., Quan, S., Aung, K., Yang, P., Manandhar-Shrestha, K., Holbrook, D., Linka, N., Switzenberg, R., Wilkerson, C. G., Weber, A. P. M., Olsen, L. J., & Hu, J. (2009). In-Depth Proteome Analysis of Arabidopsis Leaf Peroxisomes Combined with in Vivo Subcellular Targeting Verification Indicates Novel Metabolic and Regulatory Functions of Peroxisomes. *Plant Physiology*, *150*(1), 125. https://doi.org/10.1104/pp.109.137703

Reumann, S., & Singhal, R. (2014). Isolation of Leaf Peroxisomes from Arabidopsis for Organelle Proteome Analyses. In J. V. Jorrin-Novo, S. Komatsu, W. Weckwerth, & S. Wienkoop (Eds.), *Plant Proteomics: Methods and Protocols* (pp. 541–552). Humana Press. https://doi.org/10.1007/978-1-62703-631-3_36

Reumann, S., & Weber, A. P. M. (2006). Plant peroxisomes respire in the light: Some gaps of the photorespiratory C2 cycle have become filled—Others remain. *Biochimica et Biophysica Acta (BBA) - Molecular Cell Research*, *1763*(12), 1496–1510. https://doi.org/10.1016/j.bbamcr.2006.09.008

Reymond, M., Svistoonoff, S., Loudet, O., Nussaume, L., & Desnos, T. (2006). Identification of QTL controlling root growth response to phosphate starvation in Arabidopsis thaliana. *Plant, Cell & Environment*, *29*(1), 115–125. https://doi.org/10.1111/j.1365-3040.2005.01405.x

Reynolds, K. B., Taylor, M. C., Cullerne, D. P., Blanchard, C. L., Wood, C. C., Singh, S. P., & Petrie, J. R. (2017). A reconfigured Kennedy pathway which promotes efficient accumulation of medium-chain fatty acids in leaf oils. *Plant Biotechnology Journal*, *15*(11), 1397–1408. https://doi.org/10.1111/pbi.12724

Richmond, T. A., & Bleecker, A. B. (1999). A defect in beta-oxidation causes abnormal inflorescence development in Arabidopsis. *The Plant Cell*, *11*(10), 1911–1924. https://doi.org/10.1105/tpc.11.10.1911

Rinaldi, M. A., Patel, A. B., Park, J., Lee, K., Strader, L. C., & Bartel, B. (2016). The Roles of β-Oxidation and Cofactor Homeostasis in Peroxisome Distribution and Function in *Arabidopsis thaliana*. *Genetics*, *204*(3), 1089–1115. https://doi.org/10.1534/genetics.116.193169

Robinson, P. M. (1994). Efficient Tests of Nonstationary Hypotheses. *Journal of the American Statistical Association*, *89*(428), 1420–1437. https://doi.org/10.1080/01621459.1994.10476881

Roermund, C. W. T. van, IJlst, L., Majczak, W., Waterham, H. R., Folkerts, H., Wanders, R. J. A., & Hellingwerf, K. J. (2012a). Peroxisomal Fatty Acid Uptake Mechanism in Saccharomyces cerevisiae*. *Journal of Biological Chemistry*, *287*(24), 20144–20153. https://doi.org/10.1074/jbc.M111.332833

Roermund, C. W. T. van, IJlst, L., Majczak, W., Waterham, H. R., Folkerts, H., Wanders, R. J. A., & Hellingwerf, K. J. (2012b). Peroxisomal Fatty Acid Uptake Mechanism in Saccharomyces cerevisiae*. *Journal of Biological Chemistry*, *287*(24), 20144–20153. https://doi.org/10.1074/jbc.M111.332833

Ros, M. B. H., Koopmans, G. F., van Groenigen, K. J., Abalos, D., Oenema, O., Vos, H. M. J., & van Groenigen, J. W. (2020). Towards optimal use of phosphorus fertiliser. *Scientific Reports*, *10*, 17804. https://doi.org/10.1038/s41598-020-74736-z

Rosenberger, S., Connerth, M., Zellnig, G., & Daum, G. (2009). Phosphatidylethanolamine synthesized by three different pathways is supplied to peroxisomes of the yeast Saccharomyces cerevisiae. *Biochimica Et Biophysica Acta*, *1791*(5), 379–387. https://doi.org/10.1016/j.bbalip.2009.01.015

Roston, R. L., Gao, J., Murcha, M. W., Whelan, J., & Benning, C. (2012). TGD1, -2, and -3 proteins involved in lipid trafficking form ATP-binding cassette (ABC) transporter with multiple substrate-binding proteins. *The Journal of Biological Chemistry*, *287*(25), 21406–21415. https://doi.org/10.1074/jbc.M112.370213

Roughan, P. G. (1970). Turnover of the glycerolipids of pumpkin leaves. The importance of phosphatidylcholine. *Biochemical Journal*, *117*(1), 1–8. https://doi.org/10.1042/bj1170001

Rubio, V., Linhares, F., Solano, R., Martín, A. C., Iglesias, J., Leyva, A., & Paz-Ares, J. (2001). A conserved MYB transcription factor involved in phosphate starvation signaling both in vascular plants and in unicellular algae. *Genes & Development*, *15*(16), 2122–2133. https://doi.org/10.1101/gad.204401

Rudolph, M., Schlereth, A., Körner, M., Feussner, K., Berndt, E., Melzer, M., Hornung, E., & Feussner, I. (2011). The lipoxygenase-dependent oxygenation of lipid body membranes is promoted by a patatin-type phospholipase in cucumber cotyledons. *Journal of Experimental Botany*, *62*(2), 749–760. https://doi.org/10.1093/jxb/erq310

Ruiz-Lopez, N., Pérez-Sancho, J., del Valle, A. E., Haslam, R. P., Vanneste, S., Catalá, R., Perea-Resa, C., Damme, D. V., García-Hernández, S., Albert, A., Vallarino, J., Lin, J., Friml, J., Macho, A. P., Salinas, J., Rosado, A., Napier, J. A., Amorim-Silva, V., & Botella, M. A. (2021). Synaptotagmins at the endoplasmic reticulum–plasma membrane contact sites maintain diacylglycerol homeostasis during abiotic stress. *The Plant Cell*, *33*(7), 2431–2453. https://doi.org/10.1093/plcell/koab122

Russell, L., Larner, V., Kurup, S., Bougourd, S., & Holdsworth, M. (2000). The Arabidopsis COMATOSE locus regulates germination potential. *Development*, *127*(17), 3759–3767. https://doi.org/10.1242/dev.127.17.3759

Rylott, E. L., Eastmond, P. J., Gilday, A. D., Slocombe, S. P., Larson, T. R., Baker, A., & Graham, I. A. (2006). The Arabidopsis thaliana multifunctional protein gene (MFP2) of peroxisomal β-oxidation is essential for seedling establishment. *The Plant Journal*, *45*(6), 930–941. https://doi.org/10.1111/j.1365-313X.2005.02650.x

Rylott, E. L., Hooks, M. A., & Graham, I. A. (2001). Co-ordinate regulation of genes involved in storage lipid mobilization in Arabidopsis thaliana. *Biochemical Society Transactions*, *29*(2), 283–286. https://doi.org/10.1042/bst0290283

Ryu, S. B., Lee, H. Y., Doelling, J. H., & Palta, J. P. (2005). Characterization of a cDNA encoding Arabidopsis secretory phospholipase A2-alpha, an enzyme that generates bioactive lysophospholipids and free fatty acids. *Biochimica Et Biophysica Acta*, *1736*(2), 144–151. https://doi.org/10.1016/j.bbalip.2005.08.005

Sadeghipour, H. R., & Bhatla, S. C. (2002). Differential sensitivity of oleosins to proteolysis during oil body mobilization in sunflower seedlings. *Plant & Cell Physiology*, *43*(10), 1117–1126. https://doi.org/10.1093/pcp/pcf142

Saheki, Y., Bian, X., Schauder, C. M., Sawaki, Y., Surma, M. A., Klose, C., Pincet, F., Reinisch, K. M., & De Camilli, P. (2016). Control of plasma membrane lipid homeostasis by the extended synaptotagmins. *Nature Cell Biology*, *18*(5), 504–515. https://doi.org/10.1038/ncb3339

Saheki, Y., & Camilli, P. D. (2017). Endoplasmic Reticulum–Plasma Membrane Contact Sites. *Annual Review of Biochemistry*, *86*(Volume 86, 2017), 659–684. https://doi.org/10.1146/annurev-biochem-061516-044932

Saita, S., Tatsuta, T., Lampe, P. A., König, T., Ohba, Y., & Langer, T. (2018). PARL partitions the lipid transfer protein STARD7 between the cytosol and mitochondria. *The EMBO Journal*, *37*(4), e97909. https://doi.org/10.15252/embj.201797909

Saito, K. (2004). Sulfur assimilatory metabolism. The long and smelling road. *Plant Physiology*, *136*(1), 2443–2450. https://doi.org/10.1104/pp.104.046755

Saleem, R., Smith, J., & Aitchison, J. (2006). Proteomics of the Peroxisome. *Biochimica et Biophysica Acta*, *1763*(12), 1541–1551. https://doi.org/10.1016/j.bbamcr.2006.09.005

Sánchez-Fernández, R., Davies, T. G. E., Coleman, J. O. D., & Rea, P. A. (2001). The Arabidopsis thaliana ABC Protein Superfamily, a Complete Inventory *. *Journal of Biological Chemistry*, *276*(32), 30231–30244. https://doi.org/10.1074/jbc.M103104200

Sanda, S., Leustek, T., Theisen, M. J., Garavito, R. M., & Benning, C. (2001). Recombinant Arabidopsis SQD1 converts udp-glucose and sulfite to the sulfolipid head group precursor UDP-sulfoquinovose in vitro. *The Journal of Biological Chemistry*, *276*(6), 3941–3946. https://doi.org/10.1074/jbc.M008200200

Sanger, F., Nicklen, S., & Coulson, A. R. (1977). DNA sequencing with chain-terminating inhibitors. *Proceedings of the National Academy of Sciences of the United States of America*, *74*(12), 5463–5467. https://doi.org/10.1073/pnas.74.12.5463

Santos, N. C., Girik, V., & Nunes-Hasler, P. (2020). ORP5 and ORP8: Sterol Sensors and Phospholipid Transfer Proteins at Membrane Contact Sites? *Biomolecules*, *10*(6), 6. https://doi.org/10.3390/biom10060928

Saravanan, R. S., Slabaugh, E., Singh, V. R., Lapidus, L. J., Haas, T., & Brandizzi, F. (2009). The targeting of the oxysterol-binding protein ORP3a to the endoplasmic reticulum relies on the plant VAP33 homolog PVA12. *The Plant Journal: For Cell and Molecular Biology*, *58*(5), 817–830. https://doi.org/10.1111/j.1365-313X.2009.03815.x

Schapire, A. L., Voigt, B., Jasik, J., Rosado, A., Lopez-Cobollo, R., Menzel, D., Salinas, J., Mancuso, S., Valpuesta, V., Baluska, F., & Botella, M. A. (2008). Arabidopsis synaptotagmin 1 is required for the maintenance of plasma membrane integrity and cell viability. *The Plant Cell*, *20*(12), 3374–3388. https://doi.org/10.1105/tpc.108.063859

Scheible, W.-R., Morcuende, R., Czechowski, T., Fritz, C., Osuna, D., Palacios-Rojas, N., Schindelasch, D., Thimm, O., Udvardi, M. K., & Stitt, M. (2004). Genome-Wide Reprogramming of Primary and Secondary Metabolism, Protein Synthesis, Cellular Growth Processes, and the Regulatory Infrastructure of Arabidopsis in Response to Nitrogen. *Plant Physiology*, *136*(1), 2483–2499. https://doi.org/10.1104/pp.104.047019

Scherer, G. F. E., Ryu, S. B., Wang, X., Matos, A. R., & Heitz, T. (2010). Patatin-related phospholipase A: Nomenclature, subfamilies and functions in plants. *Trends in Plant Science*, *15*(12), 693–700. https://doi.org/10.1016/j.tplants.2010.09.005

Schneiter, R., Brügger, B., Sandhoff, R., Zellnig, G., Leber, A., Lampl, M., Athenstaedt, K., Hrastnik, C., Eder, S., Daum, G., Paltauf, F., Wieland, F. T., & Kohlwein, S. D. (1999). Electrospray Ionization Tandem Mass Spectrometry (Esi-Ms/Ms) Analysis of the Lipid Molecular Species Composition of Yeast Subcellular Membranes Reveals Acyl Chain-Based Sorting/Remodeling of Distinct Molecular Species En Route to the Plasma Membrane. *The Journal of Cell Biology*, *146*(4), 741–754.

Schnurr, J. A., Shockey, J. M., de Boer, G.-J., & Browse, J. A. (2002). Fatty acid export from the chloroplast. Molecular characterization of a major plastidial acyl-coenzyme A synthetase from Arabidopsis. *Plant Physiology*, *129*(4), 1700–1709. https://doi.org/10.1104/pp.003251

Schnurr, J., Shockey, J., & Browse, J. (2004). The acyl-CoA synthetase encoded by LACS2 is essential for normal cuticle development in Arabidopsis. *The Plant Cell*, *16*(3), 629–642. https://doi.org/10.1105/tpc.017608

Schrader, M., Kamoshita, M., & Islinger, M. (2020a). Organelle interplay-peroxisome interactions in health and disease. *Journal of Inherited Metabolic Disease*, *43*(1), 71–89. https://doi.org/10.1002/jimd.12083

Schrader, M., Kamoshita, M., & Islinger, M. (2020b). Organelle interplay—Peroxisome interactions in health and disease. *Journal of Inherited Metabolic Disease*, *43*(1), 71–89. https://doi.org/10.1002/jimd.12083

Schrick, K., Nguyen, D., Karlowski, W. M., & Mayer, K. F. (2004). START lipid/sterol-binding domains are amplified in plants and are predominantly associated with homeodomain transcription factors. *Genome Biology*, *5*(6), R41. https://doi.org/10.1186/gb-2004-5-6-r41

Schumann, U., Prestele, J., O'Geen, H., Brueggeman, R., Wanner, G., & Gietl, C. (2007). Requirement of the C3HC4 zinc RING finger of the Arabidopsis PEX10 for photorespiration and leaf peroxisome contact with chloroplasts. *Proceedings of the National Academy of Sciences of the United States of America*, *104*(3), 1069–1074. https://doi.org/10.1073/pnas.0610402104

Schwacke, R., Schneider, A., van der Graaff, E., Fischer, K., Catoni, E., Desimone, M., Frommer, W. B., Flügge, U.-I., & Kunze, R. (2003). ARAMEMNON, a Novel Database for Arabidopsis Integral Membrane Proteins. *Plant Physiology*, *131*(1), 16–26. https://doi.org/10.1104/pp.011577

Scorrano, L., De Matteis, M. A., Emr, S., Giordano, F., Hajnóczky, G., Kornmann, B., Lackner, L. L., Levine, T. P., Pellegrini, L., Reinisch, K., Rizzuto, R., Simmen, T., Stenmark, H., Ungermann, C., & Schuldiner, M. (2019). Coming together to define membrane contact sites. *Nature Communications*, *10*(1), 1287. https://doi.org/10.1038/s41467-019-09253-3

Seiwert, D., Witt, H., Ritz, S., Janshoff, A., & Paulsen, H. (2018). The Nonbilayer Lipid MGDG and the Major Light-Harvesting Complex (LHCII) Promote Membrane Stacking in Supported Lipid Bilayers. *Biochemistry*, *57*(15), 2278–2288. https://doi.org/10.1021/acs.biochem.8b00118

Sentenac, H., & Grignon, C. (1985). Effect of pH on Orthophosphate Uptake by Corn Roots 1. *Plant Physiology*, *77*(1), 136–141. https://doi.org/10.1104/pp.77.1.136

Seo, Y. S., Kim, E. Y., Kim, J. H., & Kim, W. T. (2009). Enzymatic characterization of class I DAD1-like acylhydrolase members targeted to chloroplast in Arabidopsis. *FEBS Letters*, *583*(13), 2301–2307. https://doi.org/10.1016/j.febslet.2009.06.021

Shah, S., Xin, Z., & Browse, J. (1997). Overexpression of the FAD3 desaturase gene in a mutant of Arabidopsis. *Plant Physiology*, *114*(4), 1533–1539. https://doi.org/10.1104/pp.114.4.1533

Shai, N., Yifrach, E., van Roermund, C. W. T., Cohen, N., Bibi, C., IJlst, L., Cavellini, L., Meurisse, J., Schuster, R., Zada, L., Mari, M. C., Reggiori, F. M., Hughes, A. L., Escobar-Henriques, M., Cohen, M. M., Waterham, H. R., Wanders, R. J. A., Schuldiner, M., & Zalckvar, E. (2018). Systematic mapping of contact sites reveals tethers and a function for the peroxisome-mitochondria contact. *Nature Communications*, *9*(1), 1761. https://doi.org/10.1038/s41467-018-03957-8

Sharma, B., Joshi, D., Yadav, P. K., Gupta, A. K., & Bhatt, T. K. (2016). Role of Ubiquitin-Mediated Degradation System in Plant Biology. *Frontiers in Plant Science*, *7*, 806. https://doi.org/10.3389/fpls.2016.00806

Shimamura, R., Ohashi, Y., Taniguchi, Y. Y., Kato, M., Tsuge, T., & Aoyama, T. (2022). Arabidopsis PLDζ1 and PLDζ2 localize to post-Golgi membrane compartments in a partially overlapping manner. *Plant Molecular Biology*, *108*(1), 31–49. https://doi.org/10.1007/s11103-021-01205-0

Shimojima, M., Madoka, Y., Fujiwara, R., Murakawa, M., Yoshitake, Y., Ikeda, K., Koizumi, R., Endo, K., Ozaki, K., & Ohta, H. (2015a). An engineered lipid remodeling system using a galactolipid synthase promoter during phosphate starvation enhances oil accumulation in plants. *Frontiers in Plant Science*, *6*, 664. https://doi.org/10.3389/fpls.2015.00664

Shimojima, M., Madoka, Y., Fujiwara, R., Murakawa, M., Yoshitake, Y., Ikeda, K., Koizumi, R., Endo, K., Ozaki, K., & Ohta, H. (2015b). An engineered lipid remodeling system using a galactolipid synthase promoter during phosphate starvation enhances oil accumulation in plants. *Frontiers in Plant Science*, *6*, 664. https://doi.org/10.3389/fpls.2015.00664

Shin, R., Berg, R. H., & Schachtman, D. P. (2005). Reactive oxygen species and root hairs in Arabidopsis root response to nitrogen, phosphorus and potassium deficiency. *Plant & Cell Physiology*, *46*(8), 1350–1357. https://doi.org/10.1093/pcp/pci145

Shin, R., & Schachtman, D. P. (2004). Hydrogen peroxide mediates plant root cell response to nutrient deprivation. *Proceedings of the National Academy of Sciences of the United States of America*, *101*(23), 8827–8832. https://doi.org/10.1073/pnas.0401707101

Shintre, C. A., Pike, A. C. W., Li, Q., Kim, J.-I., Barr, A. J., Goubin, S., Shrestha, L., Yang, J., Berridge, G., Ross, J., Stansfeld, P. J., Sansom, M. S. P., Edwards, A. M., Bountra, C., Marsden, B. D., von Delft, F., Bullock, A. N., Gileadi, O., Burgess-Brown, N. A., & Carpenter, E. P. (2013). Structures of ABCB10, a human ATP-binding cassette transporter in apo- and nucleotide-bound states. *Proceedings of the National Academy of Sciences of the United States of America*, *110*(24), 9710–9715. https://doi.org/10.1073/pnas.1217042110

Shockey, J. M., Fulda, M. S., & Browse, J. (2003). Arabidopsis Contains a Large Superfamily of Acyl-Activating Enzymes. Phylogenetic and Biochemical Analysis Reveals a New Class of Acyl-Coenzyme A Synthetases. *Plant Physiology*, *132*(2), 1065–1076. https://doi.org/10.1104/pp.103.020552

Shockey, J. M., Fulda, M. S., & Browse, J. A. (2002). Arabidopsis contains nine long-chain acyl-coenzyme a synthetase genes that participate in fatty acid and glycerolipid metabolism. *Plant Physiology*, *129*(4), 1710–1722. https://doi.org/10.1104/pp.003269

Shockey, J., Regmi, A., Cotton, K., Adhikari, N., Browse, J., & Bates, P. D. (2016). Identification of Arabidopsis GPAT9 (At5g60620) as an Essential Gene Involved in Triacylglycerol Biosynthesis. *Plant Physiology*, *170*(1), 163–179. https://doi.org/10.1104/pp.15.01563

Shukla, D., Waigel, S., Rouchka, E. C., Sandhu, G., Trivedi, P. K., & Sahi, S. V. (2021). Genome-wide expression analysis reveals contrasting regulation of phosphate starvation response (PSR) in root and shoot of Arabidopsis and its association with biotic stress. *Environmental and Experimental Botany*, *188*, 104483. https://doi.org/10.1016/j.envexpbot.2021.104483

Siao, W., Wang, P., Voigt, B., Hussey, P. J., & Baluska, F. (2016). Arabidopsis SYT1 maintains stability of cortical endoplasmic reticulum networks and VAP27-1-enriched endoplasmic reticulum–plasma membrane contact sites. *Journal of Experimental Botany*, *67*(21), 6161–6171. https://doi.org/10.1093/jxb/erw381

Simon, E. W. (1974). Phospholipids and Plant Membrane Permeability. *New Phytologist*, *73*(3), 377–420. https://doi.org/10.1111/j.1469-8137.1974.tb02118.x

Simon-Plas, F., Perraki, A., Bayer, E., Gerbeau-Pissot, P., & Mongrand, S. (2011). An update on plant membrane rafts. *Current Opinion in Plant Biology*, *14*(6), 642–649. https://doi.org/10.1016/j.pbi.2011.08.003

Simons, K., & Ikonen, E. (1997). Functional rafts in cell membranes. *Nature*, *387*(6633), 6633. https://doi.org/10.1038/42408

Sinclair, A. M., Trobacher, C. P., Mathur, N., Greenwood, J. S., & Mathur, J. (2009). Peroxule extension over ER-defined paths constitutes a rapid subcellular response to hydroxyl stress. *The Plant Journal*, *59*(2), 231–242. https://doi.org/10.1111/j.1365-313X.2009.03863.x

Singh, P., Kumari, S., Guldhe, A., Misra, R., Rawat, I., & Bux, F. (2016). Trends and novel strategies for enhancing lipid accumulation and quality in microalgae. *Renewable and Sustainable Energy Reviews*, *55*, 1–16. https://doi.org/10.1016/j.rser.2015.11.001

Skirpan, A. L., Dowd, P. E., Sijacic, P., Jaworski, C. J., Gilroy, S., & Kao, T. (2006). Identification and characterization of PiORP1, a Petunia oxysterol-binding-protein related protein involved in receptor-kinase mediated signaling in pollen, and analysis of the ORP gene family in Arabidopsis. *Plant Molecular Biology*, *61*(4), 553–565. https://doi.org/10.1007/s11103-006-0030-y

Skupień, J., Wójtowicz, J., Kowalewska, Ł., Mazur, R., Garstka, M., Gieczewska, K., & Mostowska, A. (2017). Dark-chilling induces substantial structural changes and modifies galactolipid and carotenoid composition during chloroplast biogenesis in cucumber (Cucumis sativus L.) cotyledons. *Plant Physiology and Biochemistry: PPB*, *111*, 107–118. https://doi.org/10.1016/j.plaphy.2016.11.022

Slack, C. R., Roughan, P. G., & Balasingham, N. (1977). Labelling studies in vivo on the metabolism of the acyl and glycerol moieties of the glycerolipids in the developing maize leaf. *The Biochemical Journal*, *162*(2), 289–296. https://doi.org/10.1042/bj1620289

Slee, J. A., & Levine, T. P. (2019). Systematic Prediction of FFAT Motifs Across Eukaryote Proteomes Identifies Nucleolar and Eisosome Proteins With the Predicted Capacity to Form Bridges to the Endoplasmic Reticulum. *Contact*, *2*, 2515256419883136. https://doi.org/10.1177/2515256419883136

Sm, S., Bk, K., Ca, R., S, A., Ew, E., A, A.-M., Im, M., & Gc, V. (2005). The role of alternative oxidase in modulating carbon use efficiency and growth during macronutrient stress in tobacco cells. *Journal of Experimental Botany*, *56*(416). https://doi.org/10.1093/jxb/eri146

Smith, F. W., Mudge, S. R., Rae, A. L., & Glassop, D. (2003). Phosphate transport in plants. *Plant and Soil*, *248*(1), 71–83. https://doi.org/10.1023/A:1022376332180

Somerharju, P. (2016). Is Spontaneous Translocation of Polar Lipids Between Cellular Organelles Negligible? *Lipid Insights*, *8*(Suppl 1), 87–93. https://doi.org/10.4137/LPI.S31616

Somerville, C., & Browse, J. (1996). Dissecting desaturation: Plants prove advantageous. *Trends in Cell Biology*, *6*(4), 148–153. https://doi.org/10.1016/0962-8924(96)10002-7

Soni, K. G., Mardones, G. A., Sougrat, R., Smirnova, E., Jackson, C. L., & Bonifacino, J. S. (2009). Coatomer-dependent protein delivery to lipid droplets. *Journal of Cell Science*, *122*(11), 1834–1841. https://doi.org/10.1242/jcs.045849

Speerling, P., & Heinz, E. (1993). Isomeric sn-1-octadecenyl and sn-2-octadecenyl analogues of lysophosphatidylcholine as substrates for acylation and desaturation by plant microsomal membranes. *European Journal of Biochemistry*, *213*(3), 965–971. https://doi.org/10.1111/j.1432-1033.1993.tb17841.x

Srivastava, S., Ranjan, M., Bano, N., Asif, M. H., & Srivastava, S. (2023). Comparative transcriptome analysis reveals the phosphate starvation alleviation mechanism of phosphate accumulating Pseudomonas putida in Arabidopsis thaliana. *Scientific Reports*, *13*(1), 4918. https://doi.org/10.1038/s41598-023-31154-1

Ståhl, U., Carlsson, A. S., Lenman, M., Dahlqvist, A., Huang, B., Banaś, W., Banaś, A., & Stymne, S. (2004). Cloning and Functional Characterization of a Phospholipid:Diacylglycerol Acyltransferase from Arabidopsis. *Plant Physiology*, *135*(3), 1324–1335. https://doi.org/10.1104/pp.104.044354

Stitt, M., & Hurry, V. (2002). A plant for all seasons: Alterations in photosynthetic carbon metabolism during cold acclimation in Arabidopsis. *Current Opinion in Plant Biology*, *5*(3), 199–206. https://doi.org/10.1016/s1369-5266(02)00258-3

Stoica, R., De Vos, K. J., Paillusson, S., Mueller, S., Sancho, R. M., Lau, K.-F., Vizcay-Barrena, G., Lin, W.-L., Xu, Y.-F., Lewis, J., Dickson, D. W., Petrucelli, L., Mitchell, J. C., Shaw, C. E., & Miller, C. C. J. (2014). ER–mitochondria associations are regulated by the VAPB–PTPIP51 interaction and are disrupted by ALS/FTD-associated TDP-43. *Nature Communications*, *5*(1), 3996. https://doi.org/10.1038/ncomms4996

Subramanian, V., Rothenberg, A., Gomez, C., Cohen, A. W., Garcia, A., Bhattacharyya, S., Shapiro, L., Dolios, G., Wang, R., Lisanti, M. P., & Brasaemle, D. L. (2004). Perilipin A mediates the reversible binding of CGI-58 to lipid droplets in 3T3-L1 adipocytes. *The Journal of Biological Chemistry*, *279*(40), 42062–42071. https://doi.org/10.1074/jbc.M407462200

Sussman, M. R., Amasino, R. M., Young, J. C., Krysan, P. J., & Austin-Phillips, S. (2000). The Arabidopsis knockout facility at the University of Wisconsin-Madison. *Plant Physiology*, *124*(4), 1465–1467. https://doi.org/10.1104/pp.124.4.1465

Szymanski, J., Brotman, Y., Willmitzer, L., & Cuadros-Inostroza, Á. (2014). Linking Gene Expression and Membrane Lipid Composition of Arabidopsis. *The Plant Cell*, *26*(3), 915–928. https://doi.org/10.1105/tpc.113.118919

Tabak, H. F., Braakman, I., & Zand, A. van der. (2013). Peroxisome Formation and Maintenance Are Dependent on the Endoplasmic Reticulum. *Annual Review of Biochemistry*, *82*(Volume 82, 2013), 723–744. https://doi.org/10.1146/annurev-biochem-081111-125123

Talley, J. T., & Mohiuddin, S. S. (2024). Biochemistry, Fatty Acid Oxidation. In *StatPearls*. StatPearls Publishing. http://www.ncbi.nlm.nih.gov/books/NBK556002/

Tanz, S. K., Castleden, I., Hooper, C. M., Vacher, M., Small, I., & Millar, H. A. (2013). SUBA3: A database for integrating experimentation and prediction to define the SUBcellular location of proteins in Arabidopsis. *Nucleic Acids Research*, *41*(Database issue), D1185–D1191. https://doi.org/10.1093/nar/gks1151

Tauchi-Sato, K., Ozeki, S., Houjou, T., Taguchi, R., & Fujimoto, T. (2002). The surface of lipid droplets is a phospholipid monolayer with a unique Fatty Acid composition. *The Journal of Biological Chemistry*, *277*(46), 44507–44512. https://doi.org/10.1074/jbc.M207712200

Taylor, N. L., Ströher, E., & Millar, A. H. (2014). Arabidopsis Organelle Isolation and Characterization. In J. J. Sanchez-Serrano & J. Salinas (Eds.), *Arabidopsis Protocols* (pp. 551–572). Humana Press. https://doi.org/10.1007/978-1-62703-580-4_29

Thazar-Poulot, N., Miquel, M., Fobis-Loisy, I., & Gaude, T. (2015). Peroxisome extensions deliver the *Arabidopsis* SDP1 lipase to oil bodies. *Proceedings of the National Academy of Sciences*, *112*(13), 4158–4163. https://doi.org/10.1073/pnas.1403322112

Theodoulou, F. L., Job, K., Slocombe, S. P., Footitt, S., Holdsworth, M., Baker, A., Larson, T. R., & Graham, I. A. (2005a). Jasmonic Acid Levels Are Reduced in COMATOSE ATP-Binding Cassette Transporter Mutants. Implications for Transport of Jasmonate Precursors into Peroxisomes. *Plant Physiology*, *137*(3), 835–840. https://doi.org/10.1104/pp.105.059352

Theodoulou, F. L., Job, K., Slocombe, S. P., Footitt, S., Holdsworth, M., Baker, A., Larson, T. R., & Graham, I. A. (2005b). Jasmonic Acid Levels Are Reduced in COMATOSE ATP-Binding Cassette Transporter Mutants. Implications for Transport of Jasmonate Precursors into Peroxisomes. *Plant Physiology*, *137*(3), 835–840. https://doi.org/10.1104/pp.105.059352

Thiam, A. R., Farese, R. V., & Walther, T. C. (2013). The Biophysics and Cell Biology of Lipid Droplets. *Nature Reviews. Molecular Cell Biology*, *14*(12), 775–786. https://doi.org/10.1038/nrm3699

Ticconi, C. A., Delatorre, C. A., Lahner, B., Salt, D. E., & Abel, S. (2004). Arabidopsis pdr2 reveals a phosphate-sensitive checkpoint in root development. *The Plant Journal: For Cell and Molecular Biology*, *37*(6), 801–814. https://doi.org/10.1111/j.1365-313x.2004.02005.x

Titball, R. W. (1993). Bacterial phospholipases C. *Microbiological Reviews*, *57*(2), 347–366. https://doi.org/10.1128/mr.57.2.347-366.1993

Tjellström, H., Andersson, M. X., Larsson, K. E., & Sandelius, A. S. (2008). Membrane phospholipids as a phosphate reserve: The dynamic nature of phospholipid-to-digalactosyl diacylglycerol exchange in higher plants. *Plant, Cell & Environment*, *31*(10), 1388–1398. https://doi.org/10.1111/j.1365-3040.2008.01851.x

To, A., Valon, C., Savino, G., Guilleminot, J., Devic, M., Giraudat, J., & Parcy, F. (2006). A Network of Local and Redundant Gene Regulation Governs Arabidopsis Seed Maturation. *The Plant Cell*, *18*(7), 1642–1651. https://doi.org/10.1105/tpc.105.039925

Tovar-Méndez, A., Miernyk, J. A., & Randall, D. D. (2003). Regulation of pyruvate dehydrogenase complex activity in plant cells. *European Journal of Biochemistry*, *270*(6), 1043–1049. https://doi.org/10.1046/j.1432-1033.2003.03469.x

Traver, M. S., & Bartel, B. (2023). The ubiquitin-protein ligase MIEL1 localizes to peroxisomes to promote seedling oleosin degradation and lipid droplet mobilization. *Proceedings of the National Academy of Sciences of the United States of America*, *120*(29), e2304870120. https://doi.org/10.1073/pnas.2304870120

Troncoso-Ponce, M. A., Cao, X., Yang, Z., & Ohlrogge, J. B. (2013). Lipid turnover during senescence. *Plant Science: An International Journal of Experimental Plant Biology*, *205–206*, 13–19. https://doi.org/10.1016/j.plantsci.2013.01.004

Trull, M. C., & Deikman, J. (1998). An Arabidopsis mutant missing one acid phosphatase isoform. *Planta*, *206*(4), 544–550. https://doi.org/10.1007/s004250050431

Tuller, G., Nemec, T., Hrastnik, C., & Daum, G. (1999). Lipid composition of subcellular membranes of an FY1679-derived haploid yeast wild-type strain grown on different carbon sources. *Yeast (Chichester, England)*, *15*(14), 1555–1564. https://doi.org/10.1002/(SICI)1097-0061(199910)15:14<1555::AID-YEA479>3.0.CO;2-Z

Tyburski, J., Dunajska, K., & Tretyn, A. (2009). Reactive oxygen species localization in roots of Arabidopsis thaliana seedlings grown under phosphate deficiency. *Plant Growth Regulation*, *59*(1), 27–36. https://doi.org/10.1007/s10725-009-9385-9

Tzen, JTC., Cao, Yz., Laurent, P., Ratnayake, C., & Huang, AHC. (1993). Lipids, Proteins, and Structure of Seed Oil Bodies from Diverse Species. *Plant Physiology*, *101*(1), 267–276.

Valentine, A. J., Kleinert, A., & Benedito, V. A. (2017). Adaptive strategies for nitrogen metabolism in phosphate deficient legume nodules. *Plant Science: An International Journal of Experimental Plant Biology*, *256*, 46–52. https://doi.org/10.1016/j.plantsci.2016.12.010

van der Graaff, E., Schwacke, R., Schneider, A., Desimone, M., Flügge, U.-I., & Kunze, R. (2006). Transcription analysis of arabidopsis membrane transporters and hormone pathways during developmental and induced leaf senescence. *Plant Physiology*, *141*(2), 776–792. https://doi.org/10.1104/pp.106.079293

van Meer, G., Voelker, D. R., & Feigenson, G. W. (2008). Membrane lipids: Where they are and how they behave. *Nature Reviews. Molecular Cell Biology*, *9*(2), 112–124. https://doi.org/10.1038/nrm2330

van Roermund, C. W. T., IJlst, L., Baker, A., Wanders, R. J. A., Theodoulou, F. L., & Waterham, H. R. (2021). The Saccharomyces cerevisiae ABC subfamily D transporter Pxa1/Pxa2p co-imports CoASH into the peroxisome. *FEBS Letters*, *595*(6), 763–772. https://doi.org/10.1002/1873-3468.13974

Vance, C. P., Uhde-Stone, C., & Allan, D. L. (2003). Phosphorus acquisition and use: Critical adaptations by plants for securing a nonrenewable resource. *New Phytologist*, *157*(3), 423–447. https://doi.org/10.1046/j.1469-8137.2003.00695.x

Vandana, S., & Bhatla, S. C. (2006). Evidence for the probable oil body association of a thiol-protease, leading to oleosin degradation in sunflower seedling cotyledons. *Plant Physiology and Biochemistry: PPB*, *44*(11–12), 714–723. https://doi.org/10.1016/j.plaphy.2006.09.022

Verleur, N., Hettema, E. H., Van Roermund, C. W. T., Tabak, H. F., & Wanders, R. J. A. (1997). Transport of Activated Fatty Acids by the Peroxisomal ATP-binding-cassette Transporter Pxa2 in a Semi-Intact Yeast Cell System. *European Journal of Biochemistry*, *249*(3), 657–661. https://doi.org/10.1111/j.1432-1033.1997.00657.x

Vincent, A. E., White, K., Davey, T., Philips, J., Ogden, R. T., Lawless, C., Warren, C., Hall, M. G., Ng, Y. S., Falkous, G., Holden, T., Deehan, D., Taylor, R. W., Turnbull, D. M., & Picard, M. (2019). Quantitative 3D Mapping of the Human Skeletal Muscle Mitochondrial Network. *Cell Reports*, *26*(4), 996-1009.e4. https://doi.org/10.1016/j.celrep.2019.01.010

Vincent, P., Chua, M., Nogue, F., Fairbrother, A., Mekeel, H., Xu, Y., Allen, N., Bibikova, T. N., Gilroy, S., & Bankaitis, V. A. (2005). A Sec14p-nodulin domain phosphatidylinositol transfer protein polarizes membrane growth of Arabidopsis thaliana root hairs. *The Journal of Cell Biology*, *168*(5), 801–812. https://doi.org/10.1083/jcb.200412074

Visser, W. F., van Roermund, C. W. T., Ijlst, L., Waterham, H. R., & Wanders, R. J. A. (2007). Metabolite transport across the peroxisomal membrane. *Biochemical Journal*, *401*(Pt 2), 365–375. https://doi.org/10.1042/BJ20061352

Viswanath, K. K., Varakumar, P., Pamuru, R. R., Basha, S. J., Mehta, S., & Rao, A. D. (2020). Plant Lipoxygenases and Their Role in Plant Physiology. *Journal of Plant Biology*, *63*(2), 83–95. https://doi.org/10.1007/s12374-020-09241-x

Voelker, D. R. (2003). New perspectives on the regulation of intermembrane glycerophospholipid traffic. *Journal of Lipid Research*, *44*(3), 441–449. https://doi.org/10.1194/jlr.R200020-JLR200

Voinnet, O., Rivas, S., Mestre, P., & Baulcombe, D. (2003). An enhanced transient expression system in plants based on suppression of gene silencing by the p19 protein of tomato bushy stunt virus. *The Plant Journal: For Cell and Molecular Biology*, *33*(5), 949–956. https://doi.org/10.1046/j.1365-313x.2003.01676.x

Walter, M., Chaban, C., Schütze, K., Batistic, O., Weckermann, K., Näke, C., Blazevic, D., Grefen, C., Schumacher, K., Oecking, C., Harter, K., & Kudla, J. (2004). Visualization of protein interactions in living plant cells using bimolecular fluorescence complementation. *The Plant Journal: For Cell and Molecular Biology*, *40*(3), 428–438. https://doi.org/10.1111/j.1365-313X.2004.02219.x

Wang, C., Ying, S., Huang, H., Li, K., Wu, P., & Shou, H. (2009). Involvement of OsSPX1 in phosphate homeostasis in rice. *The Plant Journal: For Cell and Molecular Biology*, *57*(5), 895–904. https://doi.org/10.1111/j.1365-313X.2008.03734.x

Wang, L., Kazachkov, M., Shen, W., Bai, M., Wu, H., & Zou, J. (2014). Deciphering the roles of Arabidopsis LPCAT and PAH in phosphatidylcholine homeostasis and pathway coordination for chloroplast lipid synthesis. *The Plant Journal: For Cell and Molecular Biology*, *80*(6), 965–976. https://doi.org/10.1111/tpj.12683

Wang, L., Shen, W., Kazachkov, M., Chen, G., Chen, Q., Carlsson, A. S., Stymne, S., Weselake, R. J., & Zou, J. (2012). Metabolic Interactions between the Lands Cycle and the Kennedy Pathway of Glycerolipid Synthesis in Arabidopsis Developing Seeds[W]. *The Plant Cell*, *24*(11), 4652–4669. https://doi.org/10.1105/tpc.112.104604

Wang, P., Richardson, C., Hawkins, T. J., Sparkes, I., Hawes, C., & Hussey, P. J. (2016). Plant VAP27 proteins: Domain characterization, intracellular localization and role in plant development. *The New Phytologist*, *210*(4), 1311–1326. https://doi.org/10.1111/nph.13857

Wang, Q., Sullivan, R. W., Kight, A., Henry, R. L., Huang, J., Jones, A. M., & Korth, K. L. (2004). Deletion of the Chloroplast-Localized Thylakoid Formation1 Gene Product in Arabidopsis Leads to Deficient Thylakoid Formation and Variegated Leaves. *Plant Physiology*, *136*(3), 3594–3604. https://doi.org/10.1104/pp.104.049841

Wang, X. (2001). PLANT PHOSPHOLIPASES. *Annual Review of Plant Physiology and Plant Molecular Biology*, *52*, 211–231. https://doi.org/10.1146/annurev.arplant.52.1.211

Wang, X., Wang, Y., Tian, J., Lim, B. L., Yan, X., & Liao, H. (2009). Overexpressing AtPAP15 enhances phosphorus efficiency in soybean. *Plant Physiology*, *151*(1), 233–240. https://doi.org/10.1104/pp.109.138891

Wang, X., Wang, Z., Zheng, Z., Dong, J., Song, L., Sui, L., Nussaume, L., Desnos, T., & Liu, D. (2019). Genetic Dissection of Fe-Dependent Signaling in Root Developmental Responses to Phosphate Deficiency. *Plant Physiology*, *179*(1), 300–316. https://doi.org/10.1104/pp.18.00907

Wang, Z., Xu, C., & Benning, C. (2012). TGD4 involved in endoplasmic reticulum-to-chloroplast lipid trafficking is a phosphatidic acid binding protein. *The Plant Journal: For Cell and Molecular Biology*, *70*(4), 614–623. https://doi.org/10.1111/j.1365-313X.2012.04900.x

Wang, Z.-A., Li, Q., Ge, X.-Y., Yang, C.-L., Luo, X.-L., Zhang, A.-H., Xiao, J.-L., Tian, Y.-C., Xia, G.-X., Chen, X.-Y., Li, F.-G., & Wu, J.-H. (2015). The mitochondrial malate dehydrogenase 1 gene GhmMDH1 is involved in plant and root growth under phosphorus deficiency conditions in cotton. *Scientific Reports*, *5*(1), 10343. https://doi.org/10.1038/srep10343

Wanner, B. L. (1993). Gene regulation by phosphate in enteric bacteria. *Journal of Cellular Biochemistry*, *51*(1), 47–54. https://doi.org/10.1002/jcb.240510110

Ward, J. T., Lahner, B., Yakubova, E., Salt, D. E., & Raghothama, K. G. (2008). The effect of iron on the primary root elongation of Arabidopsis during phosphate deficiency. *Plant Physiology*, *147*(3), 1181–1191. https://doi.org/10.1104/pp.108.118562

Weber, H., Vick, B. A., & Farmer, E. E. (1997). Dinor-oxo-phytodienoic acid: A new hexadecanoid signal in the jasmonate family. *Proceedings of the National Academy of Sciences of the United States of America*, *94*(19), 10473–10478.

Welti, R., Li, W., Li, M., Sang, Y., Biesiada, H., Zhou, H.-E., Rajashekar, C. B., Williams, T. D., & Wang, X. (2002). Profiling membrane lipids in plant stress responses. Role of phospholipase D alpha in freezing-induced lipid changes in Arabidopsis. *The Journal of Biological Chemistry*, *277*(35), 31994–32002. https://doi.org/10.1074/jbc.M205375200

Wideman, J. G., & Muñoz-Gómez, S. A. (2016). The evolution of ERMIONE in mitochondrial biogenesis and lipid homeostasis: An evolutionary view from comparative cell biology. *Biochimica et Biophysica Acta (BBA) - Molecular and Cell Biology of Lipids*, *1861*(8, Part B), 900–912. https://doi.org/10.1016/j.bbalip.2016.01.015

Williamson, L. C., Ribrioux, S. P., Fitter, A. H., & Leyser, H. M. (2001). Phosphate availability regulates root system architecture in Arabidopsis. *Plant Physiology*, *126*(2), 875–882. https://doi.org/10.1104/pp.126.2.875

Winichayakul, S., Scott, R. W., Roldan, M., Hatier, J.-H. B., Livingston, S., Cookson, R., Curran, A. C., & Roberts, N. J. (2013). In Vivo Packaging of Triacylglycerols Enhances Arabidopsis Leaf Biomass and Energy Density1[W][OA]. *Plant Physiology*, *162*(2), 626–639. https://doi.org/10.1104/pp.113.216820

Wiszniewski, A. A. G., Bussell, J. D., Long, R. L., & Smith, S. M. (2014). Knockout of the two evolutionarily conserved peroxisomal 3-ketoacyl-CoA thiolases in Arabidopsis recapitulates the abnormal inflorescence meristem 1 phenotype. *Journal of Experimental Botany*, *65*(22), 6723–6733. https://doi.org/10.1093/jxb/eru397

Wiszniewski, A. A. G., Zhou, W., Smith, S. M., & Bussell, J. D. (2009a). Identification of two Arabidopsis genes encoding a peroxisomal oxidoreductase-like protein and an acyl-CoA synthetase-like protein that are required for responses to pro-auxins. *Plant Molecular Biology*, *69*(5), 503–515. https://doi.org/10.1007/s11103-008-9431-4

Wiszniewski, A. A. G., Zhou, W., Smith, S. M., & Bussell, J. D. (2009b). Identification of two Arabidopsis genes encoding a peroxisomal oxidoreductase-like protein and an acyl-CoA synthetase-like protein that are required for responses to pro-auxins. *Plant Molecular Biology*, *69*(5), 503–515. https://doi.org/10.1007/s11103-008-9431-4

Wolter, F. P., Schmidt, R., & Heinz, E. (1992). Chilling sensitivity of Arabidopsis thaliana with genetically engineered membrane lipids. *The EMBO Journal*, *11*(13), 4685–4692. https://doi.org/10.1002/j.1460-2075.1992.tb05573.x

Wriessnegger, T., Gübitz, G., Leitner, E., Ingolic, E., Cregg, J., de la Cruz, B. J., & Daum, G. (2007). Lipid composition of peroxisomes from the yeast Pichia pastoris grown on different carbon sources. *Biochimica Et Biophysica Acta*, *1771*(4), 455–461. https://doi.org/10.1016/j.bbalip.2007.01.004

Wu, P., Ma, L., Hou, X., Wang, M., Wu, Y., Liu, F., & Deng, X. W. (2003). Phosphate starvation triggers distinct alterations of genome expression in Arabidopsis roots and leaves. *Plant Physiology*, *132*(3), 1260–1271. https://doi.org/10.1104/pp.103.021022

Xiao, K., Katagi, H., Harrison, M., & Wang, Z.-Y. (2006). Improved phosphorus acquisition and biomass production in *Arabidopsis* by transgenic expression of a purple acid phosphatase gene from *M. truncatula*. *Plant Science*, *170*(2), 191–202. https://doi.org/10.1016/j.plantsci.2005.08.001

Xie, W., Nielsen, M. E., Pedersen, C., & Thordal-Christensen, H. (2017). A Split-GFP Gateway Cloning System for Topology Analyses of Membrane Proteins in Plants. *PLOS ONE*, *12*(1), e0170118. https://doi.org/10.1371/journal.pone.0170118

Xiong, Y., DeFraia, C., Williams, D., Zhang, X., & Mou, Z. (2009). Characterization of Arabidopsis 6-phosphogluconolactonase T-DNA insertion mutants reveals an essential role for the oxidative section of the plastidic

pentose phosphate pathway in plant growth and development. *Plant & Cell Physiology*, *50*(7), 1277–1291. https://doi.org/10.1093/pcp/pcp070

Xu, C., Fan, J., Cornish, A. J., & Benning, C. (2008). Lipid trafficking between the endoplasmic reticulum and the plastid in Arabidopsis requires the extraplastidic TGD4 protein. *The Plant Cell*, *20*(8), 2190–2204. https://doi.org/10.1105/tpc.108.061176

Xu, C., Fan, J., Froehlich, J. E., Awai, K., & Benning, C. (2005). Mutation of the TGD1 Chloroplast Envelope Protein Affects Phosphatidate Metabolism in Arabidopsis. *The Plant Cell*, *17*(11), 3094–3110. https://doi.org/10.1105/tpc.105.035592

Xu, C., Fan, J., Riekhof, W., Froehlich, J. E., & Benning, C. (2003). A permease-like protein involved in ER to thylakoid lipid transfer in Arabidopsis. *The EMBO Journal*, *22*(10), 2370–2379. https://doi.org/10.1093/emboj/cdg234

Xu, C., & Shanklin, J. (2016). Triacylglycerol Metabolism, Function, and Accumulation in Plant Vegetative Tissues. *Annual Review of Plant Biology*, *67*, 179–206. https://doi.org/10.1146/annurev-arplant-043015-111641

Xu, J., Carlsson, A. S., Francis, T., Zhang, M., Hoffman, T., Giblin, M. E., & Taylor, D. C. (2012). Triacylglycerol synthesis by PDAT1 in the absence of DGAT1 activity is dependent on re-acylation of LPC by LPCAT2. *BMC Plant Biology*, *12*, 4. https://doi.org/10.1186/1471-2229-12-4

Xu, Y.-N., Wang, Z.-N., Jiang, G.-Z., Li, L.-B., & Kuang, T.-Y. (2003). Effect of various temperatures on phosphatidylglycerol biosynthesis in thylakoid membranes. *Physiologia Plantarum*, *118*(1), 57–63. https://doi.org/10.1034/j.1399-3054.2003.00067.x

Yamaguchi, T., & Osumi, T. (2009). Chanarin-Dorfman syndrome: Deficiency in CGI-58, a lipid droplet-bound coactivator of lipase. *Biochimica Et Biophysica Acta*, *1791*(6), 519–523. https://doi.org/10.1016/j.bbalip.2008.10.012

Yamaoka, Y., Yu, Y., Mizoi, J., Fujiki, Y., Saito, K., Nishijima, M., Lee, Y., & Nishida, I. (2011). PHOSPHATIDYLSERINE SYNTHASE1 is required for microspore development in Arabidopsis thaliana. *The Plant Journal*, *67*(4), 648–661. https://doi.org/10.1111/j.1365-313X.2011.04624.x

Yamaryo, Y., Dubots, E., Albrieux, C., Baldan, B., & Block, M. A. (2008). Phosphate availability affects the tonoplast localization of PLDzeta2, an Arabidopsis thaliana phospholipase D. *FEBS Letters*, *582*(5), 685–690. https://doi.org/10.1016/j.febslet.2008.01.039

Yamashita, A., Fujimoto, M., Katayama, K., Tsutsumi, N., & Arimura, S.-I. (2016). Mitochondrial outer membrane forms bridge between two mitochondria in Arabidopsis thaliana. *Plant Signaling & Behavior*, *11*(5), e1167301. https://doi.org/10.1080/15592324.2016.1167301

Yamashita, A., Fujimoto, M., Katayama, K., Yamaoka, S., Tsutsumi, N., & Arimura, S.-I. (2016). Formation of Mitochondrial Outer Membrane Derived Protrusions and Vesicles in Arabidopsis thaliana. *PloS One*, *11*(1), e0146717. https://doi.org/10.1371/journal.pone.0146717

Yang, J. W., Fu, J. X., Li, J., Cheng, X. L., Li, F., Dong, J. F., Liu, Z. L., & Zhuang, C. X. (2014). A Novel Co-immunoprecipitation Protocol Based on Protoplast Transient Gene Expression for Studying Protein–protein Interactions in Rice. *Plant Molecular Biology Reporter*, *32*(1), 153–161. https://doi.org/10.1007/s11105-013-0633-9

Yang, S. U., Kim, J., Kim, H., & Suh, M. C. (2019). Functional Characterization of Physcomitrella patens Glycerol-3-Phosphate Acyltransferase 9 and an Increase in Seed Oil Content in Arabidopsis by Its Ectopic Expression. *Plants*, *8*(8), 8. https://doi.org/10.3390/plants8080284

Yang, W., Gutbrod, P., Gutbrod, K., Peisker, H., Song, X., Falz, A.-L., Meyer, A. J., & Dörmann, P. (2022). 2-Hydroxy-phytanoyl-CoA lyase (AtHPCL) is involved in phytol metabolism in Arabidopsis. *The Plant Journal*, *109*(5), 1290–1304. https://doi.org/10.1111/tpj.15632

Yang, Y., & Benning, C. (2018). Functions of triacylglycerols during plant development and stress. *Current Opinion in Biotechnology*, *49*, 191–198. https://doi.org/10.1016/j.copbio.2017.09.003

Yang, Y., Yu, X., Song, L., & An, C. (2011). ABI4 Activates DGAT1 Expression in Arabidopsis Seedlings during Nitrogen Deficiency1[C][W][OA]. *Plant Physiology*, *156*(2), 873–883. https://doi.org/10.1104/pp.111.175950

Yang, Z., & Ohlrogge, J. B. (2009). Turnover of Fatty Acids during Natural Senescence of Arabidopsis, Brachypodium, and Switchgrass and in Arabidopsis β-Oxidation Mutants. *Plant Physiology*, *150*(4), 1981–1989. https://doi.org/10.1104/pp.109.140491

Ye, H., Ji, C., Guo, R., & Jiang, L. (2020). Membrane Contact Sites and Organelles Interaction in Plant Autophagy. *Frontiers in Plant Science*, *11*. https://doi.org/10.3389/fpls.2020.00477

Yoshida, Y., Niwa, H., Honsho, M., Itoyama, A., & Fujiki, Y. (2015). Pex11mediates peroxisomal proliferation by promoting deformation of the lipid membrane. *Biology Open*, *4*(6), 710–721. https://doi.org/10.1242/bio.201410801

Youn, D. H., Kim, Y., Kim, B. J., Jeong, M. S., Lee, J., Rhim, J. K., Kim, H. C., & Jeon, J. P. (2021). Mitochondrial dysfunction associated with autophagy and mitophagy in cerebrospinal fluid cells of patients with delayed cerebral ischemia following subarachnoid hemorrhage. *Scientific Reports*, *11*(1), 16512. https://doi.org/10.1038/s41598-021-96092-2

Yu, B., Wakao, S., Fan, J., & Benning, C. (2004). Loss of plastidic lysophosphatidic acid acyltransferase causes embryo-lethality in Arabidopsis. *Plant & Cell Physiology*, *45*(5), 503–510. https://doi.org/10.1093/pcp/pch064

Yu, B., Xu, C., & Benning, C. (2002a). Arabidopsis disrupted in SQD2 encoding sulfolipid synthase is impaired in phosphate-limited growth. *Proceedings of the National Academy of Sciences of the United States of America*, *99*(8), 5732–5737. https://doi.org/10.1073/pnas.082696499

Yu, B., Xu, C., & Benning, C. (2002b). Arabidopsis disrupted in SQD2 encoding sulfolipid synthase is impaired in phosphate-limited growth. *Proceedings of the National Academy of Sciences of the United States of America*, *99*(8), 5732–5737. https://doi.org/10.1073/pnas.082696499

Yu, L., Shen, W., Fan, J., Sah, S. K., Mavraganis, I., Wang, L., Gao, P., Gao, J., Zheng, Q., Meesapyodsuk, D., Yang, H., Li, Q., Zou, J., & Xu, C. (2023). A chloroplast diacylglycerol lipase modulates glycerolipid pathway balance in Arabidopsis. *The Plant Journal: For Cell and Molecular Biology*, *115*(2), 335–350. https://doi.org/10.1111/tpj.16228

Yuan, D., Wu, Z., & Wang, Y. (2016). Evolution of the diacylglycerol lipases. *Progress in Lipid Research*, *64*, 85–97. https://doi.org/10.1016/j.plipres.2016.08.004

Yuzawa, Y., Nishihara, H., Haraguchi, T., Masuda, S., Shimojima, M., Shimoyama, A., Yuasa, H., Okada, N., & Ohta, H. (2012). Phylogeny of Galactolipid Synthase Homologs Together with their Enzymatic Analyses Revealed a Possible Origin and Divergence Time for Photosynthetic Membrane Biogenesis. *DNA Research*, *19*(1), 91–102. https://doi.org/10.1093/dnares/dsr044

Zakhleniuk, O. V., Raines, C. A., & Lloyd, J. C. (2001). pho3: A phosphorus-deficient mutant of Arabidopsis thaliana (L.) Heynh. *Planta*, *212*(4), 529–534. https://doi.org/10.1007/s004250000450

Zhang, L., Joshi, A. K., & Smith, S. (2003). Cloning, expression, characterization, and interaction of two components of a human mitochondrial fatty acid synthase. Malonyltransferase and acyl carrier protein. *The Journal of Biological Chemistry*, *278*(41), 40067–40074. https://doi.org/10.1074/jbc.M306121200

Zhang, M., Fan, J., Taylor, D. C., & Ohlrogge, J. B. (2009). DGAT1 and PDAT1 acyltransferases have overlapping functions in Arabidopsis triacylglycerol biosynthesis and are essential for normal pollen and seed development. *The Plant Cell*, *21*(12), 3885–3901. https://doi.org/10.1105/tpc.109.071795

Zhang, Y., Song, G., Lal, N. K., Nagalakshmi, U., Li, Y., Zheng, W., Huang, P.-J., Branon, T. C., Ting, A. Y., Walley, J. W., & Dinesh-Kumar, S. P. (2019). TurboID-based proximity labeling reveals that UBR7 is a regulator of N NLR immune receptor-mediated immunity. *Nature Communications*, *10*(1), 3252. https://doi.org/10.1038/s41467-019-11202-z

Zhang, Y., Wang, X., Lu, S., & Liu, D. (2014). A major root-associated acid phosphatase in Arabidopsis, AtPAP10, is regulated by both local and systemic signals under phosphate starvation. *Journal of Experimental Botany*, *65*(22), 6577–6588. https://doi.org/10.1093/jxb/eru377

Zhang, Y., Wang, X., Wang, X., Wang, Y., Liu, J., Wang, S., Li, W., Jin, Y., Akhter, D., Chen, J., Hu, J., & Pan, R. (2023). Bioinformatic analysis of short-chain dehydrogenase/reductase proteins in plant peroxisomes. *Frontiers in Plant Science*, *14*. https://doi.org/10.3389/fpls.2023.1180647

Zhao, L., Katavic, V., Li, F., Haughn, G. W., & Kunst, L. (2010). Insertional mutant analysis reveals that long-chain acyl-CoA synthetase 1 (LACS1), but not LACS8, functionally overlaps with LACS9 in Arabidopsis seed oil biosynthesis. *The Plant Journal: For Cell and Molecular Biology*, *64*(6), 1048–1058. https://doi.org/10.1111/j.1365-313X.2010.04396.x

Zheng, Z., Xia, Q., Dauk, M., Shen, W., Selvaraj, G., & Zou, J. (2003). Arabidopsis AtGPAT1, a Member of the Membrane-Bound Glycerol-3-Phosphate Acyltransferase Gene Family, Is Essential for Tapetum Differentiation and Male Fertility. *The Plant Cell*, *15*(8), 1872–1887. https://doi.org/10.1105/tpc.012427

Zhou, J., Jiao, F., Wu, Z., Li, Y., Wang, X., He, X., Zhong, W., & Wu, P. (2008). OsPHR2 is involved in phosphate-starvation signaling and excessive phosphate accumulation in shoots of plants. *Plant Physiology*, *146*(4), 1673–1686. https://doi.org/10.1104/pp.107.111443

Zhou, X.-R., Shrestha, P., Yin, F., Petrie, J. R., & Singh, S. P. (2013). AtDGAT2 is a functional acyl-CoA:diacylglycerol acyltransferase and displays different acyl-CoA substrate preferences than AtDGAT1. *FEBS Letters*, *587*(15), 2371–2376. https://doi.org/10.1016/j.febslet.2013.06.003

Zhou, Y., Hölzl, G., Vom Dorp, K., Peisker, H., Melzer, M., Frentzen, M., & Dörmann, P. (2017). Identification and characterization of a plastidial phosphatidylglycerophosphate phosphatase in Arabidopsis thaliana. *The Plant Journal: For Cell and Molecular Biology*, *89*(2), 221–234. https://doi.org/10.1111/tpj.13378

Zhou, Y., Peisker, H., & Dörmann, P. (2016). Molecular species composition of plant cardiolipin determined by liquid chromatography mass spectrometry. *Journal of Lipid Research*, *57*(7), 1308–1321. https://doi.org/10.1194/jlr.D068429

Zhou, Z., Wang, Z., Lv, Q., Shi, J., Zhong, Y., Wu, P., & Mao, C. (2015). SPX proteins regulate Pi homeostasis and signaling in different subcellular level. *Plant Signaling & Behavior*, *10*(9), e1061163. https://doi.org/10.1080/15592324.2015.1061163

Zhu, S., Liang, C., Tian, J., & Xue, Y. (2022). Advances in Plant Lipid Metabolism Responses to Phosphate Scarcity. *Plants*, *11*(17), 2238. https://doi.org/10.3390/plants11172238

Zinser, E., Sperka-Gottlieb, C. D., Fasch, E. V., Kohlwein, S. D., Paltauf, F., & Daum, G. (1991). Phospholipid synthesis and lipid composition of subcellular membranes in the unicellular eukaryote Saccharomyces cerevisiae. *Journal of Bacteriology*, *173*(6), 2026–2034.

Zolman, B. K., Silva, I. D., & Bartel, B. (2001). The Arabidopsis *pxa1* Mutant Is Defective in an ATP-Binding Cassette Transporter-Like Protein Required for Peroxisomal Fatty Acid β-Oxidation. *Plant Physiology*, *127*(3), 1266–1278. https://doi.org/10.1104/pp.010550

Zolman, B. K., Yoder, A., & Bartel, B. (2000). Genetic analysis of indole-3-butyric acid responses in Arabidopsis thaliana reveals four mutant classes. *Genetics*, *156*(3), 1323–1337.

Zou, J., Wei, Y., Jako, C., Kumar, A., Selvaraj, G., & Taylor, D. C. (1999). The Arabidopsis thaliana TAG1 mutant has a mutation in a diacylglycerol acyltransferase gene. *The Plant Journal*, *19*(6), 645–653. https://doi.org/10.1046/j.1365-313x.1999.00555.x

Zrenner, R., Stitt, M., Sonnewald, U., & Boldt, R. (2006). Pyrimidine and Purine Biosynthesis and Degradation in Plants. *Annual Review of Plant Biology*, *57*(1), 805–836. https://doi.org/10.1146/annurev.arplant.57.032905.105421

Role of peroxisome and β-oxidation in membrane lipid remodeling in response to phosphate starvation in *Arabidopsis thaliana*

Phosphate (Pi) starvation is a frequent abiotic stress encountered by plants in nature and significantly affecting plant growth and crop yield. To adapt to Pi starvation, plants activate various mechanisms to ensure their survival, including increasing Pi uptake from soil and remobilizing intracellular phosphorus reserve. Notably, during Pi starvation, phospholipids (PL) located at extra-plastidial membranes are partially degraded to release Pi, while plastidial digalactosyldiacylglycerol (DGDG), a non-phosphorous plastid-synthesized lipid, is transferred to extra-plastidial organelles to substitute PL in order to maintain their integrities and functions. Previous studies have revealed that the DAG backbone of newly formed DGDG originated from extra-plastidial PC, indicating that the partially degraded PC is recycled to synthesize DGDG. However, we uncovered that the total lipid content drastically decreased under Pi deprivation. Given that, we hypothesized a potential association between lipid remodeling and β-oxidation, a lipid degradation pathway occurring in peroxisomes. It prompted us to further investigate if the β-oxidation pathway would be important in recycling free fatty acids derived from the partially degraded PL under Pi deprivation and, more generally, if peroxisomes would be involved in lipid remodeling during Pi starvation.

We attempt to purify peroxisome from Arabidopsis calli grown under both Pi-enriched and Pi-deprived conditions using an adapted isolation protocol from previous studies, to refine our understanding of peroxisomal lipid composition in *Arabidopsis thaliana* and to study its lipidomic and proteomic responses to Pi starvation. Using this optimized protocol, we enrich peroxisomes with satisfactory yields for analyses under both standard and stress conditions, and de-enrich other organelles. Our results highlight the major phospholipid composition of peroxisomal membranes, similar across various species. We also identify proteins related to oxidative stress response and nitrogen metabolism that exhibit significant differences between normal growth conditions and Pi deficiency. However, low purity of the isolated peroxisomes is insufficient to conclusively assess the lipidomic and proteomic differences in response to Pi deprivation.

In order to elucidate the role of β-oxidation process in lipid remodeling in response to Pi starvation, we selected two enzymes involved in β-oxidation pathway, PXA1 and MFP2, and employed multiple approaches, such as gene expression profiling, growth phenotype assessment, lipidomic analyses, and subcellular imaging, onto the wild type and mutant strains deficient in these two genes under Pi-replete and Pi-deplete conditions. Our results show that β-oxidation pathway is not involved in the metabolic processes of lipid remodeling in response to Pi starvation in *A. thaliana* cell cultures. Interestingly, a resistant phenotype of *pxa1* calli under Pi-starved conditions is observed. The phenotypic behavior of *pxa1* plants in response to Pi starvation requires further investigations. Moreover, an abnormal mitochondrial morphology, that remain to be investigated, is observed in these two β-oxidation mutants, particularly under standard conditions. Additional studies remains to be conducted to assess the redox status of these two mutant calli under both conditions.

Overall, we revealed that peroxisomal β-oxidation pathway does not play a major role in the metabolic flow of phospholipid degradation in response to Pi starvation, and characterized notable cellular responses in β-oxidation mutants.

Keywords: peroxisome, β-oxidation, membrane lipid remodeling, phosphate starvation, *Arabidopsis thaliana*

Rôle du peroxysome et de la β-oxydation dans le remodelage des lipides membranaires en réponse à la carence en phosphate chez *Arabidopsis thaliana*

La carence en phosphate (Pi) est un stress abiotique fréquemment rencontré par les plantes dans la nature, affectant considérablement leur croissance et les rendements agricoles. Pour s'adapter à la carence en Pi, les plantes activent divers mécanismes pour assurer leur survie, y compris l'augmentation de l'absorption du Pi présent dans le sol et la remobilisation des réserves intracellulaires de phosphore. Notamment, lors de la carence en Pi, les phospholipides (PL) situés dans les membranes extra-plastidiales sont partiellement dégradés pour libérer du Pi, tandis que le digalactosyldiacylglycérol (DGDG) plastidial, un lipide sans phosphore synthétisé dans les plastes, est transféré aux organites extra-plastidiaux pour remplacer les PL afin de maintenir leur intégrité et leurs fonctions. Des études antérieures ont révélé que le squelette du diacylglycérol (DAG) du DGDG nouvellement synthétisé provenait de la phosphatidylcholine (PC) extra-plastidial, indiquant que la PC partiellement dégradée etait recyclée pour synthétiser le DGDG. Cependant, nous avons découvert que le contenu lipidique total des cellules diminuait drastiquement en cas de privation de Pi. Cela nous a amenés à émettre l'hypothèse d'une association potentielle entre le remodelage des lipides et la β-oxydation, une voie de dégradation des lipides se produisant dans les peroxysomes. Cela nous a incités à examiner si la voie de la β-oxydation serait importante pour recycler les acides gras provenant des PL partiellement dégradés en cas de privation de Pi et, plus généralement, si les peroxysomes seraient impliqués dans le remodelage des lipides pendant la carence en Pi.

Nous avons tenté de purifier les peroxysomes à partir de cals d'Arabidopsis cultivés dans des conditions enrichies ou sans Pi en utilisant un protocole d'isolation adapté d'études précédentes, afin d'affiner notre compréhension de la composition lipidique des peroxysomes chez *Arabidopsis thaliana* et d'étudier leurs réponses lipidomiques et protéomiques à la carence en Pi. En utilisant ce protocole optimisé, nous avons enrichi les peroxysomes avec des rendements satisfaisants pour les analyses dans des conditions standard et de stress, tout en réduisant quantité des autres organites. Nos résultats mettent en évidence la composition majeure des phospholipides des membranes peroxysomales, similaire à travers différentes espèces. Nous avons également identifié des protéines liées à la réponse au stress oxydatif et au métabolisme de l'azote qui présentent des différences significatives entre les conditions de croissance normale et de carence en Pi. Cependant, la faible pureté des peroxysomes isolés ne permet pas d'évaluer de manière significative les différences lipidomiques et protéomiques en réponse à la privation de Pi.

Afin d'élucider le rôle du processus de β-oxydation dans le remodelage des lipides en réponse à la carence en Pi, nous avons sélectionné deux enzymes impliquées dans la voie de la β-oxydation, PXA1 et MFP2, et employé plusieurs approches, telles que l'analyse de l'expression des gènes, l'évaluation des phénotypes de croissance, les analyses lipidomiques et l'imagerie subcellulaire, sur les souches de type sauvage et les mutants déficients en ces deux gènes dans des conditions riches en Pi et déficientes en Pi. Nos résultats montrent que la voie de la β-oxydation ne joue pas un rôle majeur dans les processus métaboliques de remodelage des lipides en réponse à la carence en Pi dans les cultures cellulaires d'*A. thaliana*. Fait intéressant, un phénotype résistant des cals *pxa1* en conditions de carence en Pi a été observé. Le comportement phénotypique des plantes *pxa1* en réponse à la carence en Pi nécessite des investigations supplémentaires. De plus, une morphologie mitochondriale anormale a été observée chez ces deux mutants de la β-oxydation, particulièrement dans des conditions standards, suggérant une association potentielle avec l'accumulation de ROS. Des études supplémentaires restent à mener pour évaluer le statut redox de ces deux lignées mutantes dans les deux conditions.

En conclusion, nous avons révélé que la voie de la β-oxydation peroxysomale ne joue pas un rôle majeur dans le flux métabolique de la dégradation des phospholipides en réponse à la privation de Pi, et nous avons caractérisé des réponses cellulaires notables chez les mutants de la β-oxydation.

Mots clés : peroxysome, β-oxydation, remodelage des lipides membranaires, carence en phosphate, *Arabidopsis thaliana*

CEA Grenoble
Laboratoire de Physiologie Cellulaire et Végétale (LPCV)
UMR 5168 CEA / CNRS / Université Grenoble Alpes / UMR 1417 INRAE
17, Avenue des Martyrs
38054 Grenoble cedex 9